FEBRUARY · 1953

Proceedings of the I·R·E

Journal of Communications and Electronic Engineering

Gauging Mica Holes

Sylvania Elec. Prod. Inc.

nsuring snug fits of tube elements passing through mica cers, and avoidance of tube microphonics, require measuret of hole diameters to 1/20,000th of an inch (despite the ence of loose mica flakes which must be pushed back into body of the spacer).

Volume 41 Number 2

IN THIS ISSUE

Table of Contents, Indicated by Black-and-White Margin, Follows Page 64A

The Institute of Radio Engineers

PROCEEDINGS OF THE I.R.E.®

Published Monthly by

The Institute of Radio Engineers, Inc.

VOLUME 41 — *February, 1953* — NUMBER 2

Changes of address (with advance notice of fifteen days) and communications regarding subscriptions and payments should be mailed to the Secretary of the Institute, at 450 Ahnaip St., Menasha, Wisconsin, or 1 East 79 Street, New York 21, N. Y.

PROCEEDINGS OF THE I.R.E.

INSTITUTE NEWS AND RADIO NOTES SECTION

Responsibility for the contents of papers published in the PROCEEDINGS OF THE I.R.E. rests upon the authors. Statements made in papers are not binding on the Institute or its members.

S. R. Kantebet

VICE-PRESIDENT, 1953

Shankar R. Kantebet was born in Bombay, India, December, 1900. He graduated with the highest honors in physics and mathematics from the Bombay University, in 1922, and was awarded the University's Sir Mangaldas Nathubai Technical Scholarship.

During the following three years, Mr. Kantebet took a course in electrical technology, specializing in radio engineering at the Indian Institute of Science, Bangalore, and then traveled to the United Kingdom for advanced study at the Marconi Wireless College, Chelmsford, England. At Marconi, he participated in the installation and testing of shortwave stations for radio-telegraph services between England and Canada, Australia, and South Africa.

Joining the Marconi Wireless Telegraph Company Limited, in 1925, as an assistant engineer, Mr. Kantebet returned to India to direct the installation of the England-India beam-telegraph service. From 1928–1932, he was head of electrical communication engineering at the Institute of Bangalore, where he organized a post-graduate course in theory and practice of long-distance line and radio communication.

In 1932, Mr. Kantebet became engineer-in-chief of installations and projects of the Indian Radio and Cable Communications Company Limited, Bombay, and then served as the liaison officer at Delhi, between that company and the Government of India and South East Asia Command. In 1947, when the company became a part of the Government of India, Mr. Kantebet was named general manager of that organization, now called Overseas Communications Service, which is responsible for the cable and radio services between India and other countries.

Mr. Kantebet joined the Institute as an Associate in 1925, transferred to Member and Senior Member in 1931 and 1943, respectively, and became an IRE Fellow in 1949. He is also a member of the Institution of Electrical Engineers.

Electronic Design for the Military

John D. Reid

The present sharp differentiation in construction, appearance, and cost between military radio equipment and the corresponding apparatus for civilian use may well deserve critical examination by government specification officials, commercial manufacturers, and design engineers. Economy, compactness, and reliability are obviously some of the guiding characteristics in determining the optimum construction of electronic devices.

This subject is clearly analyzed in the following guest editorial by a Fellow of the Institute, who is vice president in charge of engineering, American Radio and Television, Incorporated, North Little Rock, Arkansas.

—The Editor.

Industry, it seems, has been remiss in not applying its commercial knowledge, which it has gained in radio and television mass production, to military electronic design.

It is unfortunate that the engineering groups working on military designs have been isolated from similar groups working on commercial designs. Many of the new engineering companies organized to work on government plans lack mass production design experience. Even the government product design groups of existing large radio manufacturers are isolated from the commercial groups in the same kind of work.

The radio engineer who designs for mass production has of necessity learned efficient design by his intimate contacts with production problems. This experience, which he has gained the hard way, should not be wasted.

Government purchasing groups demand a pleasing appearance of neatness and symmetry in their electronic chassis. When they observe the lack of symmetry and the maze of wires in commercial designs, they fall into a common error of thinking that quality has been sacrificed.

Nothing could be more false, as it is a primary requirement that commercial designs for mass production, such as radio and television sets, must have the highest reliability. No reputable manufacturer sacrifices reliability for price considerations, nor could a manufacturer who did so remain in such a highly competitive market. For example, the use of component mounting boards, screw machine soldering terminals, and cabled wiring was abandoned by the radio industry for commercial receivers in the middle thirty's; we still find these the rule rather than the exception in present day government equipment.

Most to be deplored is the trend in military electronic equipment towards the breaking up of the designs into units and the use of plugs and sockets for interconnection. This trend is particularly unfortunate when applied to expendable items such as guided missiles, where reliability is of the utmost importance. While the radio industry makes effective use of subassemblies, it shuns and abhors plugs and cables with their attendant friction contacts, short leakage paths, and increased circuit intercoupling. It costs the industry money to learn that such designs jeopardize their reliability.

Good commercial design principles are sorely needed in military electronic equipment. Cardinal design principles are: soldered connections, point-to-point wiring, and a layout for accessibility so that all joints may be inspected.

Industry has been remiss in not selling commercial designs to government purchasers and in not using their experienced commercial design engineers on government projects. Government purchasers have been remiss in buying by appearance and not demanding the improved reliability and reduction of man hours which may be afforded by commercial radio design.

The 100-KW ERP Sutton Coldfield Television Broadcasting Station*

P. A. T. BEVAN†

Summary—**This paper describes the planning, design, construction, and service performance of the 100-kw ERP Sutton Coldfield television broadcasting station built by the British Broadcasting Corporation as the first of the group of four new high-power stations required by the plan to extend the London television service to provide national coverage for the United Kingdom.**

It represents the basic general arrangement which has been used at the subsequent stations, although at each of these, some variations have been desirable because of differences and improvements in the type of transmitter and combining equipment.

The relation of the operating channel of Sutton Coldfield to the over-all frequency-allocation plan for the 41- to 68-mc band used for television broadcasting in the United Kingdom, and the reasons for adopting a vestigial sideband characteristic for the vision signal, are briefly discussed.

The construction details of the complete vision and sound transmitting equipment, transmission lines, combining diplexer, mast and antenna system are described, and information about the performance of the station in service is given.

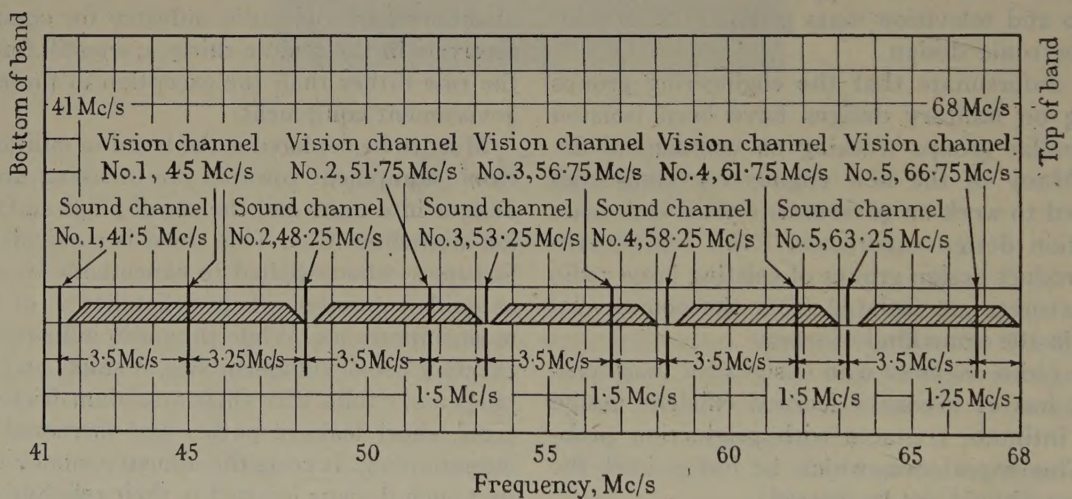

Fig. 1—The BBC's television service frequency allocation plan.

1. Introduction

THE SUTTON COLDFIELD television transmitting station, which was officially opened for public service on December 17, 1949, marked the first step in extending the British Broadcasting Corporation's 405-line 2:1 interlaced scanning 25-pictures per second television service from London to serve the rest of the United Kingdom. It has an effective radiated power (ERP) of 100 kw and represents the basic general arrangement used for the three subsequent high-power stations now either in service or nearing completion in the north of England (Holme Moss), Scotland (Kirk O'Shotts), and South Wales (Wenvoe). Some variations were desirable at the later stations, however, because of the different types of transmitters and output combining equipment.[1] The over-all engineering of the station was carried out by the BBC's Planning and Installation department in collaboration with the Research department and Building department. The station is situated some ten miles north of Birmingham, and occupies a 24-acre site 550 feet above sea level. The vision program is relayed to the station from the London Studio Centre, either by the London-Birmingham uhf radio link,[2] or the coaxial cable link,[3] which form a part of the 1,200-mile bi-directional television distribution network to be provided and operated by the General Post Office. The accompanying sound program is conveyed via the BBC's normal telephone line network.

There are two vhf transmitters: a 50-kw vision transmitter and a 12-kw sound transmitter, operating on carrier frequencies of 61.75 mc and 58.25 mc, respectively, corresponding to channel 4 of the British Television Service frequency allocation plan for the 41- to 68-mc band, as shown in Fig. 1. In accordance with this plan, a vestigial sideband transmission, based on the receiver-attenuation (r.a.) system, is used for the vision program, and five independent channels, which is the required minimum if the greater part of the population of

* Decimal classification: R583. Original manuscript received by the Institute, December 14, 1951; revised manuscript received August 27, 1952.

† British Broadcasting Corporation, Broadcasting House, London, W.1, England.

[1] P. A. T. Bevan, "Television Broadcasting Stations," paper no. 1299, British Television Convention, session 4; 1952.

[2] R. T. Clayton, D. C. Espley, G. W. S. Griffiths, and J. M. C. Pinkham, "The London-Birmingham radio-relay link," *Proc. IEE*, vol. 98, part 1, p. 204; 1951.

[3] T. Kilvington, F. J. M. Laver, and H. Stanesley, "The London-Birmingham television-cable system," *Proc. IEE*, vol. 99, part 1, p. 44; 1952.

the United Kingdom is to receive a television service in this waveband, have been obtained.[4]

With the exception of the double-sideband channel occupied by the original Alexandra Palace station, the spacing between the four new channels is 5 mc, and each has been allocated an over-all channel width of 4.75 mc. The appropriate transmitter and receiver transmission characteristics are shown in Fig. 2. The sound carrier is placed 3.5 mc below the vision carrier. The lower vision sideband is transmitted substantially in full from a frequency 3.0 mc below the carrier, while the upper vision sideband is substantially attenuated (see section 4.5) for frequencies more than 0.75 mc above the carrier. Both vision and sound transmissions are amplitude modulated, positive modulation being used for the vision signal.

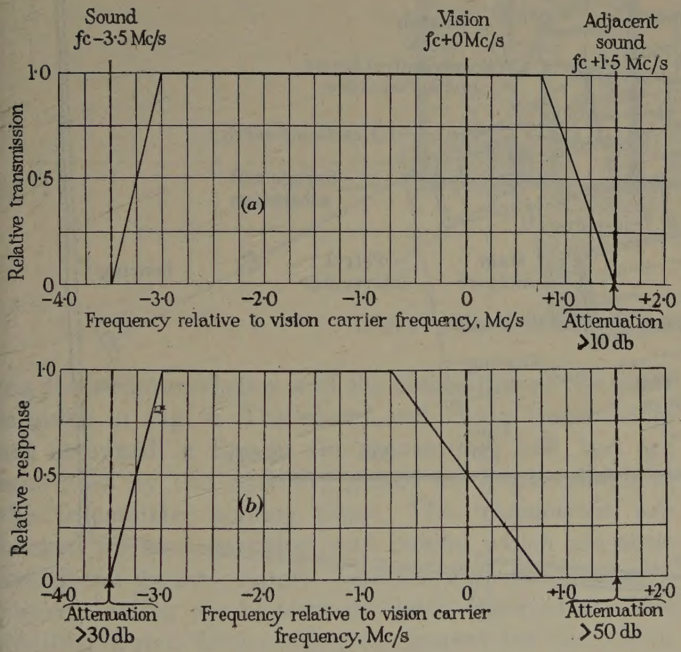

Fig. 2.—Idealized transmitter and receiver characteristics for the vestigial sideband channels.

A scheme of regional distribution, rather than the local or urban distribution more favored in the United States, was decided upon for the United Kingdom, partly because of the relatively small number of channels available, and also in order to assure the maximum possible coverage in these circumstances. This requires, therefore, high-power transmitters with high sites and high antennas. Sutton Coldfield was the first of the four new high-power stations built to implement this scheme (which also includes the provision of five low-power stations, using 5-kw transmitters and 20-kw ERPs to cover other smaller areas not adequately served by the high-power stations[1]). These stations will operate with the high-power stations and use horizontal polarization.

The London Television Service showed that a field strength of some 500 microvolts per meter at a height of 30 feet is needed to ensure consistently good reception under existing conditions of average interference, and to obtain the required coverage, this field strength had to be realized at a range of some 50 to 60 miles from each of the high-power stations. Reception is practical at 100 microvolts per meter, but its acceptability is greatly dependent on local conditions and automobile interference, while tropospheric conditions may often cause serious fading at ranges beyond 50 miles.

It was on this general basis that the ERP for Sutton Coldfield and the subsequent high-power stations was determined. One decisive factor was the possible power of the vision transmitter itself. Calculations indicated that the output obtainable from a pair of the largest vhf transmitting tubes, type CAT.21, available at the time (1947), when operated as a linear modulated amplifier of appropriate bandwidth at frequencies of the order of 60 mc, was about 35 kw for a conventional earthed-cathode circuit and 50 kw for an earthed grid circuit.[5] Little development in earthed-grid amplifier technique at this frequency and power level had, however, occurred, so for preliminary field strength calculations the power of the transmitter was arbitrarily fixed at 35 kw, it being appreciated that higher powers would be realized as tube and circuit development proceeded. The tube situation was, in fact, serious, as only experimental ring grid-seal vhf types were available with anode dissipations in excess of about 5 kw.

On this basis, and since the Sutton Coldfield site was not high, a mast having an over-all height of 750 feet was chosen to support an unstayed, vertically polarized television antenna, while an antenna power gain of 4 db over a single half-wave vertical dipole was deemed a satisfactory compromise between the other conflicting requirement of bandwidth, the production of a robust high power antenna capable of withstanding adverse weather with wind speeds of 110 mph, and the cost of the support mast. A higher antenna gain would have been justified had more time for development been available, but, even so, a reasonable limit must be set for the mechanical forces which a cantilever extension exerts at the apex of a high supporting mast, the cost of which rises steeply as these forces increase. This tends to place a practical limit on the height of the cantilever, and hence on the gain of omnidirectional, vertically polarized antennas for the 41 to 68 mc band.

With horizontal polarization it is somewhat easier to provide television antennas of much higher gain, because a number of stacks of horizontal dipole radiators may be supported from a central structure whose cross section has little effect on the radiation even when it is relatively large, while the complete array may be stayed with conducting guy ropes. A further factor affecting the mast design was the decision to provide, at each of the

[4] Sir Noel Ashbridge, "The British Television Service," Joint Engineering Conference; 1951.

[5] P. A. T. Bevan, "High power television transmitters," *Electronic Eng.* (London), vol. 19, pp. 138, 181; 1947.

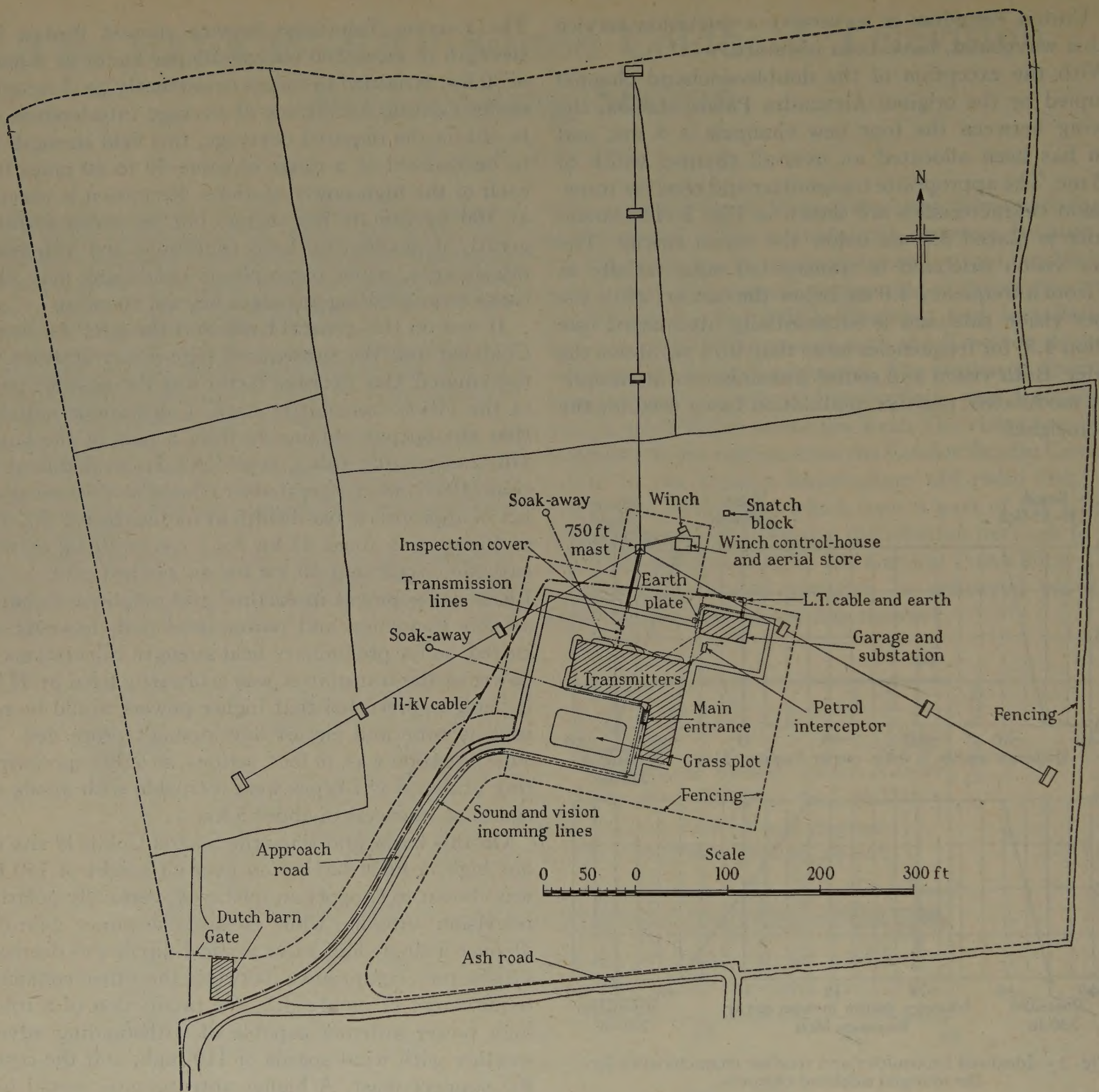

Fig. 3—Site plan of the Sutton Coldfield station.

television stations, a horizontally polarized antenna for a possible future vhf sound broadcast service in the 88- to 108-mc band. This led to the use of a mast antenna system consisting of a stayed lattice structure supporting a stayed tubular section slot antenna which, in turn, is surmounted by the cantilever topmast carrying the television antenna.

When it went into service, Sutton Coldfield was the highest powered television transmitting station constructed in any country, although it has now either been equalled or superseded in this respect by the three later stations. The antenna gain at all four stations is substantially the same, namely, approximately 4 db, but at Holme Moss, the high-level modulated vision transmitter has an output power in excess of 50-kw peak white, while the most recent design of vision transmitter, installed at both the Kirk o' Shotts and Wenvoe stations, is capable of approximately 75-kw peak white, if required. These transmitters are of the low-level modulated type. Modulation is effected at about the 600-watt level, the modulated signal then being amplified by three push-pull earthed-grid class B linear wide band power amplifiers in cascade, a description of which is given by the author in another paper.[1]

2. The Site and Buildings

A site near Birmingham was chosen because it provided the correct "center of gravity" for the Midland's population density. A plan of the site indicating the position of the buildings and mast is given in Fig. 3. The main building is of single storey construction in brick and stone, and is "L" shaped. A plan view show-

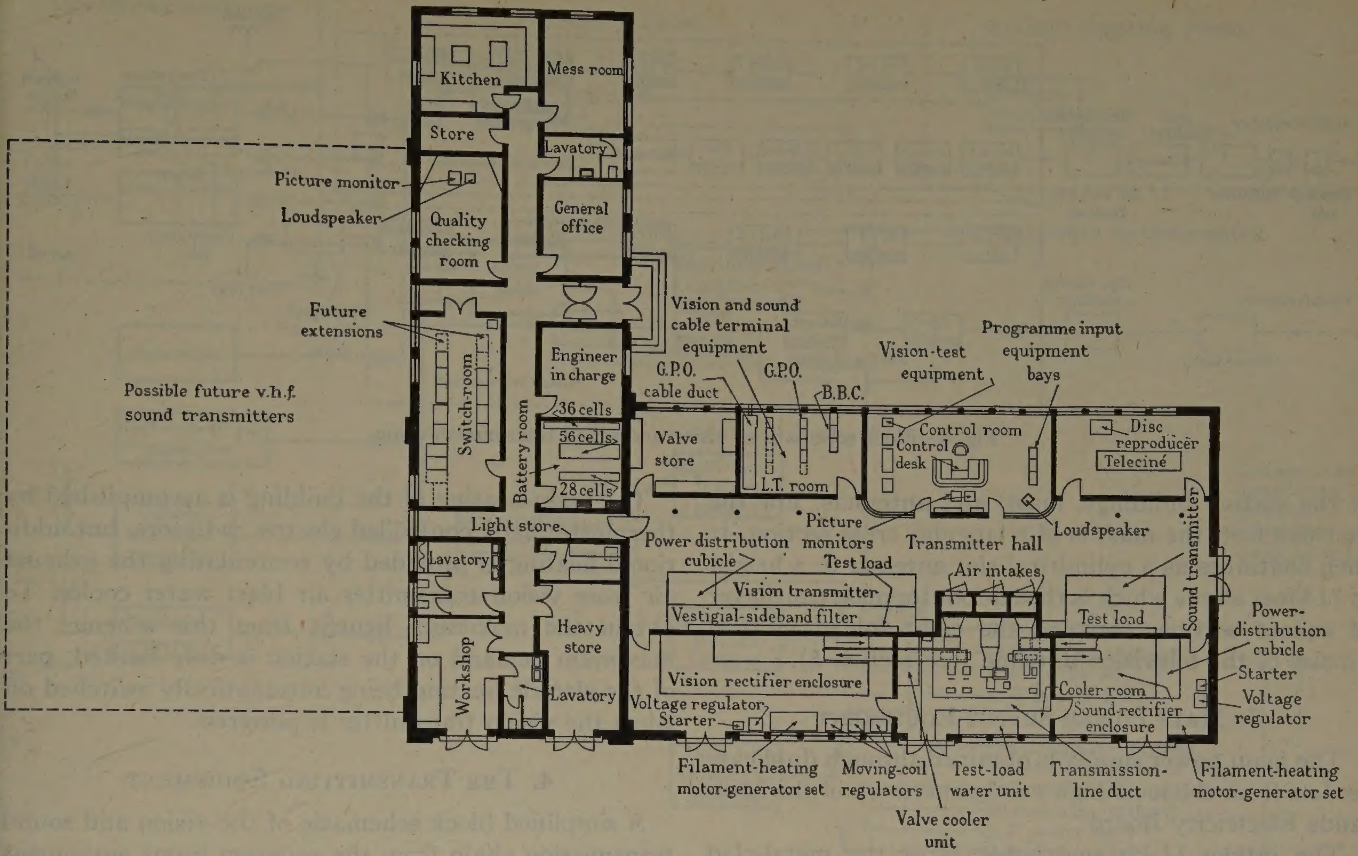

Fig. 4—Plan of transmitter building showing layout of equipment.

ing the accommodation and the disposition of the plant is given in Fig. 4. The sound and vision transmitters are arranged in line in the transmitter hall, but are separated by the centrally placed air intake shafts of the transmitter cooling plant. The transmitters are backed up to a partition wall behind which are their associated power supply cubicles and the centrally placed cooling air blowers for both transmitters, the distilled water tube cooling equipment for the vision transmitter, and the common water supply unit for the test loads of each transmitter. Facing the transmitters is the glass fronted control room containing the control desk, from which both transmitters are remotely controlled, the video- and audio-frequency program input and monitoring equipment, and the vision transmitter pulse-testing equipment. Flanking the control room is the lines termination room housing the video- and audio-frequency incoming terminal equipment, the telecine room originally containing a standby film scanner which has now been replaced by monoscopes, and a record playing desk. An annex building contains the power intake substation and a garage for station transport and visiting outside broadcast vehicles.

Some 150 feet to the north of the main building is the main mast-antenna system. Separate coaxial copper-tube transmission lines carry the radio-frequency outputs of the sound and vision transmitters to the top of the mast where they terminate in a combining unit of the nonfrequency discriminative diplexer type, which,

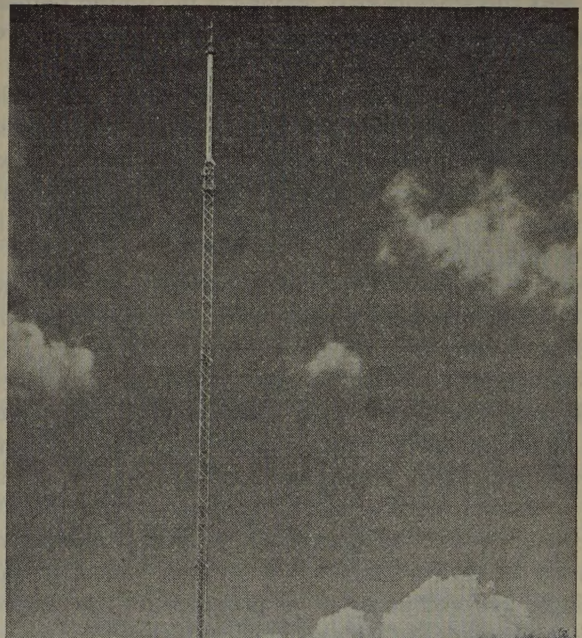

Fig. 5—General view of station buildings and mast antenna system.

in turn, feeds the combined vision and sound signals to the television antenna system. Fig. 5 is a photograph

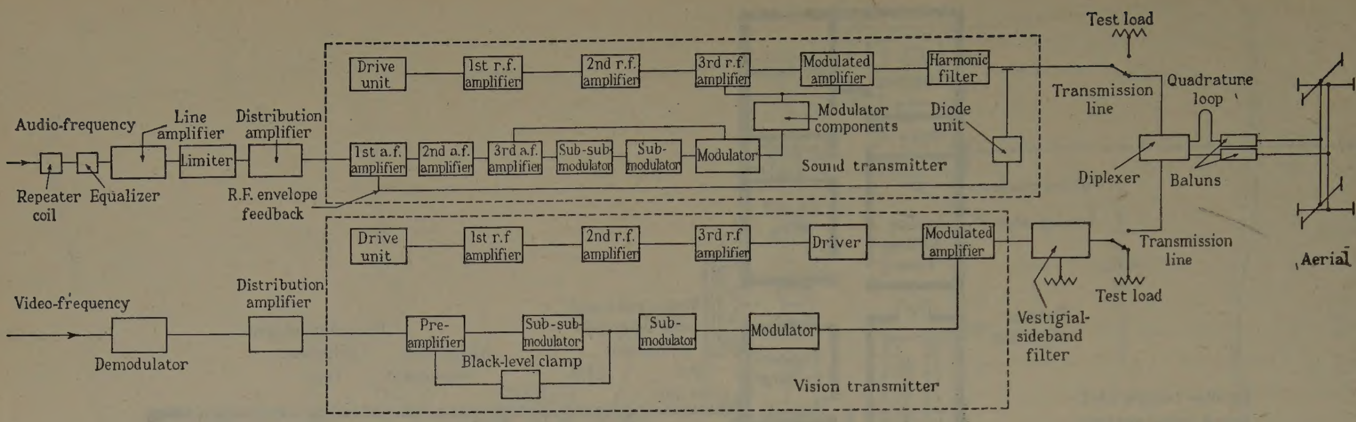

Fig. 6—Block schematic of vision and sound transmission chain.

of the station buildings, mast, and antennas. For the first 600 feet, the mast is of triangular cross section. It then continues as a cylindrical slot antenna to a height of 715 feet above which is the 35-foot topmast cantilever of square section, carrying the eight folded vertical dipoles of the television antenna (see section 5).

3. Main Power Supply Equipment

The main power supply is obtained through duplicate feeders from the local high voltage network of the Midlands Electricity Board.

The intake 11-kv switchgear is of the metal-clad vertical isolation type with a breaking capacity of 150 mva and the station load, having a maximum demand of approximately 400 kva, is supplied through two 500-kva 11,000 per 415 volts transformers installed in roofed, open-sided bays integral with the substation building. A spare bay is provided for a third transformer to accommodate the increase in load if a vhf sound broadcast extension is built at a later date. Normally, the two transformers are operated in parallel during program.

The transformer output cables terminate on a 415-volt 3-ph$+N$ switchboard incorporating vertical-isolation oil-filled circuit breakers for the incoming circuits and fuse-switch units for the outgoing circuits. The circuit breakers are equipped with conventional over-current and earth-leakage protection with intertripping of the 415-volt and 11-kv circuit breakers provided to ensure that a transformer cannot be energized from the 415-volt busbars. The transmitters and their auxiliaries are supplied at 415 volts, but a separate automatically regulated 240-volt ac supply is provided for the program input equipment and an automatically regulated 50-volt dc supply for the transmitter control and interlock circuits. General service supplies include antenna dipole de-icing, maintained lighting, and a controlled heating supply. Maintained lighting is achieved by selected lighting points in key position fed from a separate lighting circuit. Normally, this circuit is supplied at 240-volts ac, but in the even of a supply failure, contactors automatically change over to a 240-volt emergency battery.

The main heating of the building is accomplished by thermostatically controlled electric radiators, but additional heating is provided by recirculating the exhaust air from vision transmitter air blast water cooler. To obtain the maximum benefit from this scheme, the maximum demand on the station is duly limited, part of the electric heating being automatically switched off when the vision transmitter is powered.

4. The Transmitting Equipment

A simplified block schematic of the vision and sound transmission chain from the program input equipment to the antenna is given in Fig. 6 and is described in more detail in the sections which follow. Fig. 7 gives a view of the transmitter hall. The vision transmitter is on the right and the sound transmitter on the left, while the projecting windows of the control room can be seen on the left, facing the transmitters.

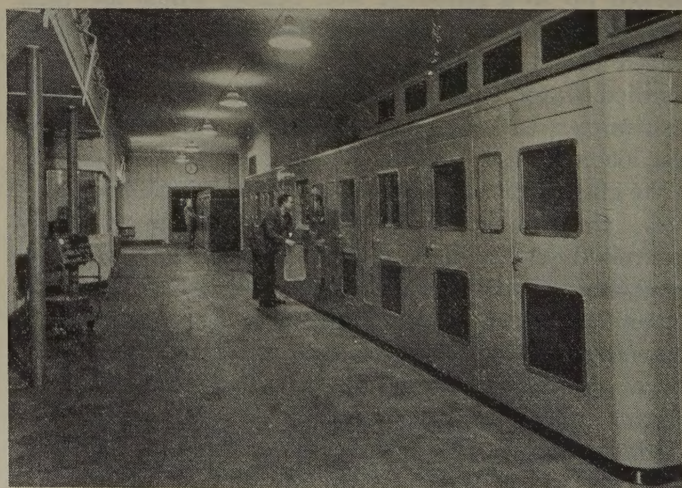

Fig. 7—Transmitter hall; vision transmitter in foreground and sound transmitter in background.

4.1 *The Vision Program Input Equipment*

The vision program input equipment consists of the Post Office vision cable terminal equipment for the program coming in over the television distribution network together with the BBC local distribution and

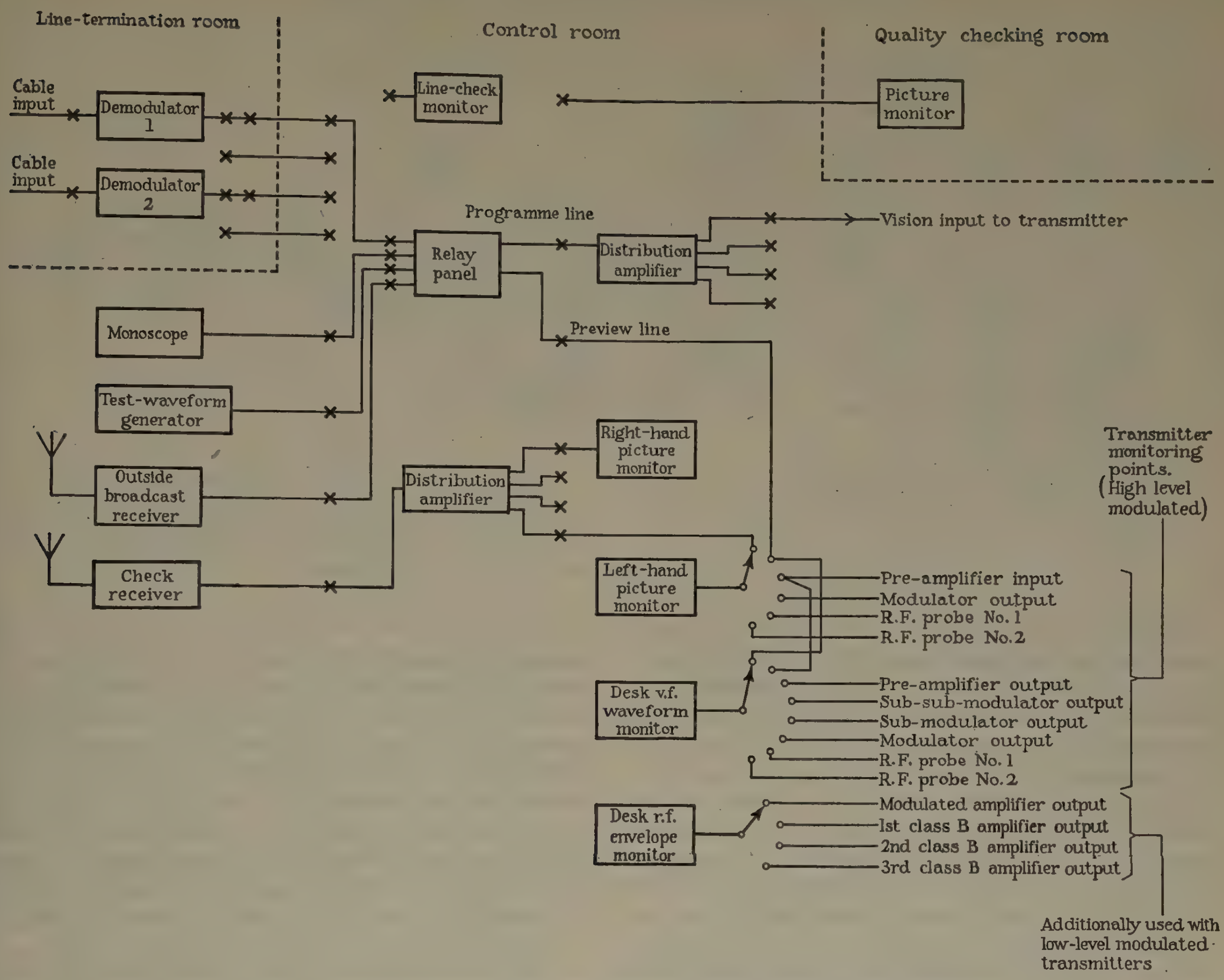

Fig. 8—Schematic of vision program input and transmitter monitoring equipment.

monitoring equipment. A test card and emergency "breakdown" caption is produced locally by monoscope units. A circuit is provided for locally injected outside broadcasts, while a test signal generator gives a source of signal for maintenance purposes. A line diagram of this equipment is given in Fig. 8.

The normal program arrives from the vision link terminal at Telephone House, Birmingham, over a 10-mile spur of 0.975-inch coaxial tube. Two circuits are available: one for transmission in the normal direction, and the other for transmitting signals in the reverse direction, for use when the station acts as a receiving point for injecting a local outside broadcast into the program distribution system. A vestigial sideband carrier system of cable transmission, which has a carrier frequency of 6.12 mc is used, the upper sideband being partially suppressed.

The two tubes are laid in a single cable which also contains a number of screened telephone pairs and unscreened quads for miscellaneous purposes, including remote control and supervision of the cable terminal equipment. This consists of the terminal repeater equipment and the demodulating equipment for deriving the video signal from the carrier signal arriving over the cable, both of which are in duplicate. It is unattended and controlled from Telephone House, Birmingham. The equipment gives at its output an ac video signal of the standard BBC Television Service waveform having an over-all amplitude of 1-volt double amplitude peak within limits of about ± 2 db. This is fed to a distribution jackfield on the vision and sound program input bays in the control room. The monoscope, outside broadcast, and test signals are also brought to this jackfield, all sources then terminating at a relay panel operated by a multiposition key on the transmitter control desk which selects the appropriate signal for transmission. Signal distribution is at 1-volt double amplitude peak, 75-ohm double screened coaxial lines being used, while line switching is by General Post Office-type low capacitance relays. The selected signal is passed to the transmitter via a level setting distribution amplifier and a 6-db control attenuator. The input signals are examined on a precision video-frequency waveform monitor, located on the transmitter control

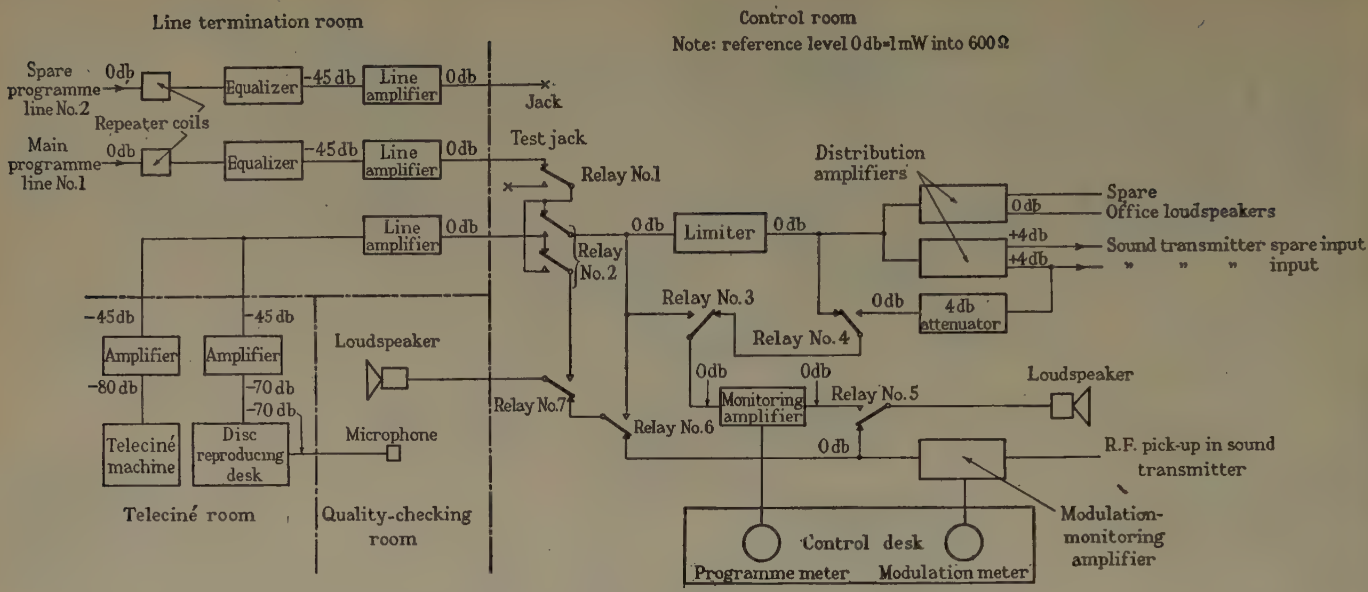

Fig. 9—Schematic of sound program input and monitoring equipment.

desk, and also on one of two picture monitors, before being selected for transmission. The control desk waveform monitor is, in fact, the master instrument for the routine setting up of program levels and for monitoring the operation of the transmitter itself. It is thus one of the most important devices of the installation.

Two picture monitors with 12-inch tubes are positioned side by side in front of the transmitter control desk. A selector switch on the transmitter control desk permits the left-hand monitor to be connected to preview any of the four sources of input signal or to observe the picture at the transmitter input, at selected points in the modulator, or as presented by either of two RF pick-up probes on the output transmission line prior to the vestigial sideband filter. The right-hand picture monitor normally observes the radiated picture as received by a high quality vestigial sideband radiocheck receiver, which is regarded as the final criterion. The video monitoring arrangements are completed by a general purpose picture monitor in the program input bay and a high-grade 15-inch tube monitor located in the quality checking room, which may be fed from any signal source.

The vestigial sideband receiver is designed with a high degree of accuracy because the results are otherwise open to question since it is difficult to determine whether any observed transients are generated in the transmission or by the monitoring system. Furthermore, the close proximity of the receiver to the transmitter necessitates a high degree of screening and a filtered power supply. The receiver is of the TRF type using three RF stages, diode detector, and video amplifier. The input signal is injected into a sound rejection filter, providing attenuation of the sound carrier of better than 46 db, and is then passed to an 80-db attenuator adjustable in 20-db steps. The signal is then applied to the first RF stage via a correction filter. The stage gain is continuously variable, and, with the input attenuator, provides an accurate level setting arrangement. The remaining RF stages are conventional and feed a diode operated at high level to maintain good linearity. The resultant video signal passes via a dc coupled cathode follower to the video amplifier, which is also dc coupled. The first two stages of this amplifier, in conjunction with an over-all feedback loop, are used mainly to obtain frequency and phase response correction. Finally, the signal passes to an output cathode-follower stage which gives an output video signal of the standard 1-volt overall amplitude.

The unit feeds a standard video distribution amplifier, one of whose outputs is connected to the monitor selector circuits to enable the picture to be observed on the appropriate transmission picture monitor. The receiving antenna is a proprietary type, having a front-to-back ratio of some 22 db, and is critically positioned on the site to avoid reflections.

4.2 *Sound Program Input Equipment*

The program input chain to the sound transmitter is shown in Fig. 9. The program input line and a spare line, which are routed through Broadcasting House, Birmingham, terminate in the line termination room at Sutton Coldfield. The input chain to the transmitter includes a line amplifier in the line termination room and a limiter and distribution amplifier in the control room. Local standby sound program is given by the disk reproducing desk, and an announcement microphone is provided in the acoustically treated quality checking room, the appropriate source of program for transmission being selected by relays controlled by keys on the transmitter control desk.

The program monitoring arrangements are conventional. A loudspeaker is installed in the control room and a peak program meter and modulation meter are

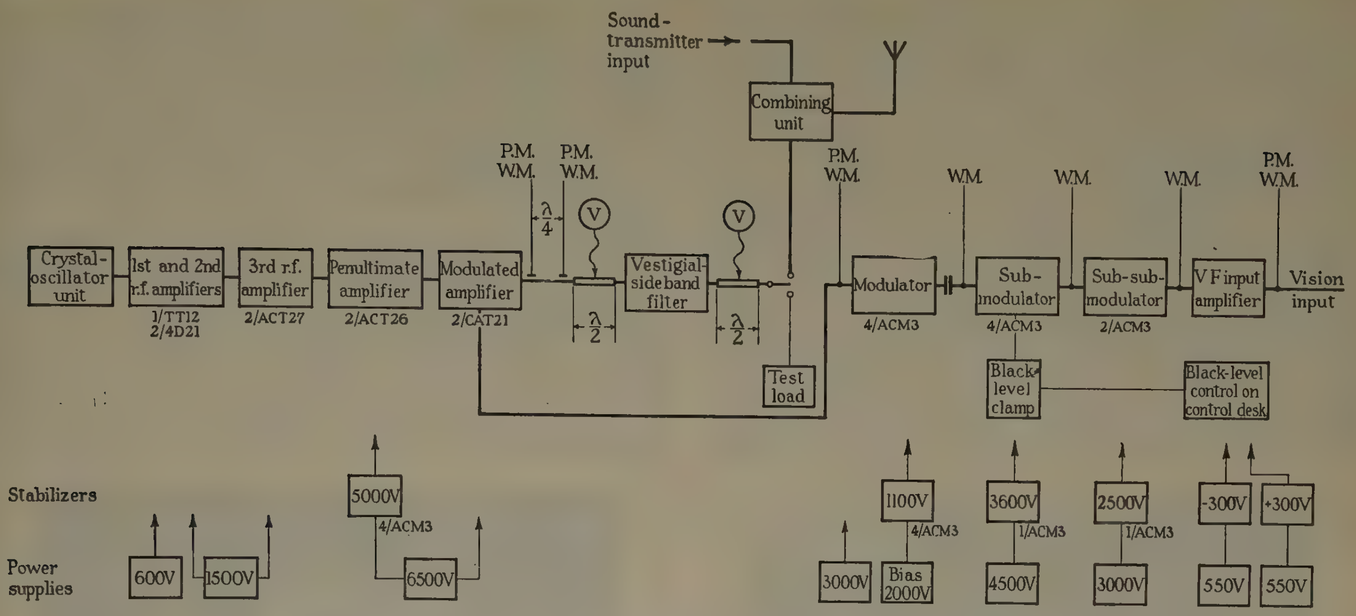

Fig. 10—Block schematic of 50 kw high level modulated vision transmitter.

mounted on the transmitter control desk. The monitoring amplifier operating the program meter may be switched to the output of either the line amplifier, the limiter, or to the input of the sound transmitter. The loudspeaker may be switched either to the monitoring amplifier, which links it to whatever point is selected for the program meter, or to a modulation monitoring amplifier fed from an RF probe in the sound transmitter output transmission line. A loudspeaker is installed in the quality checking room and may be appropriately switched for comparison listening tests.

4.3 *The Vision Transmitter*

The vision transmitter,[6] a block schematic of which is given in Fig. 10, is of the high-level modulated type, modulation being applied to the grids of the final RF output amplifier. The transmitter unit is contained in ten similar sheet-steel cubicles arranged in line. Viewed from the front, the modulation amplifier stages are arranged in increasing power level from left to right and the radio-frequency stages from right to left, so that the modulator output stage is next to the final RF power amplifier. Three of the cubicles at the right hand of the transmitter form a self-contained power-distribution cubicle on the panels of which are mounted the transmitter power supply isolating switch, subcircuit isolators, high-rupturing capacity fuses, and power intake metering. Within the cubicle is the majority of the contactor control gear for the hot cathode mercury vapor rectifier units and the filament-heating equipment. The over-all dimensions of the transmitter are 38 feet long by 9 feet wide by 7 feet high.

The video-frequency modulation amplifier has four stages. The first is a preamplifier which accepts a vision signal having an over-all amplitude of approximately 1 volt and a 70:30 picture-to-sync ratio. This ratio is adjusted in the preamplifier by stretching the synchronizing pulse amplitude to compensate for bottom bending in the RF output amplifier and to maintain the correct 70:30 ratio in the transmitted waveform. An appreciable amount of amplitude correction is also applied to the picture component (white stretching) to compensate for the nonlinearity in the modulation characteristics of the subsequent VF stages and the modulated RF output amplifier. Duplicate preamplifiers are used, the change-over from one to the other in event of a fault being made from the control desk. The preamplifier delivers an output containing the dc component to the sub-submodulator stage, which is a linear amplifier of the balanced amplifier cathode-follower type. This is ac coupled to the submodulator stage, which is similar but uses two tubes in parallel for both its amplifiers and cathode follower. Between these two stages is the black-clamp of the pulse-converter type which applies a 4-microsecond pulse to the grids of the submodulator tubes during the post-line synchronizing signal suppression period for appropriately stabilizing the black-level output of the modulation amplifier.

The submodulator, which uses four tubes in parallel, gives an output of some 1,400-volts double amplitude peak, and drives the modulator output stage, consisting of four tubes in parallel, connected as a cathode follower. This stage has a gain slightly less than unity, but provides an output of sufficiently low impedance (about 10 ohms) to supply, without appreciable regulation, the grid current of about 3.5 amperes, taken by the final modulated RF amplifier, plus the large capacitance current due to the 300-pf effective input capacitance of this amplifier. With the exception of the preamplifiers which use receiver type tubes, a single type of forced-air-cooled tube, the ACM3, is used throughout the modulation amplifier. This tube has a

rated anode dissipation of 2 kw and a mutual conductance of about 27. Fig. 11 shows the front view of the submodulator and modulator output stages.

The radio-frequency section of the transmitter has five amplifying stages preceded by a self-contained drive unit consisting of a precision crystal oscillator with a frequency stability of ± 10 parts in 10^6, and two stages of frequency multiplication. The output from this unit is amplified successively by a single-tube pentode stage, a push-pull tetrode stage, and a push-pull earthed-grid triode stage, having an output of 2.5 kw, housed in one cubicle. The adjacent cubicle contains the final modulated output stage and its driving stage, the latter consisting of two ACT26 air cooled voltage of 6.5 kv. This stage is grid-modulated, and its anode line is coupled to the 51-ohm coaxial output transmission line through a triple tuned band pass balance-to-unbalance coupling circuit,[6] as shown in Fig. 12. This circuit is flat to within 0.5 db over a total bandwidth of 6.0 mc arranged symmetrically about the carrier.

The high-voltage dc power supplies for the transmitter are obtained from hot cathode mercury-vapor rectifiers housed in cubicles similar to those of the transmitter. These contain oil-filled apparatus, and are placed in a separate room behind the transmitter hall wall to reduce fire risk. The output voltages of the rectifiers supplying the preamplifier, sub-submodulator,

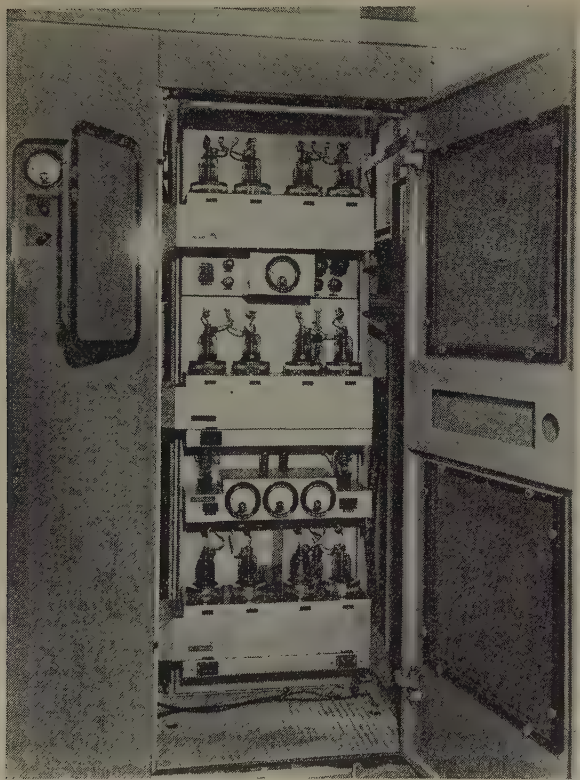

Fig. 11—Modulation amplifier cubicle. From top to bottom the units are, respectively, output bias stabilizer, modulator, modulator bias, submodulator.

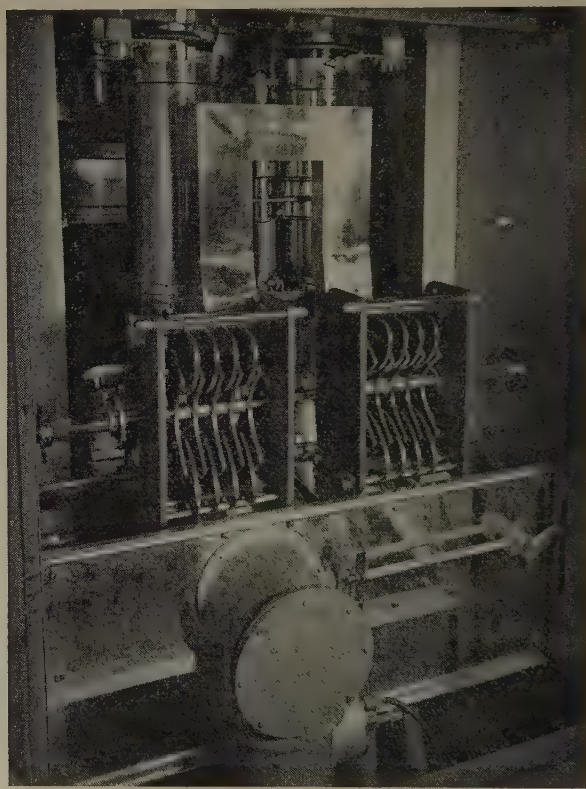

Fig. 12—50-kw earthed-grid parallel line grid modulated power amplifier of vision transmitter. Rear view shows anode line and output coupling circuit.

triode tubes in a grid-driven push-pull, Class C, cross neutralized amplifier. The load on this stage varies with modulation from about 0.3 kw during synchronizing pulses to about 10 kw at peak white, and precautions are taken to give it a good regulation characteristic to preserve a constant driving voltage for the output stage.[6] The output stage is a push-pull, earthed-grid, linear, wide band parallel line, power amplifier, which gives a peak white output of approximately 45 kw., using two CAT 21 water cooled triodes, or 50 kw with a pair of the new, equivalent BW 165 thoriated tungsten filament triodes, operating with an anode supply

[6] E. A. Nind and E. McP. Leyton, "The vision transmitter for the Sutton Coldfield television station," *Proc. IEE*, vol. 98, part 3, p. 442; 1951.

submodulator, and the RF driver stage are electronically stabilized with shunt type stabilizers. The higher power rectifiers supplying the modulator and modulated RF amplifier are not stabilized, but have smoothing circuits designed as substantially constant-resistance networks to ensure a satisfactory response to the variable load imposed on these supplies over the picture-signal range.

To obtain constant operating conditions in the transmitter and to prevent the inevitable variations in the voltage of the station power supply from affecting the radiated vision signal, the three phases of the input ac power supply to the transmitter are stabilized and phase-balanced by moving coil regulators. The reduction of any unbalance occurring between the three phase voltages of this supply minimizes the 100- and

50-cps components appearing in the output of the various high-voltage supply rectifiers, and from the point of view of the smoothing circuit design, an easement in the degree of attenuation of these low-frequency hum-producing components is very desirable.[6] It may be shown that unless the unbalance components are less than 2/9 of the normal ripple voltage at the input to the smoothing circuit, the design of the circuit is dictated by the unbalance components. To obtain this optimum ratio, it is necessary that the phase unbalance of the supply mains should not be greater than about 2.5 per cent for a six-phase rectifier of the type used. The moving-coil regulators installed are connected in star across the incoming supply and provide a total throughout of 240 kva at a constant phase to neutral voltage of 240 volts for supply voltage between 6 per cent and -10 per cent of this value. They are operated by induction disk motors controlled by an electronic regulator control unit. The filaments of all tubes in the transmitters are ac heated, with the exception of the tubes in the RF output amplifier, which are supplied by dc from a motor generator. An electronic regulator holds the output voltage of this generator constant with 0.1 per cent of its nominal value, and also automatically limits the filament starting current to 110 per cent of normal at the instant of switching on.

The chain of video-frequency stages forming the modulation amplifier is equipped with a comprehensive system of signal monitoring. Resistance capacitance potential dividers tap down the signal voltage at strategic points in the chain, and cathode-follower units feed an ac signal of standard 1.0-volt over-all amplitude to 75 coaxial lines which terminate within the control room. The system is such that the signal waveform at any selected point can be observed on either the control desk waveform monitor or the portable test equipment waveform monitor, as required.

In addition, two radio-frequency monitoring points, situated one-quarter wavelength apart on the output transmission line to the antenna immediately before the vestigial sideband filter, are included to provide an indication of the correctness of the antenna match.

On the center cubicle of the transmitter itself is a waveform monitor giving a continuous display of the unrectified modulation envelope of the radio-frequency output to the antenna transmission line.

4.4 *The Vestigial Sideband Filter*

This filter is introduced between the output of the transmitter and the input to the antenna transmission line to provide the asymmetric characteristic decided upon for the radiated vision signal. It was initially thought that a filter of this type would prove necessary to prevent interference with the 63.25-mc sound transmission of the future channel 5 (see Fig. 1) and possibly with the lower vision sideband of channel 5 for frequencies below about 64.5 mc. On this basis, the attenuation of the filter should be a maximum at 63.25 mc and furthermore, it appeared necessary that it should continue to introduce some attenuation above this frequency so that the interference with a vision transmission on channel 5 would not be visible.

In deciding upon the amount and form of attenuation characteristic required for the upper vision sideband, the condition of equal strength for the wanted and interfering signals at the receiving point was postulated, as this represents the limiting case in practice. At that time, however, there was no precise information available regarding the ratio of wanted to interfering signal which must be realized under conditions of television transmission in this country. The American specification implied at least 40-db attenuation of the vision sideband at the frequency of the sound carrier of the adjacent channel, but this was considered unnecessarily stringent as applied to the conditions which would obtain in the United Kingdom. The American specification also assumed that this degree of attenuation would be maintained over the frequency band in which the vision sidebands of adjacent channels would overlap. This also appeared unnecessary for the reason that only one program is available and therefore the viewer never wishes to receive the weaker of the two channels. Laboratory measurements were therefore carried out to obtain more precise information on the problem of adjacent-channel interference. The result was most enlightening and showed, for example, that for equal received field strengths from the wanted and unwanted transmitting station, the wanted AM sound carrier could be received with very little interference although operating with only 1.5-mc frequency separation from the unwanted AM double-sideband vision carrier. A reduction of the unwanted vision signal by 10 db, either by the use of a vestigial sideband filter or by such means as a reflector associated with the receiving antenna, sufficed to remove the interference. The only exception to this statement was the occurrence of considerably increased interference when the picture forming the unwanted vision signal was composed entirely of vertical stripes arranged at a spacing to give the maximum amplitude of vision sideband at 1.5-mc video frequency.

In this case, some 30-db discrimination is required for no detectable interference. This condition is not to be expected in practice, and it was realized that if a small degree of interference were permitted, a television service according to the scheme shown in Fig. 1 could be planned on the basis of omitting the vestigial sideband filter altogether at the transmitting end, provided the receivers themselves have the appropriate receiver-attenuation type of vestigial sideband response characteristic. This somewhat surprising result can be explained in terms of the very low energy content occurring in any small region of the vision sidebands.

This result notwithstanding, it was decided that Sutton Coldfield, in common with other future television transmitting stations, should have the upper vision sideband substantially attenuated for all video

frequencies above 0.75 mc (see Fig. 2). One reason for this decision was to discourage the use of double-sideband receivers in the Sutton Coldfield service area prior to the time at which channel 5 came into operation. Such receivers would experience considerable interference on their pictures from the sound carrier of the future channel 5, which is spaced only 1.5 mc from Sutton Coldfield's vision carrier frequency. At least 50 db of attenuation at the frequency of the sound carrier of the channel next above is required, and this attenuation must be provided in the response characteristic of a properly designed vestigial sideband receiver of the receiver-attenuation type for the British System (see Fig. 2).

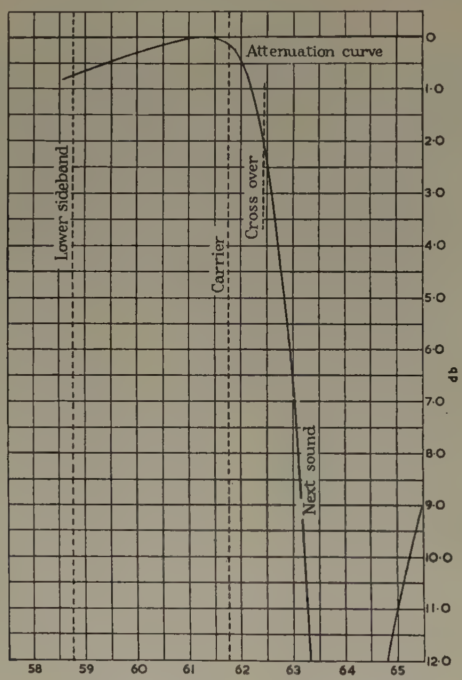

Fig. 13—Vestigial sideband filter; attenuation characteristic.

Taking all factors into account, the following specification for the attenuation characteristic of the filter for Sutton Coldfield and the future stations was decided upon: not greater than 0.5 db at carrier frequency; not greater than 3 db at 0.75 mc above carrier frequency; not less than 10 db for the range 1.5 to 3 mc above carrier frequency; not greater than 1 db from 3 mc below carrier frequency to carrier frequency.

It was considered that this specification and the other necessary characteristics could substantially be met with a constant-resistance filter of the transmission-line type consisting of two complementary networks, one high-pass and the other low-pass, the high-pass section being terminated by a constant-resistance absorber load and the low-pass section terminated by the antenna transmission line. The measured characteristics of the actual filter installed[7] are given in the curves of Figs. 13, 14, and 15. These give the insertion loss, phase shift, and input-impedance characteristic over a frequency range of 59 to 64.5 mc. Over the required transmission pass band range of 59 to 62.5 mc, the different group time delay corresponding to the phase shift is approximately 0.07 μs.

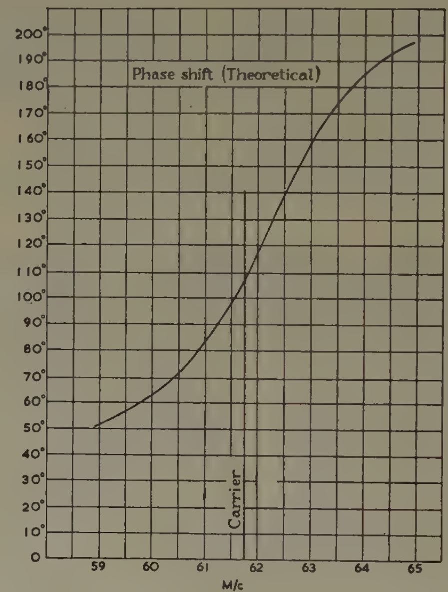

Fig. 14—Vestigial sideband filter, phase shift.

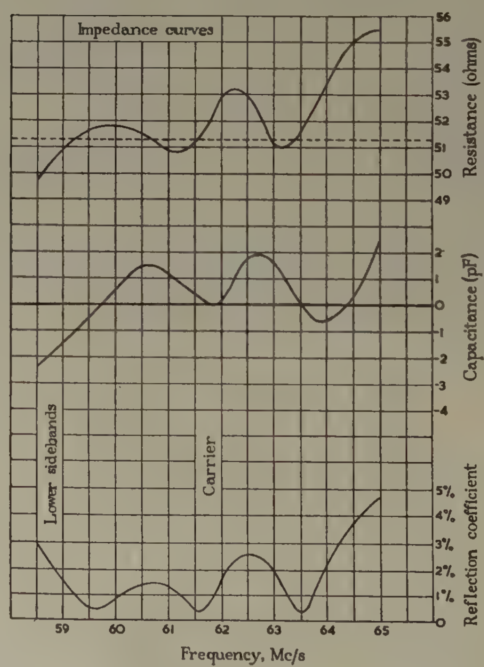

Fig. 15—Vestigial sideband filter; input impedance.

Physically, the filter is constructed from lengths of coaxial copper-tube transmission line with a 5-inch outer diameter, but with the diameter of the inner conductor varied to obtain the required characteristic impedance for the various stubs. Fig. 16 shows the filter

[7] E. C. Cork, "The vestigial sideband filter for the Sutton Coldfield television station," *Proc. IEE*, vol. 98, part 3, p. 460; 1951.

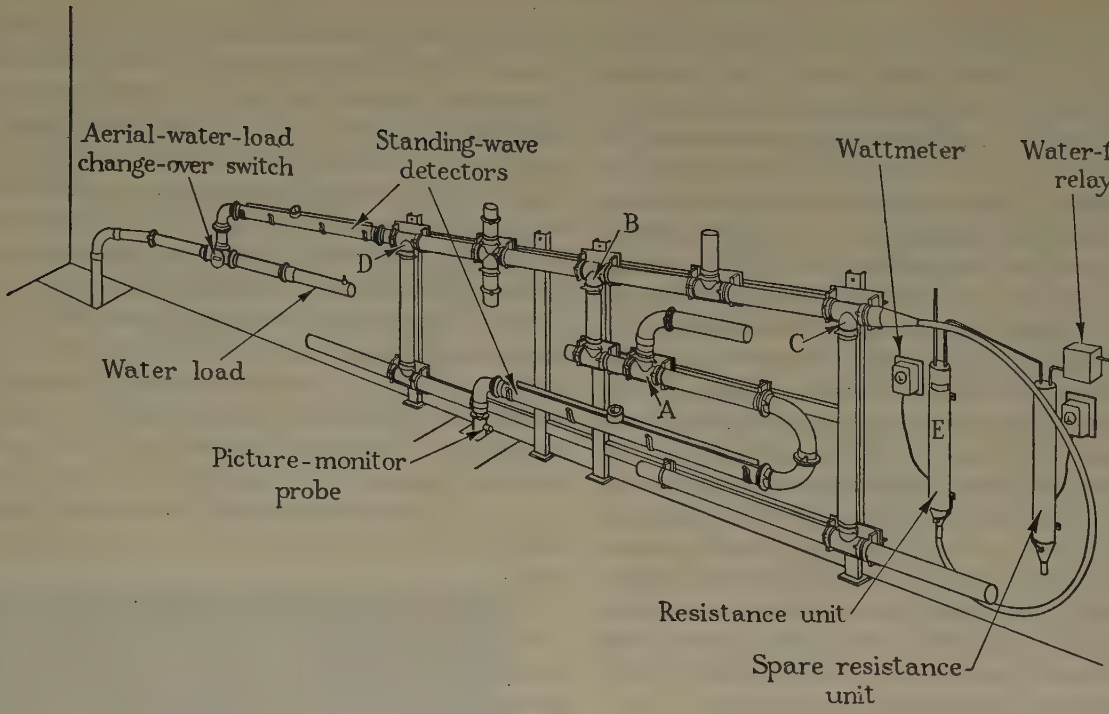

Fig. 16—Vestigial sideband filter; general arrangement.

as mounted on the wall behind the transmitter. The input of the filter at point A is connected to the vision transmitter through a standing-wave detector, and the section between points A and B is the impedance-correcting circuit. The branch BC is the high-pass section terminated in the absorber load C, while BD is the low-pass section, the output of which is taken over a second standing-wave detector to a change-over switch which enables the shaped output to be passed either to the antenna transmission line or a constant resistance water-cooled test load, which can dissipate continuously the full output of the transmitter.

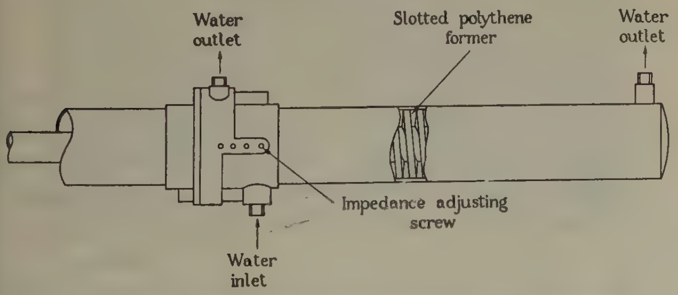

Fig. 17—Test load for vision transmitter.

The test load, which has a compact and novel construction, is shown in Fig. 17. The dissipative portion consists of a copper tape inner conductor wound in a deep spiral slot cut in a polythene former 5 inches in diameter and 30 inches long, fitting closely in the outer tubular conductor. Raw water is fed from the test-load water cooler to an inlet tube close to the RF input end of the load and emerges at two outlets, one at each end of the load. A total water flow of approximately 18 gallons per minute is used for the full continuous dissipation of 50 kw. The specific resistivity of the cooling water in which the power is dissipated is required to be maintained at about 2,000 ohms per cubic cm at 18°C, and as the input impedance of the test load varies with water temperature the water supply unit controls the inlet water temperature to within about ±2°C to 50°C, which is a convenient operating value. In these circumstances the load has a constant resistance of 51 ohms over the full transmitted vision frequency band, the reflection coefficient being not more than 2 per cent.

The absorber load for the upper sideband (designated E in Fig. 16), which terminates the high-pass section of the filter, has a constant input resistance of 51 ohms with a reflection coefficient of about 1 per cent and is rated at 5 kw. It incorporates a coaxial resistor immersed in a liquid coolant of low permittivity from which heat is transferred to a water supply of about 1 gallon per minute. The absorber load is fitted with a voltmeter crystal cartridge and a meter calibrated to give a direct reading of the RF power in the load. The RF power dissipated in this unit, corresponding to a peak white power of 47 kw to the test load or antenna transmission line, is only 3.7 kw on unmodulated carrier and 1.6 kw when transmitting the standard BBC type C television test chart.

Before deciding to shape the radiated signal by means of a separate V.S.B. filter, other methods of obtaining the required attenuation characteristic for the upper sideband were considered. The development of the transmitter was already well advanced, however, and its RF output stage was designed to give a double-sideband output, flat to within about 0.5 db for modulation frequencies up to 3.0 mc, that is, a total bandwidth of the RF circuits of 6.0 mc. The decision to use a

vestigial sideband characteristic meant that the RF output circuits need be flat only from 3.0 mc below to 0.75 mc above the carrier so that an over-all bandwidth of only 3.75 mc, with a fairly rapid attenuation on the upper frequency side, was required.

It therefore appeared possible to obtain the requisite characteristic by offsetting the carrier frequency to one side of the bandpass center frequency of the output circuit, at the same time narrowing the bandwidth to about 4 mc. This also had the theoretical advantage of permitting a significant increase in the power output of the transmitter, provided the anode supply voltage could be increased from 6.5 kv to 8.5 kv. The course was not pursued for the Sutton Coldfield transmitter because it necessarily involved changes in the construction of the circuits and in the rating of major power components. Time, in fact, did not permit, and a separate filter allowed work on the transmitter to proceed unhindered. The offset carrier and narrowed bandwidth technique has, however, been introduced in the subsequent transmitters constructed for the Holme Moss, Kirk O'Shotts, and Wenvoe Stations.[1]

4.5 *The Test Signal Generating Equipment*

For checking and maintaining the performance characteristics of the vision transmitter, a video frequency test signal generating equipment has been developed to provide signals of a type useful for measuring those qualities required in the transmission channel to ensure good picture reproduction.

The following wave forms, which are complete with standard synchronizing and suppression signals, are found the most generally useful:

(a) "Bar" signal, corresponding to a black rectangular cross on a white background.
(b) Line-frequency sawtooth of variable amplitude.
(c) Lift signal of variable amplitude.
(d) Black signal } representing the extremes of picture
(e) White signal } amplitude.
(f) "Flagpole" signal, consisting of 2-microsecond pulses at line frequency delayed half a line.

One recent equipment also produces a "patch" signal corresponding to a central black square on a white background, a "grille" consisting of 24 narrow horizontal and vertical black lines on a white background, and facilities for injecting and mixing with the lift signal an external sine wave of variable amplitude and frequency.

The bar signal contains information at both line and frame frequencies, and so gives a rapid over-all check of several aspects of the transmitter performance, particularly those relating to dc restoration and low frequency response. This signal is also a useful standard modulating signal for transmitter radiation tests. The sawtooth signal is necessary for setting up the picture-bending circuits in the modulator, for adjusting the picture-signal-to-synchronizing-signal ratio, and for checking the overload level and amplitude-linearity characteristic. The black and white signals are used to observe the stability of black level by switching rapidly from white to black, whilst the white signal is also used for checking the peak-white output power of the transmitter. The lift signal permits the transmitter to be set at any arbitrary dc modulation level, and an ac signal may then be superimposed and the sine wave response of the complete transmitter thereby obtained. The short-duration flagpole signal gives information on the high-frequency response, including time of rise, and is useful for checking the performance of the antenna, transmission line, and filter circuits for reflections and delayed-image radiation. The utility of the patch signal lies in its great ability to indicate low frequency defects, whilst the grille is useful for checking the scanning linearity and over-all focus of monitor cathode-ray tubes.

As an adjunct to the test-waveform equipment, a portable waveform monitor with a wide range of facilities is used. It measures both amplitude and time, six voltage ranges between 1.5 and 500 volts and ten time-base ranges between 50 milliseconds and 1.5 microseconds being provided. Both direct and alternating voltages within the range 0 to 3 mc may be measured with high accuracy on a moving-coil meter. Illuminated cursors are provided for the X- and Y-axes, and both X- and Y-amplifiers have adjustable gain; hence, a portion of the trace may be located under the intersection of the cursors and then expanded for closer examination. The limit of accuracy to which relative times may be measured is set by the rise time of the signal amplifier, namely 0.07 microsecond. Two signals may be displayed simultaneously, which is of value in the accurate estimation of relative timing. This type of monitor is regarded by the operational staff as a considerable asset to the station testing equipment.

4.6 *The Sound Transmitter*

The vhf Sound Transmitter is exclusively air cooled, uses highpower Class B modulation, and is amplitude modulated on the anodes of both the penultimate and final RF stages. The AF and RF amplifiers are contained in cubicles, and occupy a floor area approximately 15 feet by 9 feet, the height being 7 feet.

The modulation amplifier has six stages terminating in pair of ACT.14 air-cooled triodes driven by four DET.21 tubes in a push-pull cathode-follower circuit. Approximately 14 db of audio negative feedback is applied over the last four stages from the primary side of the modulation transformer, and rectified RF feedback is used to reduce over-all noise and hum level. An audio input of 4 db above 1 mw into 600 ohms gives 40 per cent modulation of the output carrier.

The radio-frequency section consists of a crystal-drive oscillator unit followed by four stages of RF amplification. Two TT.12 tubes in push-pull drive a similar stage using four TT.16 tetrodes inductively

coupled into the penultimate, or driver stage, consisting of two BR.125 air cooled triodes in a conventional neutralized parallel line amplifier. This is inductively coupled to the output stage which consists of a single BR.128 forced-air cooled triode in an earthed-grid coaxial-line circuit giving an output of 12-kw carrier 100 per cent modulated. The anode line of the output stage is inductively coupled to a 51.5-ohm coaxial copper-tube output transmission line via an harmonic filter and an antenna/test load change-over switch mounted in the extreme right-hand cubicle. Fig. 18 shows the form of construction of the driver and output stage of the transmitter. The circuit and constructional technique of earthed-grid coaxial-line power amplifiers of the type used in the output stage has been described elsewhere by the author,[8] but a brief description here is considered useful.

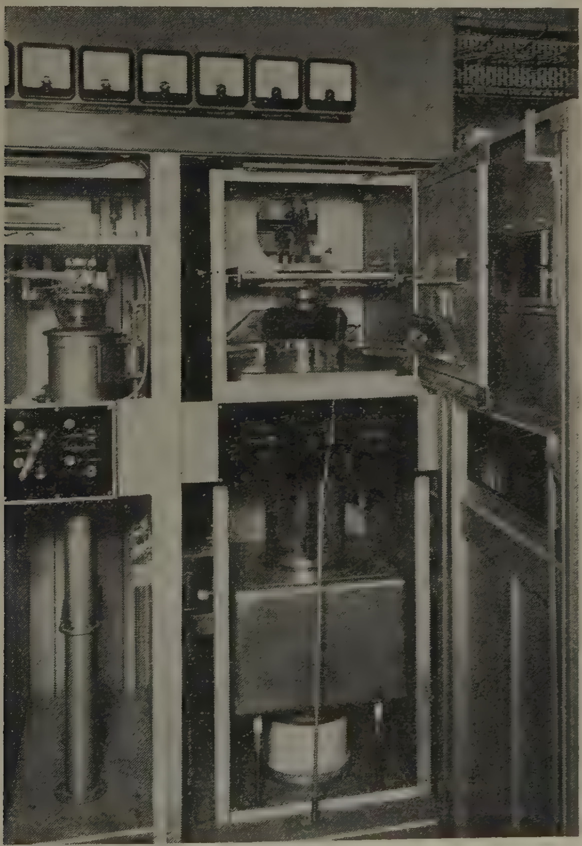

Fig. 18—12-kw coaxial earthed-grid anode modulated power amplifier of sound transmitter. Front view also shows the neutralized parallel line driver stage.

The anode-grid line is a shortcircuited, quarter-wave coaxial line the outer part of which is formed by the square-section frame of the unit and the inner by a central tubular conductor supported at its base by a ceramic ring insulator. The BR.128 triode tube is mounted in the top of the central tube, the anode-cooling radiator becoming part of this conductor. The earth plane is a hinged plate which makes contact with the square outer conductor and can be raised to remove the tube. The filament pins project through a central hole in the earth plane while the grid ring is connected to the earth plane via a grid-blocking and neutralizing capacitor mounted on the under side of the plane, the connection to the grid ring being made by a large number of spring contact fingers. The short-circuiting plunger for tuning the anode line is a movable box carried on vertical lead screws and having spring contacts engaging the inner conductor and a clearance air gap between the box and the outer conductor. A single turn loop tuned by a coaxial capacitor and located near the tube anode couples the anode line to the output 51-ohm coaxial transmission line.

An inconveniently short length of external grid-cathode line is required to tune to quarter-wave resonance with the grid-cathode tube capacitance, so the line is extended to form a capacitance-loaded three-quarter wave coaxial line. The extra length is formed by the two filament busbars which run aft, turn down at the rear of the grid-anode line, and are enclosed by a square section outer conductor. The line is short-circuited for radio-frequencies at its lower end and tuned by an air-dielectric capacitor, placed about a quarter wave from the shortcircuited end. The driving power is coupled to the cathode line by an adjustable tapping bar, fed from a balance-to-unbalance transforming circuit, and positioned near the shorted end of the line.

Basically similar earthed-grid coaxial line power amplifiers, but designed for a frequency range of 88 to 108 mc, are used in the 25-kw FM and 18-kw AM transmitters[8] at the BBC's experimental vhf sound broadcasting station at Wrotham, Kent. These transmitters used two such amplifiers, operated in parallel and driven by a third similar amplifier.

In the Sutton Coldfield transmitter, the filament of the BR.128 tube is dc heated from an electronically controlled motor-generator. All other tube filaments are ac heated, the voltages being stabilized, and the initial starting current appropriately limited.

The high voltage dc power supplies are obtained from two hot-cathode mercury vapor rectifiers located with the main modulation components in a separate enclosure part of which is a power-distribution cubicle housing the associated contactor control gear, protective relays, main isolating switch, subcircuit isolators and fuses, and power-supply meters. The transmitter is very compact and all interconnections and auxiliary circuit wiring is prefabricated on supporting cable trays.

The test load is of the conventional dissipative coaxial line type, the cooling water being the dielectric and as the source of loss. A quarter-wave line transformer raises the impedance of the load to match that of the antenna transmission line at its point of connection to the antenna load change-over switch. The cooling water flow is approximately 5 gallons per minute and is obtained from the same test-load cooler unit as the vision transmitter test load.

[8] P. A. T. Bevan, "Earthed-grid power amplifiers for vhf vision and sound transmitters," *Wireless Eng.*, vol. 26, pp. 182, 235; 1949.

4.7 *Transmitter Control*

Both transmitters are remotely controlled from a single control desk situated in the control room and placed so that the transmitters can be viewed through the windows. The desk, is U-shaped, the central section controlling the modulation amplifier and the right- and left-hand wings the RF amplifier of the vision transmitter and the complete sound transmitter, respectively. The controls for the sound transmitters are conventional, each supply being sequence-inlocked and switched on and off from the desk. The vision transmitter control is such that by the operation of two pairs of push-buttons, one pair for the modulation amplifier and the other pair for the RF amplifier, the various supplies are applied and their voltages raised to the operating value automatically and in the correct sequence with predetermined pauses between each step in the sequence. The video frequency and RF sections may be powered independently, the electromechanical interlocks on the transmitter cubicles permitting maintenance work in one section with the other section powered.

The control desk also incorporates the signal waveform monitor previously mentioned for checking the characteristics of the video-frequency signals through the modulation amplifier and at the RF output of the transmitter, together with the audio and video program switching and monitoring keys.

Because of the complex nature of the electrical and mechanical interlocking necessary for the sequence control and protection of the transmitters, interlock indicator panels are located on the wall in front of the control desk to enable the state of their control and interlock chain to be quickly assessed. The indicator units present a mimic diagram of the main interlock circuit, the position of door interlocks, air, water, filament and overload relays being indicated by miniature lamps inserted at appropriate points in the run of the diagram strip.

4.8 *Transmitter Cooling Equipment*

4.8.1. *Air Supply Installation.*—The sound transmitter is exclusively air cooled while the vision transmitter uses both air and distilled water cooling, the water cooling being confined to the tubes of final RF output amplifier. The air blowing installation consists of three separate blowers, one supplying air to the sound transmitter, one supplying air to the vision transmitter, and the third associated with a cooling radiator to form an air blast cooler unit for the distilled water cooling system. The blowers are located in a cooler room placed centrally between and behind the two transmitter units. The blower intakes are built up to openings at the base of one wall of a vertical air intake chimney, constructed as an integral part of the building, which is partitioned into three separate intake shafts to facilitate independent control of the air supply to each blower. The air intakes to each blower are fitted with removable filters and the thermostatically controlled electric heaters are placed in the intake shafts to avoid taking in air at an abnormally low temperature and to minimize the ingress of mist or low cloud.

The air blowers deliver to main intake ducts which are run horizontally along the wall behind the transmitters. Spur ducts are taken off below and at right angles to the main ducts and are brought through the wall into the rear of the transmitter cubicles. The exhausts from the cubicles are similarly arranged and feed into main exhaust ducts which run alongside the main intake ducts, and finally through the cooler room roof into external discharge ducts. Thermostatically controlled motor-driven louvres in the discharge ducts permit the exhaust air to be discharged to atmosphere or, alternatively, to re-enter the intake shafts for recirculation so that the cooling air temperature may be set at the most desirable value.

The water cooling blower has a multitube cooling radiator in its intake and the exhaust air is passed straight through the roof of the cooler room to its discharge duct, which is also fitted with automatic louvres to permit an appropriate proportion of the warm exhaust air to be transferred to an interior ventilation duct for spacing heating.

All blowers are of the centrifugal fan-type V belt, driven by induction motors, and running at about 1,000 rpm. The sound transmitter blower delivers approximately 4,000 cubic feet per minute of air at 5-inch water gauge, the vision transmitter blower 8,000 cubic feet per minute at 5-inch water gauge, while the water cooler blower delivers some 6,000 cubic feet per minute at relatively low pressure. With this quantity of air at maximum inlet maximum inlet temperature of 30°C, the water cooler is rated to dissipate 60 kw continuously with a water flow of 18 gallons per minute and a water inlet temperature not exceeding 60°C.

The remainder of the cooling equipment consists of the vision transmitter tube cooling distilled water supply unit and the transmitter test loads cooling the water supply units, which are described in the following section.

4.8.2. *The Vision Transmitter Tube Cooling Water Supply Unit.*—The tube cooling distilled water system is fairly conventional. Its various components, except for the separate cooling radiator previously described, are mounted together on a frame to form a self-contained unit. All parts are of nonferrous construction and the system operates on a closed circuit to exclude air. The amount of water in the system is approximately 75 gallons and expansion is taken up by a 15-gallon expansion tank in which the space above the water level is pressurized with nitrogen at some 5 pounds per square inch above atmosphere. The normal water flow for the pair of CAT21 or BW165 tubes is approximately 18 gallons per minute and the flow is metered by Electroflo units having interlock contacts introduced into the

transmitter main interlock circuit to ensure that the transmitter cannot be powered until the water flow is correct.

4.8.3. *Test Load Cooling Water Supply Unit.*—The test loads are required to present to the transmitters substantially the same impedance as the antenna, within very close limits, and for a water of given specific resistivity, they will do so provided the temperature of the water flowing through the load is maintained constant within limits of about ±3°C. The water supply system is accordingly designed to raise quickly the temperature of the water supplied to the loads to a predetermined value and thereafter maintain it at this value during the period of test. The normal period of test is unlikely to exceed an hour or more, and the heat capacity of the system is proportioned accordingly. The system used is shown diagrammatically in Fig. 19.

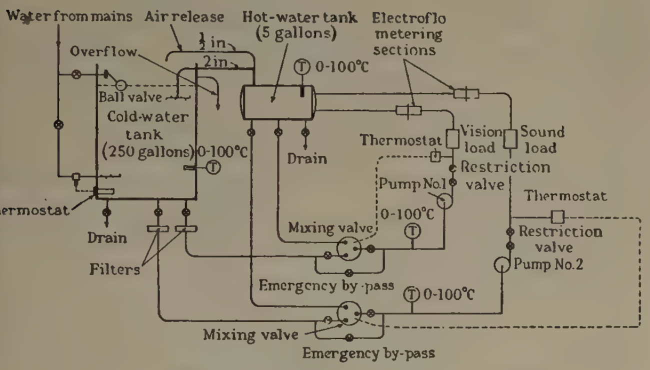

Fig. 19—Schematic of test-load cooling water supply unit.

On initially starting up, water is circulated from a small (5-gallon) tank via a mixing valve through the test load. The relatively small quantity of water is quickly raised to the predetermined operating temperature of approximately 50°C at the inlet to a load (measured thermostatically for convenience at the pump inlet). When this temperature is reached, the thermostat opens up the cold water inlet of the mixing valve to introduce cold water from a 250-gallon storage tank into the hot water in the circulating system, thereby maintaining the circulating water temperature at the correct value. To cover prolonged periods of testing when the water in the storage tank would also eventually rise above the operating limit, a thermostat is provided in the base of the storage tank which opens a valve to admit cold water from the mains into the tank. By this means, the water temperature in the tank is not allowed to rise above 45°C. The hot water displaced then overflows to waste.

The water flow for the test loads is 5 gallons per minute for the sound transmitter and 18 gallons per minute for the vision transmitter at their full rated power, and with normal commercial thermostatically controlled valves the system maintains the temperature of the water supplied to the loads within ±1°C, which is better than the limit required.

4.9 *Measured Performance Characteristics*

The Sound Transmitter

Output power	12.3-kw unmodulated carrier. 18-kw 100 per cent tone modulated carrier.
Over-all frequency response	Level within ±0.5 db from 30 to 10,000 cps.
Audio frequency harmonic distortion	Less than 2 per cent for any fundamental frequency between 30 and 10,000 cps at any modulation level between 0 and 95 per cent.
Carrier noise level	64 db unweighted, and better than 70 db weighted, below 100 per cent modulation.
RF harmonics	Less than 200-mw radiated power.
Input power consumption	50 kw on unmodulated carrier. 75 kw at 100 per cent modulation.
Operating frequency range	Adjustable from 40 to 67 mc.

The Vision Transmitter

Maximum peak white power output (using BW165 tubes)	47 kw delivered to the antenna transmission line, when not modulated but adjusted to give the maximum carrier amplitude corresponding to a full white picture; 3.5 kw delivered to vestigial sideband filter absorber load.
Over-all frequency response (sine wave)	Measured at transmission line output of modulated RF amplifier.

f(mc)	0.025	0.4	1.0	1.5	2.0	2.5	3.0	3.5
db	0	−0.1	−0.2	+0.3	+0.6	−0.4	−0.9	−2.0

Modulation linearity	The departure from a linear amplitude relationship between an input video signal, consisting of a linear line frequency sawtooth, and the corresponding rectified RF output signal does not exceed 2 per cent.
Black level stability	When switching from a white to a black input video signal, the instantaneous change in the amplitude of the RF output black level is negligible. Subsequently, after approximately 2 seconds, the output black level falls by 1.8 per cent of the overall output signal amplitude.
50-cps square-wave response	The droop in the output pulse amplitude from the start of the finish does not exexceed 2 per cent of the pulse step amplitude.
500-cps square-wave response	With an input pulse requiring a rise time of 0.074μs to increase its amplitude from 10 to 90 per cent of its maximum amplitude, the output pulse rise time is 0.18μs. There is no overshoot.
Residual carrier level	The amplitude of the residual carrier at the trough of the synchronizing signals does not exceed 2 per cent of the maximum carrier amplitude.
Radiated hum	No visible noise and/or hum patterns can be perceived on a hum-free receiver when the transmitter is being modulated by suitable test signals, the frame frequency of which is not exactly synchronized with the main power supply.
Input power consumption	180 kw for an all white picture and synchronizing signals; 114 kw for synchronizing signals only.

5. The Mast, Antenna and Transmission Line System

The considerations governing the general arrangement of the mast-antenna system have already been mentioned, and as will be seen from Fig. 4, the mast consists of three main sections. A lattice steel triangular support mast, 9 feet across each face, rises from the base pedestal to a height of 600 feet. Surmounting this is the cylindrical vhf slot antenna structure 110 feet high, 6.5 feet in diameter, and containing 32 slots, each 8 feet long by 1 foot wide. The slots are arranged in eight tiers, each tier having four slots spaced at 90° intervals around the surface of the cylinder. Each

slot is screened by backing it with a series of horizontal bars placed one above the other at intervals of 1 foot. The cylinder is formed by a thin skin of mild steel plate and is sectionalized in quadrants 10.5 feet high, each containing one slot. The slots are provided with "Perspex" covers to protect the future distribution transmission lines, which feed the slots, from the weather, and to prevent wind eddies inside the structure.

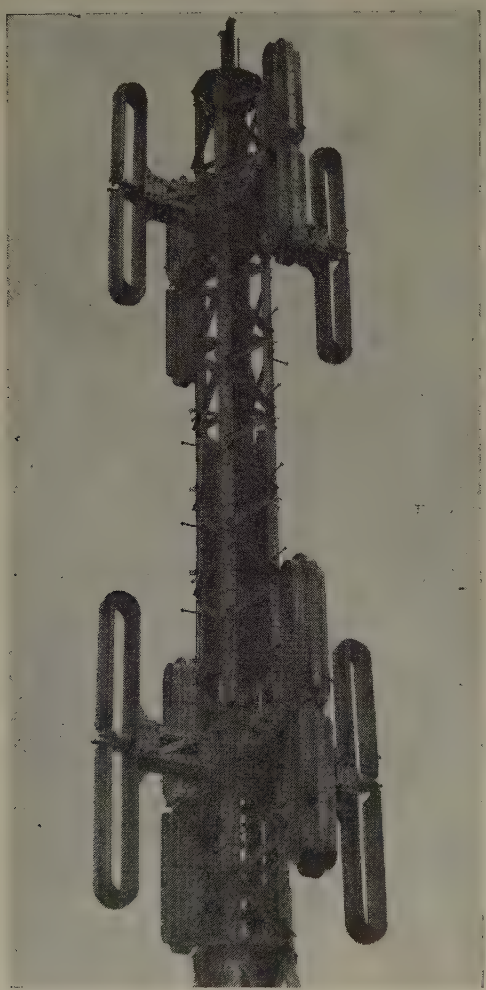
Fig. 20—Two stack folded dipole television antenna (vertically polarized).

The support mast and cylinder are stayed by steel ropes spaced at 120° and attached at heights of 200, 400, 600, and 710 feet. Above the cylinder and stays is the short unstayed lattice steel topmast of square section with 1.5-foot sides carrying the eight vertical dipoles of the television antenna and reaching to a height of 750 feet. In the support mast, a small lift is installed which rises to a point close to the base of the slot antenna, its operating motor being located at this level. The "all up" weight of the complete structure is some 140 tons and the maximum thrust on the base pedestal including the vertical components of the stay tension, is 336 tons. The mast structure is located by a 2-inch diameter steel ball, placed at the center of the base pedestal, which permits some angular movement under wind pressure. A movement at the mast head of about 7 feet from the perpendicular is envisaged under the most severe conditions.

The two-phase vertically polarized television antenna has an over-all height of 35 feet and consists of two tiers of four vertical half-wave folded dipoles supported by horizontal lattice steel arms built from the central lattice steel topmast, as shown in Fig. 20. Both the sound and vision signals are radiated from the same antenna,

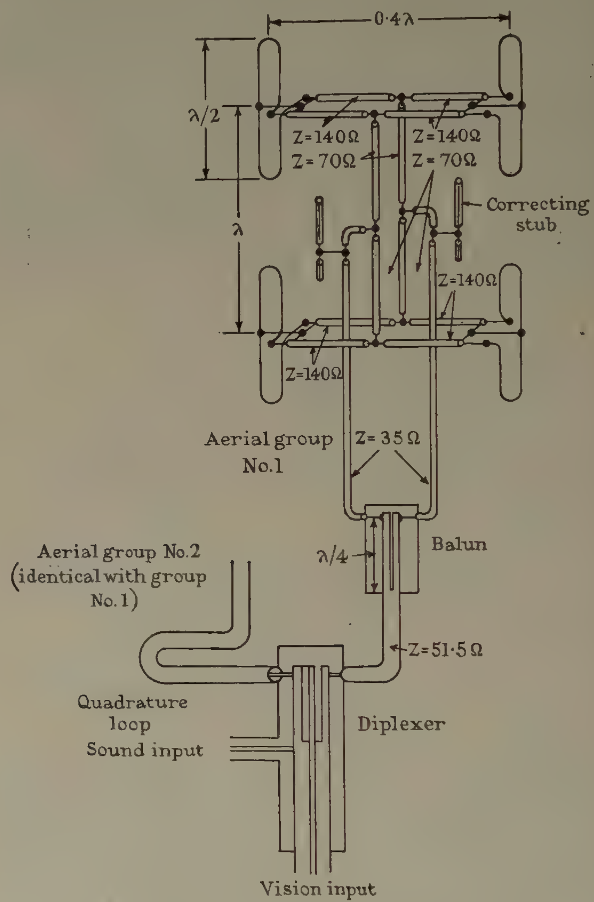

Fig. 21—Schematic of television antenna system.

but are conveyed to the antenna by separate coaxial transmission lines running from the outputs of their respective transmitters to the base of the topmast, where they are combined in the diplexer. The diameter of each tier is 0.4 wavelength, representing a compromise between uniformity of horizontal radiation and constancy of impedance over the working frequency band. The vertical spacing between the tiers is 1 wavelength, giving the optimum power gain for a two-tier system. In each of the two tiers, the four dipoles are fed with currents of the same amplitude, but with the phase changing progressively around the ring in steps of 90°. Reference to Fig. 21 will indicate how this is achieved.

Electrically, the complete antenna array may be considered as consisting of two groups of antennas, each group containing four dipoles made up from a pair of diametrically opposite dipoles in the upper tier and a similar pair in the lower tier. The correct phase relationship between the dipole currents in each group is effected by the arrangement of balanced transmission lines which connect them while the correct phase rela-

tionship between the two groups is obtained by the introduction of an additional quarter wavelength of line in the feed to one of the groups (designated "quadrature loop" in Fig. 24).

Both groups of antennas are fed from the diplexer which gives two outputs of combined vision and sound signals. These outputs are unbalanced and a balun is provided in each output to convert to the balanced feed required by each group of antennas. The diplexer combines the sound and vision signals, separately conveyed to it by the sound and vision main unbalanced transmission lines, the method of combining being such that, at the two outputs of the diplexer, the sound signals are presented in phase and drive the antenna groups in push-push while the vision signals are oppositely phased and drive the antenna groups in push-pull. The net result is that for the complete antenna array the phase rotation of the sound signals in the dipoles is in one direction and that of the vision signals in the opposite direction. The antenna system is similar in principle to the turnstile antenna used in America, but is adapted for vertical polarization. In addition to being a relatively simple and mechanically robust structure, the advantages of the arrangements are as follows: (a) The central support mast is in a region of low field strength, and therefore has a negligible effect on the performance; (b) The progressive phasing of the dipole currents increases the antenna gain; (c) The impedance of the combined groups of antennas, one fed through an additional quarter wavelength of line is more constant than that of either group separately. This results from the well known impedance inversion effect of a quarter-wavelength line; (d) There is no mutual coupling between one group of antennas and the other, so that measurements and adjustments are simplified.

A folded dipole made of galvanized steel strip forms the unit around which the complete array is built, and its leading dimensions are shown in Fig. 22. This construction has the advantage of being mechanically robust and of permitting the dipoles to be directly bolted to the lattice steel support arms built out from the topmast. Furthermore, by an appropriate choice of dimensions, the impedance can be made much more constant with frequency than the simpler type of center-fed dipole. The connection between the dipole and the transmission line which feeds it is made by appropriate shaping of the profiles which, at the same time, gives the required phase reversal in the feed to the diametrically opposite dipole. The web in the center of the strip serves to stiffen the dipole and also to provide a housing for the $7\frac{1}{2}$-kw heating elements used to prevent ice formation, which would change the dipole impedance and affect the performance adversely. The heating is switched on when the temperature falls below 2°C.

Coaxial transmission lines are used to supply the dipoles, a binocular pair being used to form a balanced feed, as shown in the diagram. The impedance of individual dipoles is 280 ohms, and in each tier diametrically opposite dipoles are connected by a pair of 140-ohm coaxial lines. The two tiers are then joined by a pair of 70-ohm lines which, in turn, are fed by a pair of 35-ohm coaxial lines from the balun output where the balanced impedance is 70 ohms.

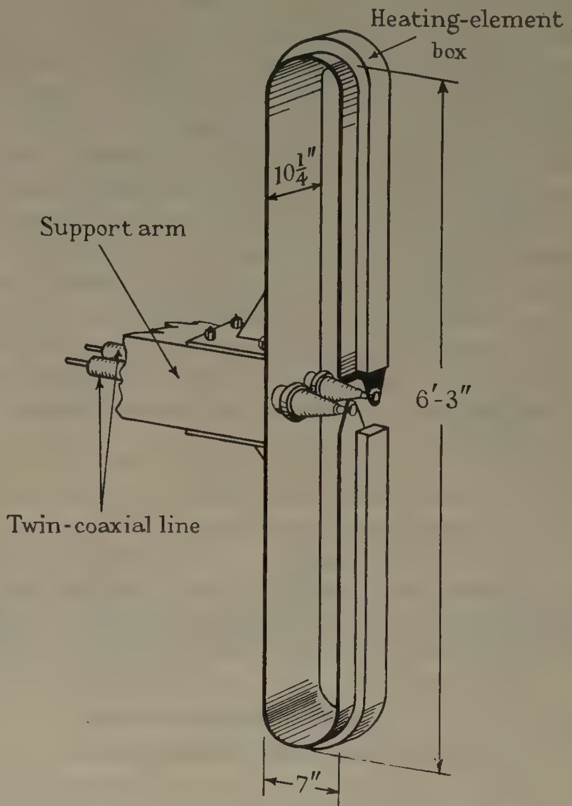

Fig. 22—Vertical folded dipole element.

Close to the driving point of the inter-tier feeders, a stub is included to make the impedance of each group of antennas more constant over the working frequency band. The stub consists of an open circuited and short circuited line in parallel, so that its effective characteristic impedance can be varied. The balun, as shown in Fig. 23, consists of a coaxial line with a slot in the outer

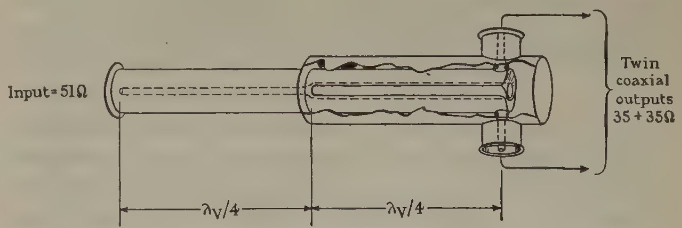

Fig. 23—Balun.

conductor one-quarter wavelength long. The balanced load is connected across the extremities of the slotted outer, and the inner of the coaxial lines connected to one of the extremities of the outer. The balun input impedance is required to match the output impedance of the diplexer unit, namely 51 ohms, and the required impedance transformation is made within the balun itself by two separate quarter-wavelength transforming sections between the balun input and the diplexer out-

put. At the input to the balun, there is thus a single unbalanced feed to one group of antennas, the impedance being substantially constant over the frequency band. The second group of antennas is similarly connected, but is fed through the quadrature loop. The diplexer is similar in construction to the balun and is represented pictorially in Fig. 24. The slot length is made one quarter of the vision wavelength, and the vision signal is fed to the two groups of antennas in series, i.e., in phase opposition. The sound signal is fed to the two groups in parallel, i.e., in the same phase, the inner of the sound line being connected to the outer of the slotted tube at a point below the end of the slot. The unit has a band pass impedance-frequency characteristic over the vision band and also gives a convenient, purely resistive impedance at the sound input, which is then matched to the impedance of the main transmission line by a subsidiary quarter-wavelength transformer.

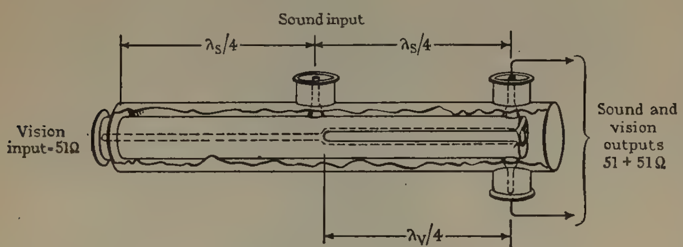

Fig. 24—Vision and sound combining diplexer.

Provided the impedance of each group of antennas over the working frequency band is a pure resistance equal to the characteristic impedance of the quadrature loop, the required current distribution in the dipoles is obtained. The impedance is not absolutely constant over the band, and the consequences of deviations of impendance from the ideal are as follows:

If the deviations are small, the combined impedance of the two groups of antennas will be constant, so that the impedance of the antenna system as a whole is insensitive to equal changes in the impedance of individual groups. Deviations also result in a difference in power delivered to the two groups of antennas, and hence to a change in the shape of horizontal radiation pattern. The most serious result, however, is the radiation of delayed images. Vision signals traveling toward the two groups of antennas are in antiphase at the diplexer output terminals; these will be reflected at the dipoles, equal reflections occurring at the terminals of group. Because of the quadrature loop in one path, the reflected signals appear in phase at the diplexer output terminals, and hence travel down the sound main transmission line. If the signal is again reflected at the transmitter end of the sound line, as will generally be the case, a delayed image will be radiated. The reflected signal does not travel down the vision line, however, so that measurements made on the latter would indicate a perfect match.

This is a fundamental limitation of this particular non-frequency discriminating diplexer system, and means that the inversion property of the quadrature loop is not fully exploited. With a straightforward series or parallel connection of the two groups of antennas, this difficulty disappears.

At the subsequent Holme Moss, Kirk O'Shotts, and Wenvoe stations, parallel connection of the antenna is used, together with a single transmission line and a frequency-discriminative type combining unit adjacent to the transmitters.[1]

The above limitation may be overcome by inserting in the sound line a network to absorb the reflected vision signal, which would eliminate the changes in horizontal radiation pattern with frequency; but the design of such a network is complicated by the requirement that it must not appreciably affect the transmission of the sound signal. Subjective tests, however, showed that such an absorption filter was unnecessary.

A further possible consequence of this effect is mutual interaction between the transmitters. Visible or audible interference which results from a second-order nonlinearity term is unlikely, but the sum and difference frequencies of the sound and vision carriers, corresponding to the first-order nonlinearity term, although not affecting television reception, may interfere with other services. As a result of consideration of these problems, it was necessary to restrict the deviations of the impedance of a single group of antennas, and an impedance characteristic corresponding to a standing wave ratio of 0.9 was chosen as a practicable compromise.

5.1. *Antenna Performance*

To assist in the design of the antenna, a small-scale model was made, measurements being carried out at a correspondingly higher frequency. A mid-band frequency of 500 mc, corresponding to a scale ratio of approximately 8:1 was used. This appeared to offer a good compromise between the difficulty of making the model and the carrying out of accurate measurements of the horizontal and vertical radiation patterns, power gain, and impedance. The jull-size antenna was made by scaling up the model with provision for controlling the impedance over a small range at appropriate points. The value of this preparation prior to installation is evidence by the fact that the antenna was erected and adjusted at the site within only a few days.

The horizontal radiation pattern of the final antenna when the dipole currents are of the correct amplitude and phase, is shown in Fig. 25, the deviation in field strength from the mean being ±0.6 db. The theoretical vertical radiation pattern of the antenna in free space is shown in Fig. 26. It was not practicable to check this experimentally on the final antenna, but measurements made on the model showed close agreement with the theoretical curve.

The mean gain of the antenna over a single half-wave dipole is 4.0 db, the deviation from this figure

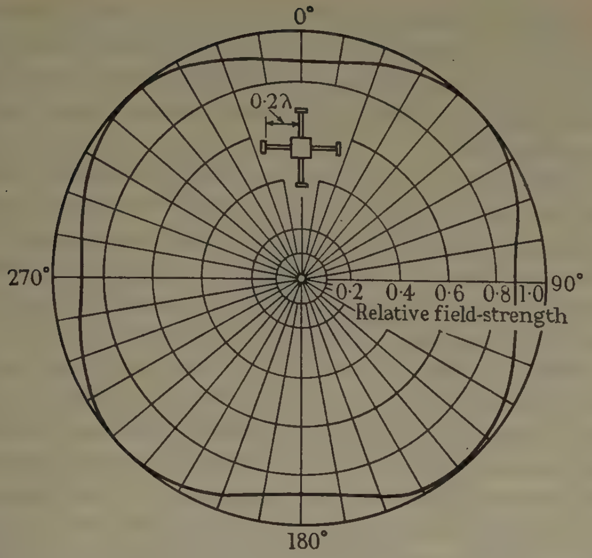

Fig. 25—Theoretical horizontal radiation pattern of antenna.

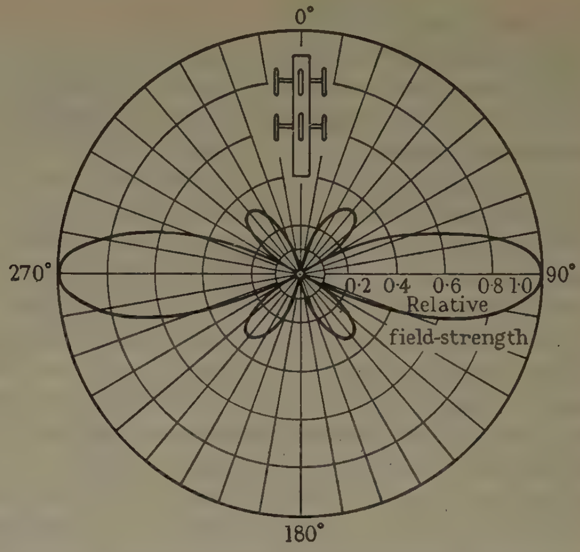

Fig. 26—Theoretical vertical radiation pattern of antenna.

in different horizontal directions being as shown in Fig. 25. The gain was measured by radiating the same power from both a standard half-wave antenna and the model, and comparing the field strength at a distant point. The theoretical and measured figures agreed within the measurement accuracy, which was ±0.2 db, indicating that the supporting structure does not introduce any significant loss. Impedance measurements were made using a bridge accurate to within ±1 per cent. Two results of interest, which are plotted in terms of conductance and susceptance normalized with respect to a characteristic admittance of 19.5 millimhos (characteristic impedance 51 ohms, are shown. Fig. 27 shows the impedance of each separate group of antennas, one of which includes the quadrature loop. The impedance of the combined groups is shown in Fig. 28, which illustrates powerful effect of this method of connection in improving the constancy of impedance over the frequency band.

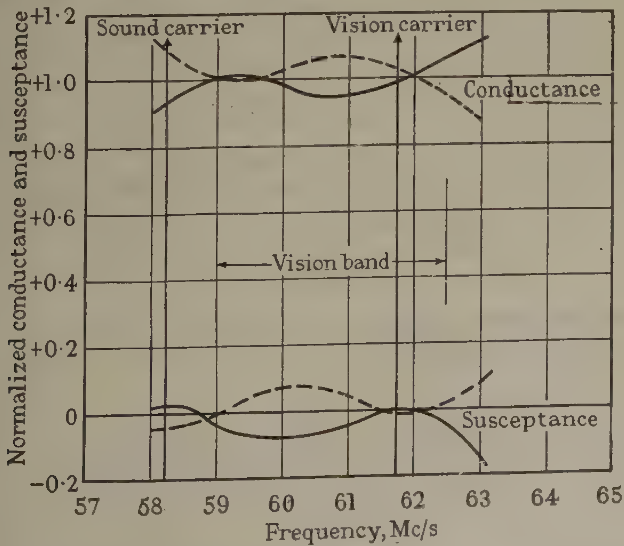

Fig. 27—Admittance/frequency characteristic of each antenna group at diplexer output flanges. Group 1 indicated by solid line; group 2 indicated by broken line.

The diplexer, and two subsequent bends in the main transmission line before connection is made to the main vertical run, cause a slight deterioration in the impedance characteristic, and one additional stub is used below the diplexer to correct this. At the point where the antenna is connected to the main transmission line, the standing wave ratio is better than 0.97, so that the reflection coefficient does not exceed 1.5 per cent.

For reasons previously mentioned, deviation of the impedance of one group of antennas from the ideal results in interaction between the sound and vision transmitters. The magnitude of the interaction can be predicted from the impedance, but a direct measurement of the insertion loss was made as a check on the impedance measurements. The measured insertion loss is shown in Fig. 29. At the vision carrier it is 40 db, falling to a minimum of 26 db at 1.5 mc below the vision carrier. Subjective tests showed that this performance was satisfactory in terms of delayed image radiation.

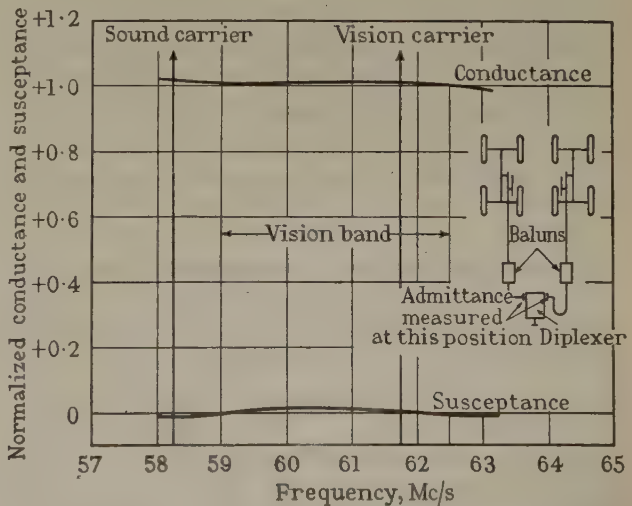

Fig. 28—Admittance/frequency characteristic of both antenna groups combined at diplexer output flanges.

5.2 *Main Transmission Lines*

The two separate coaxial copper-tube main transmission lines which connect the sound and vision transmitters to the corresponding inputs on the diplexer at the masthead are made to strict dimensional limits from copper of high purity. Their characteristic impedance is 51.5 ohms, the outside diameter of the inner tube being 2.128 inches and the inside diameter of the outer tube, 5 inches. The tubes are spaced by ½-inch diameter radial frequentite rod insulators set at 90° to each other.

It is important that the electrical characteristics of the vision lines should be uniform along the whole length, as discontinuities lead to the radiation of delayed images. The permissible tolerance on the dimensions of the copper tubes and on the uniformity of the spacing insulators is, therefore, small. The two transmission lines start at the antenna-load change-over switches of their respective transmitters, emerge from the building below the entrance door of the cooler room and are then taken in a culvert to appear above ground halfway toward the mast base. One mechanical problem was the support of the long vertical section of inner tubular conductor. The total weight of the 700-foot length used is approximately 2,000 pounds, and it is impracticable to support this either from the base or from the top of the mast. The vertical run was therefore divided into sections approximately 140 feet long, the weight of the inner of each section being taken by a conical insulator in compression, in an anchor box. The capacity introduced by the insulator is corrected by tapering the diameter of the inner conductor, a small trimming capacitor also being provided. Similar boxes are used at bends in the transmission line at the base of the mast.

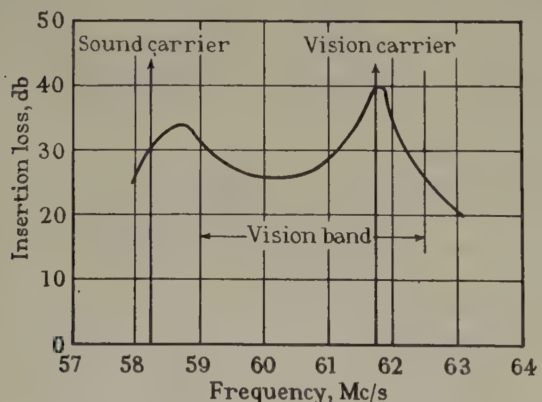

Fig. 29—Insertion loss between vision and sound transmitters.

The 140-foot sections are composed of standard 12-foot lengths; the inners are joined using sprung copper plugs and sockets, and the outers by bolted flanges with rubber sealing washers. A sliding expansion joint is provided in both inner and outer of the transmission line just below each anchor box. To prevent moisture entering the transmission lines, the whole of the system is hermetically sealed and dry air is blown through the lines continuously, the flow being 1 cubic foot per minute.

The total loss in the 900-foot length of transmission line is 0.6 db over the working frequency band. The effective gain of the antenna system relative to a half-wave dipole fed from a lossless transmission line is therefore 3.4 db.

Adjustments on the transmission line were carried out using an oscillator swept cyclically over the working frequency band, the modulus of the impedance being delineated on a cathode-ray tube. Check measurements were also made in the final condition using an impedance bridge having an accuracy of ±1 per cent.

Adjustments were carried out from the base on the first 140-foot section by terminating the distal end in an adjustable impedance. A mismatch between the line and terminating impedance results in ripples in the base impedance as the oscillator sweeps over the frequency band. These can be minimized by adjusting the termination. The discontinuity due to the anchor box, which is much nearer the base, can be distinguished by the difference in the ripple frequency and corrected. The terminating impedance and the anchor box control were therefore adjusted successively to give the optimum result. Thereafter, 140-foot sections of line were added and adjustments continued until the whole line was satisfactory. The standing wave ratio obtained by this method for the complete length of 900 feet from the transmitter to the antenna was 0.98. The corresponding figure for the complete antenna and transmission line system was 0.96, so that the over-all reflection coefficient of the vision line does not exceed 2 per cent.

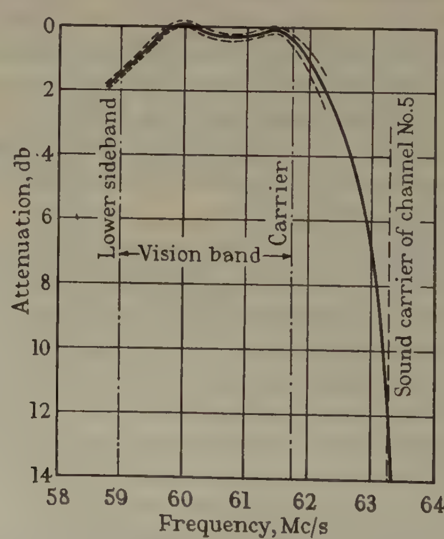

Fig. 30—Over-all transmission characteristic of radiated vision signal. (The dotted lines indicate the maximum deviation in different horizontal directions.)

At the Holme Moss station, the single transmission line is basically similar, but incorporates improvements which substantially reduce the erection time since section-by-section adjustment is not necessary. In this line the lengths of inner conductor are joined by plugs, expanded into the tube ends by hardened tapered screws, the outer tubes being coupled by cone joints in which the tube ends are forced on to an inserted steel ring,

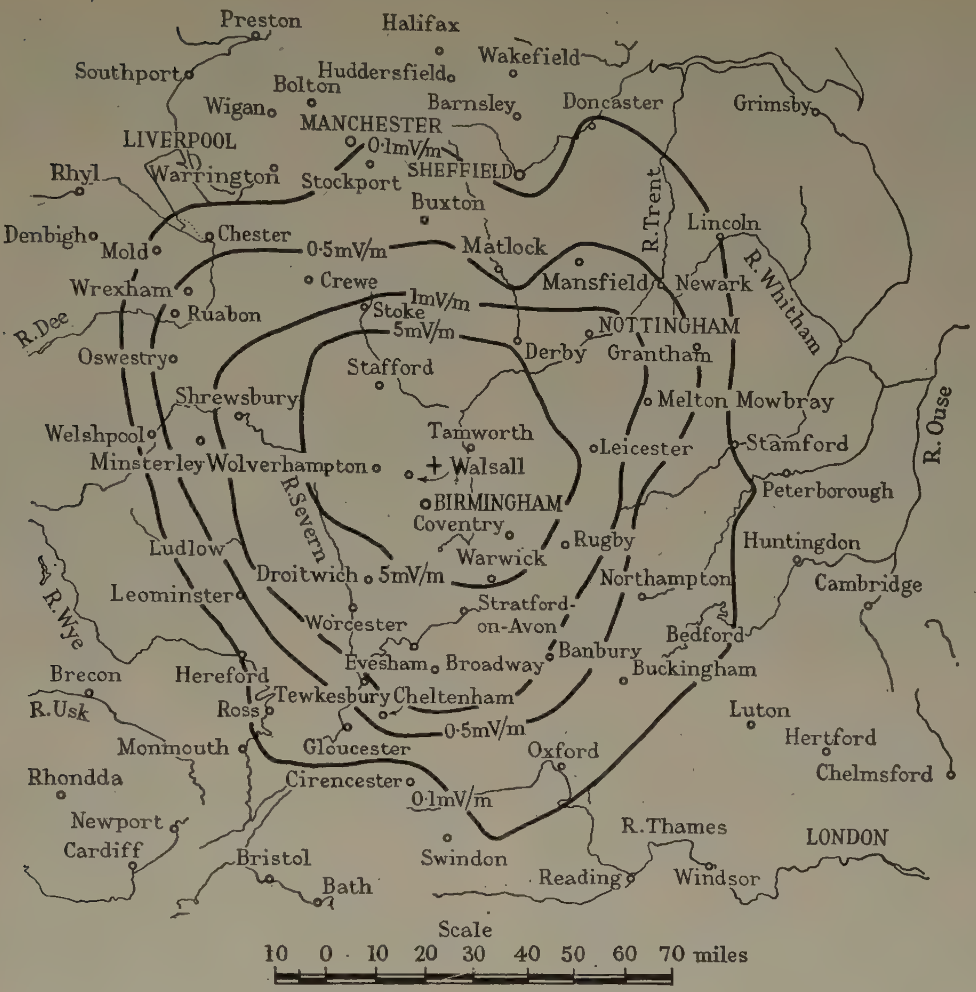

Fig. 31—Field strength contours for the Sutton Coldfield vision transmission.

which results in their being air tight without the use of sealing material. Impedance-compensated expansion joints have been developed, and both anchor box and angle box have been redesigned so that very little disturbance is introduced into the regular line constants. This line was erected completely without adjustment and gave a standing wave ratio slightly less than 0.98 with a matched termination. After a small capacitance correction had been made at the anchor boxes, the over-all standing wave ratio for the complete transmission line and antenna system was better than 0.97.

It is of interest to mention here that for the later Kirk O'Shotts and Wenvoe stations, an entirely new type of high-power coaxial transmission line has been developed.[1,9] Both the inner and outer conductors are suspended, pendulum fashion, from the top of the mast, the inner being constructed on the principle of locked-coil ropes which have excellent characteristics as winding ropes from the aspect of straightness, freedom from rotation, locking of strands, elasticity, and a smooth surface. The characteristic impedance is 78 ohms, the standing wave ratio is better than 0.99, and the loss is about 0.8 db per 100 feet.

5.3 *Over-all Performance*

The over-all frequency characteristic of the transmitted vision signal is shown in Fig. 30, the full line being the combined characteristic of the transmitter and vestigial sideband filter. For reasons already mentioned, the horizontal radiation pattern of the antenna changes slightly with frequency so that the over-all characteristic lies between the dotted lines which indicate the maximum deviations in different horizontal directions

The reflection coefficient at any point in the vision transmission does not exceed 2 per cent at any frequency in the working band, so that any delayed image radiation from this cause would be imperceptible. More likely was the possibility of delayed images being produced by vision signals, reflected from the two groups of antennas, traveling down and up the sound line and being reradiated, as already discussed. Calculations based on Fig. 29 showed that the effective reflection coefficient from this point of view (assuming the worst case of complete reflection at the base of the sound line)

[9] E. C. Cork, "Suspended Locked-Coil-Rope Television Feeder Systems," paper no. 1243, British Television Convention, session 4; 1952.

varied from 1 per cent at the vision carrier to a maximum of 5 per cent at a frequency 1.5 mc lower. Subjective tests carried out at a number of points round the site showed this performance to be satisfactory. With normal viewing conditions, no delayed images could be observed, but by adjusting the picture brightness to the most sensitive condition for this type of observation, delayed images were just perceptible to a critical observer and could be eliminated by a matched termination at the base of the sound line.

The results of the service area survey of the station are illustrated in Fig. 31 which shows the measured field strength at 30 feet above ground level of the vision transmission with the transmitter delivering a peak white power of 42 kw to the antenna corresponding to an effective radiated power of 100 kw at 730 feet, approximately. The field strength for the sound transmission will be correspondingly smaller due to its lower power. Field strengths at vhf tend to vary widely over short distances if the country is hilly or built-up, and the map shows the mean positions of the field strength contours.

Interpreted in terms of normal home viewing, the results may be summarized as follows: Up to a range of about 30 miles, the field strength is mainly greater than 5 mv/m; reception conditions are excellent and generally free from interference. Up to about 50 miles, the field strength is mainly greater than 0.5 mv/m; reception is first class but may be subject to interference where local conditions are severe. A useful signal can be received up to 70 miles from the transmitter, but may be subject to severe interference and some fading. When the terrain is accommodating and tropospheric conditions are favorable, good reception at a much greater distance is possible but not consistent, provided, once again, that the general level of interference in the area of reception is low. The estimated population served by the station is between six and seven million.

6. Acknowledgments

The author wishes to thank R. B. T. Wynn, the Chief Engineer of the BBC, for permission to publish this paper, and the I.E.E. for permission to reproduce certain of the diagrams. He also wishes to acknowledge the work of colleagues in the BBC's Planning and Installation Department, Research Department, and Building Department who collaborated in engineering the project. In particular, he acknowledges the information on antenna performance contributed by his colleague H. Page, who was responsible for developing the v.h.f. slot and television antennas.

Great credit is due to the engineers of the various manufacturers responsible for constructing the equipment to BBC specification, notably the research and development staffs of E.M.I. Research Laboratories Ltd. and Metropolitan Vickers Co. Ltd., who developed the vision transmitter, and Marconi's Wireless Telegraph Co. Ltd., who constructed the sound transmitter, transmission lines, diplexer, and baluns, and, who were responsible, jointly with the BBC for the final construction of the television antenna. In this connection, mention should also be made of the collaboration of British Insulated Callender's Construction Co. Ltd., who constructed the support mast with its integrated slot antenna.

Correction

Louise Roth and W. E. Taylor, co-authors of the paper, "Preparation of Germanium Single Crystals," which appeared on pages 1338–1341 of the November, 1952 issue of the Proceedings of the I.R.E., have brought the following errors to the attention of the editors:

Footnote 5, page 1338 should read: However, an analysis of these crystals showed large amounts of impurities: 1.83 per cent Fe, 0.3 per cent Al, 1.04 per cent SiO_2, 0.08–0.10 per cent Zn, and traces of C and Mn. H. J. Seeman, "Zur Elektrische Leitfahigkeit des Siliziums Nachtrag," *Phys. Zeit.*, vol. 29, p. 94; 1928. Therefore, the high conductivity, we conclude, must have been due to the impurity content.

Footnote 6, page 1338 should read: K. Lark-Horovitz, "Preparation of Semiconductors and Development of Crystal Rectifiers," Final Report NDRC 19-585, U. S. Dept. of Commerce; 1945. "The New Electronics," A.A.A.S. Symposium, Section 2; 1949. We are indebted to Dr. Lark-Horovitz for the use of this manuscript.

A separate footnote to the last sentence in the second paragraph of page 1338 should read: This was later substantiated by careful measurements at Bell Telephone Laboratories. The correct value is 1.12 electron volt.

Footnote 10, page 1338 should read: In 1949 Wartenberg found similar values on silicon needles obtained by the same process. H. V. Wartenberg, "Über Silicium," *Z. f. anorg. Chem.*, vol. 265, p. 186; 1951.

Footnote 11, page 1339 should read: Recently large single crystals of silicon have been grown at Bell Telephone Laboratories. G. K. Teal and E. Buehler, "Growth of silicon single crystals and of single crystal silicon *p-n* junctions," *Bull. Am. Phys. Soc.*, vol. 27, no. 3, p. 14; 1952.

Footnote 17, page 1340 should read: See also, G. K. Teal and J. B. Little, "Growth of germanium single crystals," *Phys. Rev.*, vol. 78, p. 647; 1950.

Instrument Approach System Steering Computer*

W. G. ANDERSON†, ASSOCIATE, IRE AND E. H. FRITZE†, ASSOCIATE, IRE

This paper was procured by and is published with the approval of the IRE Airborne Electronics Group.—*The Editor.*

Summary—This paper is concerned with the theory of an airborne electronic steering computer and associated instrumentation used in aircraft guidance during an instrument approach. It is shown that this guidance problem may be analyzed with advantage as one of feedback control. Means are discussed for achieving a stable flight path in the resultant variable gain feedback control system. Principles of complementary linear filtering are presented and combination of certain control signals in a complementary filter is shown to result in an improved system. The importance of the form of cockpit instrumentation in this guidance problem is indicated.

Introduction

THE INSTRUMENT LANDING APPROACH SYSTEM (ILAS) ground-radio aids provide a radiation pattern in space defining the proper aircraft approach path to a designated runway. Marker beacons are installed along this approach path to provide discontinuous distance to touchdown information.

This ground-radio equipment has been installed at airports throughout the United States and abroad to make possible the landing of properly equipped aircraft under instrument weather conditions.[1] The airborne radio equipment used with the ILAS consists of separate receivers for reception of lateral guidance (localizer), vertical guidance (glide path), and marker beacon information. Signals are obtained from the localizer and glide-path receivers regarding the lateral and vertical deviation of the aircraft from the correct approach path. In its basic form, the system provides the pilot with direct visual indications of such deviations. The aircraft must be maneuvered by attitude and power control to bring the indicated deviations to zero and these must be held to a suitable minimum during the approach. During the final phase of the approach, some of the displacement tolerances are comparable to the wingspan of the aircraft. Flying this path is an exacting task which requires an inordinate amount of the pilot's attention during a critical phase of the flight. The steering computer to be described is designed to aid the pilot in making these instrument approaches down to an altitude of approximately 200 feet. Since the flare out and touchdown are not included as functions of the computer, the vertical guidance problem is rather straightforward. Therefore, this paper will be concerned for the most part with the lateral guidance problem of the ILAS approach.

A pilot makes use of visual information from three principal sources in flying an aircraft into lateral correspondence with a localizer approach path. Such visual information includes bank angle from the vertical gyro, heading with respect to the runway from the directional gyro, and lateral flight path deviation from the localizer receiver. In such a manual approach with the basic instrumentation the pilot must continually estimate the present correct attitude control action which will achieve a future desired position. Bracketing oscillations of the aircraft about the correct flight path usually result. The steering computer to be described utilizes data regarding aircraft bank angle, heading, and localizer deviation to automatically compute a steering indication for the pilot which, if followed, will result in a smooth entry and tracking of the correct approach flight path. A manual instrument approach with the aid of a steering computer is closely related to the completely automatic approach possible with autopilot control. In either case an electrical unit is necessary for combining data from attitude gyro, compass, and radio to obtain aircraft steering information. In the case of the steering computer, the steering information is presented visually to the pilot for his manual control action. In the case of the autopilot the combining unit is termed an approach coupler and the steering information actuates control surface servomechanisms. Where control is by a pilot, the form of cockpit instrumentation is of considerable importance. It is desirable that pictorial methods be employed in the presentation of visual information to the pilot to aid rapid interpretation of a given situation and to reduce the probability of pilot error. Benefits are also derived from any reduction possible in the number of cockpit instruments requiring pilot attention.

The Control Problem

The procedure of flying an aircraft into proper correspondence with an ILAS radio beam is basically a process of feedback control. The problem of lateral

* Decimal classification: R526.2. Original manuscript received by the Institute, June 21, 1952; revised manuscript received September 30, 1952.

† Collins Radio Co., Cedar Rapids, Iowa.

[1] P. Caporale, "The C.A.A. instrument landing system," *Electronics*, vol. 18, pp. 116–124; February, 1945.

guidance is illustrated pictorially in Fig. 1, and is shown in simplified block diagram form in Fig. 2.

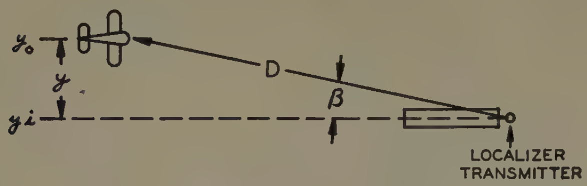

Fig. 1—Geometry of the localizer approach.

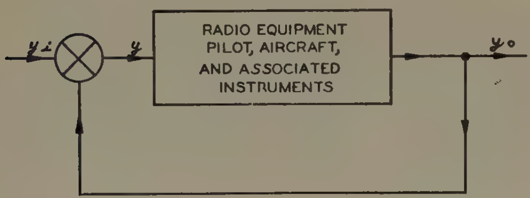

Fig. 2—Simplified block diagram of the localizer approach.

It is desired that an aircraft which is at present flying laterally displaced from the runway extension, as defined by the localizer radio link, smoothly enter and maintain a flight path coinciding with this correct line of approach. The source of information regarding the position of the aircraft relative to its desired position is an error signal derived from the instrumentation circuits of the localizer receiver. The error output of the receiver is proportional to the angular deviation of the aircraft from the correct line of approach as indicated by angle β of Fig. 1. With current standard instrumentation, a $2\frac{1}{2}$ degree deviation from the runway line corresponds to full-scale deflection of the deviation indicator.

In order to make an analysis of the beam-approach problem on the basis of a linear-co-ordinate system, we will deal with the lateral motion of the aircraft in terms of position y and its derivatives. From Fig. 1,

$$y = y_i - y_0$$

$$y = D \sin \beta,$$

where y_i is the position of the localizer approach path, y_0 is the lateral position of the aircraft, and D is the distance from the aircraft to the localizer transmitter. For the small angles involved in the localizer approach,

$$y \cong \beta D. \tag{1}$$

Consideration of the system of Fig. 1 shows that the process of bringing the aircraft into correspondence with the approach path corresponds to reducing the position error "y" to zero in the feedback control system diagrammatically shown in Fig. 2. A more complete diagram of the system, as shown in Fig. 3, is obtained by expansion of the single box of Fig. 2. The current i deflects the deviation indicator in accordance with position error y; δ is an aileron deflection set up by the pilot in response to indications of the flight instruments.

The fact that the deviation signal depends directly on angular error from the approach path rather than on lateral position error results in an inverse variation of position loop gain with distance D from aircraft to localizer transmitter. The pilot is informed of the response of the aircraft to his control in terms of attitude from vertical gyro and heading from the directional gyro, in addition to the position information obtained from the radio deviation indicator. The attitude and heading indications represent feedback loops internal to the aircraft position loop in the formulation of Fig. 3.

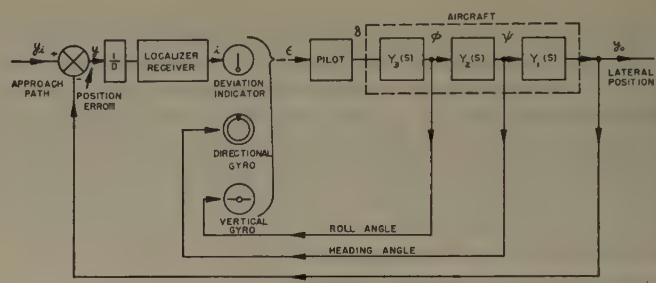

Fig. 3—Block diagram representation of the control system involved in flying a localizer approach.

The transfer functions $Y_1(s)$ and $Y_2(s)$ relating the aircraft bank angle, heading, and position relative to the localizer course can be derived from simple geometrical considerations for the case of co-ordinated turns. Fig. 4 illustrates these relations.

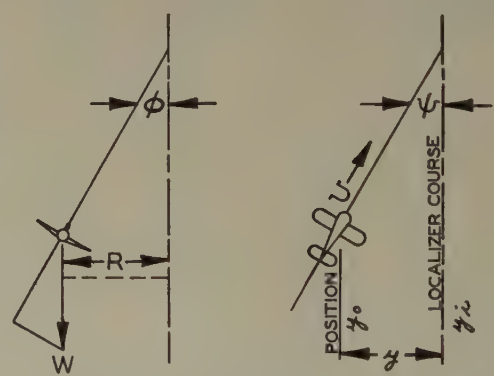

Fig. 4—Geometry of bank, heading, and position relations.

From consideration of the forces in a co-ordinated turn, we obtain

$$W \sin \phi = \frac{WU^2}{gR} \cos \phi,$$

where

W = weight of aircraft
ϕ = angle of roll
U = airspeed
g = gravitational constant
R = radius of turn.

For reasonably small angles of bank involved in normal maneuvers $\sin\phi = \phi$ and $\cos\phi = 1$. This approximation leads to a bank angle to heading transfer function.

$$\phi \cong \frac{U^2}{gR}$$

$$\phi \cong \frac{U}{g}\frac{d\psi}{dt}$$

$$\bar{\psi} \cong \frac{g}{Us}\bar{\phi}. \tag{2}$$

Neglecting the effect of wind:

$$\frac{dy_0}{dt} = U \sin\psi,$$

where ψ is the heading of the aircraft relative to the localizer course. For the normal range of heading angles:

$$\psi \cong \sin\psi$$

$$y \cong \int U\psi dt$$

$$\bar{y}_0 \cong \frac{U}{s}\bar{\psi}. \tag{3}$$

The relation between ψ and ϕ and that between y_0 and ψ is expressed in terms of the LaPlace transform variable s for zero initial conditions.

For a constant approach airspeed these transfer functions become

$$\bar{\psi} = \frac{K_A}{s}\bar{\phi} \tag{4}$$

and

$$\bar{y}_0 = \frac{K_B}{s}\bar{\psi}. \tag{5}$$

Thus $(dy_0/dt) \propto \psi$ and $(d^2y_0/dt^2) \propto \phi$, where K_A and K_B are constants.

An approximate transfer function relating roll angle to aileron deflection can be derived as follows: A differential equation representing the simplified relationship between δ and ϕ is given in the following:

$$C_\delta \delta = J_{xx}\frac{d^2\phi}{dt^2} + f\frac{d\phi}{dt}. \tag{6}$$

This equation states that the torque applied by the aileron deflection $(C_\delta\delta)$ is opposed by the torque required to accelerate the inertia of the aircraft about the roll axis $[J_{xx}(d^2\phi/dt^2)]$ and by the viscous damping torque $f(d\phi/dt)$. C_δ is a constant relating aileron deflection and torque in roll at approach airspeed, J_{xx} is the inertia, and f is the linearized damping coefficient in roll.

Applying the LaPlace transformation to this time equation yields a transfer function of the form

$$Y_3(s) = \frac{\bar{\phi}}{\bar{\delta}} = \frac{\dfrac{C_\delta}{f}}{s\left(\dfrac{J}{f}s + 1\right)} = \frac{K_R}{s(T_R s + 1)}, \tag{7}$$

where $K_R = C_\delta/f$ and $T_R = J/f$ a time constant.

The transfer functions of the aircraft given in (4), (5), and (7) are first-order approximations. They do not include any cross coupling between the roll and yaw axes nor any of the higher-order dynamic effects associated with the maneuvering aircraft. More inclusive transfer functions could be obtained by applying the LaPlace transform to the asymmetric equations of motion of an aircraft as found in the aerodynamic literature. However, for the steering problem considered here, the simplified transfer functions are sufficient.

The only other elements shown in Fig. 3, whose transfer functions contain significant dynamic terms, are the deviation indicator and the pilot. The deviation indicator is simply a d'Arsonval movement containing a mechanical mass J_m, a spring of constant K_m, and electrical damping denoted by the constant f_m. It is therefore a second-order system and can be represented by the familiar transfer function

$$\frac{\bar{\epsilon}}{\bar{i}} = \frac{K_m}{J_m s^2 + f_m s + K_m}, \tag{8}$$

where ϵ is the meter deflection in response to current i.

The transfer function of the pilot involves nonlinear human behavior which cannot be expressed explicitly by any simple transfer function. In this paper, his behavior is denoted by the generalized form

$$\frac{\delta}{\bar{\epsilon}} = K_p G_p(s). \tag{9}$$

Fig. 5 illustrates a computer system which combines by direct linear addition signals from vertical gyro, compass, and radio to produce as an output a steering indication for the pilot. The computer relieves the pilot of the task of mentally determining correct steering action on the basis of visual observation of separate instruments.

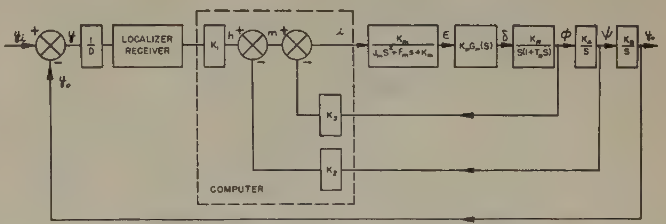

Fig. 5—Block diagram of lateral guidance utilizing a computer.

The pilot acts as an error detector in this feedback control system, and is constrained to take up a bank angle as required to continuously center the steering indicator. The steering indicator is dynamically similar to

the deviation indicator described previously. The inner feedback loop encloses the indicator, the pilot, and the aileron to roll transfer function of the aircraft. The closed loop transfer function for this loop is

$$\frac{\phi}{m} = \left[\frac{\dfrac{K_R}{s(1+T_Rs)} \cdot \dfrac{K_m}{(J_ms^2+f_ms+K_m)} \cdot K_pG_p(s) \cdot K_3}{1 + \dfrac{K_R}{s(1+T_Rs)} \cdot \dfrac{K_m}{(J_ms^2+f_ms+K_m)} \cdot K_pG_p(s) \cdot K_3} \right] \cdot \frac{1}{K_3},$$

where K_3 is the gain constant of the bank feedback loop. Assuming that the term

$$\frac{K_RK_mK_pG_p(s)K_3}{s(1+T_Rs)(J_ms^2+f_ms+K_m)}$$

is much greater than 1, the terms within the brackets reduce approximately to unity, and the transfer function simplifies to

$$\frac{\phi}{m} \cong \frac{1}{K_3}. \tag{10}$$

This condition holds at low frequency without requiring a loop gain great enough to cause a stability problem. The derivation and the included assumptions are equivalent to saying that the pilot can set up a required bank angle as called for by the computer without an oscillatory response. The pilot is effectively enclosed and controlled by the inner bank loop over the frequency range of interest to the remainder of the system during the approach.

A useful analysis of the localizer control system of Fig. 5 can be made on the basis of above simplification.

$$\frac{\bar{\psi}}{\bar{m}} = \frac{K_A}{K_3s}$$

$$\frac{\bar{\psi}}{\bar{n}} = \frac{\dfrac{K_A}{K_3s}}{1 + \dfrac{K_2K_A}{K_3s}}$$

$$\frac{\bar{v}_0}{\bar{v}} = \frac{\dfrac{K_1K_AK_B}{DK_3s^2}}{1 + \dfrac{K_2K_A}{K_3s}}$$

$$\frac{\bar{y}_0}{\bar{y}_i} = \frac{\dfrac{K_1K_AK_B}{D}}{K_3s^2 + K_2K_As + \dfrac{K_1K_AK_B}{D}}. \tag{11}$$

Equation (11) expresses the lateral position of the aircraft y_0 with respect to the reference input localizer position y_i in terms of a second-order system. The characteristic equation of this system (denominator of (11)) is of the form

$$A\frac{d^2y_0}{dt^2} + B\frac{dy_0}{dt} + Cy_0 = 0$$

$$A \propto K_3 \qquad B \propto K_2 \qquad C \propto \frac{K_1}{D}.$$

As is well known, the nature of the response of such a system may be oscillatory or exponential in form dependent on the relative value of the coefficients.

It is analogous to the familiar second-order mechanical system consisting of a mass, a spring, and a viscous damper. The bank feedback gain K_3, the heading feedback gain K_2, and the radio displacement gain K_1/D are respectively proportional to the mass, the damping, and the spring of the mechanical system. Thus the undamped natural frequency ω_n of the system is proportional to

$$\omega_n \propto \sqrt{\frac{K_1}{DK_3}}.$$

As the transmitter is approached, D will decrease, thereby increasing the natural frequency of the system, and also the amount of damping required for a non-oscillatory system.

Variable Gain and Cross-Wind Effects

Although the use of a computer of the form shown in Fig. 5 much eases the pilot's task in flying an ILAS approach, the system suffers from some limitations. Because of the variation in radio deviation gain as a function of distance, it is not possible to make a damping setting which is completely satisfactory over the range from the early approach phase to touchdown. A compromise setting results in the approach being rather heavily overdamped in the region of early approach. This results in a long exponential phase before the aircraft comes into correspondence with the approach path. A reduction in damping in this region is limited by the requirement that the system must not become oscillatory in the region of high position gain near touchdown. At the present state of development distance to touchdown information of a continuous form is not available in the aircraft. Were this information available, the effect of variable position gain could of course be compensated.

A second difficulty arises from the effect of cross wind during the approach. Since the damping term $B(dy_0/dt)$ is proportional to heading of the aircraft with respect to the runway, a steady angle of crab, as required under cross-wind conditions, appears in the system as a steady rate component across the course. This results in a standoff position error of the aircraft to the downwind side of the correct approach path. A similar standoff results from any error made in setting the runway

direction into the system. This standoff error may be corrected by filtering out the dc component of the heading signal by passing it through a single-section, high-pass filter having a very large time constant. Another scheme would involve integrating the radio displacement signal in order to reduce the standoff error to zero. Both of these methods remove the steady-state error due to cross wind, but necessarily at a slow rate due to stability considerations. Hence they are of little value when the aircraft is confronted with a changing cross wind during the final phase of the approach. In addition, during initial maneuvering the integrator stores up false information usually making it necessary for the plane to overshoot the desired course.

A third conventional attack on this type of problem involves abandonment of heading as the damping signal. Instead, the damping signal is derived by differentiation of the radio-position signal by electrical networks or other means. Using this method, cross wind causes no difficulty and theoretically the system damping increases as the transmitter is approached. This increase in damping is not objectionable since the natural frequency of the system is also increased as D decreases. The principal deterrent to the use of this technique results from the "noisy" nature of the radio-position signal. A considerable amount of disturbing noise is present in this signal as a result of siting effects. This noise is at times bothersome in the radio-position indication, and is generally removed by low-pass filtering. Differentiation of the radio signal results, as would be expected, in considerable emphasis of the noise. Noise effects in the radio-derived damping signal are at times severe enough to make such a system scarcely flyable.

The Complementary Filter

The problem of designing a suitable control system has been resolved into one of synthesizing a suitable damping signal. The basic heading damped system is in error in the presence of a cross wind and the noise contained in the differentiated radio signal is very undesirable.

Examining the two damping signals on a frequency basis yields an interesting result. The heading signal (due to cross wind) is in error at the very low frequencies including dc, whereas the differentiated radio signal has undesirable high-frequency components. It thus becomes apparent that the optimum damping signal would contain low-frequency information derived from the differentiated radio signal and high-frequency information obtained from the heading signal. The complementary filter, first suggested by Wirkler,[2] is a means of accomplishing this desired result.

The filter derivation will be carried out in terms of the angular frequency operator $j\omega$ since it is helpful to think of synthesizing the signal on a frequency basis, i.e., low frequencies from differentiated radio and high frequencies from heading. In addition, the derived results will be applicable to further consideration using the techniques and terminology of attenuation-phase feedback control-system analysis.

It can be shown that for steady-state analysis multiplying a function of $(j\omega)$ by the operator $j\omega$ is equivalent to taking the derivative as a function of time. In equation form the latter statement is represented as

$$\frac{df(t)}{dt} = j\omega F(j\omega).$$

This equivalence will be used in applying the complementary filter principle.

Combination of signals from relative heading and radio sources will first be considered for a fixed distance D from aircraft to localizer transmitter. Fig. 6 shows diagrammatically the manner in which a first derivative damping signal could be derived under these conditions. The heading signal $j\omega y_2$ is passed through the high-pass RC filter to attenuate its low-frequency components;

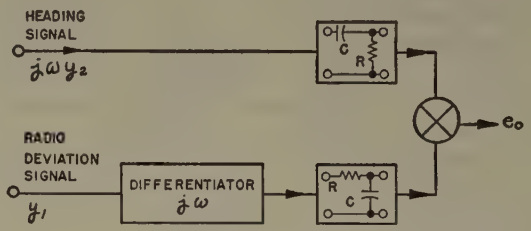

Fig. 6—Deriving a rate signal from two sources.

the radio signal y_1 is differentiated and then filtered by the low-pass RC filter to attenuate the high-frequency components including the noise. The outputs of the two filters are then added together to make up an improved damping signal.

The frequency response functions of the filters and the differentiator are

$$\text{high pass} = \frac{j\omega RC}{1 + j\omega RC}, \tag{12}$$

$$\text{low pass} = \frac{1}{1 + j\omega RC}, \tag{13}$$

$$\text{differentiator} = j\omega.$$

Therefore,

$$e_0 = j\omega y_2 \cdot \frac{j\omega RC}{1 + j\omega RC} + y_1 \cdot j\omega \cdot \frac{1}{1 + j\omega RC},$$

$$e_0 = \frac{j\omega y_2 \cdot j\omega RC + j\omega y_1}{1 + j\omega RC}. \tag{14}$$

If y_1 and y_2 are equivalent, e_0 reduces to

$$e_0 = j\omega y \frac{(1 + j\omega RC)}{(1 + j\omega RC)} = j\omega y. \tag{15}$$

[2] W. H. Wirkler, "Aircraft Course Stabilizing Means," U. S. Patent No. 2,548,278; April 10, 1951.

A simplification is possible in view of the fact that the cascade combination of a differentiator and a low-pass filter is equivalent in form to a high-pass filter. Thus Fig. 6 can be redrawn as shown in Fig. 7. The operations indicated in this figure give the same result as that obtained from the system of Fig. 6, provided that the radio input is reproportioned by the factor 1/RC.

$$e_0 = \left(\frac{y_1}{RC} + j\omega y_2\right)\cdot\frac{j\omega RC}{1 + j\omega RC} = \frac{j\omega y(1 + j\omega RC)}{(1 + j\omega RC)},$$

$$e_0 = j\omega y. \tag{16}$$

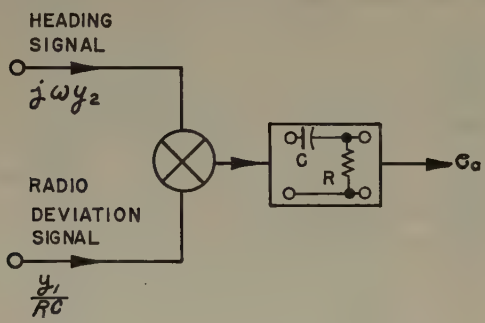

Fig. 7—Simplified circuit for derivation of rate signal from two sources.

Thus passing heading and radio signal through a high-pass filter results in a synthesized damping signal free of static cross-wind error and with the radio noise attenuated as compared to the use of a pure differentiated radio signal.

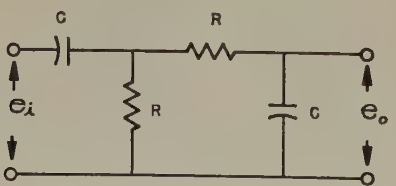

Fig. 8—Two-section complementary filter.

It would be advantageous to attenuate, by an additional amount, the noise in the complementary-derived damping signal. This is possible by obtaining the very high-frequency components of the damping signal from a third source, the bank or roll angle which is approximately equivalent to $(j\omega)^2 y_3$. For this derivation, a two-section complementary filter shown in Fig. 8 is used. The frequency response function of this filter is

$$\frac{e_0(j\omega)}{e_i(j\omega)} = \frac{j\omega RC}{1 + 3j\omega RC - \omega^2R^2C^2}. \tag{17}$$

Let $e_i(j\omega)$ be a linear combination of signals from the three sources

$$e_i(j\omega) = Ey_1 + F\dot{y}_2 + G\ddot{y}_3,$$

where $E = 1/RC$, $F = 3$, $G = RC$, and for sinusoidal signals

$$\dot{y}_2 = j\omega y_2$$

$$\ddot{y}_3 = -\omega^2 y_3.$$

Thus

$$e_0(j\omega) = \left[\frac{j\omega RC}{1 + 3j\omega RC - \omega^2R^2C^2}\right]\left[\frac{1}{RC}y_1 + 3j\omega y_2 - \omega^2 RC y_3\right]$$

$$= \frac{j\omega y_1 + 3j\omega RC(j\omega y_2) - \omega^2R^2C^2(j\omega y_3)}{1 + 3j\omega RC - \omega^2R^2C^2}. \tag{18}$$

If the three sources are consistent,

$$e_0(j\omega) = \left[\frac{1 + 3j\omega RC - \omega^2R^2C^2}{1 + 3j\omega RC - \omega^2R^2C^2}\right]j\omega y = j\omega y. \tag{19}$$

The resultant signal is obtained in complementary fashion without loss of any component frequencies while the undesired components of the input signals are attenuated.

The opportunity for complementary filtering exists in general whenever more than one source of information is available describing a given variable and its derivatives. Single-section low-pass and high-pass complementary filters require information from only two sources, while the two-section filter requires information from three sources.

As stated earlier, the preceding derivations were made assuming the aircraft to be a fixed distance D out from the localizer. The fact that the gain of the radio deviation signal varies inversely with distance means that the radio, heading, and bank signals will be truly complementary in the manner of (19) for only one distance D_0. When the aircraft is at a lesser distance from the transmitter, the radio feed to the filter will be higher than the nominal setting of (19). When the aircraft is at a greater distance, this feed will be lower. Since lateral acceleration and velocity are represented by ϕ and ψ only approximately, we might also expect some deviation from the foregoing results.

Despite these effects, a damping signal derived from the three sources through the complementary filter of Fig. 8 proves very satisfactory for use in the localizer channel of a steering computer. The standoff error caused by cross wind or small errors made in setting runway heading into the system is eliminated and radio noise in the damping signal is attenuated in the frequency region above that associated with the filter time

constant. The value of this time constant must be chosen as a compromise. Too large a time constant will make the system oversensitive to low-frequency disturbances such as shifting cross wind. Too small a time constant will result in the passage of excessive radio noise. A block diagram of the over-all system using the two-section complementary filter is shown in Fig. 9.

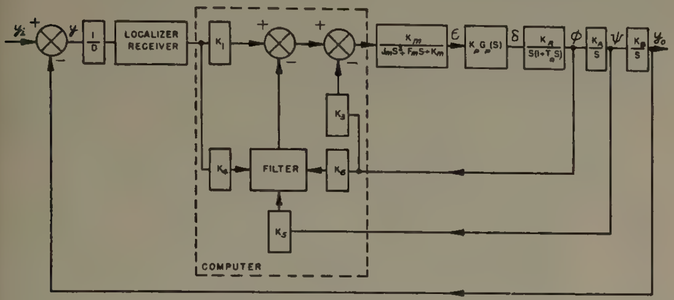

Fig. 9—Block diagram of system with complementary filter.

the use of the equivalent diagram is advantageous in separating effects caused by different loop parameters.

One of the advantages of the frequency response (attenuation-phase) method of analysis lies in the ready use which can be made in theoretical work of experimentally determined frequency-response data on all or a part of the system. In the present case this applies

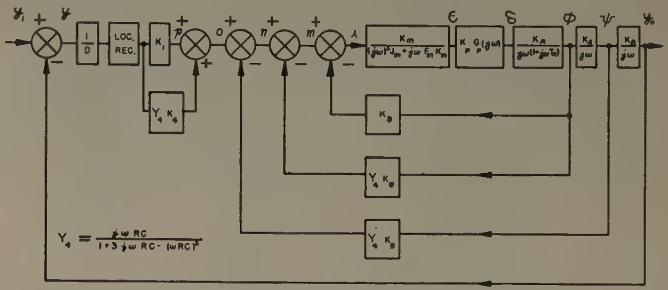

Fig. 10—System of Fig. 9 redrawn for attenuation-phase analysis.

Having determined the over-all nature of a system with the desired characteristics, questions of parameter adjustment and stability tolerance are of concern. A satisfactory adjustment of this steering computer system has been determined by use of correct complementary filter feed factors at an experimentally determined set-up point in the region of the approach several miles from touchdown. Operation has been checked by analog simulation and flight test. Although workable, this method of adjustment does not give as complete a picture of the "damping" characteristics of the filter derived signals as desired. Nor is it straightforward to determine the optimum feed factors for the filter by the experimental approach.

The effect on the transient performance of the system of variation in damping is clearly defined in connection with a second-order system such as that associated with the approximate representation of (11). The system of Fig. 9 is of much higher order. Although the system equation can be derived by sufficient algebraic manipulation, it is not possible to easily identify the parameters with corresponding effects on transient behavior as in the less complicated system.

The frequency-response method of analysis as applied to this multiloop feedback control system offers a means of obtaining considerable information regarding stability ranges, optimum adjustment, and tolerances. Significant results of the application of this method follow.

Frequency-Response Analysis

For ease in dealing with this system as a multiloop feedback problem the block diagram of Fig. 9 can be redrawn in the form of Fig. 10. In this arrangement the signals from bank, heading, and radio sources are each fed through separate identical RC filters (as shown in Fig. 8), after which the three output signals are combined. While the actual system involves only one filter, particularly to the innermost loop of Fig. 10 which describes pilot control of bank angle in response to the input, m, from the rest of the system. Instead of neglecting the dynamic characteristics of this innermost loop as was done in the previous simplified treatment, the approximate frequency response can be determined experimentally and included in the analysis.

It is sufficient to obtain an adequate representation of the closed-loop response over the frequency band of interest. At low frequencies this closed-loop response will be essentially $1/K_3$ as given in (10). The point at which the closed-loop response starts to fall off will, of course, vary somewhat in frequency dependent on the particular aircraft and pilot involved. As would be expected, the frequencies involved in the over-all position response of the controlled aircraft during the approach are considerably lower than that at which bank loop cutoff begins. Measurements made in a twin-engined Beech aircraft used in system flight tests show that the bank closed-loop response (with the inner loop only closed) is essentially flat out to an angular frequency of approximately 2 radians per second. This frequency is considerably above that at which gain cutoff occurs in the position (outer) loop. An attenuation rate of 12 db per octave has been used beyond this frequency to establish the phase contribution of this portion of the system at the lower frequencies significant in the outer loops.

Starting with this innermost closed loop response, the attenuation and phase characteristics of the encircling outer loops can be obtained by graphical procedures. The closed-loop responses of ϕ/n and ψ/o in terms of attenuation and phase are obtained by a successive process of graphical addition of the complementary filter characteristic to the inner closed-loop characteristic followed by application of the Nichols chart for conversion of open-loop response to corresponding

closed-loop response.[3,4] The attenuation and phase characteristics of the complementary filter are shown in Fig. 11 for a 2-second time constant.

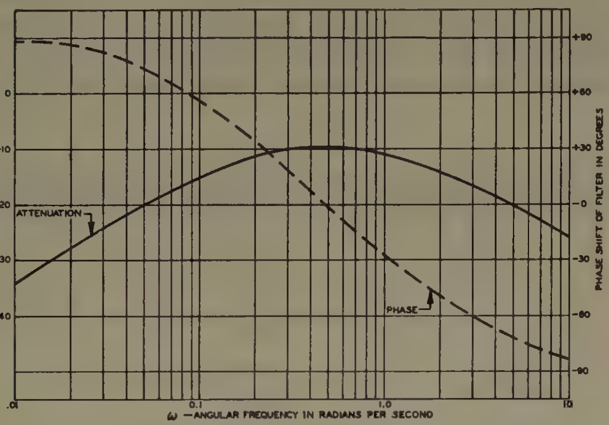

Fig. 11—Attenuation-phase characteristics of the two-section complementary filter. (Time constant = 2 seconds.)

The attenuation and phase of the outermost position open loop are obtained by addition of the attenuation and phase of ψ/o to those for the parallel combination of K_1, the direct radio feed and the filter feed associated with constant K_4, and also that of the transfer function y_0/ψ. Insertion of the quantity $1/D$ in terms of open-loop gain gives a graphical picture of the relation of the system gain cutoff to the distance of the aircraft from the localizer transmitter. The resultant position open-loop attenuation and phase diagram for the approach of a twin-engined Beech aircraft at 120 mph is shown in Fig. 12. Constants of the steering computer have been adjusted to achieve a suitable stable range for the system. The attenuation-phase analysis leads to a filter feed factor ratio in which a somewhat higher bank feed is used than would result from complementary adjustment.

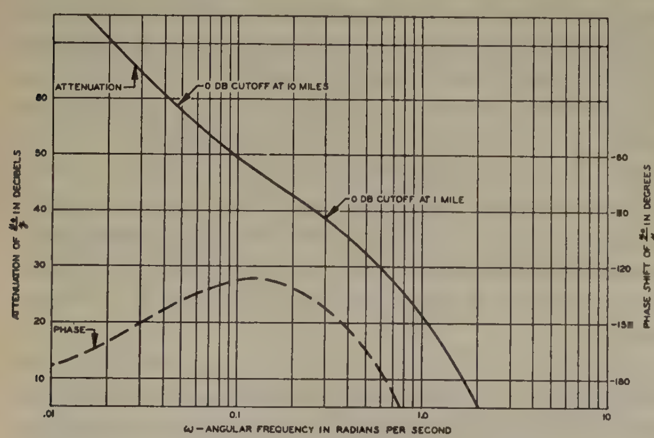

Fig. 12—Attenuation-phase curves for open displacement loop.

[3] H. M. James, N. B. Nichols, and R. S. Phillips, "Theory of Servo-Mechanisms," McGraw-Hill Book Co. Inc.; New York, N. Y., chap. 4, sec. 11 and 12; 1947.

[4] H. Chestnut and R. W. Mayer, "Servomechanisms and Regulating System Design," John Wiley and Sons, Inc., chap. 11–14; 1951.

This open loop has an attenuation rate of 12 db per octave and a phase shift of 180 degrees at very low frequencies. This rate of attenuation and negative phase shift decreases through the region of gain cutoff as required for stability according to the Nyquist criterion. The system has a phase margin of 40 degrees or more throughout the approach region from 10 miles to touchdown. In Fig. 13 the open-loop attenuation and phase have been transferred to a Nichols chart.

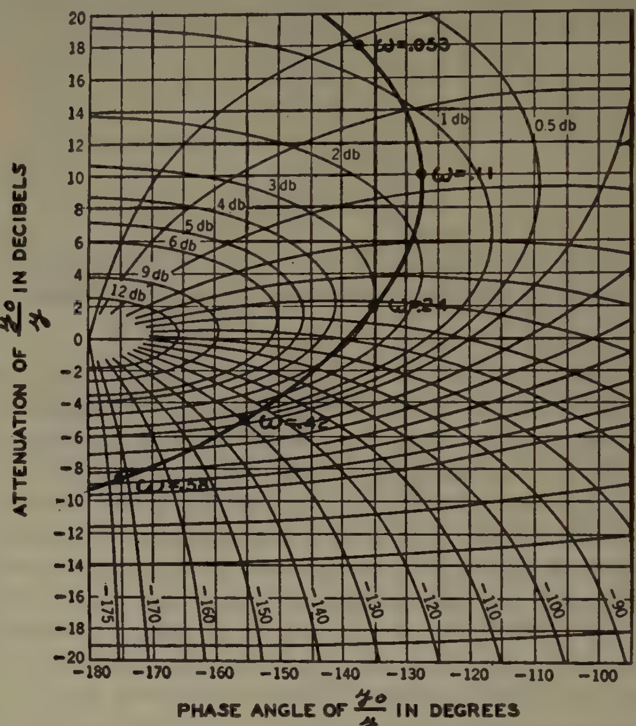

Fig. 13—Open-loop characteristics plotted on a Nichols chart for $D = 1$ mile.

There are some important factors to be considered in applying the results of the theoretical analysis presented in the preceding paragraph to the behavior of the true system. First, this analysis was carried out on the basis of a fixed gain (aircraft-localizer transmitter distance) assumed when considering the system response at any given distance (or corresponding position loop gain). Actually the position loop-gain parameter varies continuously during the approach. Fortunately, this gain change is at a sufficiently slow rate during the major portion of the approach to make the fixed-gain results reasonably applicable. Second, the probability exists that the aircraft will at times operate under conditions differing to some degree from those assumed in deriving the simplified transfer functions of (4) and (5).

Despite these restrictions, the results of attenuation-phase analysis have proven very useful in determining proper gain settings and in predicting results of system alterations. Flight tests, during which the significant variables were recorded, have given results which are in substantial agreement with those of the theory.

Two groups of typical localizer deviation recordings made during a recent flight test evaluation of the steer-

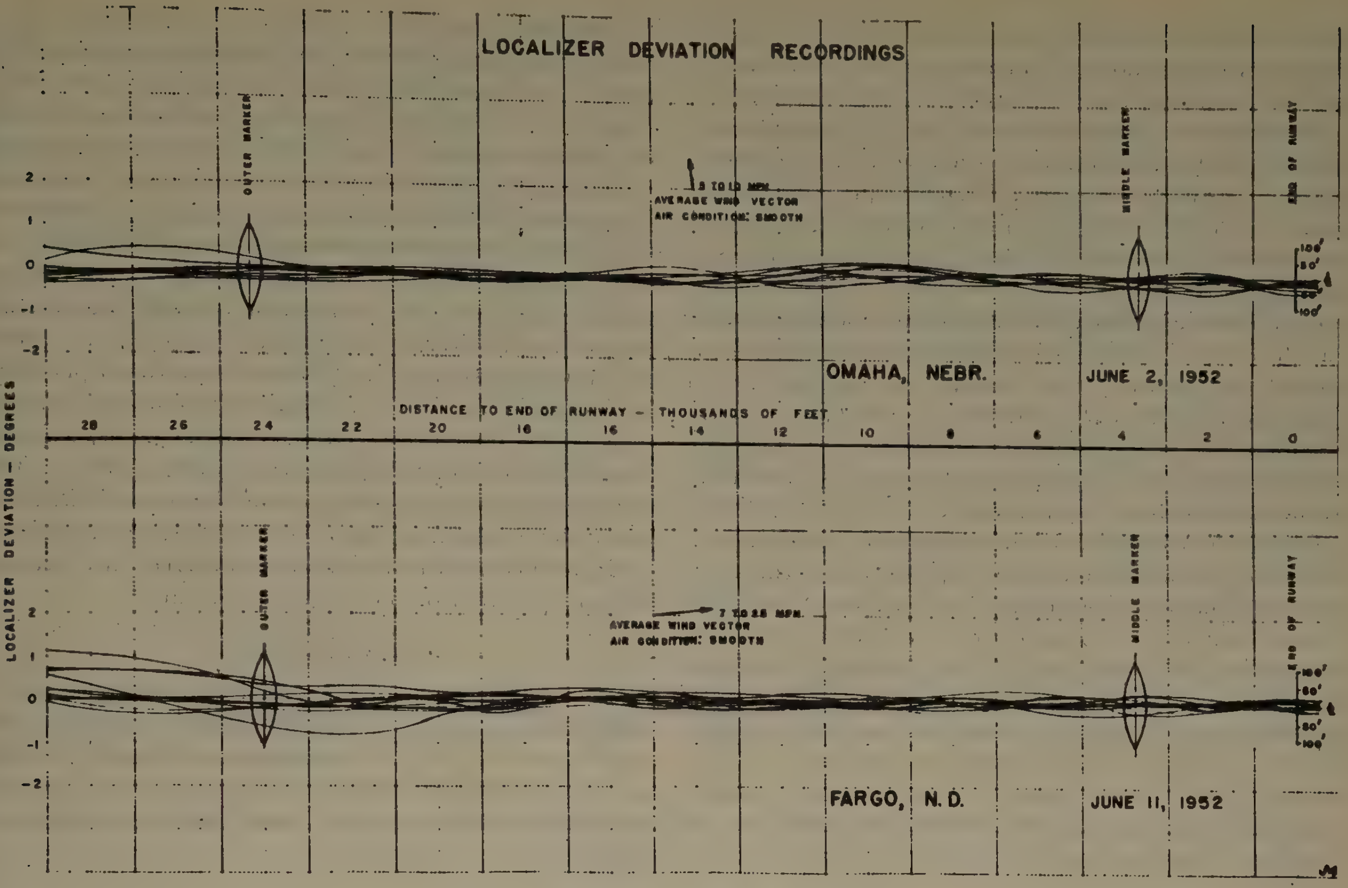

Fig. 14—Representative flight-test recordings.

ing computer are shown in Fig. 14. The data for these curves were obtained under simulated instrument conditions (pilot under the hood) at Omaha, Nebraska and Fargo, North Dakota. Ten approaches were made at each facility and the results are superimposed in the figure. Initial maneuvering including the procedure turn was accomplished with the aid of the course indicator described in the following section.

Integrated Flight Instrumentation

A photograph of the subject steering computer and associated instruments is shown in Fig. 15.

Fig. 15—Steering computer and instrumentation. (a) Steering computer. (b) Course indicator. (c) Approach horizon.

It is not intended to discuss detailed circuits here other than to say that conventional analog computer techniques of signal combination, 400-cycle modulation of dc signals, and phase sensitive detection are employed. Use of vacuum tubes is held to a minimum. Limiters are employed to prevent the computer from calling for an excessive bank angle to center the steering needle. The system includes circuitry and indicators for steering computer solution of the glide-path approach problem in addition to that of the localizer which has been discussed. In an alternate mode of operation, the computer provides steering information for maintaining the aircraft on a selected heading during cross-country flight.

A new cockpit instrumentation has been developed for use with the steering computer and also for use in general navigation during cross-country flight of the aircraft.[5] It has been the tendency in the past for each new piece of aircraft equipment to include its own separate cockpit instruments which were forced to compete for space and attention on the panel against the many others required. Of late it has been recognized that there is much need for integration of cockpit instrumentation to conserve panel space and also to make information presented to the pilot more easily assimilated.[6] Integrated pictorial displays prove to have advantages over separate symbolic displays in presenting several items

[5] S. H. Reiniger, "New picture aid for ILS-omnirange," *Aviation Week;* July 2, 1951.

[6] L. S. Beals, Jr., "Integrated instrumentation for modern aircraft," Institute of Aeronautical Sciences, Preprint No. 368.

of related information to the pilot in an easily interpreted form. Psychological factors must be considered in the choice of indicator arrangement and operation.

The course indicator shown in Fig. 15 is a multifunction pictorial instrument concerned with the navigation of the aircraft in the horizontal plane. It provides indications of compass heading, course deviation, and to-from information, and includes controls for selection of heading and omnirange or localizer courses. The display presents to the pilot a maplike picture of his position and heading relative to the selected course. It is intended that this indicator be used as reference for all maneuvers in the early phases of an ILAS approach. Heading and course selectors are set to the magnetic heading of the ILAS runway in this mode of operation. Maneuvers such as the procedure turn are readily accomplished with the aid of the continuous pictorial presentation. As used in making the intial entry on the localizer, the course indicator may be considered as a form of nonlinear pictorial computer. In this early approach phase when the pilot has time for considered decisions, he may choose the type of curved entry to the course which is most expeditious under the particular circumstances. The gain of the position control loop is low at this point and there is no need for the aircraft approach to be tied to the exponential curve which results from an automatic steering computation. When the aircraft is approximately on the localizer course, the shift can be made to the computed steering indication for the critical period of the approach from the region of the outer marker to touchdown. During this final approach phase, the pilot needs direct and precise steering instructions.

During the final approach phase the approach horizon instrument becomes the primary source of information for the pilot. It includes the steering indicator and an artificial horizon providing attitude information. Aircraft pitch angle and position of the glide slope with respect to the aircraft are presented in a manner which facilitates solution of the glide-path approach problem. The integration of these indications into a single instrument makes unnecessary frequent shifts in pilot attention during this most critical part of the approach. The heading and position situation of the aircraft with respect to the localizer path as displayed on the course indicator becomes a continuous monitoring check on the proper operation of the steering computer.

Acknowledgments

The authors wish to acknowledge the assistance of their associates at the Collins Radio Company in the work described. Mr. S. Kneemeyer of the Wright Air Development Center deserves particular mention for his original suggestions on the form of the course indicator display.

A Highly Stable Variable Time-Delay System*

Y. P. YU†, ASSOCIATE, IRE

Summary—**This paper describes a variable time-delay system having time jitter less than 0.00025 μsec, which is equivalent to 2.5 parts per million of its maximum time delay. To achieve this stability, time delay in this system is accomplished exclusively by means of linear bilateral elements. A distributed amplifier is used to compensate the losses in the delay elements. Due to the fact that only a limited number of elements can be installed in a practical circuit, the signal pulse is permitted to travel through each delay element many times in order to increase the amount of total time delay. One of the experimental units having a total time delay up to 100 μsec in step of 1 μsec has been found to be satisfactory. The usual causes of time jitter in conventional time-delay circuits such as, variations of cut-off characteristics, noise, hum, and fluctuations of supply voltages, cannot affect the stability of this system. Practical circuits as well as experimental results are described.**

Introduction

VARIABLE TIME-DELAY CIRCUITS are frequently needed for establishing the coincidence of the sweep and a given signal in high-speed oscillographs, as well as for measuring the time interval between two signals in radar or loran systems. Experience has shown that difficulties would arise in using conventional sweep-delay circuits in conjunction with high speed sweeps. These difficulties are caused chiefly by the irregular changes of total time delay which appear as time jitter on the screen of the cathode-ray tube or other indicators. For instance, when one wishes to observe a repetitive signal on a sweep of 400 inches per μsec the maximum amount of jitter along the trace should not exceed 0.1 inch, which corresponds to 2.5×10^{-4} μsec in time. Thus the constancy of the time-delay circuit should be better than 0.00025 per cent for a delay of 100 μsec.

One of the conventional methods employs a sawtooth voltage to initiate a trigger generator which is normally biased beyond cutoff with a negative dc potential.[1–3] As soon as the amplitude of the sawtooth voltage reaches a predetermined value, a switching action takes place in the trigger generator. At the end of the switch-

* Decimal classification: R143.4×R389.15. Original manuscript received by the Institute, April 24, 1952; revised manuscript received, September 24, 1952. Presented at the 1952 IRE National Convention.

† Du Mont Laboratories, Inc., Clifton, N. J.; now with the Advance Electronics Company, Passaic, N. J.

[1] J. T. Gordon, "Variable pulse delay for radar ranging," *Electronics;* October, 1951.

[2] Chance, Hughes, MacNichol, Sayre, and Williams, "Waveforms," vol. 19, Rad. Lab. Series, McGraw-Hill Book Co., Inc., New York, N. Y.; 1949.

[3] M. I. T. Radar School Staff, "Principles of Radar," chapter 2, McGraw-Hill Book Co., Inc., New York, N. Y.; 1947.

ing action, the sawtooth voltage will return to its normal minimum potential and an output pulse will be generated by the trigger generator. It is conceivable that noise, hum, or variations of tube characteristics will cause erratic switching actions and fluctuations of the resultant time delay.

Another form of conventional variable delay system is accomplished by converting electrical pulses into sonic pulses by means of a transducer, then the sonic pulses are delayed through a proper medium, such as mercury and water, and at the end of the delay the sonic pulses are changed back into electrical pulses by means of a second transducer.[4,5] The total amount of insertion losses in this type of delay system is very high, over 60 db normally. Other disadvantages include difficulties of mounting both the input and output transducers properly, poor response for short pulses, and instabilities caused by mechanical vibration, thermal variations, etc.

For short periods of fixed delay, both real and artificial delay lines[6,7] are generally suitable for most applications. However, these are not practical when the delay period is required to be either variable or longer than 10 μsec with short rise time.

It is the purpose of this paper to describe a variable time-delay system having time jitter less than 2.5 parts per million of its total time delay, yet neither requiring special components nor occupying a large amount of space and weight.

Operating Principles

The principle of operation of the system to be described may be explained with the aid of the accompanying figures. In Fig. 1, tube T_1 is the input preamplifier, tube T_2, T_3, and T_4 are connected as a distributed amplifier. There are three advantages in employing a distributed amplifier in this system, (1) good response for narrow pulses, (2) provision of correct impedance at both the input and output terminals in order to match lines A and B, and (3) the grid and plate capacitances of the tubes can be absorbed by the transmission networks as parts of their shunting elements, thus minimizing the frequency limitations and reflections caused by tube capacitances. When a positive pulse is applied to amplifier T_1, a negative pulse will travel to both ends of the line from the plate of T_1. The pulse to the right is finally absorbed by terminating resistor R. The pulse to the left will be reflected back as a positive pulse by the short-circuited end of line A. When this reflected positive pulse reaches the grids of T_2, T_3, and T_4, a negative pulse will be produced at the plates of each of these three tubes and will travel toward both left and right ends. The pulses which travel to the right will finally be absorbed by resistor R. The pulses which travel to the left will combine into a single negative pulse if the propagation constants of both grid and plate networks are made equal. When this single negative pulse reaches the short-circuited end of line A, a total reflection again occurs. Thus a positive pulse will again travel to the grids of T_2, T_3, and T_4. The left side of Fig. 2(a) shows both the incident (negative) and reflected (positive) pulses at the plate of the tube T_2 as they appear on the screen of a cathode-ray tube. The blocking oscillator generates a single positive pulse of constant amplitude for each positive reflection produced by the short-circuited end of line A. Fig. 2(b) shows the waveform of an oscillogram taken at the output of the blocking oscillator. The counter circuit serves two purposes: (1) to register the number of positive pulses generated by the blocking oscillator, and (2) to trigger the gate-pulse generator at the end of a predetermined number of reflections designated by the letter M in Fig. 2(a). Fig. 2(c) shows the waveform of a storage type counter circuit, of which the output in-

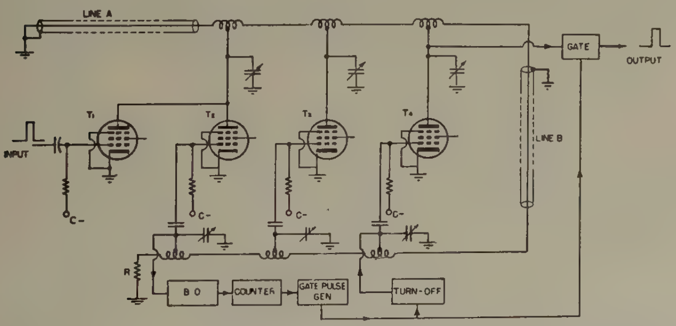

Fig. 1—A simplified block diagram of the system.

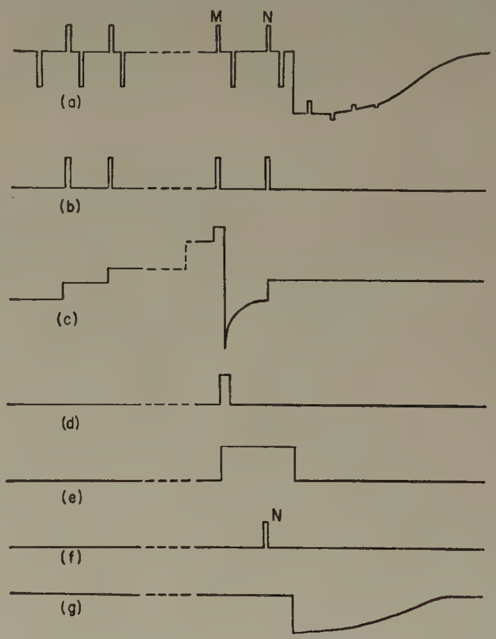

Fig. 2—Waveform at various points of the delay system.

[4] H. J. McSkinnis, "Theoretical analysis of mercury delay line," *Jour. Acous. Soc. of America*; July, 1948.
[5] J. F. Blackburn, "Components Handbook," chapter 7, vol. 17, Rad. Lab. Series, McGraw-Hill Book Co., Inc., New York, N. Y.; 1949.
[6] H. E. Kallmann, "Equalized delay lines," Proc. I.R.E.; September, 1946.
[7] A. H. Turner, "Artificial lines for video distribution and delay," *RCA Review*; December, 1949.

creases one step for each input pulse. The gate-pulse generator produces a positive gate pulse as soon as the number of reflections by the short-circuited end of line A reaches the value M. A control is provided in the counter circuit to select the value M, this in turn to control the amount of time delay. Fig. 2(d) shows the time relation between the gate pulse and pulses produced by other circuits. The gate-pulse generator serves the following two purposes: (1) to open the gate circuit for a short interval, as shown in Fig. 2(e), just sufficient to allow the positive pulse following M number of reflection in line A to go out (this pulse is designated by the letter N in Fig. 2(a)); and (2) to trigger the turn-off circuit after the pulse N has reached the output terminal of the gate circuit. Fig. 2(g) shows a long negative pulse which is produced by the turn-off circuit and is to be fed of the grids of amplifier tubes T_2, T_3, and T_4. Then the entire system returns to its quiescent condition. The right side of Fig. 2(a) shows the wave-form at lines A and B when the system returns to this condition. It is noted that the reflections become smaller due to the fact that amplifier tubes T_2, T_3, and T_4 are being cut off.

Practical Considerations

The choice of lines A and B in Fig. 1 is governed by the amount of time delay required between each reflection of the system, namely, the amount of time delay of each step. Spirally-wound delay lines generally have much more time delay per unit length then rf coaxial lines. However, the attenuation of spirally-wound delay lines is also much higher. For instance, RG65U delay line has a time delay of 41.8×10^{-9} second per foot and an attenuation of 22 db per 100 feet at 10 mc; on the other hand, RG58U coaxial line has a time delay of 1.525×10^{-9} second per foot and an attenuation of one db per 100 feet at 10 mc. The operating principle described above has shown that the time delay between two positive reflections of the system is equal to $2T_a+T_b$ plus the time delay of the grid and plate lines of the distributed amplifier, where T_a represents the total time delay of line A and T_b represents the total time delay of line B. Furthermore, the attenuation of the system is $2D_a+D_b$, where D_a is the attenuation of line A and D_b is the attenuation of line B, assuming that the attenuations of both the grid and plate lines are negligibly small.

Therefore, in order to have continuous circulation of pulses within the system, the ratio of the output signal voltage E_0 to the input signal voltage E_{in} of the distributed amplifier may be expressed as

$$\frac{E_{out}}{E_{in}} \geq 20 \log^{-1} (2D_a + D_b). \tag{1}$$

It is preferable to use m-derived sections (see Fig. 3) in the distributed amplifier of this system because constant phase shift can be obtained up to about two-thirds of the cutoff frequency, and greater bandwidth can be obtained with a given amount of grid and plate capacitances. A typical m-derived distributed amplifier is shown in Fig. 4. As long as the propagation constants of both plate and grid lines are made equal, the plate

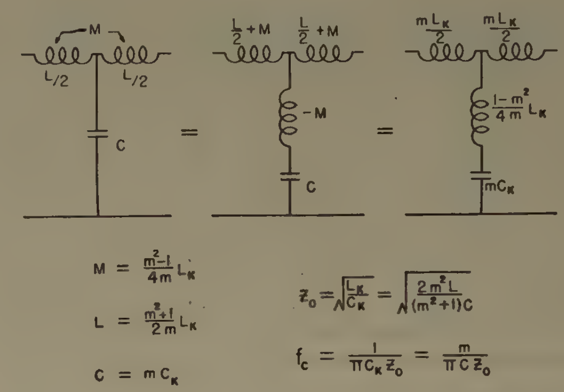

Fig. 3—Typical m-derived network.

current pulses produced by various tubes will add up as a single pulse at the right terminal of the plate line. The plate current pulse traveling to the left will be absorbed by the terminating resistor R_2. By remembering

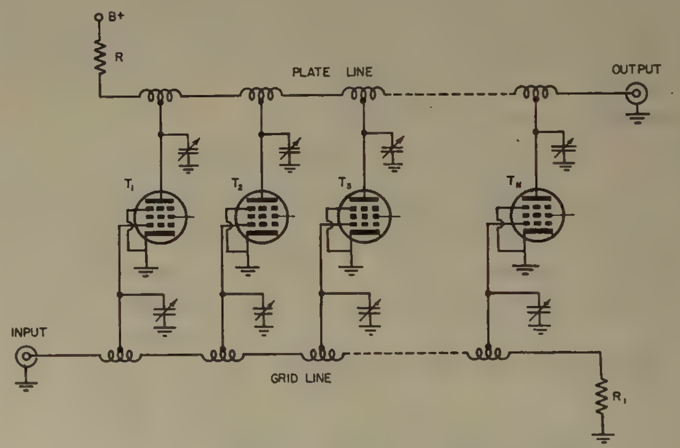

Fig. 4—A stage of distributed amplifier.

that the propagation constants of both lines should be equal,

$$\sqrt{L_{k1}C_{k1}} = \sqrt{L_{k2}C_{k2}},$$

and assuming q to be w/w_c, then that

$$q = w\sqrt{L_{k1}C_{k1}/2} = w\sqrt{L_{k2}C_{k2}/2},$$

an expression for voltage amplification can be written

$$\frac{E_0}{E_{in}} = \frac{gmZ_{02}}{2} \frac{nm^3}{\sqrt{m^2-q^2}\,[m^2+(m^2-1)q^2]}, \tag{2}$$

where n is the number of tubes, and the expression for phase shift is

$$\theta = -2n \tan^{-1} \cdot \frac{mq}{\sqrt{m^2-q^2}}. \tag{3}$$

The time delay for the stage may be found as follows.

$$t_0 = \frac{d\theta}{dw} = \frac{1}{w_c}\cdot\frac{d\theta}{d_q} = \frac{n}{w_c}\cdot\frac{m^3}{\sqrt{m^2 - q^2}\,[m^2 + (m^2 - 1)q^2]}. \quad (4)$$

The problem of impedance matching in lines A and B and the distributed amplifier should be carefully considered. If undesirable echoes are allowed to go through the system many times, the amplitude of the echoes may become high enough to trigger the blocking oscillator and counter. Undesirable echoes may be caused by stray capacitances at soldered joints, different characteristic impedance of the m-derived network at the high end of the pass band, or the lead inductance and stray capacitances of the terminating resistor. These causes can be kept to a minimum by careful design and construction. In addition, it is recommended that all tubes in the distributed amplifier unit be biased sufficiently below cutoff, so that undesirable reflections which have their amplitudes generally much lower than the main signal will not be able to circulate within the system after their generation.

Time jitter generated in lines A and B or the distributed amplifier unit would become serious since the input signal travels many times through these units. The usual causes of time jitter are hum and noise. Hum is usually introduced in power supplies, therefore the use of power supplies with low ripple percentage becomes necessary. Noise can be greatly reduced by (1) reducing the values of the characteristic impedance of lines A and B and the m-derived networks, since noise figures generally decrease with the decrease of the value of impedance in the circuit; (2) having all tubes in the distributed amplifier unit biased sufficiently below cutoff so as to eliminate from circulation noises generated during the absence of main signal pulses; and (3) raising all main signal pulses to a high level (above 50 volts) with the use of high-current tubes in the distributed amplifier to keep negligibly small noises generated during the presence of main signal pulses.

The lower limit of the time delay of one step is governed by the maximum value of the repetition rate obtained with the blocking oscillator provided that the duration of the signal pulse is less than the amount of time delay in one step. For high repetition rate the transformer employed in a blocking oscillator should have a very-high-frequency response, and a very small amount of leakage inductance, stray capacitances and core losses. The first requirement determines the rise time of the output pulse and the second determines the decay time. Pulse transformers used in the experimental units of this paper consist of three 40-turn windings of No. AWG32 Formex wire wound on the same leg of a Westinghouse Hypersil core. The pulse width can best be reduced by the use of an RC network of very small time constant in the grid coupling circuit. To further reduce recovery time a crystal diode may be connected in parallel with the grid-leak resistor for dc restoration.

Complete Circuits

Fig. 5 shows a circuit diagram of a variable delay system with one-microsecond steps and capable of giving a maximum delay of 12 μsec. T_1 and T_2 are used as a preamplifier. The transformers at the plates of these tubes not only serve for coupling but also serve to shorten the duration of the input pulses when they are longer than the system can handle. Furthermore, the frequency response of these transformers should be very high so that the shapes of narrow pulses will not be altered. Pentodes type 5763 are used in the distributed amplifier unit, because they have high power ratings and can produce output pulses of sufficiently high amplitude. All trimmers in the distributed amplifier are required to be adjusted in operating condition in order that the total shunting capacitance of each section of both the grid and plate lines of the distributed amplifier is identical and equal to a proper value. In case that two plates, or grids, are connected in parallel, the capacitance of the trimmer will be decreased by an amount equal to that contributed by the additional plate or grid, thus no discontinuity will be caused by the plate or grid capacitance of the additional tube. Both lines A and B are Type RG65U. The time delay of line B should be longer than the maximum duration of the input pulse which will be required to pass the system. Double triode 5687, T_6, is used as a blocking oscillator. This tube has a very high transconductance and can generate pulses of very rapid rise-time. Cathode follower T_7 is used to eliminate the undershoot generated by demagnetization of the transformer in the blocking oscillator.

Double diode T_8 is used as an energy storage type counter. The first half duo-triode T_9 is a cathode-follower to provide a low impedance source for discharging capacitor C_1. The second half of T_9 is arranged as a blocking oscillator to perform switching action for terminating further increase of the number of incremental steps and discharging capacitor C_2 in the counter circuit. Potentiometer R_1 serves to select the number incremental voltage steps after which switching action takes place and the system completes one cycle. Thus R_1 is the panel control for selecting the total amount of time delay. As an alternative, potentiometer R_1 may be replaced by a number of fixed resistors and a single pole multisection switch. In this case all fixed resistors are connected in series as a voltage divider, and the switch selects the quiescent dc potential at the grid of the first half of T_9, which in turn selects the number of incremental voltage steps on C_2. The output from the transformer at the plate of T_9 is used to trigger a gate-pulse generator which is also a blocking oscillator. The duration of the gate pulse is made equal to, or slightly longer than, the maximum duration of the input pulse plus the amount of time delay between each incremental voltage step in the counter circuit. To achieve this goal the frequency response of the transformer should be

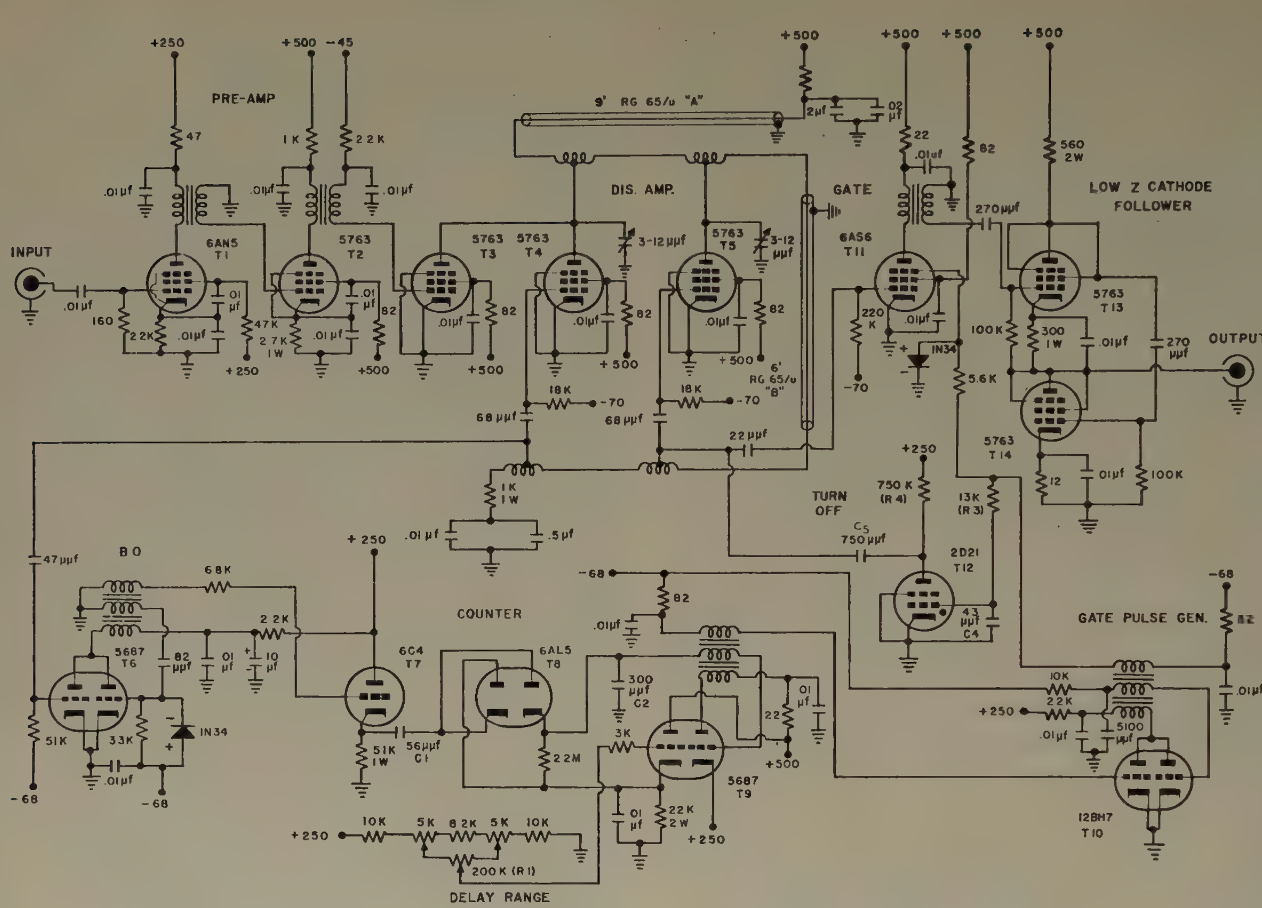

Fig. 5—Complete circuit diagram of a variable delay system with 1 μsec per step and a maximum delay of 12 μsec.

sufficiently low to allow the natural duration to be at least equal to, or exceed, the desirable value.

T_{11} is a 6AS6 pentode and used as a gate circuit. Both the control grid and suppressor grid of this tube have a very sharp cut-off characteristic. Normally both the control grid and suppressor grid are biased beyond cutoff. Thus no signal will be delivered to the grid of T_{13} unless both the control and suppressor grids receive a positive pulse simultaneously. T_{12}, type 2D21 gas tube, is nonconducting, normally. As soon as it conducts a negative pulse will be generated at its plate and is applied to the grids of the distributed amplifier unit. This will terminate further circulation of the signal pulse within the system. R_3 and C_4 are used to delay the firing of the gas tube T_{12}, until the signal pulse has completely passed the gate tube T_{11}. Additional function of R_3 is to limit the grid current of T_{12}. The maximum repetition rate of the system is limited by the recovery time of the potential at the plate of T_{12}, therefore, the time constant of R_4C_5 should not be larger than necessary. The minimum value of C_3 is determined by the amount which is capable of allowing a complete termination of the signal circulation within lines A and B and the distributed amplifier unit. Resistor R_4 cannot be made smaller than the value which is the minimum permitting the deionization of the gas tube T_{12} after its grid returns to the quiescent potential.

T_{13} and T_{14} are arranged as a very low output impedance cathode follower. In this circuit the amplification of T_{14} is used to increase the transconductance of T_{13}. If r_P/μ is much smaller than r_P and R_5, the output impedance becomes $r_P/(\mu\mu')$, where μ' is the gain of the amplifier T_{14}.

Fig. 6 shows the complete circuit diagram of another delay system of this kind. The time delay is 4 μsec per step and can provide a total time delay of over 88 μsec. The circuit is somewhat similar to that of Fig. 5. Because both delay lines are longer and have more attenuation the driver amplifier consists of two pentodes, type 5763, and the distributed amplifier unit consists of three sections. The additional shunting capacitance in the transmission network caused by connecting the grids or plates of two or three tubes in parallel is compensated by reducing the capacitance of the trimmer in that particular section. The counter circuit is somewhat similar to that of Fig. 5. An additional blocking oscillator T_9 is used to prevent the width of input pulses from affecting the amplitudes of the incremental voltage steps of the counter circuit. Because the time per step is longer and the number of steps is higher, capacitor C_1 and C_2 have higher values and a smaller ratio. The switch tube T_{13} is a duo-triode, and is connected in parallel in order that a higher current capacity is available for discharging capacitor C_2. T_{14} is arranged to

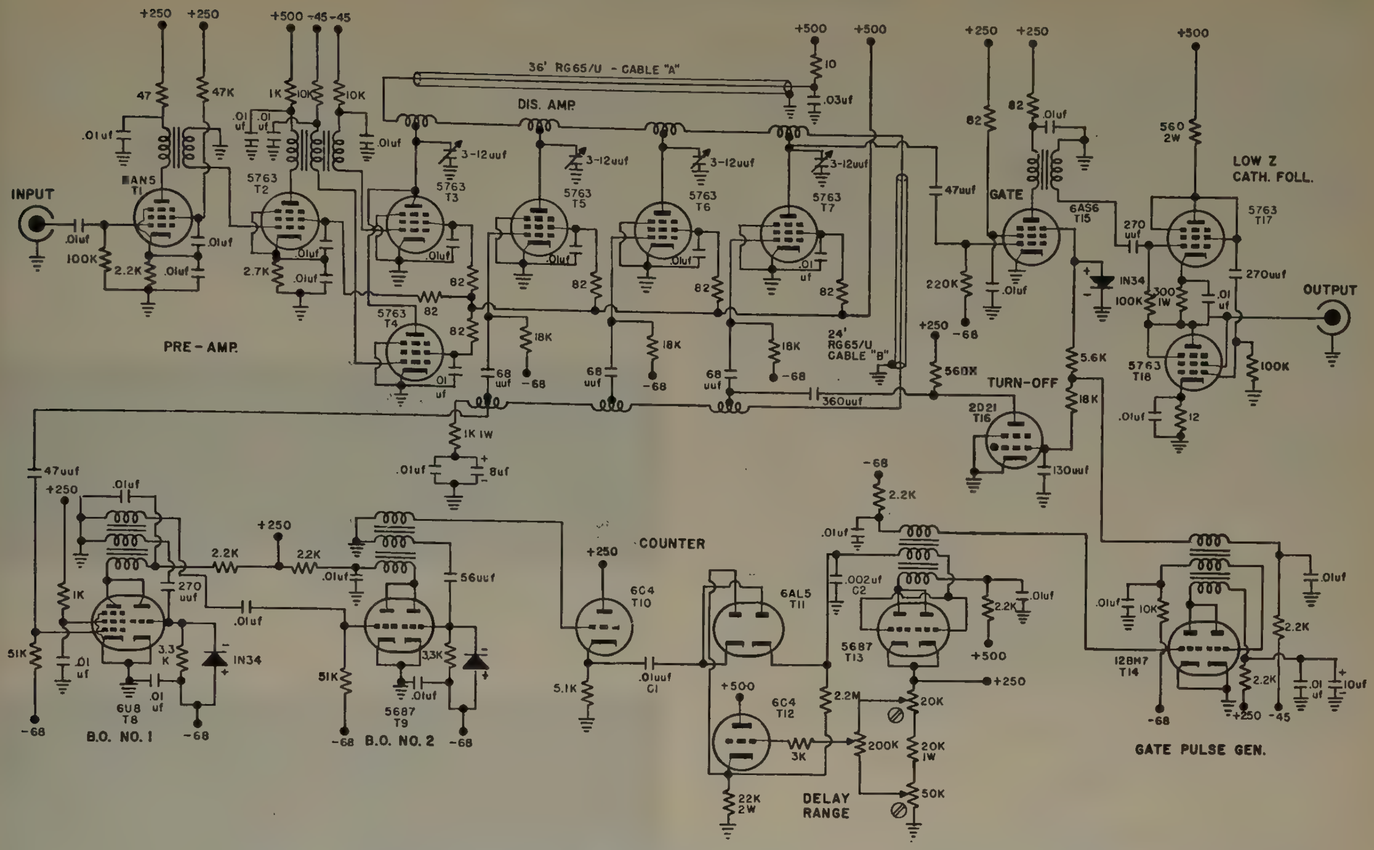

Fig. 6—Complete circuit diagram of a variable delay system with 4 μsec per step and a maximum delay of 88 mc.

generate a gate pulse of about 3 μsec in duration, which is the time required for a pulse to make a round trip in delay line A. The control grid of T_{15} is fed by signals at the plate of T_7, instead of at the grid as in Fig. 5. There are two reasons for such a change in this unit, (1) the amplitudes of the signal pulses are higher at the plate of T_7 and (2) the duration of the gate pulse can be made shorter. However, delay line B of Fig. 5 is short and does not attenuate signals as much as Fig. 6.

Experimental Results

There are numerous difficulties in determining the amount of time jitter in the system experimentally, because it requires the measurement of time interval less than 0.0001 μsec. It is suggested that a temperature-regulated crystal oscillator and a chain of frequency-dividing circuits that reduces the crystal frequency to a desirable value be used. The output of this triggers a pulse generator and the delay system. A high speed syncscope is used as indicator. A tuned RF amplifier resonated at a high harmonic of the crystal is used to excite the verticle deflecting plates. The sweep of the sync-scope is triggered directly by the output of the delay system. The chief objection to this proposal lies in the generation of a sharp pulse at the exact instant of every cycle of a low-frequency sine wave. The resultant time jitter from this method is normally much higher than can be tolerated.

The method employed to determine the amount of time jitter in the system may be described with the aid of the block diagram shown on Fig. 7. The pulse generator produces pulses of 0.1-μsec duration as a repeti-

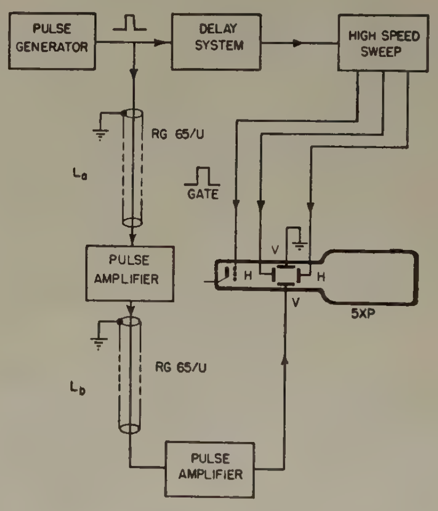

Fig. 7—Block diagram of the method adopted for time jitter test.

tion rate of 120 pulses per second. Two pulse amplifiers having a gain of 20 db each are employed to compensate for the losses of the delay lines L_a and L_b. Each of these delay lines are more than 250 feet in length. The output of the second pulse amplifier is used to excite the

vertical deflecting plates of a 5XP cathode-ray tube. The accelerating voltages of the 5XP are −4,000 volts at the cathode and +16,000 volts at the third anode.

The output of the pulse generator also enters the delay system and then triggers the high-speed sweep circuit. The high-speed sweep circuit is capable of generating a sweep speed of 400 inches per μsec and having a time jitter of less than 0.0001 μsec. The circuit diagram is shown in Fig. 8. The output of the first blocking oscillator serves as a gate pulse to switch on the beam of the cathode-ray tube, and also triggers the second blocking oscillator after differentiation. The output of the second blocking oscillator turns on the sweep tube, 4X150A, causing C_1 to discharge and C_2 to charge. If the value of C_3 is made large enough to preserve constant screen-to-cathode potential during the sweep period, the discharge of C_1 will be constant due to the constant plate current. The charge of C_2 will also be essentially constant because the sum of the plate and screen currents is very nearly constant. Thus linear push-pull sweep voltages can be obtained from the plate and cathode of the 4X150A tetrode. The choice of the sweep tube was governed by the requirements that very-high-tube current must be available during the sweep period and very small amounts of tube capacitance and lead inductance can be tolerated. Further information on the high-speed sweep circuit may be found elsewhere in the literature.[8]

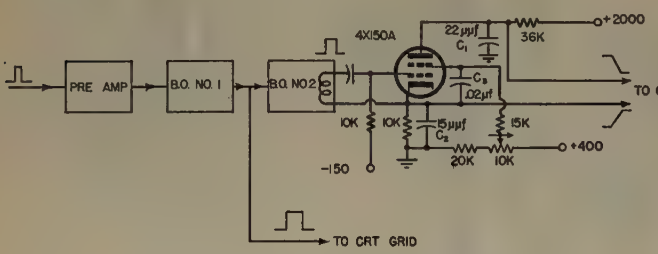

Fig. 8—Simplified circuit diagram of the high-speed sweep circuit.

By adjusting the amount of time delay in the delay system and the length of both lines L_a and L_b either the front edge of the trailing edge of the 0.1 μsec pulse can be seen on the screen of the 5XP cathode-ray tube. Fig. 9 shows the front edge of the 0.1-μsec pulse after 30-μsec delay through L_a, L_b, and pulse amplifiers, while the delay system was set to give a total delay of the same amount. Fig. 10 shows the trailing edge of the same pulse under identical conditions, except the length of L_a, was shortened by approximately 0.1 μsec. Fig. 11 shows the front edge of the same pulse with L_a, L_b, and the delay systems removed. The time of exposure employed in taking the picture in Figs. 9, 10, and 11 was 30 seconds and the repetition rate 60 per second. Thus the total number of traces in these figures is 1,800. Comparison of Fig. 9 with Fig. 11 reveals that the difference in width of the two beam traces is not more than 0.02 inch when the photographs are enlarged until the sweep length equals five inches. This indicates that the total amount of time jitter produced by the two delay systems for 30-μsec time delay is less than 5×10^{-11} seconds in 30 seconds with its sweep speed set at 400 inches per μsec.

Fig. 9—Front edge of the 0.1-μsec test pulse after 35 μsec delay; sweep duration 0.0125 μsec; time of exposure 30 seconds; and repetition rate at 60 per second.

Fig. 10—Trailing edge of the 0.1 μsec test pulse after 35-μsec delay; sweep duration 0.0125 μsec; time of exposure 30 seconds; and repetition rate at 60 per second.

Fig. 11—Front edge of the pulse shown in Fig. 9 after passing through the pulse amplifiers without delay cable; sweep duration 0.0125 μsec; time of exposure 30 seconds; and repetition rate at 60 per second.

When the total time delay approaches 100 μsec difficulties arise because a long delay line is required to delay the signal to the vertical deflecting plates. This would deteriorate the rise time of the signal pulse even if the number of pulse amplifiers were increased. Thus it is extremely difficult to measure the exact amount of time jitter when time delay is long.

The time jitter produced by the sweep circuit and the pulse amplifiers does not affect the accuracy of this method of measurement since the result is based on comparison of two beam traces, one generated with only the sweep circuit and pulse amplifier, and the other generated with the sweep circuit, pulse amplifiers, delay cables, and the variable delay systems under test.

[8] Y. P. Yu, H. E. Kallmann, and P. S. Christaldi, "Millimicrosecond oscillograph," *Electronics;* July, 1951.

Conclusion

The reason this system has much higher stability than conventional time-delay circuits is obvious. In the above description and the block diagram of Fig. 1 the signal pulse travels back and forth in lines A and B in which the attenuation is compensated for by the distributed amplifier T_2, T_3 and T_4, and finally goes out through the gate circuit. Thus the time delay is accomplished exclusively by linear bilateral elements, which includes lines A and B, inductances and capacitances at the grids, and plates of the distributed amplifier. Accordingly, the output pulse is the same one that has been fed into the system—unlike most other electronic delay systems of which the output pulse is a new pulse generated in the system. Any variation in cutoff characteristics of electron tubes, noise, hum, temperature, and change in supply voltages, which cause a major portion of time jitter in conventional electron-tube time-delay circuits, may produce time jitter only in the gate pulse and the turn-off pulse but cannot alter the number of reflections in lines A and B. Furthermore, by maintaining both the incident and reflected pulses in lines A and B at a high level, above 50 volts, and by keeping the characteristic impedance of both lines A and B below 1,000 ohms, noise, hum, or echoes due to imperfected matching can be eliminated when a high negative bias is applied to the tubes of the distributed amplifier.

There are two outstanding limitations of this system in its present form: (1) The signal pulse cannot have its duration longer than the time delay of one step of the system; (2) the time between any two adjacent input pulses is required to be longer or at least equal to the total time delay of the system plus its recovery time. These two limitations introduce no inconvenience for many applications such as sweep delay in oscillographs, pulse delay in radar ranging, or propagation studies, although objections may arise in some other applications.

While there is much remaining to be done in the way of improving and refining the circuits involved, it has been found that the method described in this paper is one of the most promising approaches for obtaining variable time delay of very high stability for unidirectional pulses. Particularly, the system has proved to be very useful for the application of sweep trigger delay in high-speed oscillographs.

Factors Affecting the Performance of Linear Arrays*

L. L. BAILIN† AND M. J. EHRLICH†, SENIOR MEMBER

Summary—The performance of a linear array, which has been designed for low side-lobe level, is markedly affected by small variations in element excitation, introduced primarily, by the inaccuracies that are inherent in the manufacture of the array. Thus, the phase and amplitude of each element contain a slight randomness and the array performance must be determined by the application of statistical methods. This method of analysis has been formulated for the generalized symmetric linear array and computed for the special cases of three 24-element linear-shunt slot arrays using a Dolph-Tchebyscheff current distribution. The statistics give the probability that the side-lobe level will exceed an arbitrary comparison value as a function of the magnitude of arbitrary manufacturing tolerances.

The results indicate that the lower the design value of the side-lobe level the greater the perturbation to be expected for the allowed tolerance. Thus, an additional restriction is imposed upon array design which forces the designer either to require very small tolerances in manufacture or to overdesign the array in order to compensate for the perturbations introduced by the manufacturing processes.

I. Introduction

A PRIMARY PROBLEM is the design of antenna arrays is the satisfaction of the requirements of side-lobe level and beamwidth. An additional major consideration which has only recently received an analytical treatment[1] is the problem of the deterioration of the beamwidth and side-lobe level arising from the variations in the excitation of each element. These variations are due primarily to the inaccuracies inherent in the manufacturing processes used to produce the array. The first problem has been discussed in great detail by many authors (see, for example, Silver[2]), and it will be the purpose of this paper to analyze the second problem. The analysis is formulated in general for a symmetrically excited broadside array and then, as a specific example, is applied to a linear shunt-slot array which uses a Dolph-Tchebyscheff[3] distribution for the element excitations. This distribution optimizes the relationship between beamwidth and side-lobe level.

The method of analysis is general and may be applied to any linear array of radiators with arbitrary excitation, if the total mutual coupling between individual radiators may be neglected and no correlation exists between the inaccuracies of any two sources. In fact, the statistical method shown here may be applied to any radiative device whose total effect is obtained by summing the effects from a large number of smaller radiators. If the amplitude and phase of the excitation from each radiator are independent functions of the

* Decimal classification: R125.1×R325.11. Original manuscript received by the Institute, November 27, 1951; revised manuscript received September 26, 1952.

† Research and Development Laboratories, Hughes Aircraft Co., Culver City, Calif.

[1] J. Ruze, Presented at IRE Meeting, New York, N. Y.; January, 1951.

[2] S. Silver, "Microwave Antenna Theory and Design," chap. 9, McGraw-Hill Book Co., Inc., New York, N. Y.; 1949.

[3] C. Dolph, "A current distribution for broadside arrays which optimizes the relationship between beam width and side-lobe level," Proc. I.R.E., vol. 34, pp. 335–346; June, 1946.

physical dimensions of the structure, size and spacing, then the technique developed in this paper may be modified to give useful results concerning the effect of manufacturing inaccuracies.

II. General Method

The general method to be used in this analysis may be applied to any distribution of N independent radiators. The magnitude of the instantaneous field strength at a point P from such an array can be given as

$$\left| E_N \right| = \left| \sum_{i=0}^{N} A_i \exp (j\delta_i) \right|, \qquad (1)$$

where A_i is the relative amplitude and δ_i, a function of P, is the relative phase of the contribution to the field pattern from the i-th source. However, the numerical computations for practical arrays become somewhat lengthy if the method is applied to the formulation given by (1) which involves the exponential factor. In the special case of $2n$ independent radiators spaced symmetrically about a center line and symmetrically excited, as shown in Fig. 1, a great simplification can be achieved in the calculations. Then, the magnitude of the field in the direction making an angle θ with the normal to the line of sources may be expressed as follows:

$$\left| \frac{E_{2n}(\theta)}{2} \right| = \left| \sum_{k=1}^{n} A_k \cos \delta_k \right|. \qquad (2)$$

The general method consists of two parts. First, from physical considerations, it will be shown that A_k and δ_k are determined by the physical dimensions and spacing of the elements. Thus, inaccuracies inherent in the manufacture of the array will produce a fluctuation of physical parameters about their design values which will be reflected in both the amplitude and phase of each radiator. It must be shown from physical considerations that, to good approximation, the individual amplitude fluctuations are independent of each other and of the phase fluctuations. Thus, A_k and δ_k can be regarded as independent random variables and, from their statistical parameters, those of the absolute value of the electric field pattern can be calculated. This is the statistical portion of the method. Finally, the probability that the magnitude of the perturbed field will exceed an arbitrary reference value is derived. Thus, the general method relates the fluctuations in the array design parameters of the individual radiators to the probability that the magnitude of the field will attain or exceed a prescribed value.

III. Symmetric Slot Array

While the analytical method is applicable to any symmetrical array, the calculations will be restricted to the special case of a symmetrical shunt-slot array on the broad face of a rectangular waveguide. This array is to be realized physically as shown in Fig. 2. The radiating elements are spaced symmetrically about a transverse center line and are symmetrically excited as shown in Fig. 1. It will then be shown that the phase of excitation of each slot depends, to good approximation, only upon the slot spacing, d, and the slot length l, and the magnitude of the excitation of each source may be considered as a function only of x, the slot's displacement from the center of the broad face of the guide. The desired pattern is obtained by the choice of proper values of the design parameters, d, l, and x for

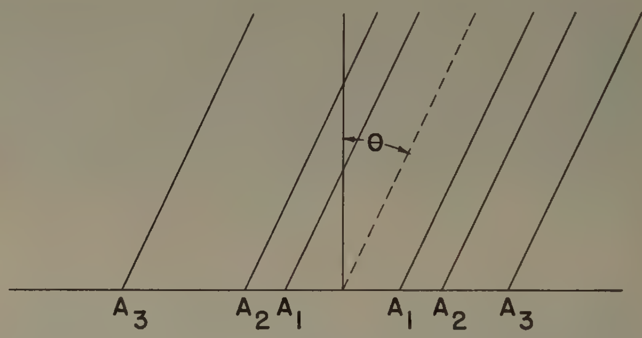

Fig. 1

each slot. However, when the slots are cut, random errors are introduced in these parameters, and it is assumed that the resulting parameter values are normally distributed about a mean or design value.

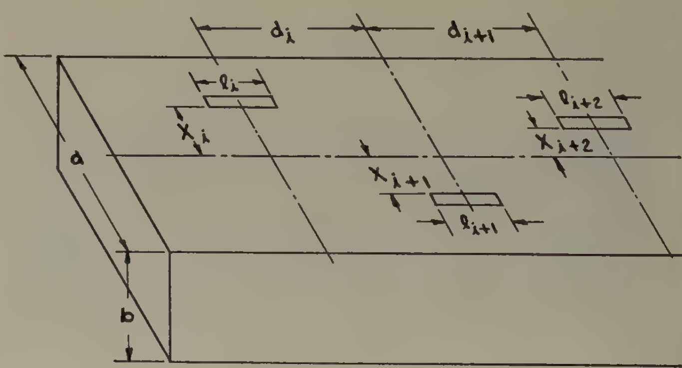

Fig. 2

The symmetrical formulation given by (2) does not imply that the same errors are introduced into the parameters of two radiators equally spaced about the center of the array. A different distribution of values may be assigned to each parameter, and only for convenience in the final computation will this distribution assume to be the same for each element in the array.

IV. Role of Physical Parameters

Before proceeding to the treatment of the particular problem chosen to illustrate the use of the method developed, it is desirable to discuss in detail the physical basis for various assumptions made in this paper. It must be emphasized that the shunt-slot arrays discussed in this paper are composed of collinear resonant

slots with approximately a half-guide-wavelength interslot spacing. It has been shown by Watson[4] that the resonant length of the slot at a fixed frequency is a slowly varying function of the transverse displacement. Accordingly, the perturbation in the impedance arising from the change in resonant length produced by a slight randomness of the transverse displacement about its mean may be neglected since it is second order compared to the other small impedance changes. It is readily seen from the transmission-line equations that for an element spacing which is very nearly half-guide wavelength, the input impedance is unaffected, to second order, by small variations in interelement spacing. The impedance then seen looking into the array is essentially real and is approximately equal to the sum of the slot conductances and the load conductance and is relatively insensitive to the random variations of the individual slot impedances. In addition, the randomness in slot length produces only a small change in impedance.[5] Consequently, the effects of impedance changes may be neglected in this analysis. The change in phase produced by the randomness in transverse displacement may be neglected as also being second order compared to the phase change arising from deviations in slot length.

The relative phase between the signals from two consecutive radiators at the field point P arises from two separate sources, the free-space path-length difference from the two radiators to the field point and the path-length difference between the radiators along the array. The latter difference is reduced by placing alternate slots on opposite sides of the waveguide center line. Thus, the total phase difference then becomes

$$\phi_d = \left(\frac{2\pi d}{\lambda_0} \sin \theta\right) + \left(\frac{2\pi d}{\lambda_g} - \pi\right), \tag{3}$$

where λ_0 is the free-space wavelength, λ_g the guide wavelength, and θ the angle measured from the direction normal to the array axis as shown in Fig. 1. The change in phase as a function of an error in slot length is now considered. It is well known that a phase change is produced in the field radiated by a slot as the slot departs from the resonant length, l_0. The magnitude of the phase change has been determined experimentally[5] for a wide range of frequencies and slot lengths. From this work, it can be seen that near resonance the phase change is proportional to increment in slot length, and is given:

$$\phi_l = \frac{K(l_0 - l)}{l_0}. \tag{4}$$

The total phase of the radiation at P may be obtained from (3) and (4) as

$$\delta = \phi_d + \phi_l. \tag{5}$$

An additional factor that must now be treated is the perturbation in the amplitude of excitation of the slots. It has been shown by Stevenson[6] that the conductance of shunt slot in the broad face of a rectangular wave guide is given by

$$G_i = C_0^2 \sin^2\left(\frac{\pi x_i}{a}\right), \tag{6}$$

where C_0 is a constant involving the guide dimensions and frequency and x_i is the transverse displacement of the i-th slot.

Then, if for purposes of obtaining simplicity in calculation we restrict our attention to resonant-spaced arrays in which the resonant shunt slots are spaced one-half guide wavelength apart, the equivalent circuit may be given as in Fig. 3 and the magnitude of the equivalent slot excitation voltage is

$$|V_i| = C_0 \sin \frac{\pi x_i}{a}. \tag{7}$$

The use of this method also requires the assumption that the total mutual coupling is negligible between the individual slot and the rest of the radiators. This assumption has been experimentally verified.[7]

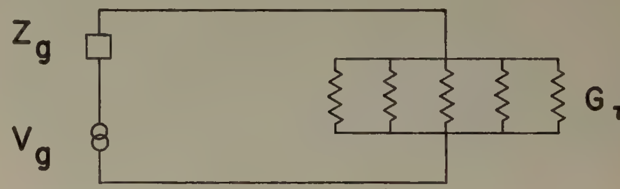

Fig. 3

The effects which must then be considered in the statistical portion are: (a) the variation in the amplitude of excitation due to the randomness in the transverse displacement, (b) the variation in phase due to the randomness in the longitudinal spacing, and (c) the variation in phase due to the randomness in slot length.

V. Statistical Analysis

The statistical problem is to investigate the behavior of the far-zone field pattern, as the amplitude and phase of the individual sources vary in a random manner as a function of their parameters. The field given by (2) may now be rewritten as

$$|E_{2N}(\theta)| = 2|Z| = 2\left|\sum_{k=1}^{n} Z_k\right| = 2\left|\sum_{k=1}^{n} X_k Y_k\right|, \tag{8}$$

[4] W. H. Watson, "The Physical Principles of Waveguide Transmissions and Antenna Systems," Oxford University Press, London; 1947.

[5] R. Stegen, "Design of Linear Arrays," I.R.E. West Coast Meeting; August 23, 1951.

[6] A. F. Stevenson, "Theory of slots in rectangular wave guides," *Jour. App. Phys.*, vol. 19, pp. 24–38; January, 1948.

[7] M. J. Ehrlich, C. W. Curtis, and R. G. Fawcett, "Mutual Coupling between Slot Radiators," I.R.E. New York Meeting; March, 1952.

where the physical description has shown that

$$X_k = C' \sin \frac{\pi x_k}{a} \quad \text{and} \quad Y_k = \cos \delta_k;$$

C' is a constant and δ_k a function of d_k and l_k. (The subscripts may now be omitted since the discussion in the next few paragraphs is applicable to each source.) We have taken d, l, and x to be normally distributed random variables where the deviations at each source are independent of the deviations at all sources. The mean values of these parameters are the design values. Their standard deviations (from these values) are denoted as σ_d, σ_l, and σ_x. If d and l are normally distributed, then δ is normally distributed about its mean value given by the linear relationship of (5) and has a standard deviation given by

$$\sigma_\delta^2 = \sigma_{\phi_d}^2 + \sigma_{\phi_l}^2, \qquad (9)$$

where

$$\sigma_{\phi_d} = \left(\frac{2\pi \sin \theta}{\lambda_0} + \frac{2\pi}{\lambda_g}\right)\sigma_d$$

and

$$\sigma_{\phi_l} = \frac{K}{l_0}\sigma_l.$$

From the function relationships described by (2) and (7), it is evident that the behavior of the cosine and sine of a random variable must be determined as one step towards the solution of this problem. The mean m, and the standard deviation, σ, of a function of a random variable y is defined[8] by the equations

$$m_{f(y)} = \int_{-\infty}^{\infty} f(y)\Phi(y)dy \qquad (10)$$

and

$$\sigma_{f(y)}^2 = \int_{-\infty}^{\infty} [f(y) - m_{f(y)}]^2\Phi(y)dy, \qquad (11)$$

where Φ is the probability density function of y. In our present problem, Φ is normally distributed; consequently,

$$m_Y = \cos \delta \exp\left(-\frac{\sigma_\delta^2}{2}\right) \qquad (12)$$

and

$$\sigma_Y^2 = \tfrac{1}{2}[1 + (\cos 2\delta) \exp(-2\sigma_\delta^2)] - m_Y^2. \qquad (13)$$

Similarly,

$$m_X = C'\left(\sin \frac{\pi x}{a}\right) \exp\left(-\frac{\sigma_X^2}{2}\right) \qquad (14)$$

and

$$\sigma_X^2 = \frac{(C')^2}{2}\left[1 - \left(\cos \frac{2\pi x}{a}\right) \exp(-2\sigma_X^2)\right] - m_X^2, \qquad (15)$$

where

$$\sigma_X = \frac{\pi}{a}\sigma_x.$$

The mean and standard deviation for Z may be determined by applying (12), (13), (14), and (15) to each source. Thus,

$$m_Z = \sum_{k=1}^{n} m_{X_k} m_{Y_k} \qquad (16)$$

and

$$\sigma_Z^2 = \sum_{k=1}^{n} (\sigma_X^2 m_{Y_k}^2) + (\sigma_{Y_k}^2 m_{X_k}^2) + (\sigma_{X_k}^2 \sigma_{Y_k}^2). \qquad (17)$$

The probability density of Z which is an essential part of this derivation can now be found by an application of the Central Limit Theorem. The theorem states, in effect, that the result of summing a sufficiently large number of products of independent random variables is normally distributed regardless of the distribution of the products themselves. Since the field at any angle θ is given by (8), the mean and the standard deviation as well as the density function for $|Z|$ must be calculated in terms of m_Z and σ_Z. Thus the probability density function for $|Z|$ may be written from the probability density of Z as

$$\Phi(|Z|, m_Z, \sigma_Z) = \frac{2}{\sqrt{2\pi}\,\sigma_Z} \exp\left[-\frac{1}{2}\left(\frac{|Z| - m_Z}{\sigma_Z}\right)^2\right]. \qquad (18)$$

Again applying (10) and (11), $m_{|Z|}$ and $\sigma_{|Z|}$ are given by

$$t' \equiv \frac{m_Z}{\sigma_Z} = \frac{2}{\sqrt{2\pi}} \exp\left[-\frac{1}{2}t^2\right] + \frac{|t|}{\sqrt{2\pi}} \int_{-|t|}^{|t|} \exp\left[-\frac{1}{2}x^2\right]dx \qquad (19)$$

and

$$\sigma^2 = \left(\frac{\sigma_{|Z|}}{\sigma_Z}\right)^2 = [1 + (t)^2 - (t')^2] \qquad (20)$$

where

$$t \equiv \frac{m_Z}{\sigma_Z}.$$

A probability can now be associated with the magnitude of the field by integrating the density function between appropriate limits. Since the basic interest in this problem is to determine the effect of the statistical variations upon the side-lobe level, we would like to

[8] See for example H. Cramer, "Mathematical Methods of Statistics," Princeton University Press, Princeton, N. J.

know the probability that side lobes will exceed some arbitrary level. The probability that the field will exceed $m_{|Z|}+\sigma_{|Z|}$ is

$$P[|Z|>m_{|Z|+\sigma|Z|}]$$

$$=1-\frac{1}{2\pi}\int_0^{t'+|t|+\sigma}\exp\left[-\frac{1}{2}x^2\right]dx$$

$$-\frac{1}{\sqrt{2\pi}}\int_0^{t'-|t|+\sigma}\exp\left[-\frac{1}{2}x^2\right]dx. \quad (21)$$

An evaluation of (21) at the position of the side lobes shows that the probability is approximately 0.16 and that the value of the field pattern will be greater than $m_{|Z|}+\sigma_{|Z|}$.

VI. Linear Shunt-Slot Array

The method is demonstrated as a practical device for assigning a probability to the side-lobe level deterioration by a consideration of several examples of shunt-slot arrays. The arrays to be considered have 24 radiators which are excited according to a Dolph-Tchebyscheff distribution where the side-lobe level is chosen to be 20, 30, and 40 db below the main beam with absolute gains of approximately 17 db, 16 db, and 15 db, respectively.

For simplicity in the calculation, consider a resonant-spaced array where the spacing between the elements is $d=\lambda_g/2$ and the sum of the slot conductances is normalized to unity. Equation (8) is then given in the notation (current I_k) of Dolph[3] with

$$X_k=I_k=N_0C_0\sin\left(\frac{\pi x_k}{a}\right) \quad (22)$$

and

$$Y_k=\cos\delta_k=\cos\left[\left(\frac{2k-1}{2}\right)\frac{2\pi d}{\lambda_0}\sin\theta\right], \quad (23)$$

where N_0 is the normalization factor obtained from

$$(N_0)^2=\sum_{k=1}^{12}I_k^2. \quad (24)$$

Upon introducing the nominal dimensions of a standard waveguide at X-band, where $a=0.9$ inch and $b=0.4$ inch and an appropriate frequency so that $\lambda_g=1.4026\ \lambda_0$, C_0 may be calculated from the equation given in footnote reference 6. Consequently, from (22), x_k may be obtained from the given set of normalized Dolph-Tchebyscheff excitation coefficients. The assumption is made also that the slot spacings are not measured serially and, consequently, the errors in spacing do not accumulate but are independent. If now the manufacturing inaccuracies in d, l_k, and x_k are normally distributed about their mean value or desired values with

$$\sigma_d=\sigma_l=\sigma_x=0.002 \text{ inch}. \quad (25)$$

The standard deviation σ_{δ_k} can be calculated from (9) where

$$\sigma_{\phi_d}=\left(\frac{2\pi\sin\theta}{\lambda_0}+\frac{2\pi}{\lambda_g}\right)\sigma_d \quad (26)$$

and

$$\sigma_{\phi_l}=\frac{K}{l_{0_k}}\sigma_l. \quad (27)$$

Here l_{0_k} is the resonant length of the k-th slot and $K=5\pi$ is a value determined from the slope of the experimental values given by Stegen.[5] From (12), (13), (14), and (15) the mean and standard deviation of Y_k and X_k can be computed. The mean and standard deviation of the perturbed field are now determined from (16) and (17) by the indicated summation. For the actual calculations, the third term in (17) may be neglected as being small in comparison to the sum of the other two terms. The mean and standard deviation of absolute value of the perturbed field can be obtained from (19) and (20) and the probability that this magnitude of the field will exceed its mean plus one standard deviation can be calculated from (21).

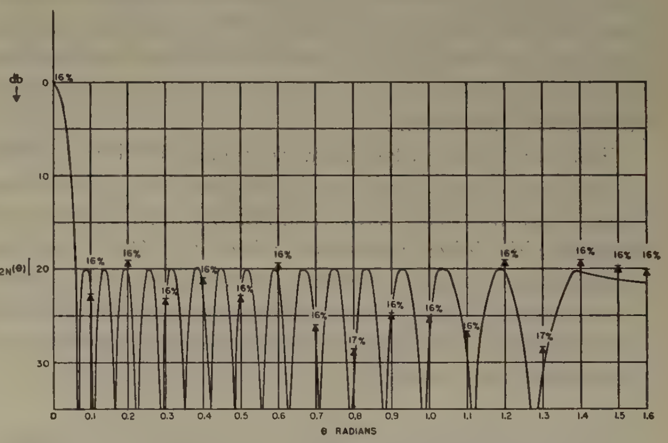

Fig. 4—$|E_{2n}(\theta)|$ versus θ for a 24-element Dolph-Tchebyscheff array designed for 20-db side lobes at X-band. The symbol (↧) denotes the comparison value of perturbed field $|Z|$. The attached percentages indicate the probability that the perturbed field will be smaller (in db) than $m_{|Z|}+\sigma_{|Z|}$ for manufacturing tolerances of 0.002 inch.

VII. Conclusion

The perturbation of the radiation pattern of the array due to the inaccuracies in manufacture has been computed for a 24-element longitudinal shunt-slot array previously described. Since the general method is a statistical one, the changes to be expected in the radiation pattern are presented as a probability that the absolute magnitude of the field will be greater than a specified amount. The value arbitrarily selected was the statistical mean plus one standard deviation. This value is shown superimposed upon the unperturbed Dolph-Tchebyscheff distribution $|E_{2n}(\theta)|$ in Figs. 4, 5, and 6, where Z is used to denote the perturbed field. The prob-

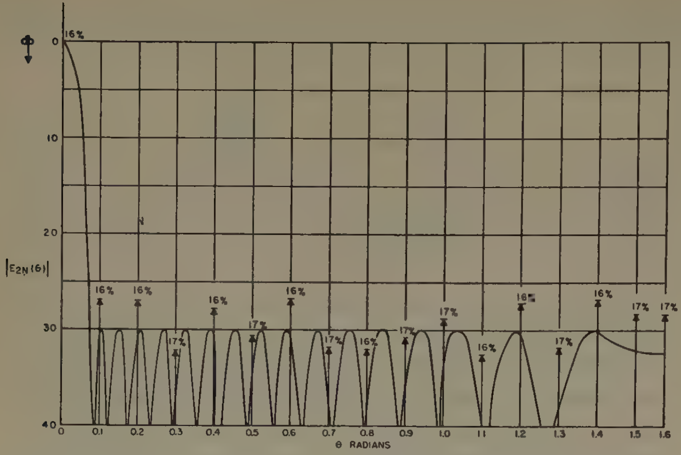

Fig. 5—$|E_{2n}(\theta)|$ versus θ for a 24-element Dolph-Tchebyscheff array designed for 30-db side lobes at X-band. The symbol (↟) denotes the comparison value of perturbed field $|Z|$. The attached percentages indicate the probability that the perturbed field will be smaller (in db) than $m_{|Z|}+\sigma_{|Z|}$ for manufacturing tolerances of 0.002 inch.

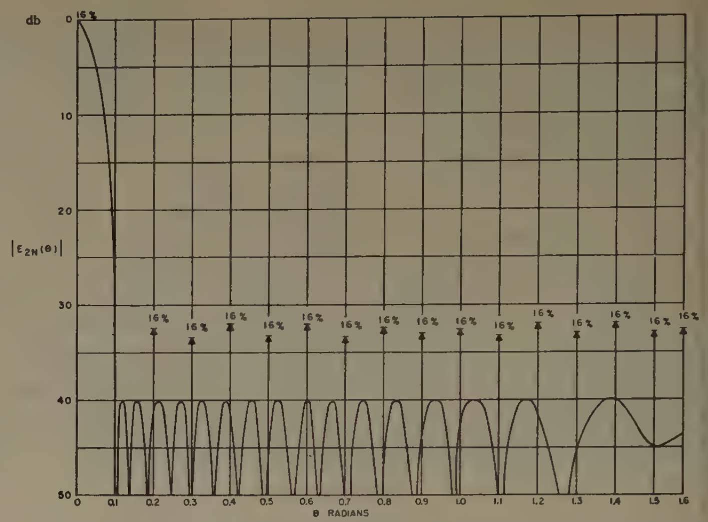

Fig. 6—$|E_{2n}\theta(\theta)|$ versus for a 24-element Dolph-Tschebyscheff array designed for 40-db lobes at X-band. The symbol (↟) denotes the comparison value of perturbed field $|Z|$. The attached percentages indicate the probability that the perturbed field will be smaller (in db) than $m_{|Z|}+\sigma_{|Z|}$ for manufacturing tolerances of 0.002 inch.

ability $P(\theta)$ of the perturbed field is less than the value $m_{|Z|}+\sigma_{|Z|}$ listed in Table I for 0.1 intervals in θ. The values for 6 were selected so as to reduce the amount of computation; consequently, some of the calculated points lie near the maxima of the side lobes and some near the minima in the pattern. It is evident that the maxima and minima are perturbed by the inaccuracies in manufacture, and it can be shown that the beamwidth is similarly affected.

The radiation patterns were measured for a 20-db, 30-db, and a 40-db 24-element X-band array which had been manufactured with a 0.002 inch tolerance.[9] The highest side lobes measured were: (a) 19 db for the 20-db array, (b) 27 db for the 30-db array, and (c) 32 db for the 40-db array. These values are in agreement with the data near any of the peaks of Figs. 4, 5, and 6 within the experimental error.

[9] The arrays were designed, constructed, and measured under the supervision of R. Stegen, Hughes Aircraft Company.

The inaccuracies of the design parameters in each instance were assumed to be normally distributed about the desired value. Studies of error distribution have shown this assumption to be valid for production manufacture processes, although any reasonable error distribution could have been used in our statistical discussion.

It can be seen from Figs. 4, 5, and 6 that the lower the design value of the side lobe the greater the perturbation to be expected for the allowed tolerance. Thus, an additional restriction is now imposed upon array design as a consequence of these results. In order to obtain the desired side-lobe level, two courses are open to the designer: The first is to require very small tolerances in manufacture. Such a procedure is prohibitive in cost, especially if a large number of arrays are to be made. The second is to overdesign the array by designing for an N-db side-lobe level if an M-db level is required, where $N>M$. The amount of overdesign, i.e., $|N-M|$,

TABLE I

θ	20 db			30 db			40 db		
	$E_{2n}(6)$ (db)	$m_{\|Z\|}+\sigma_{\|Z\|}$ (db)	$P(\theta)$	$E_{2n}(\theta)$ (db)	$m_{\|Z\|}+\sigma_{\|Z\|}$ (db)	$P(\theta)$	$E_{2n}(\theta)$ (db)	$m_{\|Z\|}+\sigma_{\|Z\|}$ (db)	$P(\theta)$
0	0	−0.097	16%	0	−0.10	16%	0	−0.11	16%
0.1	24.7	22.8	16%	30.2	26.9	16%	33.1	28.8	17%
0.2	20.2	19.1	16%	30.1	26.9	16%	42.7	32.5	16%
0.3	25.3	23.3	16%	37.0	32.2	17%	91.7	33.4	16%
0.4	22.4	21.0	16%	31.4	27.7	16%	40.4	32.1	16%
0.5	24.7	22.9	16%	36.1	30.6	17%	48.6	33.2	16%
0.6	20.4	19.2	16%	30.3	26.8	16%	40.6	32.0	16%
0.7	28.9	26.0	16%	38.6	31.8	17%	48.8	33.2	16%
0.8	33.2	28.6	17%	43.7	32.0	16%	56.1	32.2	16%
0.9	27.1	24.7	16%	36.3	30.7	17%	45.0	32.9	16%
1.0	27.8	25.2	16%	32.9	28.7	17%	43.6	32.6	16%
1.1	29.9	26.7	16%	41.4	32.5	16%	52.6	33.2	16%
1.2	20.2	19.1	16%	30.5	27.1	16%	41.3	32.0	16%
1.3	32.1	28.2	17%	39.0	31.8	17%	46.1	32.9	16%
1.4	20.2	19.1	16%	30.0	26.8	16%	40.0	31.8	16%
1.5	21.0	19.8	16%	32.1	28.2	17%	44.9	32.7	16%
$\pi/2$	21.4	20.1	16%	32.1	28.2	17%	43.6	32.5	16%

can be governed by the results given in this paper or similarly computed. However, if the length of the array is fixed, the overdesign results in reduced aperture efficiency. Consequently, the requirements of low side-lobe level must be examined carefully since, when the array dimensions are fixed, they will only be satisfied by expensive manufacturing procedures or by reduced aperture efficiency.

VIII. Acknowledgement

The authors wish to thank Professor Samuel Silver of the University of California, Dr. Robert Wehner, Dr. Leo A. Aroian, Dr. Nicholas A. Begovich, and Dr. Bela Lengyel of Hughes Aircraft Company for their helpful suggestions and critical review of this paper, and Annabelle Cordova, Harriet Ruderman, and Wilma Bottaccini for their computing services.

Analysis and Performance of Locked-Oscillator Frequency Dividers Employing Nonlinear Elements*

WILLIAM L. HUGHES†, ASSOCIATE, IRE

Summary—**The locked-oscillator frequency divider is seldom used because of its inherent instability. One method of stabilizing the locked-oscillator divider is to insert certain nonlinear elements in the oscillator circuits. It is required that these elements have a voltage characteristic that is proportional to an integral root of the current through them. If this condition is met, the locked-oscillator divider can become almost completely insensitive to extreme changes in plate voltage, driving signal voltage, and driving frequency. The fact that the nonlinearity of the elements can be described mathematically permits some analysis of the circuit nonlinear differential equations.**

Introduction

The LOCKED-OSCILLATOR frequency divider was abandoned early in the development of electronics because of its apparently hopeless instability. The early locked-oscillator dividers depended upon the nonlinearity of the tubes that were used. The nonlinearity was different for individual tubes and varied with small changes of plate and driving signal voltages. It seems reasonable, however, that if the nonlinearity requirement of the locked-oscillator divider could be fulfilled with an element that is not subject to changing characteristics with other parameter changes, the stability of the divider might be improved.

The requirements of an ideal frequency divider can be enumerated.

1. It should require no special waveform.
2. It should be independent of random tube changes.
3. It should rarely, if ever, require adjustment.
4. It should require no special plate voltage regulation.
5. It should not lose synchronization over a reasonably wide range of frequency input.
6. It should not lose synchronization over wide ranges of signal-input voltage amplitudes.
7. The principle of operation should be applicable over wide frequency ranges.

It will be shown that the locked-oscillator frequency divider can fulfill these requirements rather well.

In the analysis that follows, all calculations are made for output frequencies around 5,000 cps. Except as otherwise noted, all experimental circuits were designed for this frequency.

Design and Analysis of a Circuit to Divide by Two

In order to design a circuit to divide the frequency of a sinusoidal voltage by two, it is convenient to consider the following fundamental trigonometric identity:

$$2 + \sin \omega t = \{9/2 + 4 \sin \omega t - 1/2 \cos 2\omega t\}^{1/2}. \quad (1)$$

An electric analog of this identity could be constructed with current generators feeding a nonlinear element with a volt-ampere characteristic described by

$$E = Ki^{1/2}. \quad (2)$$

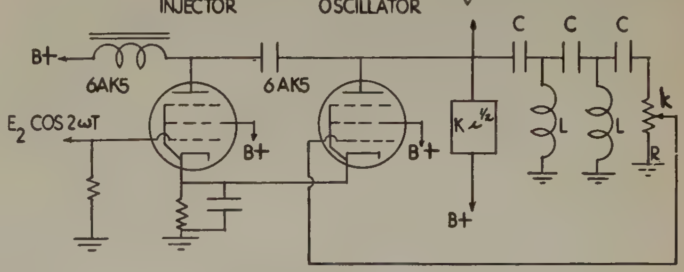

Fig. 1—Circuit designed to divide by 2.

The circuit of a possible analog is shown in Fig. 1. The equation governing the circuit is

$$V = -K\{I_0 + g_m e_{g1} + g_m e_{g2}\}^{1/2}. \quad (3)$$

* Decimal classification: R213.2×R357.3. Original manuscript received by the Institute, April 7, 1952; revised manuscript received, July 16, 1952.

† Electrical Engineering Department, Iowa State College, Ames, Iowa.

The circuit of Fig. 1 fulfills the requirements of an analog if the following proportionalities hold for all values of time.

$$\frac{9/2}{I_0} = \frac{4 \sin \omega t}{g_m e_{g1}} = \frac{-1/2 \cos 2\omega t}{g_m e_{g2}}. \qquad (4)$$

I_0 is provided by the static plate current of one of the 6AK5 current generators and is therefore relatively easy to control. e_{g2} represents the driving signal voltage on the injector current generator. Since the driving signal is considered as the time reference signal, it is necessary to control only its amplitude to satisfy the proportionality requirement. e_{g1} is the grid voltage of the oscillator current generator. It remains to be shown that e_{g1} may assume a time function that will satisfy the required conditions.[1]

It can be easily shown by means of simultaneous linear differential equations that if the input voltage of the phase shifting network is V, the output voltage is given by

$$V_{\text{out}} = \frac{kC^3L^2Rp^5V}{[C^3L^2Rp^5 + 4C^2L^2p^4 + 4C^2LRp^3 + 6CLp^2 + 2CRp + 2]}, \qquad (5)$$

where p is the differential operator d/dt. The driving voltage is arbitrarily given by

$$e_{g2} = E_2 \cos 2\omega t. \qquad (6)$$

The equation governing the circuit (3) can now be written as the operator differential equation

$$V = -K\left\{gmE_2 \cos 2\omega t + I_0 + \frac{gmkC^3L^2Rp^5V}{[C^3L^2Rp^5 + 4C^2L^2p^4 + 4C^2LRp^3 + 6CLp^2 + 2CRp + 2]}\right\}^{1/2}. \qquad (7)$$

By means of substitution and some rather extensive manipulation it can be shown that

$$V = V_0 + V_1 \sin \omega t$$

is an exact solution to (7) provided that

$$\frac{K^2gmkC^3L^2R\omega^5A_1V_1}{A_1^2 + B_1^2} = 0, \qquad (8)$$

$$\frac{K^2gmkC^3L^2R\omega^5B_1V_1}{A_1^2 + B_1^2} = 2V_0V_1, \qquad (9)$$

$$-\frac{V_1^2}{2} = K^2gmE_2, \qquad (10)$$

$$V_0^2 + \frac{V_1^2}{2} = K^2I_0, \qquad (11)$$

where

$$A_1 = 4C^2L^2\omega^4 - 6CL\omega^2 + 2 \qquad (12)$$

$$B_1 = C^3L^2R\omega^5 - 4C^2LR\omega^3 + 2CR\omega. \qquad (13)$$

Equation (8) requires that

$$A_1 = 0$$

or,

$$\omega = 1/\sqrt{LC}. \qquad (14)$$

In the three remaining condition equations (9, 10, and 11) there are five variables. Since these equations are assumed independent, it is convenient to fix two of the variables. The driving signal voltage is at our disposal so let $E_2 = -0.2$ volt and assume $V_0 = 2V_1$. It is experimentally convenient to choose the following values for circuit constants.

$K = 458$ $L = 0.506$ henry

$g_m = 5{,}000$ micromhos $R = 0.5$ megohm

$C = 2{,}000$ micromicrofarads

It is now possible to find the values of the remaining unknowns. They are:

$V_0 = -40.96$ volts $k = 0.0781$

$V_1 = -20.48$ volts $\omega = 31{,}400$

$I_0 = 0.009$ ampere

If the unknowns have these values, the circuit of Fig. 1 is a perfect analog of the original trigonometric function. Since it is a perfect analog, it is obviously a frequency divider. The input is a 10,000 cycle cosine wave and the output is a 5,000 cycle sine wave. Experimentally, the output voltage was

$$V = -40 - 18 \sin 31{,}400t.$$

If the theoretical driving voltage is plotted on the X axis against the output voltage on the Y axis, the resulting Lissajou pattern is shown in Fig. 2(a). Fig. 2(b) shows the experimentally obtained Lissajou pattern.

The behavior of the circuit for driving frequencies near 10,000 cycles can be predicted by assuming the first few terms of a Fourier series as a solution for (7). The steps will be outlined here with the conclusions. To be useful, the output voltage must be expressible in the form

[1] It is necessary to ignore the shunt-plate conductances of both current generators in this analysis. This approximation introduces negligible error because of the characteristically low-plate conductances of pentodes. In fact, this is the characteristic that allows them to act as almost perfect current generators.

$$V = V_0 + \sum_{n=1}^{\infty} \{V_{2n-1} \sin n\omega t + V_{2n} \cos n\omega t\}. \quad (15)$$

If the constant term and the first four periodic terms (involving the first two harmonics) are used as an approximate solution for (7), the following approximate conditions equations are obtained.

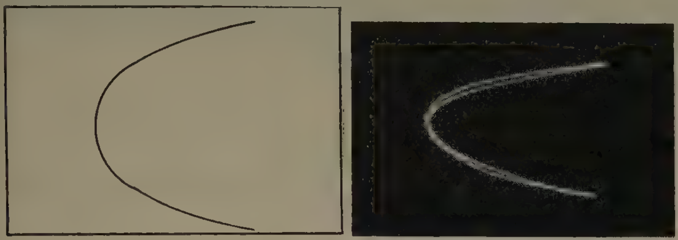

(a) (b)

Fig. 2—(a) Theoretical Lissajou pattern for division by 2. (b) Experimental Lissajou pattern for division by 2.

$$V_0^2 + \frac{V_1^2}{2} + \frac{V_2^2}{2} + \frac{V_3^2}{2} + \frac{V_4^2}{2} = K^2 I_0, \quad (16)$$

$$2V_0V_1 - V_1V_4 + V_2V_3 = \frac{K^2 gmkC^3L^2R\omega^5}{A_1^2 + B_1^2}[-A_1V_2 + B_1V_1], \quad (17)$$

$$2V_0V_2 + V_1V_3 + V_2V_4 = \frac{K^2 gmkC^3L^2R\omega^5}{A_1^2 + B_1^2}[A_1V_1 + B_1V_2], \quad (18)$$

$$2V_0V_3 + V_1V_2 = \frac{32K^2 gmkC^3L^2R\omega^5}{A_2^2 + B_2^2}[-A_2V_4 + B_2V_3], \quad (19)$$

$$2V_0V_4 - \frac{V_1^2}{2} + \frac{V_2^2}{2} = K^2 gmE_2 + \frac{32K^2 gmkC^3L^2R\omega^5}{A_2^2 + B_2^2}[A_2V_3 + B_2V_4], \quad (20)$$

$$V_2V_3 + V_1V_4 = 0, \quad (21)$$

$$-V_1V_3 + V_2V_4 = 0, \quad (22)$$

$$-\frac{V_3^2}{2} + \frac{V_4^2}{2} = 0, \quad (23)$$

$$V_3V_4 = 0, \quad (24)$$

where

$$A_n = 4C^2L^2(n\omega)^4 - 6CL(n\omega)^2 + 2$$

$$B_n = C^3L^2R(n\omega)^5 - 4C^2LR(n\omega)^3 + 2CRn\omega.$$

Equations (23) and (24) obviously require V_3 and V_4 to be equal to zero for an exact solution. This leads to the single solution previously obtained. If V_3 and V_4 are small but not zero, (21) and (22) suggest that an approximate solution might be obtained by setting V_2 equal to zero and solving for the other constants as functions of the angular velocity. This is pure speculation, of course, and any justification that it might have must come from experimental evidence. Simultaneous solution of (16) through (20) yields the solid curve of Fig. 3. This curve is the calculated percentage of second-harmonic content in the output voltage. The dotted curve shows the experimentally measured variation of second-harmonic content superimposed upon the calculated value.[2] It is indicative that both curves reach a minimum at 5,000 cycles. The straight line nature of the calculated values probably indicates, however, that the approximation is too limited to be of quantitative value.

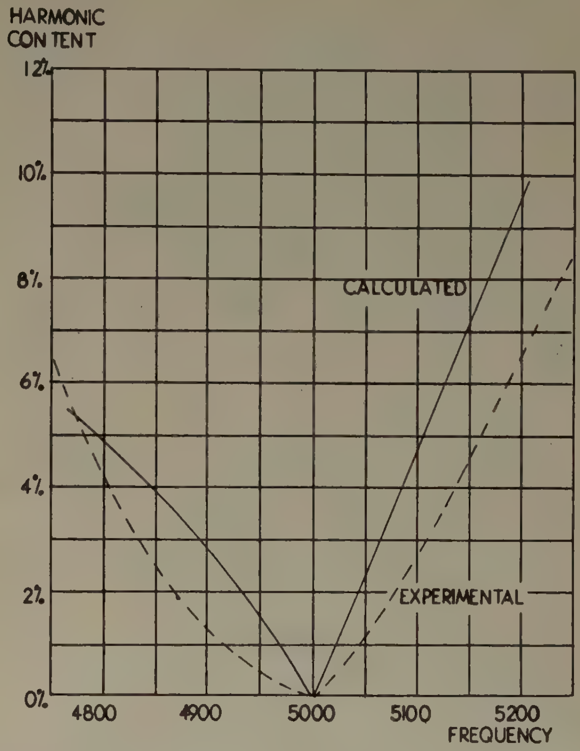

Fig. 3—Harmonic content of output voltage as a function of driving frequency.

It is possible to solve for E_2, the coefficient of the driving voltage, for various frequencies. Theoretically, these are the values of E_2 that should give a minimum of harmonic content in the output voltage. The solid curve of Fig. 4 shows the absolute value of E_2 plotted against frequency. The dotted curve of Fig. 4 gives the experimentally obtained absolute values of E_2. The minimum value of E_2 was recorded that gave stable locking for each frequency since this seemed also to be the E_2 that gave minimum second-harmonic content in the output. The most significant thing about these curves is that they both reach a minimum below 5,000 cycles. The calculated value of E_2 changes polarity about 40 cycles below 5,000 cycles. This can be interpreted as an indication of the natural frequency of oscillation of the nonlinear system since it is the output frequency when the driving voltage is zero. This is substantiated experimentally.

[2] At 5,000 cycles, the experimentally measured second-harmonic content was 1.3 per cent.

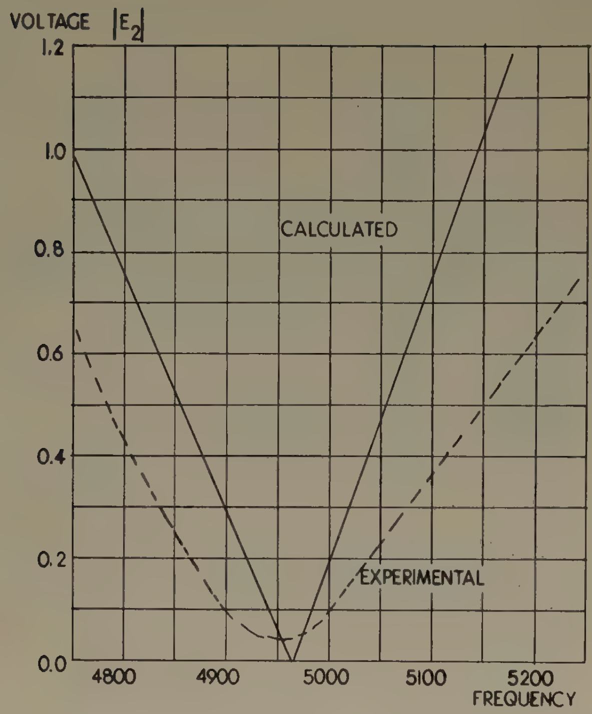

Fig. 4—Driving-signal voltage as a function of frequency.

Design of a Circuit to Divide by Three

The following fundamental identity is useful in designing a circuit to divide by three.

$$\cos \omega t = \{\tfrac{1}{4}[\cos 3\omega t + 3 \cos \omega t]\}^{1/3}. \qquad (25)$$

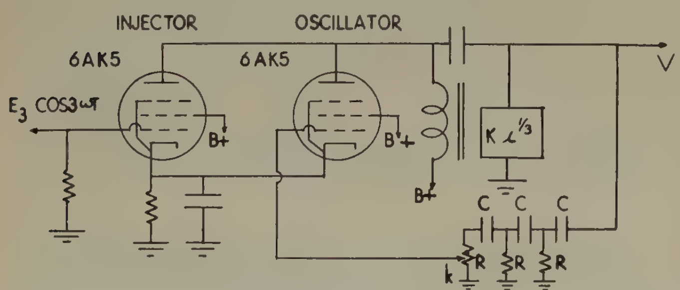

Fig. 5—Circuit designed to divide by 3.

The corresponding circuit analog is shown in Fig. 5. The differential operator equation governing the circuit is found as before. It is

$$V = -K\left\{ gmE_3 \cos 3\omega t + \frac{gmkp^3V}{p^3 + \dfrac{6p^2}{RC} + \dfrac{5p}{R^2C^2} + \dfrac{1}{R^3C^3}} \right\}^{1/3}. \qquad (26)$$

An exact solution can be shown to be

$$V = V_1 \cos \omega t,$$

provided that certain conditions are fulfilled as before. This analysis is not discussed in any detail because of its obvious similarities to the preceding one. It is interesting to note, however, that no dc component occurs. In general, dc components occur when circuits are designed to divide by even numbers but do not occur in circuits designed to divide by odd numbers.

Some information was obtained by an assumed series solution of (26). The solution indicated that the natural frequency of oscillation of the circuit was 250 cycles below 5,000 cycles. Experimentally, it was 150 cycles below 5,000 cycles. Apparently the order of magnitude was correct but quantitative indications were not dependable due to the limited approximations that were necessary to obtain a solution at all.

Design of a Circuit to Divide by Five and Seven

The fundamental trigonometric identity for a circuit designed to divide by five is

$$\cos \omega t = \left[\frac{1}{16}[\cos 5\omega t + 5 \cos 3\omega t + 10 \cos \omega t]\right]^{1/5}. \qquad (27)$$

The circuit designed to divide by five is given in Fig. 6. This circuit defies analysis by differential equations. Some insight can be gained into its operation, however,

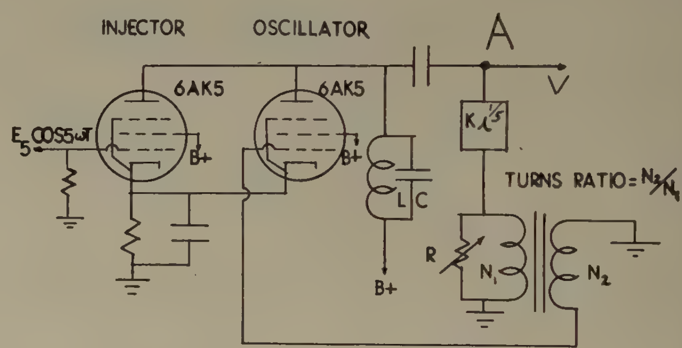

Fig. 6—Circuit designed to divide by 5 and 7.

by assuming a perfect cosine wave of voltage at point A. The LC combination is approximately resonant at ω. The volt-ampere characteristic of the nonlinear element in series with R is

$$E = Ki^{1/5} \quad \text{or} \quad i = \left(\frac{E}{K}\right)^5. \qquad (28)$$

The current through R, then, is

$$i = \frac{V^5 \cos^5 \omega t}{K^5}. \qquad (29)$$

The voltage across R is

$$E = \frac{RV^5 \cos^5 \omega t}{K^5}. \qquad (30)$$

The grid voltage on the oscillator tube is[3]

[3] It is assumed that the transformer does not load R appreciably. This is true since the secondary of the transformer is effectively open if the oscillator tube draws no grid current.

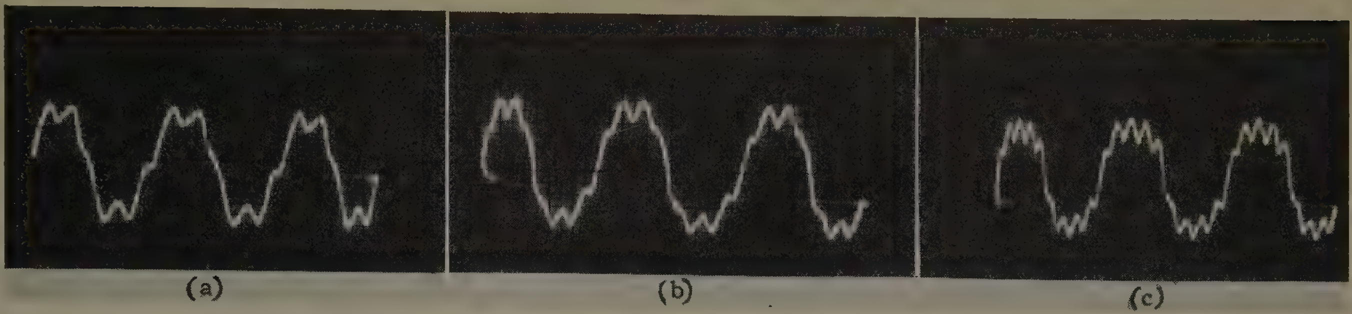

Fig. 7—(a) Waveform of output voltage for division by 5. (b) Waveform of output voltage for division by 7. (c) Waveform of output voltage for division by 9.

$$\left(\frac{N_2}{N_1}\right)\frac{RV^5}{K^5}\cos^5 \omega t. \tag{31}$$

The current in the oscillator tube is

$$gme_g = \left(\frac{N_2}{N_1}\right)\frac{RV^5 gm}{K^5}\cos^5 \omega t = \left(\frac{N_2}{N_1}\right) \cdot \frac{RV^5 gm}{16K^5}[\cos 5\omega t + 5\cos 3\omega t + 10\cos \omega t]. \tag{32}$$

The total current is

$$\left\{\left(\frac{N_2}{N_1}\right)\frac{RV^5 gm}{16K^5} + gmE_5\right\}\cos 5\omega t + \left(\frac{N_2}{N_1}\right)\frac{RV^5 gm}{16K^5}[5\cos 3\omega t + 10\cos \omega t]. \tag{33}$$

Since the cos $5\omega t$ term is in excess by $g_m E_5$, it is expected that the assumed perfect cosine wave at A would be modified by a small fifth-harmonic content. The fundamental identity is satisfied except for this small excess.

The circuit designed to divide by seven depends upon

$$\cos \omega t = \left\{\frac{1}{64}[\cos 7\omega t + 7\cos 5\omega t + 21\cos 3\omega t + 35\cos \omega t]\right\}^{1/7}. \tag{34}$$

The circuit is the same as that of Fig. 6 except that the nonlinear element theoretically should be replaced by one with a volt-ampere characteristic described by

$$V = Ki^{1/7}. \tag{35}$$

The theory is the same as before and will not be repeated. Actually, the circuit of Fig. 6 will divide very well by either five or seven, and almost as well by nine without changing the elements at all.

Figs. 7(a), 7(b), and 7(c) show the output waveforms for division by five, seven, and nine, respectively.

General Discussion

In every circuit, the nonlinear elements were either General Electric thyrite elements or Western Electric varistors. Sometimes combinations of nonlinear elements and linear resistors were used. In each case, the coefficient K was obtained by a least squares curve fitting process from experimental data on volt-ampere characteristics.

In all of the circuits described, the requirements for an ideal divider were reasonably fulfilled. The waveforms were all essentially sinusoidal. It was not possible to find any random combination of good 6AK5's that would not work together perfectly.[4] Once a circuit was properly adjusted, any tube or tubes could be plugged in and the circuit would operate perfectly without further adjustment. The plate voltage could be varied from a value where oscillation began (around 50 volts) to a value where the grids of the 6AK5's ran red (about 275 volts) without losing synchronization even momentarily while the voltage was being changed. It was not always necessary to have the feedback adjusted to allow for free oscillation. As soon as the driving-signal voltage was applied the proper submultiple output frequency would appear even though the output was zero without a driving signal. In all of the circuits just described the driving-signal voltage amplitude could be varied over a range of at least 400 per cent. In all of the circuits the driving frequency could be varied over a range of at least ±6 per cent and for the lower counts it could be varied as much as ±15 per cent.

An experimental circuit was built to divide by three with an input frequency of approximately three mc. The circuit operated satisfactorily in all respects except that the driving frequency could be varied only about ±30 kc. This was probably due to the shunt capacitive effect of the Varistor that was used. It is evident, however, that the principle is applicable at higher frequencies if suitable nonlinear elements could be obtained.

Bibliography

1. P. G. Sulzer, "An improved locked oscillator frequency divider," Proc. I.R.E., vol. 39, p. 1535; December, 1951.
2. J. J. Stoker, "Nonlinear Vibrations," Interscience Publishers Inc., New York, N. Y., pp. 104–107; 1950.
3. N. Minorsky, "Nonlinear Mechanics," J. W. Edwards Publishing Company, Ann Arbor, Mich., pp. 331–336; 1947.

[4] For the purposes of this analysis, a good 6AK5 is defined as one that checks anywhere in the satisfactory range of a mutual-conductance tube tester.

Wien Bridge Oscillator Design*

KENNETH K. CLARKE†, ASSOCIATE, IRE

Summary—The practical design of the Wien bridge type of RC oscillator or selective amplifier is discussed. A set of design curves is presented which allows the direct determination of such characteristics as frequency stability, frequency accuracy, amplifier gain and phase shift requirements, and the voltage control element requirements.

INTRODUCTION

IN THE LARGE NUMBER of references[1–3] to resistance-capacitance oscillators and to frequency selective amplifiers[4,5] little mention has been made of the frequency accuracy which could be expected. It thus appears that a straightforward method of predetermining these characteristics is needed.

It is the purpose of this paper to show how the exact amplitude and phase-shift characteristics of the Wien bridge may be presented graphically and in a form directly useful for design purposes. Using these curves it will be shown how to determine the amplifier requirements if the over-all performance characteristics are specified. It will also be shown how to treat the reverse problem as well as how to determine control element requirements, stability possibilities, and the effect of bridge element tolerances on over-all operation.

BASIC CIRCUIT AND OPERATION

The Wien bridge circuit is generally agreed to be the most suitable for variable frequency operation.[3] The basic circuit is shown in Fig. 1. It may be operated as either an oscillator or as a frequency selective amplifier. In the first case the bridge must always be slightly unbalanced so that an output or error signal will be present at, or close to, the desired frequency. The actual frequency of operation is then determined by the requirement of 2π degrees of phase shift from e_{bc} around the loop and back to e_{bc}. In the second case the bridge is balanced and degenerative feedback at all but the balance frequency gives a selective effect. The rest of this paper takes into account only the oscillator case, nevertheless, remembering the basic differences in operation, much of the data is also applicable to the frequency selective amplifier.

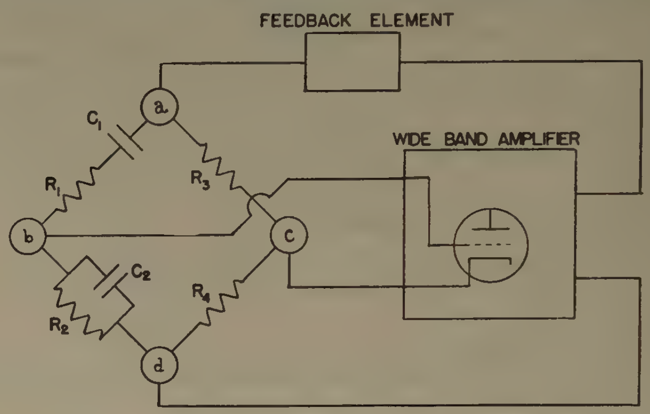

Fig. 1—Basic schematic of a Wien bridge oscillator or frequency selective amplifier.

The only mode of operation discussed is that where the theoretical balance conditions are

$$f_0 = \frac{1}{2\pi R_1 C_1} = \frac{1}{2\pi R_2 C_2}$$

and $R_1 = R_2$, $C_1 = C_2$, $R_3 = 2R_4$. Practical design factors are so simplified by this approach that almost all actual oscillators use it. Several other terms which will be used throughout the rest of this paper are defined below.

$p = f/f_0$	where f is the actual operating frequency and f_0 is the theoretical balance frequency.
p_1	equals the value of p when the output voltage e_{bc} changes its phase relative to the bridge input voltage e_{ad}. In the theoretical balance case discussed in the previous paragraph, p_1 will always be 1. However, in the case where the elements in arm 1 or 2 of the bridge vary from this ideal case, then p_1 will assume a new value.
Δp	equals the variation of p from p_1.
$Y = \dfrac{e_{ad}}{e_{cd}} = 1 + X$	where $R_3 = XR_4$. For the theoretical balance case discussed above, $X = 2$ and $Y = 3$.
ΔY	equals the variation of Y from the value $Y = Y_1$ when $p = p_1$.
net amplifier gain	equals the voltage gain, at the frequency in question, from e_{bc} through the amplifier and the feedback loop to e_{ad}.
net phase shift	equals the phase shift in the voltage around the same path.

DERIVATION OF RESULTS

The output of the bridge shown in Fig. 1 may be written as $e_{bd} - e_{cd}$. Now e_{cd} may easily be shown to be e_{ad}/Y, and e_{bd} may be shown to equal

$$e_{bd} = \frac{j\omega R_2 C_1 e_{ad}}{1 - \omega^2 R_1 R_2 C_1 C_2 + j\omega[R_1 C_1 + R_2 C_2 + R_2 C_1]} \quad (1)$$

* Decimal classification: R355.914.31. Original manuscript received by the Institute, October 16, 1951; revised manuscript received, March 5, 1952.

† Electrical Engineering Department, University of Ceylon, Colombo 3, Ceylon.

[1] C. M. Edwards, "A precision decade oscillator for 20 cycles to 200 kc," PROC. I.R.E., vol. 39, pp. 277–278; March, 1951.

[2] W. G. Shepherd and R. O. Wise, "Variable frequency bridge type frequency stabilized oscillators," PROC. I.R.E., vol. 31, pp. 255–268; June, 1943.

[3] B. Chance, F. C. Williams, V. Hughes, E. F. MacNichol, and D. Sayre, "Waveforms," Vol. 19, Radiation Laboratory Series, chap. 4, McGraw-Hill Book Co., Inc., New York, N. Y.; 1949.

[4] H. H. Scott, "A new type of selective circuit and some applications," PROC. I.R.E., vol. 26, pp. 226–235; February, 1938.

[5] G. E. Valley and H. Wallman, "Vacuum Tube Amplifiers," vol. 18, Radiation Laboratory Series, chap. 10, McGraw-Hill Book Co., Inc., New York, N. Y.; 1948.

For the given case e_{bd} reduces to

$$e_{bd} = \left\{\left[\frac{3p^2}{p^4+7p^2+1}\right] + j\left[\frac{1+p^2}{p^4+7p^2+1}\right]\right\} e_{ad}. \quad (2)$$

Now both e_{bd} and e_{cd} have been expressed in terms of e_{ad}, Y and p. Therefore it would be possible to plot the magnitude and phase of the bridge output voltage versus Y with p as a parameter. A more useful plot is obtained if several modifications corresponding to the actual operating conditions of the oscillator are made. For oscillation to occur, the phase shift in the bridge must be exactly equal but opposite to the net amplifier phase shift. Also, the minimum required net amplifier gain is that which is necessary to make up for the bridge loss or e_{bc}/e_{ad}, at the balance point. Therefore while Fig. 2 contains the characteristics of a Wien bridge, it has been labeled in terms of the amplifier parameters. Thus Fig. 2(a) is a representation of either negative bridge phase shift or positive amplifier phase shift versus Y, and Fig. 2(b) is a plot of the magnitude of e_{ad}/e_{bc} or of minimum required amplifier gain. A little manipulation will show that when the amplifier phase shift becomes negative (the high frequency end of the band) the same curves are applicable if p is replaced by $2-p$ in both figures. (For variations of p of plus or minus 5 per cent from p_1, the variation in the curves for the two cases will be so small that it may be neglected).[6]

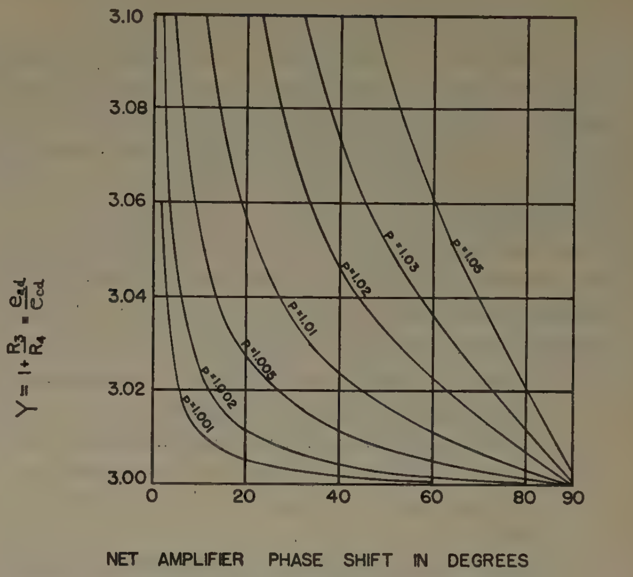

Fig. 2(a)—The relative frequency of oscillation of a Wien bridge oscillator,

$$p = \frac{f_{\text{oscillation}}}{f_{\text{theoretical balance}}}$$

as a function of the net amplifier phase shift and the bridge relation $Y \cdot Y = 1 + R_3/R_4 = e_{ad}/e_{cd}$.

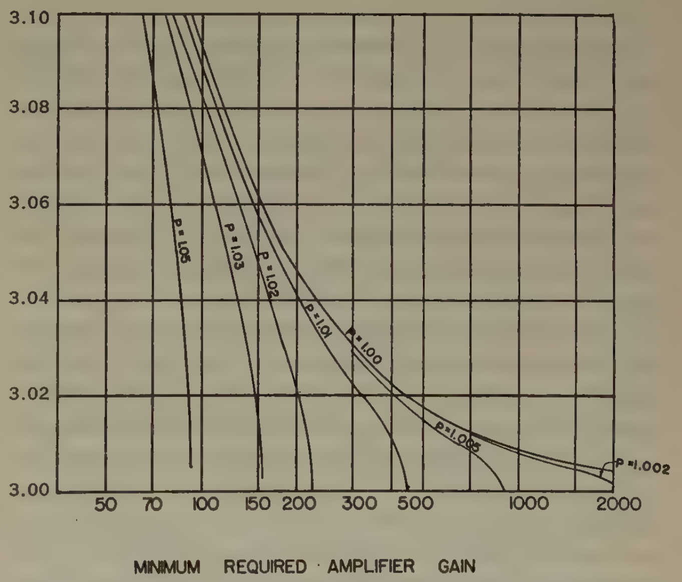

Fig. 2(b)—The minimum required net amplifier gain for oscillation of a Wien bridge oscillator as a function of relative frequency p and of the bridge relation Y.

Data Obtainable from Fig. 2

1. *Basic Design Data*

The problem is either (1) given an amplifier to find the operating characteristics of a Wien bridge oscillator using this amplifier, or (2), given the desired oscillator characteristics to find the requirements for the wide-band amplifier.

In the first case one computes or measures the phase shift and gain characteristics of the amplifier for the frequency band in question.[7] Then at any desired frequency enter Fig. 2(a) along the vertical line equal to the net amplifier phase shift at this frequency. Travel up this line, from the $Y=3$ line, until a point is reached where the value of p also simultaneously satisfies the gain specification on Fig. 2(b) for the same value of Y. This value of Y will be the minimum value of Y with which oscillations at this frequency will be possible. The value of p will give the deviation of the actual operating frequency from the theoretical balance frequency. This point, where Δp and Y are both a minimum, will be the most desirable operating point. This is true not only since Δp is a minimum, but also since the frequency stability is maximum and the amplifier is operating with the smallest allowable signal and should therefore produce a minimum of harmonic distortion.

In the second case a similar procedure is followed except that now a phase shift-gain combination must be chosen that will keep the operating point below the p curve for the maximum allowable frequency deviation.

[6] For this case the maximum variation will be between $p=0.95$ and $p=1.05$, and will occur when the phase shift equals 90°. It will always be less than 5 per cent. Since the maximum error occurs at the relatively unimportant end of the graph, its neglect is justified. Actually, by the time the phase shift has decreased to ±45°, the error has decreased below 0.5 per cent.

[7] It must be remembered that the feedback element and the bridge will both exert an effect upon net amplifier phase shift and gain. It is relatively easy to make this effect very small over the region from 1 to 10 kc. In fact, the effect of the bridge and of a capacitive feedback element can be made to practically cancel over this region. Outside this region the effect is not small and must be considered.

2. *Use of Voltage Variable Control Elements*

For any bridge there are two possible modes of operation. The first method is that where R_3 and R_4 are fixed elements which are adjusted to the "proper" values when the bridge is built. The second is that where either or both R_3 or R_4 is allowed to vary with the power flowing through it.

In the first case Y will be fixed, and the operation will necessarily be along a horizontal Y line of Fig. 2. A study of the curves will show several features of this type of operation.

(a) It may cause large frequency deviations from the theoretical balance frequency.

(b) It may cause large amplitude variations with frequency. These may not only be annoying, but may also lead to amplifier over-loading and distortion.

(c) There will be a range of frequencies, depending upon Y and the amplifier characteristics, where operation will not be possible.

This type of operation is thus seen to be practical only for the case of limited frequency coverage or where variations in amplitude and distortion are of secondary importance.

In the second, and most often used, method of operation either R_3 or R_4, or both, are allowed to vary with e_{ad}. Y will then be dependent upon e_{ad}. Now if R_3 is given a negative temperature coefficient and R_4 is given a positive temperature coefficient, then Y will always tend to decrease when e_{bc} is greater than is necessary to barely maintain oscillations. This means that the oscillator will always automatically adjust itself to the most desirable operating point. The frequency accuracy, with regard to the theoretical balance frequency, can only be improved beyond this point by decreasing the net amplifier phase shift or increasing the gain. Once the range of amplifier phase shifts to be covered is known, then the necessary range for the control elements is easily derivable from the graphs. The actual values of R_3 and R_4 will have to be determined after a consideration of the bias requirements of the first amplifier stage, the loading effect on the second amplifier stage, the effect on the net amplifier gain and phase shift, and the available control elements. In practice, R_3 will usually be a thermistor[8,9] and R_4 will be a low wattage light bulb. While many practical bridges have been built using both R_3 and R_4 as control elements, it would appear from these figures that it may be advantageous to hold R_4 constant and allow only R_3 to vary. If R_4 is adjusted for maximum desirable amplifier gain and then kept constant, the frequency stability, frequency accuracy, and the amplitude stability should always be the maximum possible. If R_4 is allowed to vary, the gain will vary somewhat with frequency and maximum stabilities will not be obtained.

[8] J. H. Bollman and J. G. Kreer, "The application of thermistors to control networks," Proc. I.R.E., vol. 38, pp. 20–26; January, 1950.

[9] J. A. Becker, C. B. Green, and G. L. Pearson, "Properties and uses of thermistors-thermally sensitive resistors," *Trans. AIEE*, vol. 65, pp. 711–725; November, 1946.

3. *Frequency Stability*

The actual effects of amplifier gain variations on the operating frequency may be read directly from the graphs, i.e., if the required phase shift is 26 degrees, and the gain is 400, then $p=1.005$ and $Y=3.02$. If the phase shift is smaller, then the stability is even greater, i.e., a 0.2 per cent change in frequency when the gain goes from 450 to 225 at a required phase shift of 11 degrees. In any case the values for any phase shift conditions are easily readable from the graphs. An approximate expression relating these quantities is given in footnote reference (1). However, the curves should allow a greater insight into the operation than the expression cited.

Effects of Component Tolerances

To find the effect of bridge component variations on over-all oscillator operation one may rewrite (1) for two simple possible variations.

When R_2 or C_1 varies from the balance value, assuming that R_1 and C_2 remain constant,

$$e_{bd} = A\left\{\frac{p^2[1+2A]+jp[1-p^2A]}{p^4A^2+p^2[4A^2+2A+1]+1}\right\}e_{ad}, \quad (3)$$

where $A=R_2/R_1$ or C_1/C_2.

When R_1 or C_2 varies from the balance value, assuming that R_2 and C_1 remain constant,

$$e_{bd} = \left\{\frac{p^2[2+B]+jp[1-p^2B]}{p^4B^2+p^2[B^2+2B+4]+1}\right\}e_{ad}, \quad (4)$$

where $B=R_1/R_2$ or C_2/C_1.

Examination of these equations will show that the effect on e_{bd} of a 1 per cent variation in the same direction of both R_2 and C_1 will produce the same effect as a 2 per cent variation of R_2 alone. A 1 per cent variation in opposite directions will cancel and have no effect. A similar relation holds for R_1 and C_2. The effect of temperature on the bridge may thus be largely removed by using elements with opposite temperature coefficients for R_1 and C_2 ,and for R_2 and C_1.

The following technique has been found applicable for finding the effect of component variations or tolerances on oscillator operation.

The effect of a change in R_2/R_1, C_2/C_1, R_1/R_2, C_1/C_2 or some combination of changes of these values from the theoretical balance values, will result in the shifting of the curves of Fig. 2 either up or down along the Y axis. While the curves are shifted they retain their same shapes so that it is necessary merely to find a new value for p_1 and Y_1 for each value of component change. To use the curves one should view the Y axis as shifted vertically until Y_1 corresponds to $Y=3$ in Fig. 2 as plotted. The p curves must then be read as p curves where p_1 is equivalent to $p=1.00$ in Fig. 2. In both cases the relative spacings remain the same.

Values for p_1 and Y_1 may be found by substituting the actual ratios into (3) or (4) in the case of simple variations, or into (1) for e_{bd} in the more complicated variations. p_1 may then be found by setting the numerator of the imaginary part of e_{bd} equal to zero. Y_1 is found by taking the reciprocal of the value of the real part of e_{bd} when p_1 is substituted for p in the equation.

From this data and Fig. 2 it is seen that in an oscillator with automatic control a variation of A or B will cause a frequency variation dependent upon the original operating point of the bridge and the sign of the required phase angle. The maximum possible deviation of the frequency under these conditions will be the sum of the original deviation and the difference between p_1 and 1. For component tolerance of less than ± 5 per cent, the average frequency deviation will be half the component deviation. The extreme value will be one and one half times the component deviation. If the original amplifier has a reasonably small phase shift over the operating region, then the original phase shift will be very small and the over-all frequency accuracy will always be approximately one half of the component tolerances.

It would therefore appear as if the use of compensating temperature coefficient components of 1 per cent accuracy would allow the construction of 1 per cent accurate oscillators directly, without the necessity of resorting to individual adjustments.

The Lock-In Performance of an AFC Circuit*

G. W. PRESTON†, ASSOCIATE, IRE AND J. C. TELLIER†, SENIOR MEMBER, IRE

Summary—**The lock-in condition of the phase-detector reactance tube-controlled oscillator afc system has been investigated. For the case of RC coupling between phase detector and the reactance tube, an explicit relation is obtained for the lock-in condition which involves the filter time constant, the initial frequency error, the phase detector constant and the reactance tube controlled oscillator sensitivity constant.**

IN CERTAIN compatible color-television systems, hue and saturation are transmitted as phase and amplitude modulation of a sine wave, the color "subcarrier." In the particular system for which specifications have been established by the National Television System Committee, the frequency of the subcarrier is approximately 3.89 mc. In order to recover the phase modulation at the receiver without ambiguity, a phase reference must be available. For this purpose, a color "reference" signal is transmitted as a burst of color carrier, just after the horizontal synchronizing pulse. The common afc system shown in block diagram form in Fig. 1 is often employed at the receiver to extract a relatively noise-free reproduction of the burst from the transmitted signal.

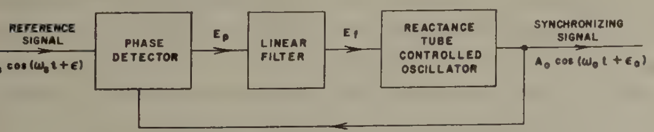

Fig. 1—Block diagram.

For the purposes of the present discussion, this burst is assumed to have been separated by gating from the synchronizing pulses, and filtered somewhat to reduce noise but without producing any significant amount of phase shift. It is permissible, moreover, to regard the synchronizing signal as being continuous rather than intermittent since the band pass of the circuit, as a whole, will always be narrow compared to the line-repetition frequency, which is 15,750 cps.

The phase-detector reactance, tube-controlled oscillator afc system functions in the following manner. The phase detector has a voltage output E_p, which is proportional to the cosine of the difference $\phi_s-\phi_0$ in the phases of the reference signal and the controlled oscillator and to twice the signal voltage amplitude, $E_p=2A_sK_1 \cos(\phi_s-\phi_0)$. This voltage is applied (disregarding for the moment the intervening linear filter) to the grid of the reactance-tube controlled oscillator. The oscillator in turn assumes a frequency which differs froms its normal value Ω (obtained when the reactance tube control voltage is zero) by an amount which is essentially proportional to the control voltage;

$$\omega_0 = \Omega + K_2E_p = \Omega + 2A_1K_1K_2 \cos(\phi_s - \phi_0).$$

If the reference signal frequency is $\omega_a+\Omega$, and if synchronization is assumed, it is seen that in the equilibrium condition there must exist a static phase difference

$$\left(\phi_s - \phi_0 - \frac{\pi}{2}\right)_{\text{static}} = \sin^{-1}\left(\frac{\omega_a}{2A_sK_1K_2}\right).$$

The noise performance of this circuit has been discussed by George[1] although his analysis involves a linearizing assumption which is valid in the steady state for IF signal-to-noise ratios of practical interest. George shows that the mean-square phase fluctuation, due to noise, of the oscillator depends upon the transient response of the coupling network and that it is also proportional to $A_sK_1K_2$. The static phase shift, on the

* Decimal classification: R361.215. Original manuscript received by the Institute, November 16, 1951; revised manuscript received August 27, 1952.
† Philco Corp., Philadelphia 34, Pa.

[1] T. S. George, "Analysis of synchronizing systems for dot-interlaced color television," PROC. I.R.E., vol. 39, pp. 124–131; February, 1951.

other hand, varies nearly inversely as $A_s K_1 K_2$. It is desirable to minimize the static phase error by maximizing $K_1 K_2$ provided the noise performance requirements can be satisfied by making the band pass of the coupling network sufficiently narrow. However, as the band pass is narrowed, a point is reached at which the oscillator may fail to synchronize following an initial frequency difference. The purpose of the present investigation was to determine constraints upon the filter characteristic within which synchronization will occur. An abrupt frequency difference between the reference voltage and the oscillator occurs in practice when switching from one station to another.

With respect to lock-in, this circuit will, in general, exhibit a peculiarity common to many types of nonlinear oscillatory systems; *it has more than one steady-state condition.* Specifically, following a step change in the reference frequency, the controlled oscillator may become synchronized to the new frequency, or it may reach the state of oscillation (with periodic perturbations) at its normal frequency Ω. Which of these final conditions is assumed depends upon the initial phase and frequency errors. If, however, suitable constraints are observed in the design of the linear filter, only the former steady-state condition will be possible, regardless of initial conditions.

By numerical and graphical methods, this constraint for a simple RC coupling network, has been found to be

$$\frac{1}{RC} \geqq 0.64 \frac{\omega_a^2}{K_1 K_2} \tag{1}$$

approximately, provided $\omega_a \leqq 0.5 K_1 K_2$.

The methods used in obtaining this condition will be discussed after a mathematical statement of the problem has been made. Unfortunately, qualitative considerations of nonlinear systems of this type contribute little to a clear understanding of their behavior.

The conventional discriminator-type balanced phase detector has a voltage output which is proportional to the difference between the absolute values of the sum and difference of the complex reference and oscillator voltages.

Thus, if the reference voltage is $A_s \exp\{j\int^t \omega_s dt\}$ and the oscillator voltage is $A_0 \exp\{j\int^t \omega_0 dt\}$, the output of the balanced phase detector is (assuming $(A_0/A_s)^2$ is small compared to unity)

$$E_p(t) = 2A_s K_1 \cos\left[\int^t (\omega_0 - \omega_s)dt\right] \tag{2}$$

approximately, in which K_1 is a constant characteristic of the phase detector.

In the particular case of low-pass RC coupling, the control voltage E_f is given by

$$\frac{dE_f}{dt} + \alpha E_f = \alpha E_p, \tag{3}$$

in which $1/\alpha = RC$.

Letting $\phi \equiv \phi_0 - \phi_s = \int^t (\omega_0 - \omega_s)dt$, then

$$\frac{d\phi}{dt} = \omega_0 - \omega_s \quad \text{and} \quad \frac{d^2\phi}{dt} = \frac{d\omega_0}{dt} = K_2 \frac{dE_f}{dt}, \tag{4}$$

where $d\omega_s/dt$ has been neglected since the synchronizing burst is crystal controlled at the transmitter and will drift very slowly.

It follows from (2), (3), and (4) that

$$\frac{d^2\phi}{dt^2} + \alpha \frac{d\phi}{dt} - 2\alpha A_s K_1 K_2 \cos\phi = -\alpha\omega_a.^2 \tag{5}$$

The equation is highly nonlinear owing to the presence of cos ϕ, and it is clear that no methods are presently available for obtaining a solution.

The appearance of this equation can be improved somewhat by making the substitutions,

$$\lambda = \sqrt{\frac{\alpha}{2A_s K_1 K_2}}, \quad \gamma = \frac{\omega_b}{2A_s K_1 K_2} \quad \text{and}$$

$$\tau = \sqrt{2\alpha A_s K_1 K_2}\, t, \tag{6}$$

which result in

$$\frac{d^2\phi}{d\tau^2} + \lambda \frac{d\phi}{d\tau} - \cos\phi = -\gamma. \tag{7}$$

This equation may be reduced to a first-order one with the elimination of the independent variable τ by the substitutions $p = d\phi/d\tau$ and hence $p dp/d\phi = d^2\phi/d\tau^2$; this gives

$$p \frac{dp}{d\phi} + \lambda p - \cos\phi = -\gamma. \tag{8}$$

The disappearance of the variable $\tau = \sqrt{2\alpha A_s K_1 K_2} t$ is no disadvantage since, in practice, the time required for look-in to occur is not significant. At lock-in, $p = 0$ and $\phi = \arccos\gamma$. Within the range of its validity, (1) gives approximately the necessary constraints upon λ and γ so that the above values are boundary conditions on *all* solutions of (8).

The behavior exhibited by this type of nonlinear oscillatory system is perhaps somewhat easier to visualize in terms of an analogue, the ideal damped pendulum acted upon by a constant torque and by the force of gravity. Then λ is analogous to the angular displacement of the bob measured from the downward vertical and p is analogous to the angular momentum.

With no torque, the pendulum is in stable equilibrium at $\phi = 0$, $p = 0$, and is in unstable equilibrium at $\phi = \pi/2$, $p = 0$. The effect of a torque γ is a shift of the stable and unstable equilibrium points by the angle arcsin γ; the stable equilibrium point is shifted in the direction of the applied torque, the unstable equilibrium point in the opposite direction.

[2] This equation is discussed at some length by J. J. Stoker, "Nonlinear Vibrations," Interscience, New York, N. Y., pp. 70–80; 1950, in connection with the pull-out torque of synchronous motors.

When the torque is increased to unity, the points of stable and unstable equilibrium coalesce at $\phi=-\pi/2$.

The applied torque supplies energy to the pendulum uniformly for each degree of rotation, whereas the energy dissipated by damping per degree of rotation is proportional to the angular velocity. The gravitational field is conservative, of course, and there is an oscillatory flow of energy from kinetic to potential. Clearly, at very high angular velocities, the dissipated energy will exceed the energy supplied by the torque and the pendulum will slow down. However, at low enough velocities, the energy gained from the applied torque per degree of rotation must exceed the dissipated energy, and the condition of rest is not stable unless the maximum gravitational torque ($\phi=\pm\pi/4$) exceeds the applied torque.

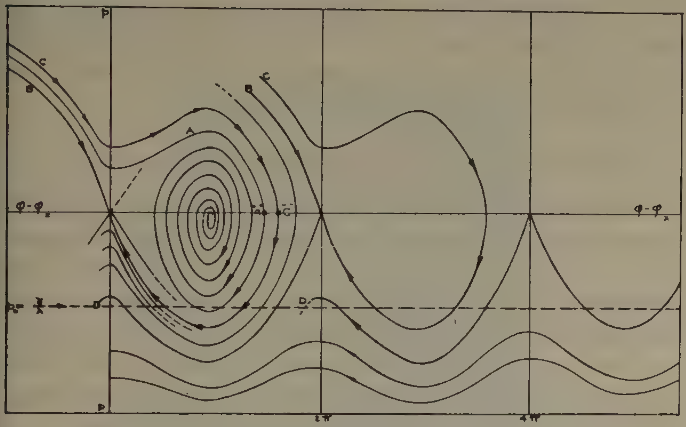

Fig. 2—Representative solution curves for λ less than λ_c—free-hand sketch.

At any instant, the phase error ϕ and the frequency error, which is proportional to p, define a point in the p, ϕ plane; and since p and ϕ are implicit functions of time, this representative point will move in time and generate a curve $p(\phi)$ which is a solution of (8) with the given initial condition. Moreover (8), when solved for $dp/d\phi$, defines uniquely the slope of the solution curve which passes through any given point, except at those points $p=0$, $\phi=\arccos(-\gamma)$, usually referred to as "saddle points." As a consequence, no two solution curves can intersect anywhere on the p, ϕ plane except at the saddle points.

Let us suppose that the initial angular velocity is large and opposite in sense to the applied torque. Then p will decrease toward zero, while ϕ steadily increases until the p axis is reached. If the initial conditions have been chosen so that the pendulum comes to rest, it will stop short of a "saddle point" and fall back, stopping and reversing its motion again at some point short of its previous turning point, and so on, oscillating about the intermediate stable equilibrium point with steadily decreasing amplitude until its energy is fully dissipated by damping; or the pendulum may stop and reverse its direction only once and eventually reach terminal rotation speed under the applied torque.

There will be one solution curve B (Fig. 2), which terminates at an unstable equilibrium point from the left, and one C from the right. Finally, the curve D represents the solution curve when the pendulum is given an infinitesimal angular impulse while in unstable equilibrium.

Since the solution curves cannot intersect, the curves A, B, C, and D divide the p, ϕ plane into two sets of regions, those to the left and above the lines C, but to the right of the B lines (the stable region), and those to the right of the C lines, but to the left of the B and D lines (the unstable region). All solution curves in the stable region spiral into a stable equilibrium point, while all solution curves in the unstable region eventually oscillate about the axis $p=-\gamma/\lambda$.

Thus, given values of γ and λ, depending upon the initial conditions of motion and displacement, the pendulum will eventually either damp out or will approach continuous rotation.

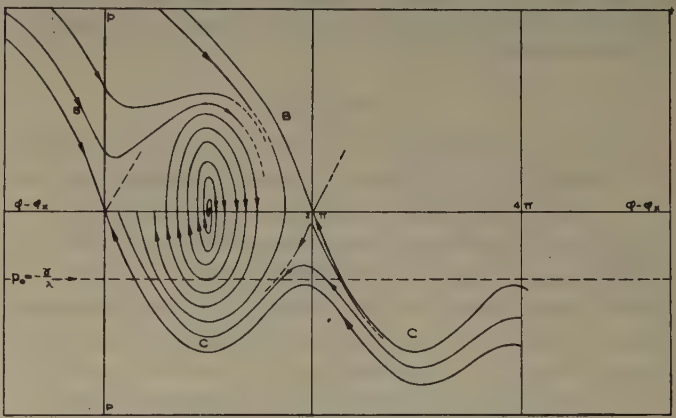

Fig. 3—Representative solution curves for λ slightly greater than λ_c—free-hand sketch.

However, for a given value of γ, as λ is increased, the point c at which the curve C crosses the p axis, moves to the right, until for a certain value λ, the point c reaches the next point of unstable equilibrium. We call this value of λ, λ_c the "second critical damping factor."[3] For λ greater than λ_c, the curve C no longer crosses p axis, and the unstable regions have completely disappeared (Fig. 3).

The values of the "second critical damping factor" for several values of γ were determined by cut and try methods. The boundary solution curves were traced by differential analysis to determine whether or not they cross the p axis.

For γ less than 0.5, the relationship is quite linear and given very nearly by $\lambda_c=0.8\ \gamma$; however, this line cannot be extrapolated with any degree of confidence.

Inserting the original parameters, we get for the lock-in condition (1).

Acknowledgment

The authors gladly acknowledge the assistance of Mrs. Florence Katz, who performed the computations and prepared the manuscript.

[3] *Ibid.*, referring to investigations by Lyon and Edgerton in which "critical damping factor" is distinct from this one.

The Use of Dielectric Lenses in Reflection Measurements*

J. R. MENTZER†

Summary—**In order to minimize the effects of Fresnel diffraction due to short range in the measurement of radar cross sections, a dielectric lens of low dielectric constant was introduced. The lens action was investigated by direct measurement of the shape of the incident phase front at the target, both with the lens in place and without it. The result of the phase measurement showed a reduction of phase variation over the exit aperture of the lens from 150 to 33°.**

In addition to the measurement of phase, the radar cross section of each of a set of metal cylinders was measured both with and without the lens, for comparison. The measured broadside radar cross section of a cylinder of length equal to about 80 per cent of the lens diameter was doubled by the addition of the lens. Calculation showed that the lens effectively eliminated phase error and that the residual error in measured results was essentially all due to anisotropy of the antenna of the simulated radar system used for the measurements.

I. Introduction

THE TECHNIQUE of modeling for the measurement of radar cross sections has been used for several years.[1] The use of models for such measurements has the principal advantage of an increase in the flexibility of frequency simulation and a frequent simplification of both the measuring site and simulated targets. However, the reduction in range obtained by scaling down to a modeled system is often insufficient for convenience and efficiency of measurement, and it is frequently desirable to operate at still further reduced ranges. Although some additional reduction of range is usually permissible, it is clear that excessive range reduction can result in improper phasing of the incident field over the model and additional error in the reception of the field components scattered from different portions of the model.

It is possible to realize the advantages of short measuring ranges without introducing excessive errors by incorporating a lens into the measuring system. The application of metal and dielectric lenses to antenna-pattern measurement has been discussed by Kock,[2] Woonton,[3] and others. However, in the past, most dielectric lens materials have been of dielectric constants of the order of that of polystyrene. The use of either a metal lens of this type of dielectric lens for the measurement of radar cross sections is usually not feasible because the echo from the lens can exceed the echo from the model; moreover, the possibility of interaction between the lens and the model is an additional source of error.

The first of these objections leads to an error signal which is superimposed on the desired echo, and correction is rarely feasible. The second source of error due to lens-model interaction can seriously modify the excitation of the model.

A compromise between long-range operation and the use of a highly reflective lens of short focal length is to use a dielectric lens of low dielectric constant. For this purpose a lens was constructed of styrofoam[4] which has a dielectric constant of about 1.03.

II. Design and Construction of the Lens

The conditions under which the lens was to be used required phase correction over an aperture of 1.1 meter at an antenna-to-target range of 10.7 meters. The modeled wavelength was 3.33 cm so that the lens diameter was 33 wavelengths. Although the validity of optical design of such small lenses is questionable, this method of design was used with the aim of determining the quality of lens performance by measurement.

Fig. 1 shows a cross section of a portion of the measuring system including the lens.

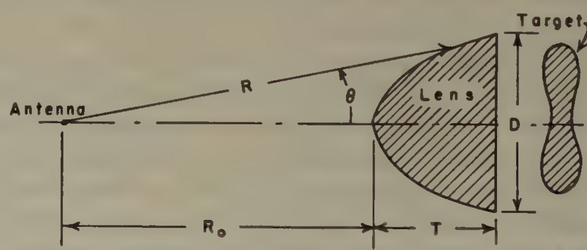

Fig. 1—Arrangement of lens and target.

The first surface of the lens is determined optically so as to produce a plane wave in the dielectric material, and the lens is terminated by a plane surface to preserve the plane phase front on exit.

The source radiates with the phase factor k_0R, where k_0 is the free-space value of $2\pi/\lambda$. To maintain a plane wave in the lens with the phase factor $k_1R\cos\theta+\text{const}$, where k_1 applies to the dielectric medium, the phase of the internal and external fields must be equal at the first surface of the lens. With the co-ordinates of Fig. 1, this gives for the first surface

$$R = \frac{\text{const}}{k_0 - k_1 \cos\theta}. \tag{1}$$

* Decimal classification: R116×R537. Original manuscript received by the Institute, June 2, 1952; revised manuscript received September 12, 1952.

† Formerly Ohio State University, Columbus, Ohio; now, Massachusetts Institute of Technology, Cambridge, Massachusetts.

[1] G. Sinclair, "Theory of models of electromagnetic systems," Proc. I.R.E., vol. 36, pp. 1364–1370; November, 1948.

[2] W. E. Kock, "Path-length microwave lenses," Proc. I.R.E., vol. 37, pp. 852–855; August, 1949.

[3] G. A. Woonton, R. B. Borts, and J. A. Carruthers, "Indoor measurement of microwave antenna radiation patterns by means of a metal lens," *Jour. Appl. Phys.*, vol. 21, pp. 428–430; May, 1950.

[4] Dow Chemical Co., Midland, Mich.

Since $k_1 > k_0$, (1) is the equation of a hyperbola, and the first surface is a hyperboloid of revolution.

In terms of the index of refraction, n, and the distance R_0 between the source and the apex of the lens, (1) may be written

$$R = R_0 \frac{n - 1}{n \cos \theta - 1}. \tag{2}$$

To find the lens thickness, let D be the diameter of the flat side (aperture) of the lens and let T be the lens thickness. With the aid of Fig. 1, it is found that the lens thickness satisfies

$$(n^2 - 1)T^2 + 2R_0(n - 1)T - \frac{D^2}{4} = 0. \tag{3}$$

Since n is nearly unity for styrofoam, (3) may be written in the simpler form

Fig. 2—Photograph of styrofoam lens.

$$T^2 + R_0T - \frac{D^2}{8(n - 1)} = 0. \tag{4}$$

It is desirable to use the more practical range R_0+T, which is nearly the model range. Letting

$$R_1 = R_0 + T,$$

(4) takes the form

$$T = \frac{D^2}{8R_1(n - 1)}. \tag{5}$$

For the lens described here, the parameters in (5) had the values $R_1=10.7$ meters and $D=1.10$ meters, and for styrofoam the value used for n was 1.015. This gave a lens thickness of 0.94 meters. Fig. 2 is a photograph of the lens.

The lens was assembled from two pieces of styrofoam which were large enough to exceed the lens volume when placed together. The pieces were rigidly attached by styrofoam dowels shaped to form dovetail joints. The resulting block was then cut to shape by means of an electrically heated wire stretched along a contour template.

A styrofoam cylinder was used to support the lens, Fig. 2. The cylinder had a diameter of about 40 cm.

III. Experimental Evaluation of the Lens

As a means of testing the result of optical design, a direct measurement of the phase variation was made across the exit aperture diameter of the lens. A top view of the arrangement for this measurement is shown in Fig. 3.

The source of radiation for the phase measurement was modulated by a square wave at 1,000 cps. The wavelength used was 3.33 cm.

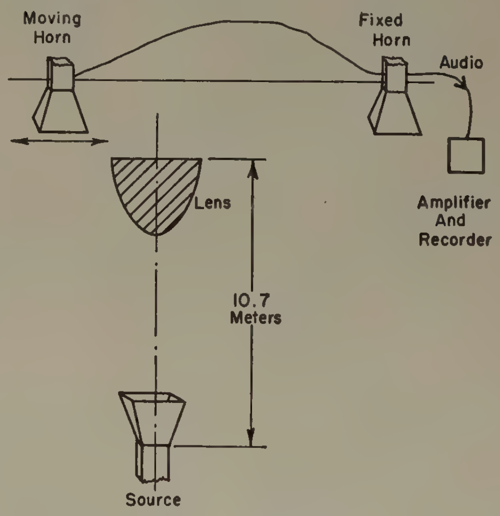

Fig. 3—Top view of arrangement for phase measurement.

As shown in Fig. 3, a moving horn traveled on a horizontal track across the aperture and received a sample of the field continuously. The sample was carried through coaxial cable and added to a sample signal received by a fixed horn. The combined signals were detected and the resulting signal at the modulation frequency was rectified to operate a recorder.

The detection of the sum of the sample signals received by the fixed and moving horns was accomplished by a crystal mounted in the waveguide section attached to the fixed horn. The square-law characteristic of the crystal resulted in recorded data proportional to the square of the sum of the sampled signals.

Since measurement of the reference signal and the unknown signal were required individually, three measurements were necessary: (a) The intensity variation across the aperture was obtained with the movable horn, while keeping the fixed horn pointed away from the source,

but with the horns connected electrically; (b) the intensity of the reference signal at the fixed horn was measured by pointing the movable horn away from the source; (c) the horns were both pointed toward the source as in Fig. 3 and the movable horn was moved along the track.

If $|V_s|$, $|V_r|$, and $|V_t|$ are the respective amplitudes of the signal of unknown phase, the reference signal, and the sum of the first two, the phase angle ϕ between the positive directions of V_s and V_r satisfies the equation

$$\cos\phi = \frac{|V_t|^2 - |V_s|^2 - |V_r|^2}{2|V_s||V_r|}. \tag{6}$$

Fig. 4 shows the result of the phase measurement in the magnetic field plane (vertical polarization). The points obtained from the measurement are shown.

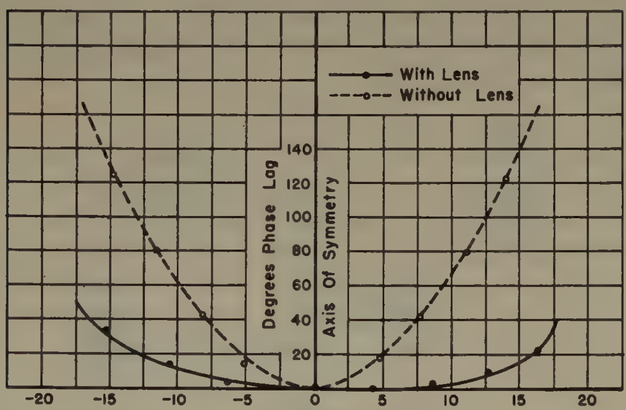

Fig. 4—Measured phase variation with distance from symmetry axis in wavelengths.

For comparison with the phase variation without the lens, a phase measurement was made over the same aperture with the lens removed. The measuring equipment and technique were identical to those described above. The result of this measurement also is plotted in Fig. 4. It is seen that without a lens the total phase variation over a distance 16 wavelengths (the lens radius) off axis is about 150°. Over the same distance with the lens in use, this variation was reduced to 33°. Moreover, when the lens is used, a model, regarded as a set of independent scatterers as long as 36 wavelengths, would not be expected to radiate components more than 90° in phase error back to the antenna; the same model without the lens could reflect components with phase errors as much as 390°.

A noteworthy conclusion from the direct measurement of phase is that a lens no more than 33 wavelengths in diameter shows nearly optical performance.

To examine the effect of the lens on measured values of radar cross section, reflection measurements at 3.33-cm wavelength were made on a series of solid metal circular cylinders. The cylinders ranged in length from 3.05 wavelengths to 36.6 wavelengths, and all were 2.28 wavelengths in diameter. Each cylinder measurement was made both with the lens in use and without it for comparison of results.

Fig. 5 is a reproduction of the recorded results of the measurements on a cylinder 27.5λ long. The radial displacement is proportional to received voltage. The polar plots are the result of rotating the cylinder about a transverse axis with the longitudinal axis of the cylinder lying in a horizontal plane. Vertical polarization was used so that the cylinder axis was always in the magnetic field plane. On each polar plot is superimposed a sketch of the cylinder outline to demonstrate the relation between the data and the cylinder orientation. The echo lobes from the ends of the cylinder extend vertically on the figure and the broadside lobes are horizontal. The reflection measurements were not made on an absolute basis but calibration was accomplished by a single measurement of the echo from a standard metal sphere. A reference echo of 1 M^2 is shown in Fig. 5 as a dotted circle.

It is seen in Fig. 5 that the echoes from the ends of the cylinders did not change appreciably with the introduction of the lens. This result would be expected since the effects of phase curvature would probably be insignificant over the region occupied by the circular section of the cylinder in the end-on position.

The broadside echoes from the cylinder, extending horizontally in Fig. 5, clearly illustrate the effect of the lens on the result of measurement. It is seen that the square root of the radar cross section was increased by the addition of the lens from 1.18 to 1.68 meters, or the measured value of the radar cross section was doubled by the addition of the lens.

It is known that the broadside radar cross section of a thick metal circular cylinder of length L and radius a is given to good approximation by the relation[5]

$$\sigma = \frac{2\pi a}{\lambda} L^2, \tag{7}$$

provided the cylinder is thick enough to be free of resonance effects with varying length. In this case it is reasonable to assume that the cylinder may be regarded as a continuous linear distribution of identical scattering elements. Then, for broadside incidence, the surface current will be in phase along the cylinder provided the lens is functioning properly, but the amplitude of the surface current along the cylinder will vary directly with the amplitude pattern of the antenna. Moreover, the received radiation from different portions of the cylinder will vary directly with the receiving pattern of the receiving antenna along the cylinder.

Under these assumptions, the measured value of broadside radar cross section would be proportional to the square of the integral of the antenna power pattern along the length of the cylinder. If the axial distance from the center of the cylinder to a point on the surface

[5] L. J. Chu, "Analysis of Window and Related Matter," Radio Research Laboratory, Report E 4, Harvard University, Cambridge, Mass.; October 22, 1942.

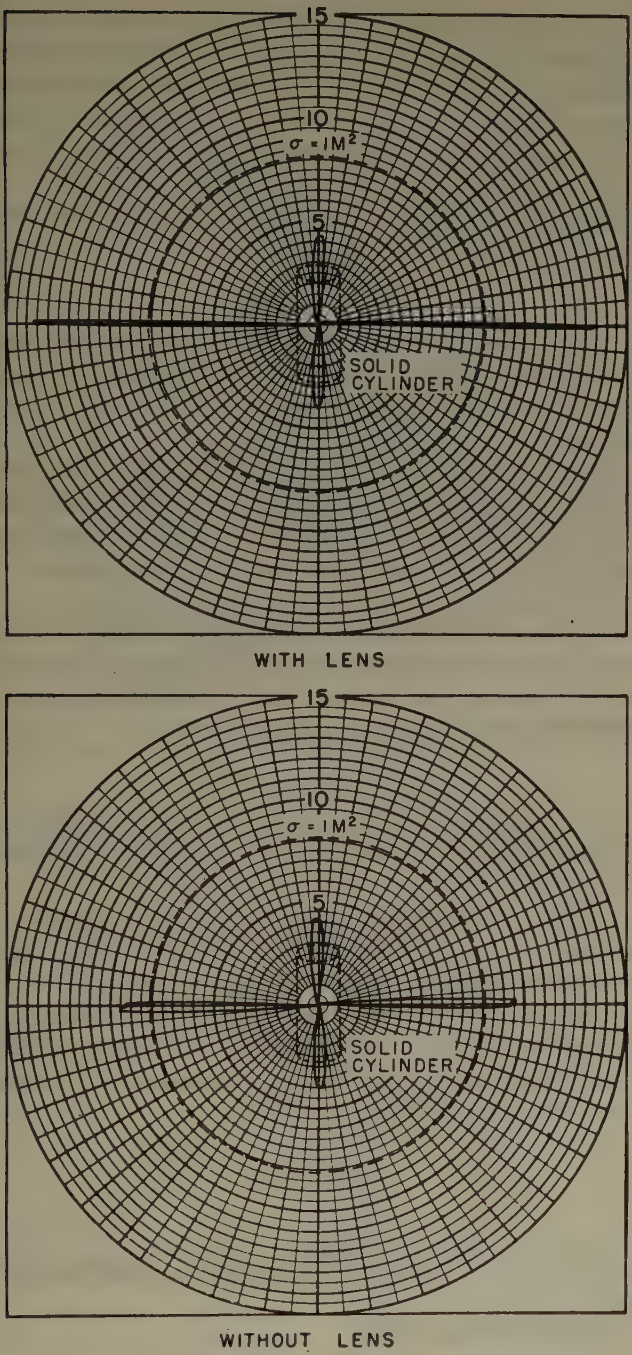

Fig. 5—Measured voltage echoes around a metal cylinder.

is x, and the power pattern of the antenna is denoted by $f(x)$, the broadside radar cross section of a cylinder of length L is

$$\sigma' = A\left[\int_0^{L/2} f(x)dx\right]^2, \tag{8}$$

where A is a constant independent of L.

Since the calibration of the measuring system was done by measurement on a metal reference sphere which was located at the center of the beam of the antenna, the value of σ' prescribed by (8) should be compared with the value one would get by a measurement in a uniform beam of strength $f(0)$. By choosing $f(0)=1$, the application of (8) to the case of a uniform beam gives for the correct value of σ

$$\sigma = \frac{AL^2}{4}, \tag{9}$$

and the ratio of measured to actual radar cross section is

$$\frac{\sigma'}{\sigma} = \frac{4}{L^2}\left[\int_0^{L/2} f(x)dx\right]^2. \tag{10}$$

It was found by measurement that the power pattern of the antenna was represented over the lens diameter in the magnetic field plane within 5 per cent by the empirical formula

$$f(x) = 0.60 + 0.40 \cos 0.175x, \tag{11}$$

where x is measured in wavelengths.

Applying this result to (10), gives for the ratio

$$\frac{\sigma'}{\sigma} = 0.505, \tag{12}$$

and from (7) the measured value of radar cross section should be

$$\sigma' = 3.04 \text{ meters}^2.$$

Referring to Fig. 5, which gives the square root of radar cross section as a function of aspect, it is seen that the measured value of the broadside radar cross section of the cylinder was 2.94 meters.[2] The resulting error between the measured and calculated result is less than 8 per cent of the measured value.

The measurements on the shorter cylinders showed a consistently reduced error in measurement with reduced length, which was correlated with calculation in the same manner as above. In every case agreement was within 10 per cent of the measured value.

The results of the measurements on cylinders showed that substantially all of the error due to phase front curvature was removed by the lens, and the remaining error could be effectively removed by the use of a wide-beam antenna.

IV. Radar Cross Section of the Lens

The low reflectivity of materials of extremely low dielectric constant is one of the most important requirements for satisfactory lens material in order to minimize interaction between the lens and the model and undesirable echoes from the lens. The second of these sources of error is probably the more serious of the two, and may be investigated by a measurement of the radar cross section of the lens alone.

The result of the lens echo measurement at 3.33-cm wavelength is presented in Fig. 6. The radial displacement is proportional to the square root of the radar cross section. As before, the angular positions on the figure corresponds to aspects of the lens as the lens was rotated about a vertical axis. For reference, a top view of the outline of the lens is sketched on the figure.

Referring to the calibration value of 0.1 meter^2 in Fig. 6, it is seen that the maximum radar cross section of the lens in the operating position, represented by the echo lobe extending vertically downward, is about 0.1 meter.^{2} Although this result may prove to be still excessive, it is seen that the lens echo can be reduced to a negligible value by rotation of the lens only one or two degrees about a vertical axis. This rotation was found to have no significant effect on performance of the lens.

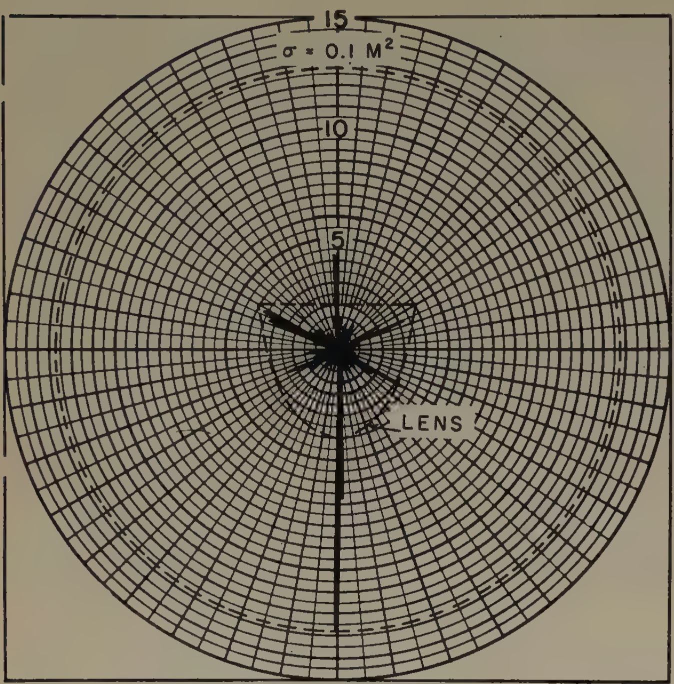

Fig. 6—Voltage echo around a styrofoam lens.

It may be noted that the maximum echo signal from the curved portion of the lens, which corresponds to the operating position, exceeded the echo from the opposite surface, which is flat. Since the principal cause of the maximum echo lobe was probably the reflection at the plane air-dielectric interface in either case, this increased echo from the curved portion is to be expected because of the lens action.

V. Conclusions

A dielectric lens of low dielectric constant has been found to be useful for the correction of phase errors in the measurement of radar cross sections by means of a modeled system at reduced ranges.

Although the long focal length of a lens of low dielectric constant is a disadvantage in cases where low reflectivity is of extreme importance, such lenses can provide highly increased accuracy of measurement at workable ranges.

With respect to lenses of high effective dielectric constant, some definite advantages of lenses of low dielectric constant are ease of machining, light weight, and low required mechanical tolerances.

Acknowledgments

The work described in this paper was sponsored by the Signal Corps. Engineering Laboratories, Fort Monmouth, N. J.

The material presented here is a slightly modified extraction from a dissertation submitted at The Ohio State University for the Ph.D. degree in physics.

Appreciation is expressed for helpful discussions with Professor V. H. Rumsey, Research Supervisor at the Antenna Laboratory and for measurements by Messrs. Daniel Yaw and S. A. Redick.

The Optimum Piston Position for Wide-Band Coaxial-to-Waveguide Transducers*

W. W. MUMFORD†, FELLOW, IRE

Summary—**A coaxial line can be matched to a waveguide by means of a probe antenna located ahead of a short-circuiting plunger. An impedance match can usually be achieved by varying any two of the following three dimensions: (a) the off-center position of the probe, (b) the probe length, (c) the piston position.**

This paper points out that there is, theoretically, an optimum piston position for greatest bandwidth, and presents some evidence corroborating this theory. Bandwidths greater than ±10 per cent to the 1 db swr points have been realized by fixing the piston at its optimum position and varying (a) and (b) above to obtain a match.

* Decimal classification: R117.12. Original manuscript received by the Institute, April 2, 1952; revised manuscript received August 1, 1952. Presented at the 1952 IRE National Convention.
† Bell Telephone Laboratories, Inc., Holmdel, N. J.

Introduction

Coaxial lines and waveguides are both used extensively for the transmission of radio-frequency energy in the microwave region. Since both of these mediums are inherently capable of transmitting wide bandwidths, it should be possible to connect one to the other without too much degradation of the transmission bandwidth. This, in fact, has already been achieved in ridged waveguide,[1] but it requires a transformer which is long compared with the simple

[1] S. B. Cohn, "Design of simple broad-band waveguide-to-coaxial-line junctions," Proc., I.R.E., vol. 35, pp. 920–926; September, 1947.

"cup" type of transducer in which a portion of the inner conductor of a coaxial line is exposed to the wave energy inside a standard waveguide ahead of a short-

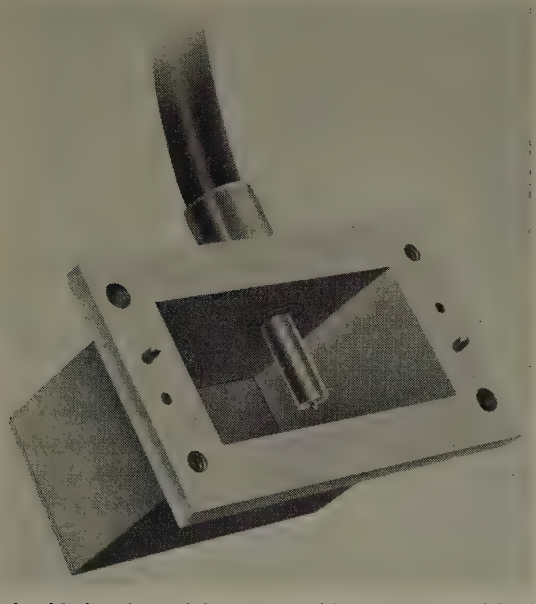

Fig. 1—A wide-band coaxial-to-waveguide transducer with dielectric sheath cut short so the end of the metal probe may be seen.

circuiting piston or plunger, as shown in Fig. 1. The pertinent dimensions for this type of transducer are

(a) the off-center position of the probe,
(b) the probe length, and
(c) the piston position (see Fig. 2.)

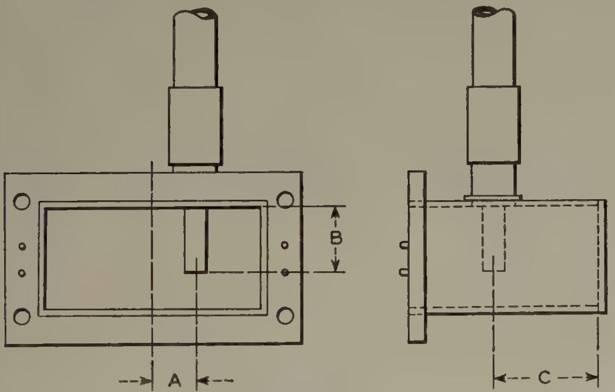

Fig. 2—A probe may be matched to a waveguide by varying (A) the off-center position, (B) the probe length, and (C) the piston position.

An impedance match can usually be achieved by varying any two of these dimensions. In this simple "cup" transducer the bandwidth is limited by the reactance of the piston and also by the fact that the characteristic impedance of the waveguide varies with the frequency. A discussion of these limitations and the search to find conditions which are favorable for wide-band transmission follow.

Theoretical Discussion

The impedance presented to the probe by the waveguide consists of the characteristic impedance of the waveguide in parallel with the reactance of the plunger. This combination of parallel impedances is presented to the coaxial line through the reactance of the probe. There may be some transformation of impedance along the probe if it is a long one, but this may be neglected if the probe is short and is connected directly to the opposite wall of the waveguide. Consider first that this is the case and that the impedance transformation is negligible. Under these conditions, the impedance presented to the coaxial line may be written[2]

$$Z = Z_{0g} \sin^2 \frac{2\pi l}{\lambda_g} \cos^2 \frac{\pi d}{a} + jX, \tag{1}$$

where

- l is the length from piston to probe,
- λ_g is the wavelength in the guide,
- d is the distance of the probe from the center line of the waveguide,
- a is the width of the waveguide,
- X includes reactive components introduced by the probe inductance and the shorting piston, and
- Z_{0g} the characteristic impedance of the waveguide, is given by the relation[2]

$$Z_{0g} = 240\pi \frac{b}{a} \cdot \frac{\lambda_g}{\lambda}, \tag{2}$$

where b is the height of the waveguide.

$$\frac{\lambda_g}{\lambda} = \sqrt{1 + \left(\frac{\lambda_g}{2a}\right)^2}. \tag{3}$$

The impedance, Z of (1), must match the impedance of the coaxial line and since this is ordinarily a purely real impedance, we direct our attention to the real part of Z and the factors which control it.

$$R = 240\pi \frac{b}{a} \sqrt{1 + \left(\frac{\lambda_g}{2a}\right)^2} \sin^2 \frac{2\pi l}{\lambda_g} \cos^2 \frac{\pi d}{a} \cdot \tag{4}$$

It is seen that by changing the piston position, l, or the off-center position, d, any resistance less than the characteristic impedance of the waveguide can be obtained. But it may change rapidly with frequency if the wrong piston position is used, consequently the band might be unnecessarily narrow.

The bandwidth of the transducer depends partly upon how rapidly this resistive component departs from the matching value as the frequency is changed, and will tend to be greatest when the slope of R with respect to the wavelength is zero, i.e., when R is maximum. This would occur with the piston a quarter wavelength from the probe if the characteristic impedance of the waveguide were constant. Ordinarily, however, Z_{0g} changes with wavelength so that the maximum resistance oc-

[2] S. A. Schelkunoff, "Electromagnetic Waves," D. Van Nostrand Co., New York, N. Y., pp. 319, 495; 1943; and J. C. Slater, "Microwave Transmission," McGraw-Hill Book Co., Inc., New York, N.Y., chap. VII; 1942.

curs when the piston position is somewhat less than a quarter wavelength. This is illustrated in Fig. 3, where the factors contributing to R are plotted as a function of frequency for the particular case of dominant waves in a 1 inch$\times$2 inch waveguide with the piston located 2.38 cm (0.936 inch) from the centrally located probe. The quarter-wave position lies at a frequency of 4,450 mc, whereas the slope of R is zero at 4,162 mc.

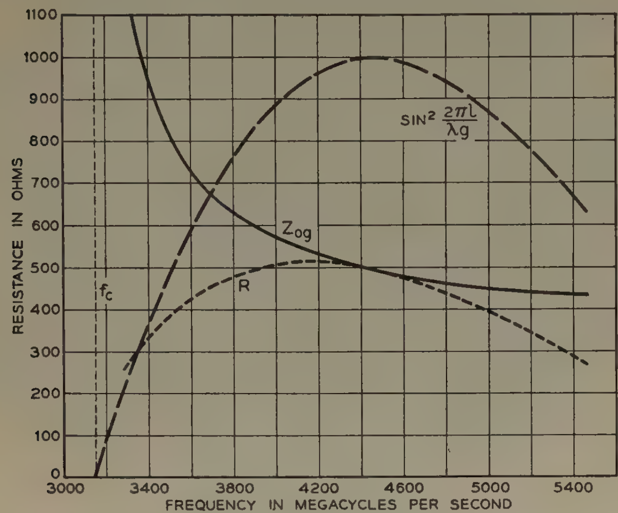

Fig. 3—A plot of the factors which determine the optimum piston position.

The piston position which yields an unchanging value of R, and hence the greatest bandwidth for an excellent impedance match, may be derived from (4) by setting the first derivative of R with respect to λ_g equal to zero. When this is done, we find that the following transcendental equation needs to be satisfied.

$$\frac{\tan \dfrac{2\pi l}{\lambda_g}}{\dfrac{2\pi l}{\lambda_g}} = \frac{2}{\left(\dfrac{\lambda}{2a}\right)^2}. \tag{5}$$

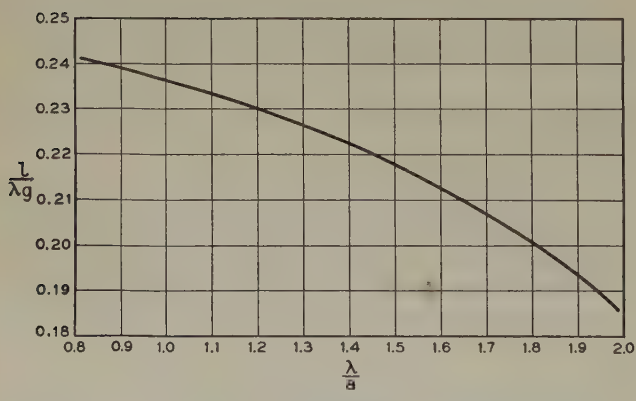

Fig. 4—The optimum piston position, l/λ_g, as a function of the ratio of free-space wavelength to waveguide width.

Values of λ/a and l/λ_g, which give optimum piston position according to this relation, are plotted in Fig. 4. Likewise, values of λ/a and l/a are plotted in Fig. 5.

For example, if we choose a 1 inch $\times$2 inch waveguide (a=1.872 inch id) and a wavelength of 7.2 cm (4,162.5 mc), λ/a=1.51. From Fig. 5, we find λ/a=0.5, whence l=0.936 inch or 2.38 cm. As shown in Fig. 3, R has a maximum value of 514 ohms at 7.2 cm or 4,162.5 mc.

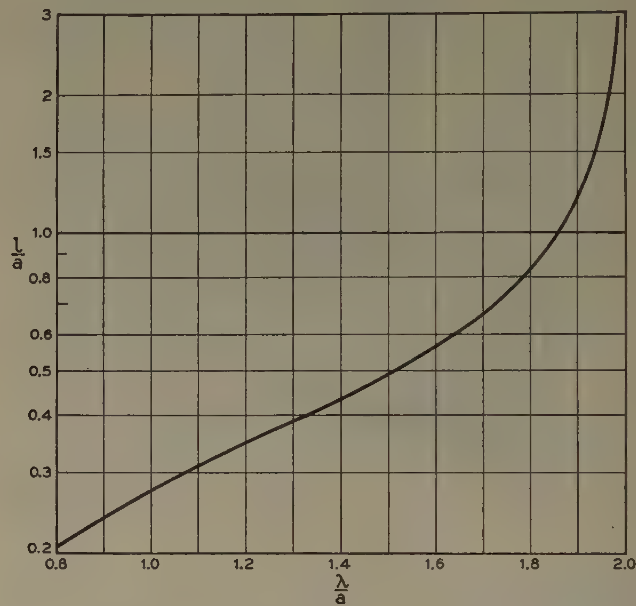

Fig. 5—The optimum piston position, l/a, plotted versus λ/a.

The calculated swr of a transducer designed to match the wave impedance of 514 ohms at 4,162 mc is plotted in Fig. 6. In this calculation the reactive mismatch has been neglected, hence it represents about the best that we should expect from a transducer in 1 inch$\times$2 inch-waveguide at this frequency without resorting to complicated designs. It is seen from the plot that the bandwidth is 970 mc to the 1 db swr point, or expressing it in terms of percentage bandwidth, it is 4,200 mc $\pm$11.5 per cent.

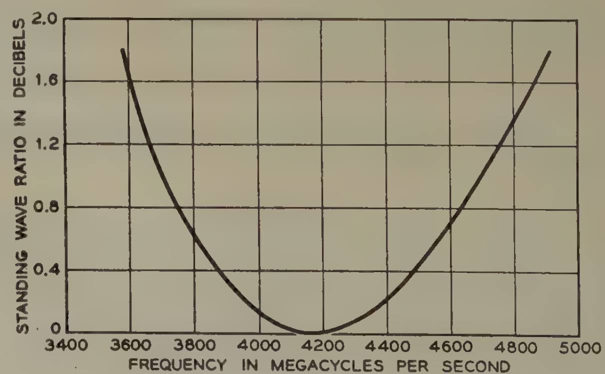

Fig. 6—The calculated swr 20 log $R/514$, for the resistance plotted in Fig. 3.

In the foregoing we assumed that the current in the probe was uniform and that the transformation ratio was unity. This condition exists in waveguides that are not very high, i.e., it exists when the waveguide dimen-

sion parallel to the E vector is small compared with the wavelength and when the probe is connected directly to the opposite wall of the waveguide. In most practical cases the waveguide is so high and the probe is so long that the current cannot be uniform, and a transformation of impedance takes place. This transformation may be taken into account, according to Slater, by defining a coupling coefficient which is independent of the wavelength and of the piston position. Such a coupling coefficient can be assigned to a probe antenna whether it extends all the way across the waveguide and connects to the other side, or merely projects part of the way into the waveguide and is left open circuited. The open-circuited probe is the one of practical importance in wide-band transducers, since its capacity can be used to advantage; the inductive reactance introduced by a piston which is located at the optimum position can be cancelled by the capacitive probe over a wide band.

Some theoretical work has been done[3] on the reactance of probes in waveguides and this may be used as a guide to determine the proper probe length and diameter for bare cylindrical probes. However, when the dielectric of the coaxial line is allowed to cover the probe, as is often done in order to maintain continuity at the junction, the analytical solution becomes quite involved, and for practical reasons it is more convenient to determine the correct dimensions empirically.

Experimental Results

To verify satisfactorily the kind of theory advanced above would take a great deal more data than we have available. The theory deals with but one of so many variables that indeed a comprehensive program involving many detailed side issues would need to be inaugurated and executed carefully in order to prove the theory. No such program has been carried out or even planned. However, our experience has shown us that the coaxial-to-waveguide transducers which have had bands as wide as ± 10 per cent to the 1-db swr points have used piston positions which were close to the optimum position given by (5). Likewise, many narrow-band transducers did not use this optimum position. There is thus a strong presumption that this theory of the optimum piston position will reduce the problem of design from one of three to one of two variables. The following will be of interest to the design engineer.

Let us consider some measurements of the admittance of probes in a waveguide when the piston is held stationary. From these measurements one may see how the probe length and off-center position affect the admittance which is presented to the waveguide by the probe.

Fig. 7 presents these data at a single frequency. It is readily seen that the trend of admittance versus probe length is nearly orthogonal to that of admittance versus off-center position. Hence, by varying these two parameters, an impedance match can be achieved quickly.

These curves are presented with this thought in mind: Trends similar to those of Fig. 7 would be observed in other coaxial-to-waveguide transducers when the optimum piston position is used, so that by a single measurement of admittance one may estimate whether the probe is too long or too far off center.

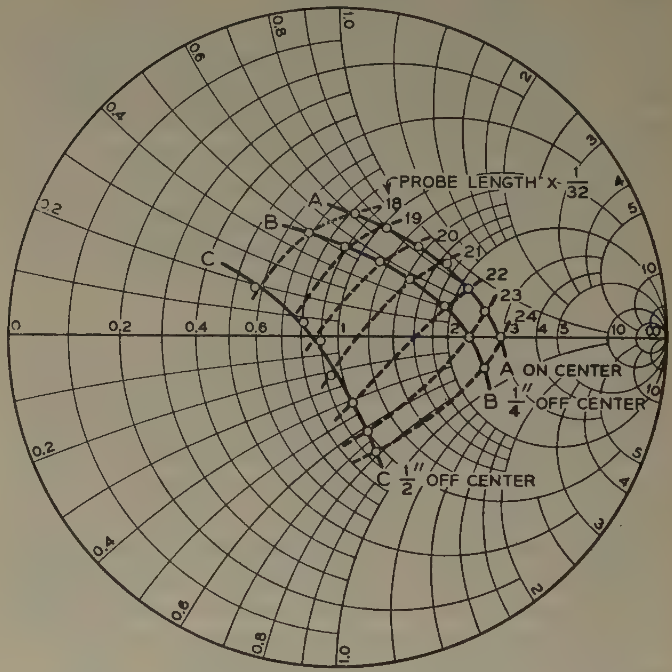

Fig. 7—Smith chart showing the admittance (measured in the waveguide) for probes as a function of the length and off-center position.

For practical reasons, these admittance measurements were made in the waveguide instead of in the coaxial line. This was done to avoid the complication of trying to measure the standing waves in dielectric loaded coaxial lines such as KS-8086 and RG6/u as are commonly used. There can be no question about reversing the point of view from the coaxial line to the waveguide since a broad-band transducer will have the same bandwidth whether one looks at it from the coaxial line or from the waveguide.

The measurements were made in 1 inch$\times$2 inch od rectangular waveguide at a frequency of 4,343 mc. The optimum piston position for 4,162 mc., 0.936 inch, was used throughout, as determined by (5) and Fig. 5. The probe was a bare wire 0.025 inch in diameter and the coaxial line was KS-8086, a lossy cable with rubber dielectric. An adequate length was attached to the probe so as to terminate the probe properly. Measurements of swr and position of the minimum in the waveguide were made versus probe length for three different probe positions: on-center, $\frac{1}{4}$ inch off center, and $\frac{1}{2}$ inch off center. These measurements were interpreted in terms of the admittance seen by the waveguide at the probe. The measurements given by the curve A-A were made with

[3] T. Pearcey, "An Antenna Theory of The Waveguide Probe," Council for Scientific and Industrial Research RPR 72, Sydney, Australia, April, 1947.

the probe on the center line and included probe lengths from 24/32 inch (0.275λ) to 18/32 inch (0.206λ) in 1/32 inch steps. A minimum swr of 6.4 db was recorded for a probe length of 19/32 inch. The admittance at this point was $1.02+j.79$. One might be tempted to move the piston up so as to cancel the susceptance and obtain a match ($1.02+j0$) with the probe length; but this, according to our earlier analysis, would result in a narrower transmission band than necessary.

The next curve, *B-B*, was obtained with the probe ¼ inch off center, with a minimum swr of 4.9 db at a probe length of about 19.5/32 inch. The third curve, *C-C* was obtained with the probe ½ inch off center, with a minimum swr of about 1 db at a probe length of about 20/32 inch.

It is evident that the desired admittance match exists in this case when the probe is about 20.5/32 inch long and a little less than ½ inch off center.

Transducer Design Tips

It will be noted that the amount that the probe had to be moved off center could be estimated from the curve taken when the probe was on center, (*A-A*). There it was observed that the minimum swr was 6.4 db at a probe length of 19/32 inch. If this were purely a resistive mismatch it would correspond to a resistance of 0.478 Z_{0g} across the waveguide, or, looking from the coaxial line into the probe, the resistance would be 2.09 Z_0. Now according to (1), the resistance that the probe presents to the coaxial line can be written.

$$R = R_0 \cos^2 \frac{\pi d}{a}. \tag{6}$$

Setting $R=Z_0$, and $R_0=2.09Z_0$, we have $d=\frac{1}{2}$ inch. From the data of Fig. 7 we know that ½ inch was too far to move the probe off center, but apparently not much too far.

When the probe is too far off center, the coupling to the probe is too weak and can be increased either by moving nearer the center, or by increasing the concentration of the electric field near the probe. Pushing the coaxial line further into the waveguide produces this effect: An increase in conductance, without changing the susceptance, was observed when the threaded outer conductor was screwed further into the waveguide. (The probe length from the end of the outer conductor was not changed; the probe as well as the outer conductor extended further into the waveguide.) This adjustment, when used in conjunction with one which changes the susceptance, is a convenient one for trimming the match.

One means for changing the susceptance slightly is to introduce a metal plug in the waveguide wall opposite the coaxial line probe. This causes a change in admittance almost in the same direction as moving the probe nearer the center of the waveguide. Both the susceptance and the conductance are being changed simultaneously, and although the admittance path is not orthogonal to that caused by screwing in the outer conductor of the coaxial line, small mismatches may be trimmed out by a series of successive adjustments. When it is desired to build both of these two trimming adjustments into the transducer, it is necessary to have the probe a little too far off center, since both tend to make the probe look as if it were nearer the center.

Design Procedure

The data shown in Fig. 7 and discussed above leads us to a rather straightforward design procedure which may (and may not) produce the wide bandwidth predicted by (4). Accepting the optimum piston position given by (5), the procedure for designing coaxial-to-waveguide transducers can be reduced to a logical process consisting of the following steps:

1. Make the coaxial probe too long, i.e., greater that a quarter wavelength.
2. Insert it in the center of the waveguide ahead of a piston, the piston position being determined by 5 (Fig. 4 or Fig. 5).
3. Terminate the coaxial line in its characteristic impedance.
4. Measure the swr (amplitude and minimum position) in the waveguide as a function of the probe length. There will be a probe length for which the swr is least, σ_m. Calculate the admittance for this probe length.

Three conditions of admittance seen by the waveguide are possible; namely,

(a) the admittance is too low,
(b) the admittance is too high,
(c) the admittance is just right.

Condition (c) is unlikely, but it can happen. If it does, one is lucky, for the job may be finished.

5. If the admittance is too low, try to concentrate the field in the waveguide around the probe, for instance, by (a) a metal plug or (b) by screwing in the outer conductor of the coaxial line. Then repeat step 4.
6. If the admittance is too high, it can be lowered by moving the probe off center. One can estimate by (6) how far to move it, setting

$$\frac{1}{\sigma_m} = \cos^2 \frac{\pi d}{a} \quad (\sigma_m \geqq 1). \tag{7}$$

Repeat 4, moving the off-center position of the probe again, if necessary, until the desired condition of match is obtained.

If one has been lucky, the match will be as good as that indicated by (4).

Examples

By way of illustrating the results which may be obtained by following the procedure outlined above, two

examples of coaxial to 1 inch×2 inch waveguide will be quoted in which practically all the bandwidth of (4) was realized. These examples involved the same size of rectangular waveguide, and the same midband wavelength, 7.2 cm (f=4,162.5 mc.). As we have seen in the discussion of the curves in Fig. 3, the calculated optimum piston position is 0.936 inch and substantially this dimension was used in both cases, which involved two different coaxial cables. One coaxial line was the KS-8086 cable mentioned previously, and the other was RG42/u, which has a nominal characteristic impedance of 76 ohms and uses polyethelene dielectric around a nichrome inner conductor. The off-center position in both cases was the same, being 0.368 inch, but the lengths of the dielectric-covered probes were different, being 0.515 inch for the KS-8086 cable and 0.564 inch for the RG42/u cable. The measured swr versus frequency for the KS-8086 transducer is plotted in Fig. 8, showing the semblance of being double humped, with a swr of ½ db at 4,000 mc.

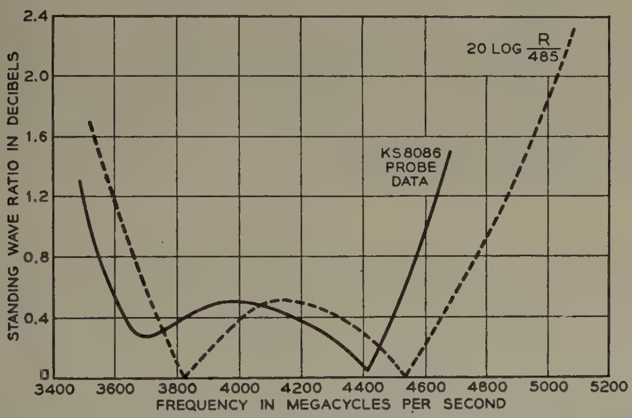

Fig. 8—The measured and calculated swr for a slightly over-coupled transducer.

To compare these results with the theoretical formula (4), the resistance plotted in Fig. 3 was used, assuming ½ db swr due to an over-coupled mismatch at the frequency of maximum resistance, to calculate the swr versus frequency. This curve of 20 log R/485 is included in Fig. 8. The similarity between the calculated and observed curves is good, although there is a frequency shift of about 100 mc between the two. The percentage bandwidths, to the 1-db swr points, are: calculated, ±14.2 per cent, measured, ±13.3 per cent, which represents a reasonable agreement.

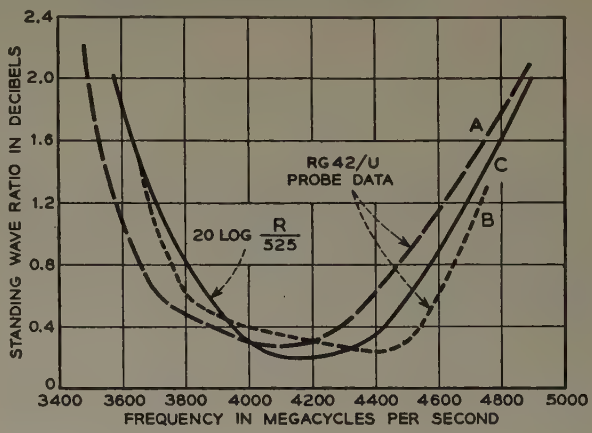

Fig. 9—Measured (curves A and B) and calculated (curve C) swr for a slightly undercoupled transducer.

Similar data for RG42/u coaxial cable are plotted in Fig. 9. They were obtained on two different pieces of cable without resorting to any fine trimming adjustments to improve the match. Neglecting some small anomalous effect at 3,800 mc, both curves A-A and B-B are similar in shape and not too much different from a calculated curve (C-C) based upon an undercoupled mismatch corresponding to 0.2-db swr at mid-band (20 log R/525). The percentage bandwidths to the 1-db swr points are

Calculated (C-C)	±10.5 per cent
Measured (A-A)	±11.2 per cent
Measured (B-B)	±11.6 per cent

These represent reasonable agreement.

Conclusions

This theory of optimum piston position for coaxial-to-waveguide transducers is based upon assumptions which may seem only tolerably acceptable. Yet when one designs transducers in accordance with this theory, one often obtains transmission bandwidths which agree reasonably well with the predicted ones. These instances of reasonable agreement may be fortuitous, but such luck seems unlikely.

The supporting evidence seems to justify the recommendation of a design procedure which is based on this theory.

Fixed-Length Transmission Lines as Circuit Elements*

ALAN A. MEYERHOFF†, ASSOCIATE, IRE AND ROBERT GRAHAM, JR.†, ASSOCIATE, IRE

Summary—**The use of short-circuited transmission-line sections as wide-range resonant circuits in the 50- to 500-mc region is attended with one or more of these disadvantages: restricted tuning range with ordinary variable capacitors, limited choice of susceptance variation, poor impedance matching, and mechanical complexity. An analysis of an alternate method, using short, fixed-length transmission lines with a capacitor at each end, which overcomes these disadvantages, is carried through in normalized form to permit rapid graphical design of the lines and capacitors. The analysis is extended to include interstage coupling circuits and output circuits with a fixed coupling point.**

1. Introduction

At FREQUENCIES in the 50- to 500-mc region it is often desirable to use transmission lines as circuit elements. Usually these are made by short-circuiting the end remote from the circuit under consideration so that, at the end near the circuit, such a line, if less than one-quarter wavelength long, presents a negative susceptance to the circuit. If the line is to be part of a tuned circuit, its susceptance can be tuned out by the equal positive susceptance of a capacitor. By making this capacitor variable, or by changing the length of the line (moving the short), we can tune over a frequency range. If the range obtainable in these ways is not enough, both the capacitor and the length can be changed simultaneously. Some disadvantages of this use of shorted lines are: (1) movable shorts are usually expensive and often unreliable in making contact; (2) the minimum tuning capacitance is limited by the tube interelectrode capacitances; (3) when a certain variation with frequency of effective susceptance at resonance is desired, there is often not sufficient latitude of choice; (4) shorted lines cannot easily be used for impedance matching between two radio-frequency amplifier stages; and, (5) the optimum coupling point for a loop or probe in a shorted line varies considerably over a tuning range.

The alternate method of fixed-length transmission lines as tunable circuit elements described here overcomes these disadvantages.

2. Wide-Range Tuned Circuits

Consider the dissipationless transmission line with air dielectric represented in Fig. 1. For convenience it is shown as a two-wire line, but it may be any cylindrical structure for which a resistive characteristic impedance Z_0 is defined.

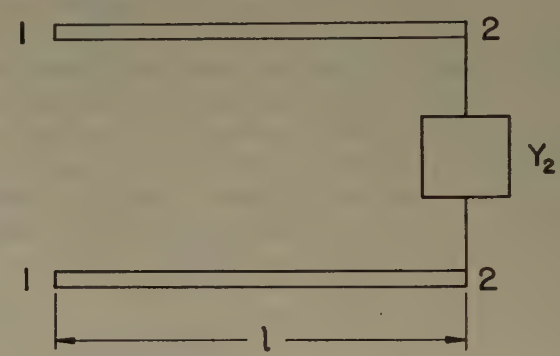

Fig. 1—Transmission-line section.

The formula for the admittance, y, presented by the line at terminals 1-1,

$$y = jy_0 \frac{-j\dfrac{y_2}{y_0} + \tan\theta}{1 + j\dfrac{y_2}{y_0}\tan\theta}, \qquad (1)$$

where $\theta = \omega l/v$ is the electrical length of the line in radians and v is the speed of light, can easily be transformed into the form

$$\frac{y}{y_0} = j\tan\left[\theta + \arctan\frac{y_2}{jy_0}\right], \qquad (2)$$

where $y_0 = 1/Z_0$ is the characteristic admittance. Since we are interested in having y a pure susceptance, y_2 must be a pure susceptance, and since the ordinary tunable susceptances are capacitors, $y_2 = j\omega C_2$.

Equation (2) as it stands does not permit a reasonably simple plot of curves for design purposes since it contains the variables y, y_0, θ, ω, and C_2. But, since $\theta = \omega l/v$, the equation can be written

$$-j\frac{y}{y_0} = \tan\left[\theta + \arctan(n\theta)\right], \qquad (3)$$

where

$$n \equiv \frac{vC_2}{ly_0}.$$

Now, $|y/y_0|$ is plotted as a function of θ with n as a parameter as in Figs. 2 and 3. Fig. 2 is for negative val-

* Decimal classification: R141.2×R117.1. Original manuscript received by the Institute, December 17, 1951; revised manuscript received July 21, 1952. Presented before the Chicago Section of the IRE and Professional Groups on Circuit Theory and on Broadcast Transmission Systems, October 19, 1951.

† Signal Corps Engineering Laboratories, Fort Monmouth, N. J.

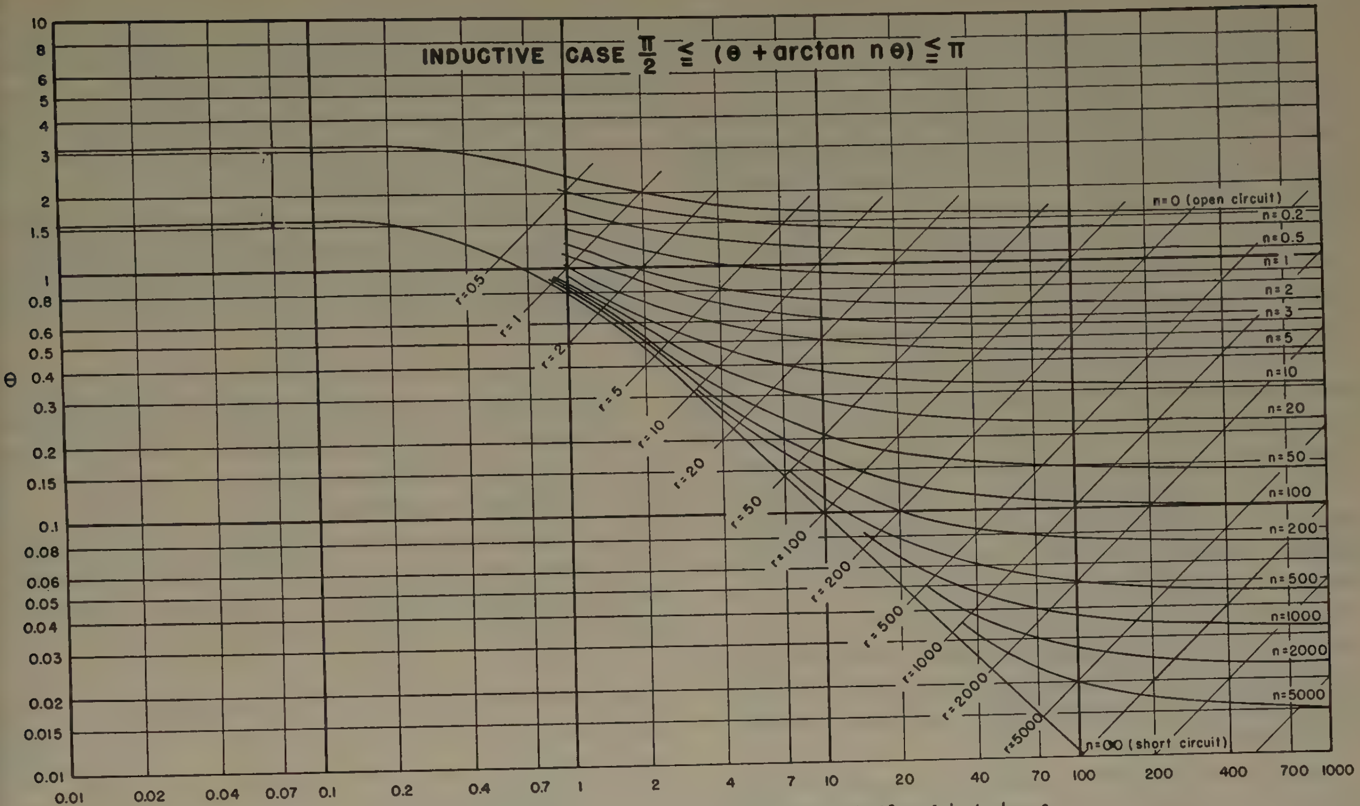

Fig. 2—Graphs of the functions, $|y/y_0| = \tan[\theta + \arctan(n\theta)]$ and $|y/y_0| = r\theta$.

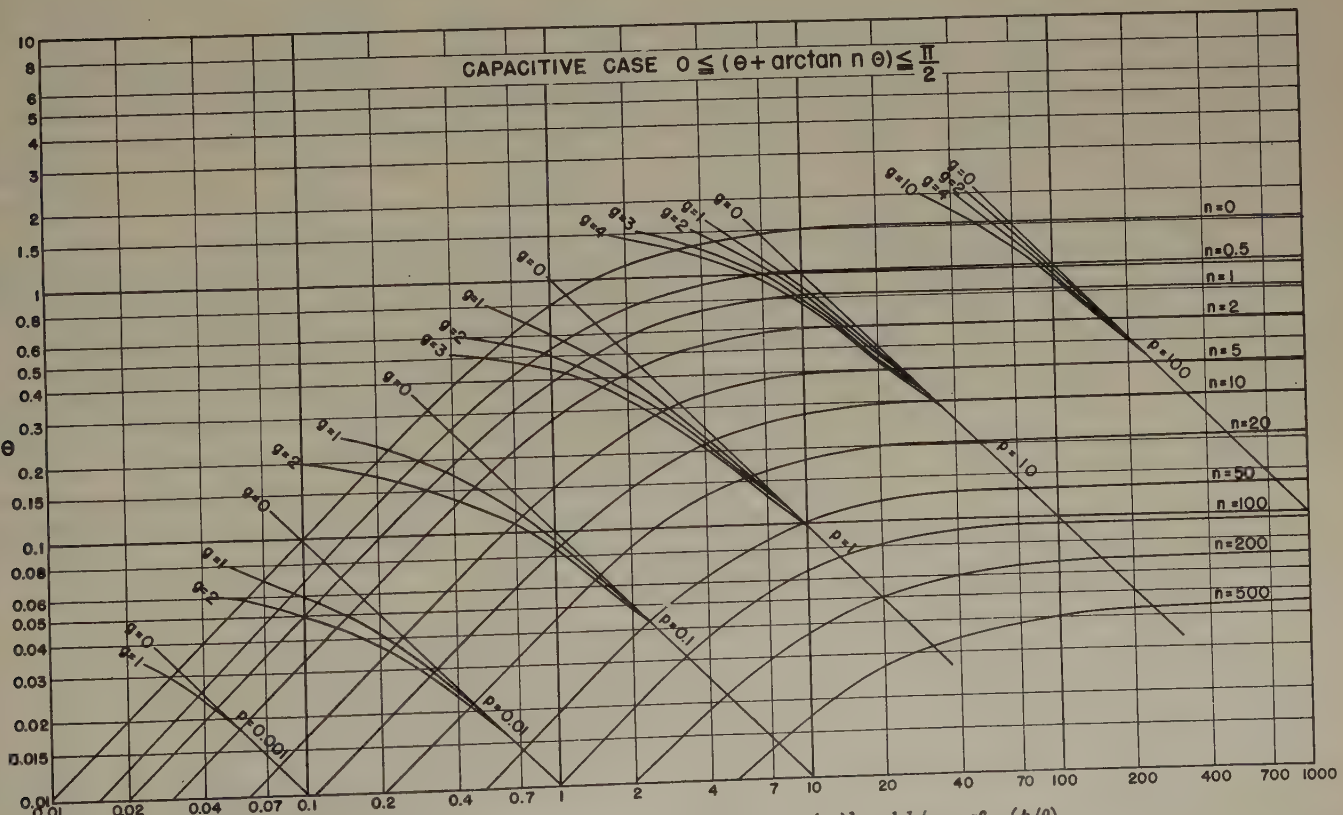

Fig. 3—Graphs of the functions, $b/y_0 = \tan[\theta + \arctan(n\theta)]$ and $b/y_0 = g\theta - (p/\theta)$.

ues of y/y_0 and Fig. 3 is for positive values. The negative values can be resonated by capacitors at terminals 1-1 and the positive values can be resonated by inductors. Consider first the former case.

In keeping with the notation used before, we define $r \equiv vC_1/ly_0$, where C_1 is a capacitor at terminals 1-1, and plot $r\theta = \omega C_1/y_0$ as a function of θ for various values of r. These are the straight lines of Fig. 2. Now, wherever an $r\theta$ line (representing the susceptance of the tuning capacitor) intersects a tan $[\theta + \arctan(n\theta)]$ line (representing the net inductive susceptance of the line) a resonance condition exists and the corresponding values of r, n, and θ can be read off. From these, l, y_0, C_1, and C_2 are suitably chosen. The usual type of tuned circuit has a fixed length, a fixed C_1, and a variable C_2. Then the operation is along any $r\theta$ line. Since θ is plotted on a logarithmic scale, we can mark on a movable straight-edge parallel to the $r\theta$ lines two fixed points representing a desired θ ratio (ω ratio) and slide this straight edge to a position which gives reasonable ratios of r to the two limits of n. Observe that $r/n = C_1/C_2$, so that it is a simple matter to choose these ratios in accordance with available capacitors. There is also no problem with tube capacitances since r can always be made large enough to enable them to be included in C_1.

The cases where the line presents a positive susceptance are of limited usefulness in this application because they require the use of an inductor, L_1, for resonating. If the inductor is at the tube end of the line, the susceptance of the tube capacitance must be added algebraically to the susceptance of the inductor. Fig. 3 contains curves of tan $[\theta + \arctan(n\theta)]$ with n as a parameter and curves of $(p/\theta) - g\theta$ with p as a parameter for several values of g, where $p = l/vL_1y_0$ and $g = vC_t/ly_0$ (C_t is the tube capacitance).

The design of lines by this method usually involves some trial and error as to the relative values of p and g. We shall see later a useful application of these curves in the design of impedance-matching devices.

3. Prescribed Susceptance Variations

Suppose we wish to have a tuned circuit which presents a given variation with frequency of the total effective capacitive or inductive susceptance at resonance, e.g., a reactance tube circuit. The line of Fig. 1 can be replaced, for a certain band of frequencies about any given frequency, by a parallel LC circuit. To find the values of equivalent L and C, write the expressions for the admittances of the line and the LC circuit,

$$\frac{y}{y_0} = j \tan[\theta + \arctan(n\theta)] \quad \text{(for the line)},$$
$$\frac{y}{y_0} = j\left(\frac{b_{sc}}{y_0} + \frac{b_L}{y_0}\right) \quad \text{(for the LC circuit)}, \tag{4}$$

and their derivatives,

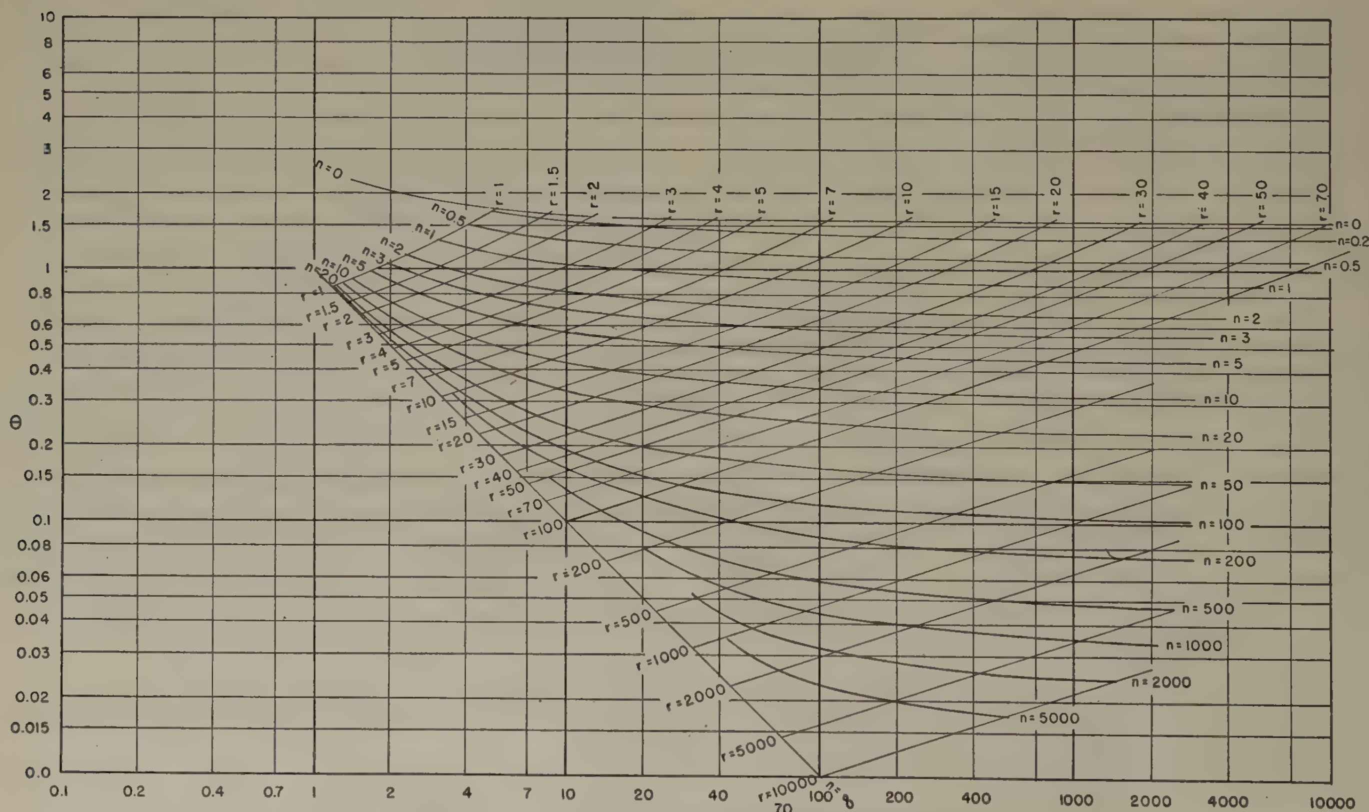

Fig. 4—Graph of the function,

$$\left|\frac{b_L}{y_0}\right| = \frac{\theta}{2}\left[1 + \frac{n}{1+(n\theta)^2}\right]\sec^2[\theta + \arctan(n\theta)] + \tfrac{1}{2}r\theta.$$

$$\frac{d\left(\frac{y}{y_0}\right)}{d\theta} = j\left[1 + \frac{n}{1+(n\theta)^2}\right]\sec^2\left[\theta + \arctan(n\theta)\right], \tag{5}$$

$$\frac{d\left(\frac{y}{y_0}\right)}{d\theta} = j\left(\frac{b_{sc}}{\theta y_0} - \frac{b_L}{\theta y_0}\right),$$

and set the functions equal to each other and the derivatives equal to each other. The simultaneous solution of these equations yields

$$\frac{b_L}{y_0} = \frac{1}{2}\tan\left[\theta + \arctan(n\theta)\right] - \frac{\theta}{2}\sec^2\left[\theta + \arctan(n\theta)\right]\cdot\left[1 + \frac{n}{1+(n\theta)^2}\right]; \tag{6}$$

$$\frac{b_{sc}}{y_0} = \frac{1}{2}\tan\left[\theta + \arctan(n\theta)\right] + \frac{\theta}{2}\sec^2\left[\theta + \arctan(n\theta)\right]\cdot\left[1 + \frac{n}{1+(n\theta)^2}\right]. \tag{7}$$

Since we are interested in cases where the net susceptance presented by the line is negative, the tuning will be brought about by an additional capacitor effectively in parallel with b_{sc}/y_0. Thus the total inductive or capacitive susceptance has the same numerical value as b_L/y_0. This function is plotted in Fig. 4 for various values of n. For convenience, the corresponding values of r for the resonance condition are included.

In most cases the desired variation of b_L/y_0 with frequency is of the form $b_L/y_0 = a\theta^d$ where a and d are constants. Since b_L/y_0 and θ are plotted on logarithmic scales, this variation is represented by any line whose slope is d. Therefore, we need only move, parallel to a line with slope d, a straight edge having two marked points corresponding to the desired frequency ratio and choose convenient values of r and n for the two limits of θ. Since in this case both r and n vary, variable capacitors are required at both ends of the line. Normally the choice of θ, r, and n only at the two extremes will be adequate to provide a sufficiently good realization of the desired power-law variation of b_L/y_0 between the extremes when the capacitors are ganged; however, if a more exact realization is desired, the function r/n can be plotted versus θ and special capacitors can be built to give the proper tracking.

4. Interstage Coupling Device

It is possible, by the following method, to couple efficiently between two radio-frequency stages, over a wide tuning range, through the use of a section of tuned line with a variable capacitor at each end as an interstage impedance-transforming device:

The input admittance to a section of line with any termination is defined by (1). Let

g_1 = equivalent grid-circuit conductance at frequency of operation,
g_2 = plate-circuit conductance,
b_1 = grid susceptance to be introduced in the form of a tuning capacitor including strays and C_{gk},
b_2 = plate susceptance to be introduced in the form of a tuning capacitor including strays and C_{pk}.

The condition for maximum power transfer is

$$y^*_{\text{load or source}} = y_{\text{in}}; \tag{8}$$

hence,

$$\frac{g_1 - jb_1}{y_0} = \frac{\left(\frac{g_2 + jb_2}{y_0}\right) + j\tan\theta}{1 + j\left(\frac{g_2 + jb_2}{y_0}\right)\tan\theta}, \tag{9}$$

and

$$\frac{g_2 - jb_2}{y_0} = \frac{\left(\frac{g_1 + jb_1}{y_0}\right) + j\tan\theta}{1 + j\left(\frac{g_1 + jb_1}{y_0}\right)\tan\theta}. \tag{10}$$

If (9) and (10) are solved simultaneously, the result is

$$\frac{b_1}{y_0} = \frac{1}{\tan\theta}\left[1 + \sqrt{\frac{g_1}{g_2}\left(\sec^2\theta - \frac{g_1 g_2}{y_0^2}\tan^2\theta\right)}\right]; \tag{11}$$

$$\frac{b_2}{y_0} = \frac{1}{\tan\theta}\left[1 + \sqrt{\frac{g_2}{g_1}\left(\sec^2\theta - \frac{g_1 g_2}{y_0^2}\tan^2\theta\right)}\right]. \tag{12}$$

In most practical cases,

$$y_0^2 \gg g_1 g_2; \tag{13}$$

also, for the small values of θ generally used, $\sec^2\theta \gg \tan^2\theta$. Making these approximations reduces (11) and (12) to

$$\frac{b_1}{y_0} \simeq \frac{1}{\tan\theta}\left[1 + \sqrt{\frac{g_1}{g_2}}\sec\theta\right]; \tag{14}$$

$$\frac{b_2}{y_0} \simeq \frac{1}{\tan\theta}\left[1 + \sqrt{\frac{g_2}{g_1}}\sec\theta\right]. \tag{15}$$

By the same reasoning as before let

$$\frac{b}{y_0} = n\theta.$$

Then (14) and (15) reduce to

$$n\theta = \frac{b}{y_0} = \frac{1}{\tan\theta}\left[1 + m\sec\theta\right], \tag{16}$$

where m may take on values either greater than or less than 1.

Both members of (16) are plotted in Fig. 5. First, the values between which m varies are computed. Working on a convenient portion of the curve, the highest value of $\sqrt{g_2/g_1}$ may be plotted and the point of operation on the curve for the lower value of $\sqrt{g_2/g_1}$ is determined by the frequency range. At the values of θ thus determined the values of $\sqrt{g_1/g_2}$ are plotted. Four values of n may now

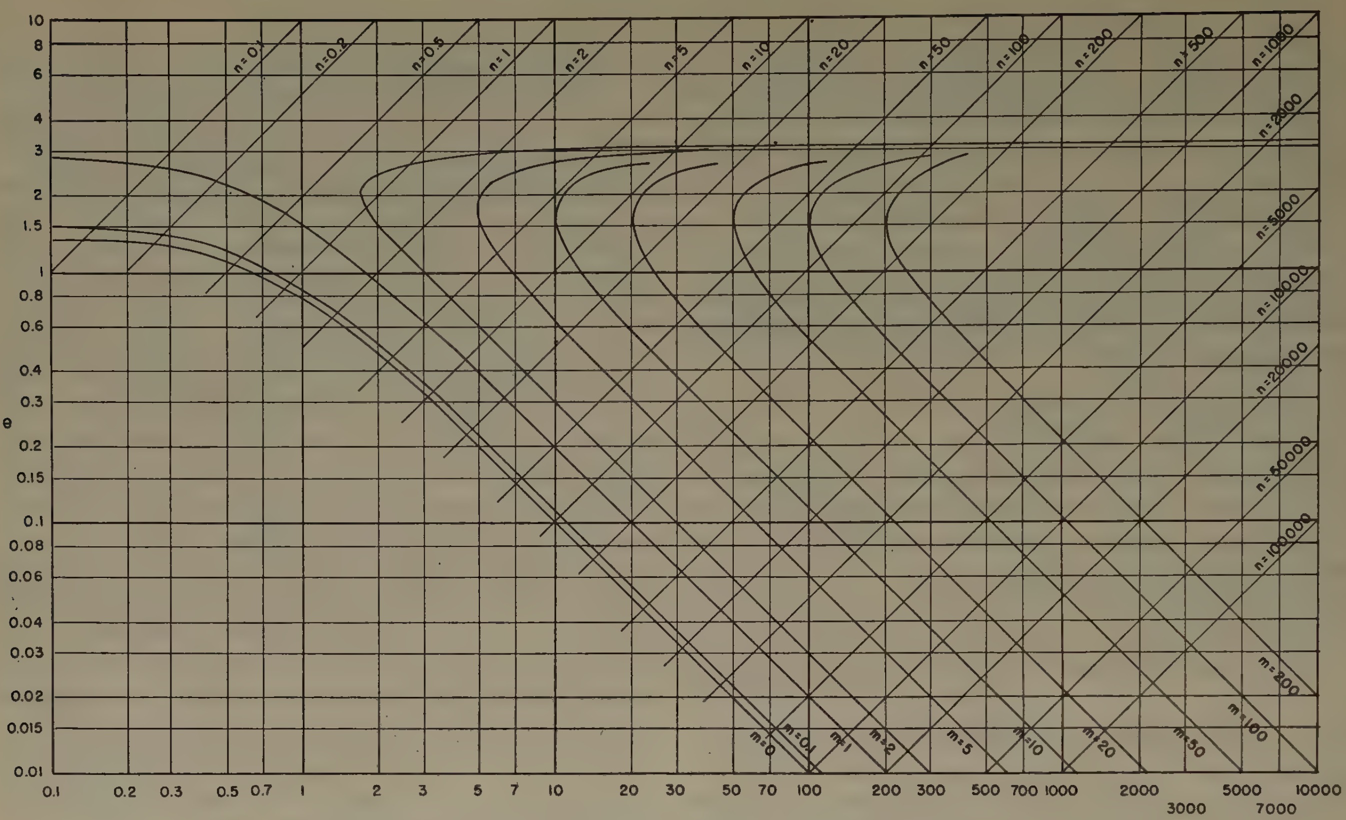

Fig. 5—Graph of the functions, $b/y_0=(1+m \sec \theta)/\tan \theta$ and $b/y_0=n\theta$.

be read from the curves; these determine the maximum and minimum values of capacitance necessary at each end of the line to accomplish the desired match.

5. Antenna Coupling

The foregoing analysis presents a simple method of coupling between the output stage of a transmitter and an antenna over a wide frequency range. If the impedance-matching curves (Fig. 5) are used alone, rather prohibitive values of capacitance are found to be necessary at the low-impedance end of the line because of the usually large ratio of impedances to be matched. If, however, we use this family of curves in conjunction with the family of curves plotted in Fig. 3, a practical solution to the problem results. Since resistive loads constant with frequency are to be matched, operation will be along constant-m lines. The values of m are computed and tentative values assigned Z_0 and θ. The range of θ is determined by the frequency range; the line length is computed. Values of n may now be read off from the appropriate curve of m smaller than 1 in Fig. 5, which determine the maximum and minimum values of capacitance needed at the tube end of the line.

From the appropriate m curve, which is greater than 1, values of b/y_0 corresponding to the limits of θ are read off and plotted on Fig. 3. Values of n are now read off which determine the variation of capacitance necessary at the end of a section of line, the same length and characteristic impedance as the original line, to present the necessary variation in capacitive susceptance at the antenna end. In this application, care must be exercised to ensure that condition (13) is satisfied. The complete device is represented in Fig. 6.

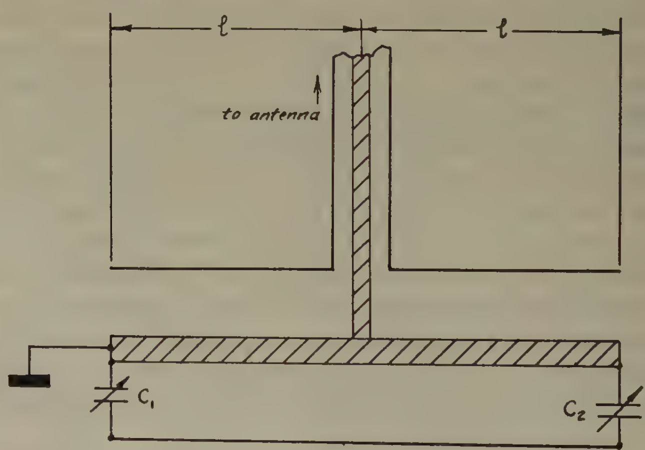

Fig. 6—Antenna coupling line.

6. General Design Considerations

For several reasons, one must be careful in using the right-hand portions of the curves where the normalized input susceptance of the line increases indefinitely. The first reason is the magnification of the loading effect on the circuit of a conductance at the far end of the line or of the copper losses in the transmission line. A second reason arises in connection with reactance-tube prob-

lems. For a given value of characteristic impedance, the susceptance presented by the line increases to the right; therefore, the deviation sensitivity for a given reactance tube decreases. Thirdly, in circuits where a relatively great bandwidth is required, the input susceptance must be kept low, or the Q of the tuned circuit, when determined by the conductance associated with the tube, may become so high as to limit the bandwidth. Finally, the effect of lead inductances becomes pronounced when large input susceptances are used.

7. Examples

1. Design a tuned circuit covering the range 120 to 300 mc with fixed capacitance greater than 20 $\mu\mu$f at the tube end.

Solution: Sliding a straight edge on Fig. 2 parallel to the r lines, we find reasonable values of r, n, and θ at the extremes of the frequency range to be

for $f = 300$ mc,	for $f = 100$ mc,
$\theta_1 = 0.88$	$\theta_2 = 0.35$
$n_1 = 1$	$n_2 = 13$
$r_1 = 20$	$r_2 = 20.$

Then,

$$l = \frac{\theta v}{\omega} = 14 \text{ cm},$$

$$C_2 = \frac{nl}{vZ_0} = 4.67n\ \mu\mu\text{f where } Z_0 = 100 \text{ ohms},$$

$$C_1 = 4.67r\ \mu\mu\text{f},$$

C_2 goes from 54.67 to 60.7 $\mu\mu$f,

$$C_1 = 93.3\ \mu\mu\text{f}.$$

2. Design an oscillator tank circuit tuning 100 to 200 mc for constant deviation for use with a reactance tube which presents an incremental capacitive susceptance of the form

$$\Delta b = a\omega_0.$$

Solution: Analysis of a tuned circuit consisting of L contributed by the line; C, including the capacitance contributed by the line, tube capacitance, fixed capacitances of the reactance tube and strays; and $\Delta C = \Delta b/\omega_0$, yields an expression for the deviation, $\Delta\omega$,

$$\Delta\omega = -\frac{\Delta b}{2C} = \frac{-a\omega_0\omega_0^2 L}{2};$$

then,

$$\frac{1}{\omega_0 L y_0} = \frac{b_L}{y_0} = \frac{a}{2y_0(-\Delta\omega)}\omega_0^2.$$

If $\Delta\omega$ is to be constant, $\theta = \omega_0 l/v$ must vary as $(b_L/y_0)^{1/2}$. Thus, moving a straight edge on Fig. 4 parallel to any line having an actual slope of 1/2, we choose the following values of the parameters for the extremes of the frequency range:

for $f = 100$ mc,	for $f = 200$ mc,
$\theta = 0.54,$	$\theta = 1.08,$
$n = 10,$	$n = 0.8,$
$r = 5;$	$r = 4.$

Then,

$$l = \frac{\theta v}{\omega} = 25.8 \text{ cm},$$

$$C_2 = \frac{nl}{vZ_0} = 8.6n\ \mu\mu\text{f for } Z_0 = 100 \text{ ohms},$$

$$C_1 = 8.6r\ \mu\mu\text{f},$$

C_2 = goes from 6.9 to 86 $\mu\mu$f,

C_1 = goes from 34 to 43 $\mu\mu$f.

3. Design a line to operate as an interstage coupling device in a radio-frequency amplifier tuning the range 100 to 200 mc. The driver plate resistance is 5,000 ohms; the equivalent grid resistance of the driven stage is 1,000 ohms at 100 mc and varies inversely with ω^2.

Solution: The values which m assumes are, for $f=100$ mc, $m=2.24$ and $m=0.447$; for $f=200$ mc, $m=4.47$ and $m=0.224$. Moving these points along their respective m lines on Fig. 5 we find reasonable values of n to be

for $\theta = 0.5,$	for $\theta = 1,$
$n_1 = 5.8,$	$n_1 = 1$ (plate end),
$n_2 = 14;$	$n_2 = 5.7$ (grid end).

Then,

$$l = \frac{\theta v}{\omega} = 23.9 \text{ cm},$$

$$C_1 = \frac{nl}{vZ_0} = 7.97n_1\ \mu\mu\text{f for } Z_0 = 100 \text{ ohms},$$

$$C_2 = 7.97n_2\ \mu\mu\text{f},$$

C_1 goes from 7.97 to 46.2 $\mu\mu$f,

C_2 goes from 45.4 to 112 $\mu\mu$f.

4. Design a line to couple the output of a radio-frequency amplifier stage having a plate resistance of 10,000 ohms to an antenna feed line having a characteristic impedance of 50 ohms over the range 200 to 400 mc.

Solution: For the antenna end, $m=14.1$ and for the tube end $m=0.071$. Moving along $m=0.071$ on Fig. 5, we find reasonable values to be

$\theta = 0.8,$	$n = 1.3,$
$\theta = 0.4,$	$n = 6.5.$

Then,

$$l = \frac{\theta v}{\omega} = 9.55 \text{ cm},$$

$$C_1 = \frac{nl}{vZ_0} = 6.37n\ \mu\mu\text{f for } Z_0 = 50 \text{ ohms}.$$

At the tube end, C_1 goes from 8.28 to 41.4 $\mu\mu$f. From the $m=14.1$ curve the values of b/y_0 are, for $\theta=0.8$, $b/y_0=20.5$; for $\theta=0.4$, $b/y_0=40$. Note that the corresponding n-values are very high, calling for large capacitances. We now plot these values of b/y_0 versus θ on Fig. 3, and read off values of n as 1 and 5. Again, $l=9.55$ cm and $C_2=6.3\ n$. Then, C_2 goes from 6.37 to 31.8 $\mu\mu$f at the open end of the line now 19.1 cm long with the antenna feed line at the midpoint.

Figs. 7 and 8 show details of the construction of lines designed by the methods given here.

Fig. 7—Exploded view of interstage coupling line for 100 to 225 mc., showing tuning capacitors, center conductor, and lucite supports.

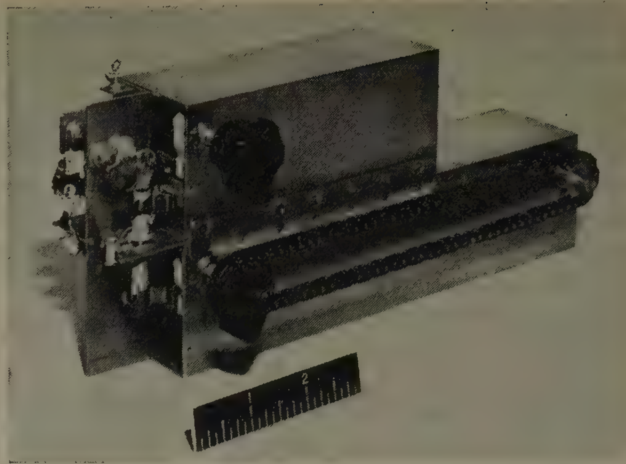

Fig. 8—Oscillator and reactance-tube circuits for constant deviation.

ACKNOWLEDGMENT

Thanks are due Dr. R. Guenther for suggesting several of the subjects treated here and Mr. V. Chewey for reviewing the manuscript.

Correlation Versus Linear Transforms*

MARCEL J. E. GOLAY†, SENIOR MEMBER, IRE

Summary—**A criticism is made of the emphasis recently placed by communication engineers on correlative concepts and devices. Specific suggestions, illustrated by an example borrowed from radar, are offered about other possible attacks on the problems presented by the submergence of wanted data in noise.**

Introduction

An important concept, much applied by Michelson to his interferometric work in optics, is that of the visibility curve of a series of interference fringes. In the particular case of a symmetrical spectrum, this visibility curve constitutes the autocorrelation function of the light amplitude "heterodyned" with respect to the spectrum center, and its Fourier transform in cosines yields the spectral distribution of the source of light. In his latest writings, Michelson recognized the vectorial character of this autocorrelation function for the general case of an asymmetrical spectrum.

More recently, the correlation concept has come very much to the fore in communication engineering, thanks to the use which Wiener, Lee, Brillouin, and others have made of this powerful tool to add new and brilliant chapters to communication theory.

Unfortunately, there appears to have been a hope in many quarters that this recently revived concept might spark the invention of new communication devices,—a hope not particularly encouraged by those who have contributed most to communication theory. This hope must be contrasted with the circumstance that, to this day, there have been no outstanding useful applications specifically derived from it.

A plausible philosophical view of this circumstance is that the correlation concept permits a rationalization of what takes place in a complete communication system, with a human observer as its end organ, and that we should not, at this time, anticipate machines with a rudimentary intelligence, that is, capable of reaching conclusions and decisions from given information by means of correlation computations, when the end organ is a human observer.

We may consider briefly the enormous capacity of this human end organ for discerning patterns, for noting the small irregularities which are of physical significance, for reaching conclusions and decisions. Some of these properties can be quantitatively gauged by the reader, who will look at any supposedly uniform shade of grey obtained by the half tone process, and who will immediately detect slightly brighter or darker spots. On closer examination, he will discover that these smaller or darker spots are caused by a few black dots in a million, which are slightly smaller or larger than the rest. In a somewhat coarser pattern of regularly spaced dots, the reader will also detect, with surprising ease, individual dots of the same size as the rest, which are slightly displaced with respect to their assigned lattice positions.

* Decimal classification: R116×510. Original manuscript received by the Institute, July 31, 1951; revised manuscript received June 9, 1952.

† Signal Corps Engineering Laboratories, Fort Monmouth, N. J.

Conversely, few readers will not recall the feeling of frustration experienced when failing to count with certainty, say, twenty equally spaced identical black bars separated by white bars of the same width—a counting operation most easily performed by electronic means—unless helped in this by the presence of small irregularities in the pattern—a circumstance difficult to register electronically.

As we consider these extraordinary properties of the human end organ in a communication system, his shortcomings, and the kind of dualism which exists between him and electronic systems which perform with ease where he fails and with difficulty where he excels, we may be led to accept the thesis that what should be expected of an efficiently designed electronic system is the predigestion of the primary information by means of linear transformations, followed by cinematographic presentation of the linear transforms to the human end organ, who shall do his own correlations and decisions.

It is not the intent of this discussion to give a proof of this thesis, if, indeed, a proof could be given for a general recommendation in instrumental policy. Rather, an illustration will be given of the application of this thesis to the relatively simple and clean-cut problem of processing digitally and displaying on a cathode-ray scope the full information contained in coherent radar returns. This illustration will also be designed to indicate quantitatively the enormous memory and information processing requirements of an efficiently designed system, and suggestions not borrowed from modern communication theory will be made for practical solutions.

The Coherent Radar Display Problem

Consider the "*A*" scope display of the coherent video returns of 2-μsec pulses emitted at a 1,000-pulse per second repetition rate. In this display, large clutter will appear as fixed hills or valleys, large moving targets will appear as "butterflies," small clutter is detectable by virtue of our eye's ability to recognize a molehill under the grass, but small moving targets remain undetected because our visual senses and our brain cannot make the Fourier analysis required for this.

The display of these small targets can be achieved either by a correlation method or by a Fourier transformer method. With both methods, dual video returns will be obtained by heterodyning the radar returns with two cw radar frequency signals in quadrature, and these returns will be separated into 500 different range intervals by means of 500 pairs of gates. Thus, the returns passed by one pair of gates during some arbitrarily chosen time, say 1/10 second, will form two series of 100 amplitudes,

$$a_1, a_2, \cdots, a_n \text{ and } b_1, b_2, \cdots, b_n \quad (n = 100).$$

Both methods will consist in making a finite number of arithmetical operations, in keeping with the digital treatment postulated above, and the methematical expressions for the processes carried out will contain the sum signs rather than the integral signs. Hence the correlation functions will be approximated by correlation series; and the Doppler spectra of moving targets derived from these series will consist of a finite number of spectral samples. Likewise, there will be a correspondingly finite number of Fourier transforms of the amplitudes.

This approximation of continuous functions by discrete series represents the inverse of the process followed when defining these continuous functions as the limits of indefinitely detailed series, and the mathematical implications of this approximation need not be recalled here.

The correlation method consists in forming the autocorrelation series A and B of the a and b series, as well as their cross-correlation series C, defined as follows:

$$A_j = \sum^m a_m a_{m+j}, \qquad B_j = \sum^m b_m b_{m+j} \text{ and}$$
$$C_j = \sum^m a_m b_{m+j}, \tag{1}$$

where the summations are to extend over values of m and $m+j$ which range from 1 to 100 only.

These correlation series contain all the statistical information which is of physical interest in the a and b series taken as representing an isolated series of events, within the assumed 1/10-second interval, and the Doppler power spectrum of the moving targets can be obtained from these series by means of the summations

$$S_k = \sum^j (A_j + B_j) \cos \frac{2\pi jk}{n} + 2 \sum^j C_j \sin \frac{2\pi jk}{n} \cdot \tag{2}$$

By giving k the 100 values $-50, -49, \ldots +49$, one hundred spectral samples, which contain the pertinent physical information inherent in the correlation series in a form suitable for display and convenient survey, will be obtained. If these hundred spectral samples are displayed on a cathode-ray screen, the eye will quickly note the large spectral value in the center of the display, corresponding to $k=0$, which represents fixed clutter, whereas approaching or receding moving targets will appear as abnormally high values left or right of center.

As the spectra computed for successive 1/10-second intervals are displayed at that same rate, the faculty of the observer's eye to average these displays will permit him to recognize small targets which might have been mistaken for an accidental burst of noise in a single display. However, the enhancement of the signal-to-noise power ratio thus obtained will be in proportion of the square root only of the number of displays, for we deal here with post-detection integration. The phase information of the 1/10-second groups of returns has not been retained by the correlating computations, hence the information contained in the correlations between these successive groups has been lost.

The Fourier transform method consists in forming the two sets of summations

$$t_k = \sum^m a_m \cos \frac{2\pi mk}{n} + \sum^m b_m \sin \frac{2\pi mk}{n} \tag{3}$$

and

$$u_k = \sum^{m} a_m \sin \frac{2\pi mk}{n} - \sum^{m} b_m \cos \frac{2\pi mk}{n} \qquad (4)$$

for the 100 values of k: $-50, -49, \ldots +49$.

The hundred pairs of values thus obtained preserve all the information contained in the original a and b series, and can be considered as the pairs of projections of hundred vectors. When the ends of the vectors thus obtained for successive 1/10-second intervals are displayed on a cathode-ray screen with respect to a vertical linear array of vector origins, they will appear to dance about if due to noise, the average noise vector being scaled down to a conveniently small length, say 0.5 mm. One vector will rotate slowly on a circle 1.5 mm in diameter if it represents a target having a speed which is nearly an exact multiple of one hundredth the speed of light times the ratio of the repetition rate over twice the radar frequency, and produces individual radar returns some 10 db below the noise (10 db above the noise for the 100 returns summed over the 1/10-second interval). Two neighboring vector ends will bounce regularly and in unison on their respective circles, if they represent a target having a speed intermediate between the two speeds at which one or the other of these two vectors would be maximized and remain stationary.[1,2]

If the observer's eye is attracted by an apparently large vector, an instant's observation, coupled with mental correlation, will reveal whether the vector singled out was a chance noise burst, or represents a target the speed of which could be determined with any desired accuracy by means of a stop watch. And if the returns passed by 500 pairs of range gates are similarly processed and displayed side by side on a cathode-ray screen, the observer will view the display of the complete predigested returns of the radar postulated in this discussion.

In this two-dimensioned display, the abscissa and ordinates of the 100,000 vector ends will represent the range and amplitude of the targets. The quick registration by the eye of a few out of 100,000 dots which are displaced with respect to the regular pattern in which most fit, may be near the limit of the eye's capacity, but alternate displays may be easier to survey. For instance, the t_k values may be displayed as vertical displacements of the vector ends, as assumed above, while the u_k values are displayed as a "Z" modulation. Thus, instead of appearing to move on a circle in the screen, the vector ends corresponding to a target will appear to move up and down and in and out of the screen, on a circle perpendicular to the screen, and the modulation of intensity may make for an easier survey of the pattern.

It must be noted that the Fourier analysis carried out with the second method consists in making linear transformations of the amplitudes received at a high rate, and that these transformations are presented at cinematographic speed. Since the phase information is preserved by these linear transformations, the observer can make his own antedetection integrations and correlations, up to the instant of decision, and the enhancement of the signal-to-noise power ratio thus realized is in direct proportion of the number of displays.

It will be noted also that the power spectrum of the Dopler signals can be obtained directly by squaring the lengths of the vectors yielded by the Fourier analysis, for we have, identically

$$S_k = u_k^2 + t_k^2. \qquad (5)$$

It can be verified easily that, in the example treated here, the correlation method requires the order of 40,000 ($4n^2$) independent multiplications to compute the 100 S_k's from the a and b series derived from one pair of gates during 1/10 second, whereas the Fourier transform method requires the order of 20,000 independent multiplications only to compute the equivalent $(u_k^2+t_k^2)$'s.

As it is the spectrum which is most often of physical interest in operational problems (as against analytical problems), the use of the correlation method appears thus to have the further disadvantage of requiring twice the number of computations required by the Fourier transform method, because an intermediate step is required to determine the auto- and cross-correlation series of the signals.

As indicated above, this does not detract from the value of the correlation series or correlation functions as analytical tools. It merely underlines their inappropriateness as operational tools, when dealing with signals the amplitudes of which can be measured, that is, when coherent measurements can be made, as is the case for most radio waves. In this connection it should be remembered that the correlation function can constitute a most useful operational tool in certain problems dealing with incoherent radiation. Michelson's work in optics is a case in point. Another one is the use of the interferometric method to obtain the spectrum of small infrared sources. This method yields directly the autocorrelation function of the radiation amplitude, and permits recording of information about

[1] In the case where the gated 2-μsec interval covers exactly the return of a target, and where this target's speed is exactly one of said multiples, the length of the corresponding vector (without noise will be $\sqrt{E/kT}$ larger than the rms length of the noise vectors, where E designates the total energy returned from the target during the 1/10-second interval, divided by the noise factor of the radar receiver. The probability that a longer vector be due to noise alone is exp $(-E/KT)$. The probability that any vector be due to a target can be computed by an application of Bayle's rule, if an assumption is made about the distribution of target probabilities as a function of target size. It is noteworthy that we deal with Boltzmanns' probability in an efficiently attacked detection problem, in which the phase is unknown, whereas we would deal with the gaussian probability,

$$\frac{1}{\sqrt{2\pi}} \int_{\sqrt{2E/kT}}^{\infty} e^{-x^2/2} dx,$$

when treating the communication problem presented by two cooperating observers who can prearrange the phase of their signals.

[2] A smoother cinematographic display could be obtained by an "interleaving" process. For instance, there could be 20 displays per second of the linear transforms of the returns obtained during overlapping 1/10-second periods.

the entire infrared spectrum of the source in the time otherwise required, with a conventional spectrometer, to obtain information about the small spectral region defined by the slit width.

Consider now the practical problem of computing with adequate speed the various transforms of the radar returns discussed above. Let K designate the number of places in the binary number into which one sampled amplitude is resolved. The multiplication of two such numbers will involve the order of $K(2K+lg_2K)$ gating operations if a high-speed computer of the von Neumann type is used. The number $2K$ includes the partial carrying operation performed after each addition, and lg_2K is a fair figure for the number of operations needed at the end to take care of all the carries. This expression also has the virtue of having the value 2 when $K=1$, i.e., when multiplication of numbers is reduced to a mere multiplication of signs, which can be performed with one pair of gates.

Since 20,000 multiplications are needed to obtain the linear Fourier transforms of the 100 pairs of video returns passed by one pair of gates, $10^7K(2K+lg_2K)$ gating operations will be needed to process all the video returns passed during 1/10 second by the 500 pairs of gates required to cover all range intervals.

The number of operations involved for the complete processing of these radar signals, and the corresponding extensiveness of memory and gating circuits, appear forbidding, at first glance, for any value of K which might be considered reasonable. For instance, for $K=10$, which corresponds to the requirement that the amplitude of the returns be measured and stored with an accuracy of one thousandth of some preassigned amplitude range, the rate at which gating operations should be performed to process all 500 pairs of video returns for presentation on as many columns on a cathode-ray screen is 2.4×10^{10} sec^{-1}. If 10^6 sec^{-1} is assumed for the rate of an individual gating circuit, some 24,000 such circuits would form the bulk of the processing portion of the computer, and provisions should be made for the storage of the 10^6 bits representing the 100,000 pairs of video returns obtained during the aggregate sampling period of 0.1 second.

The very size of the instrumentation involved may explain why the radars of today are still rather primitive and inefficient instruments, when gauged with the standards established for telegraphic circuits, for instance.

Fortunately, an examination of the merits of a large K value reveals the curious mathematical circumstance that, for $K=1$, i.e., when the sign only of each video return is stored, the loss of information incurred is equivalent to less than a 2-db loss in transmitting power, a loss cheerfully accepted when integration over a 0.1-second period yields a 20-db gain in signal-to-noise ratio.

This circumstance exists only when any large fixed clutter which would mask small moving targets is reduced to the level of noise with one of the well known methods, and can be gathered immediately from a comparison of the information value expected of a channel,

$$Wt\, lg_2\left(1+\frac{S}{N}\right)\cong\frac{WtS}{WkT}\, lg_2\, e=\frac{E}{kT}\, lg_2\, e,$$

with the information value of the very doubtful "bit" registered when an energy E, much smaller than kT, is available for its reception. The probability of correctness of this bit is

$$p=1-q=\frac{1}{\sqrt{2\pi}}\int_{\sqrt{+2E/kT}}^{\infty}e^{-x^2/2}dx\cong\frac{1}{2}+\sqrt{\frac{E}{\pi kT}}. \tag{6}$$

Its value is

$$1-p\, lg_2\, p-q\, lg_2\, q\cong\frac{2}{\pi}\,\frac{E}{kT}\, lg_2\, e. \tag{7}$$

Hence, the equivalent power loss[3]

$$10\, lg_{10}{}^{\pi/2}=1.96\text{ db}. \tag{8}$$

With $K=1$, the storage requirement of the example considered above is reduced to 100,000 bits. The repetitive, predetermined character of the linear transformation permits convenient storage on magnetic tapes, and when square functions instead of sinusoidal functions are used for the Fourier analysis, the number of gating circuit is reduced to a most reasonable 200. Actually, in this case, the harmonic production and totalization requirements outweigh the multiplication requirements.

Conclusion

A justification is found for the view that the correlation concept is a useful analytical concept in communication theory, but does not constitute a useful operational concept in communication or radar practice.

On the other hand, it is believed that a useful developmental trend of many systems could be based on the storage on magnetic tapes and linear transformation of the sign only of the amplitude of signals submerged in noise, with presentation at cinematographic speed of the linear transforms thus obtained.

[3] The case $K=1$ can also be treated by the classical probability theory: Assume that a signal pulse of amplitude A is available for the transmission of some information in a low pass channel in which the rms noise is unity. Let the energy available for the transmission of this signal be subdivided into n small pulses of amplitude $A/\sqrt{n}$. If the amplitude of these n small pulses is recorded and added, the value $\sqrt{n}\,A$ will be found, while the incoherently added noise will be $\sqrt{n}$, and the same signal-to-noise ratio is obtained as formerly. On the other hand, if a tally is made of only the positive and negative signals received, the number thus tallied will differ from $n/2$ by the quantity

$$\frac{n}{\sqrt{2\pi}}\int_0^{A/\sqrt{n}}e^{-x^2/2}dx\cong A\sqrt{\frac{n}{2\pi}}.$$

As the rms random fluctuation to be expected in such tallying processes is $\sqrt{n/4}$, the signal-to-noise ratio thus obtained will be $A\sqrt{2/\pi}$, corresponding to an equivalent power reduction of $2/\pi$, as found above. The case $K=2$ is more complicated to treat and requires the application of Shannon's entropy formulas. When it is assumed that a tally is made of whether the signals received are positive or negative, and of absolute magnitude greater or smaller than the rms noise, the equivalent power loss is found to be 0.7 db.

A Theoretical Study of an Antenna-Reflector Problem*

W. C. JAKES, JR.†, ASSOCIATE, IRE

Summary—This paper gives the results of a theoretical investigation of an antenna used with a plane reflector. This finds application in microwave relay stations, where the antenna is placed at ground level facing up and the reflector is located some distance above it.

The results given show that there are certain values of λ, separation distance, reflector and antenna size for which the received power is greater than for the same antenna alone at the elevated location.

I. Introduction

THIS PAPER PRESENTS the results of a theoretical study of an antenna-reflector combination. As shown in Fig. 1(a), the reflector is mounted at an elevated location and reflects incoming energy down towards a receiving antenna. The reflector is assumed to be plane with an elliptical periphery, so that when oriented at 45 degrees to the vertical the projected reflector area is circular, both horizontally and vertically. The diameter of the projected circle is $2a$. (See Fig. 2)

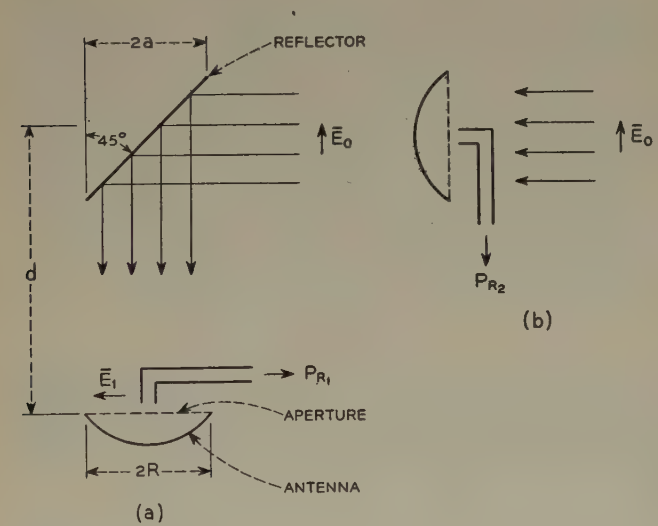

Fig. 1(a)—Antenna-reflector combination. (b)—Antenna alone, subjected to incident field E_0.

The antenna is here assumed to have a circular aperture of diameter $2R$, and when used as a transmitter the aperture field is assumed to be plane, circularly symmetric in amplitude, and parabolically tapered 10 db, with maximum field at the center.

The incoming field is assumed to be a uniform plane wave of value E_0. With the antenna located beneath the reflector, as shown in Fig. 1(a), the received power output is assumed to be P_{R1}. With the antenna located in the position occupied by the reflector (i.e., subject to the incoming plane wave E_0), as shown in Fig. 1(b), the received power output is assumed to be P_{R2}. The problem is then to calculate P_{R1}/P_{R2} for various values of the parameters a, R, λ, and d.

II. Solution

The problem may be divided into two parts. First, the distribution of the reflected field over the antenna aperture must be calculated. Then this field is integrated over the antenna aperture, taking into account the assumed 10 db tapered field distribution of the antenna as a transmitter.

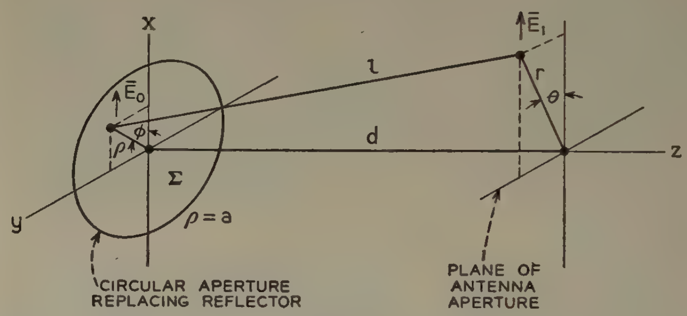

Fig. 2—Replacement of the reflector by a circular aperture for purpose of calculation of the field incident on the antenna.

Treatment of the problem runs as follows, with mathematical details being given in the Appendix: The reflector is replaced by a circular aperture of diameter $2a$ having a uniform plane field of value E_0, polarized in the x-direction, impressed upon it. The diffracted field is assumed to be plane and also polarized in the x-direction. By use of Huygens' principle the diffracted field, E_1, may be brought to the form

$$E_1 = E_0 e^{-i\beta d} g(\xi),$$

where $\beta = 2\pi/\lambda$, d is the separation between reflector and antenna, $\xi = r/a$, r is the radial distance out from the z-axis, and a is the radius of the projected reflector circle. The cross-sectional distribution function $g(\xi)$ has real and imaginary parts, $u(\xi)$ and $v(\xi)$, respectively. Representative variations of u and v are plotted in Fig. 3 for a value of dimensionless parameter $k = (4a^2/\lambda d) = 4$.

When $g(\xi)$ is integrated over the antenna aperture in conjunction with the assumed transmitted aperture field distribution the ratio P_{R1}/P_{R2} may be calculated. Fig. 4 gives the variation of $\eta = 10 \log P_{R1}/P_{R2}$ with $1/k$ ($1/k$ is proportional to the separation, d) for various values of the parameter $l = 2R/2a$.

* Decimal classification: R325.7. Original manuscript received by the Institute April 4, 1952; revised manuscript received July 2, 1952.

† Bell Telephone Laboratories, Holmdel, N. J.

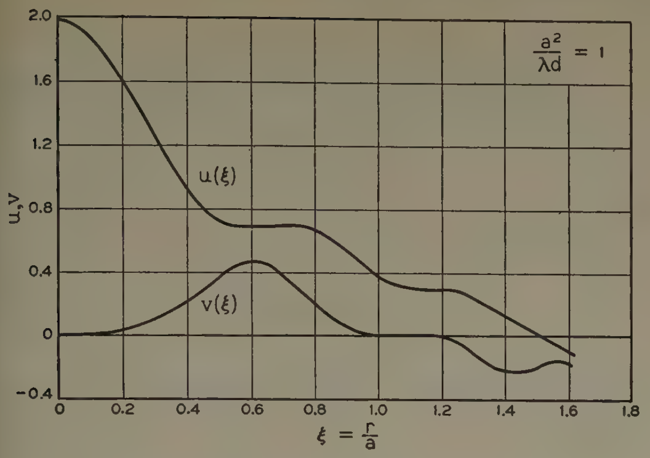

Fig. 3—Real and imaginary components (u and v) of the field variation over the antenna aperture for $d=a^2/\lambda$.

It is obvious from Fig. 4 that for values of $l<0.8$ adn $(\lambda d/4a^2)<0.6$ the power received under the reflector exceeds that which the antenna would receive if it were subject to the field incident on the reflector. For $l=0.8$

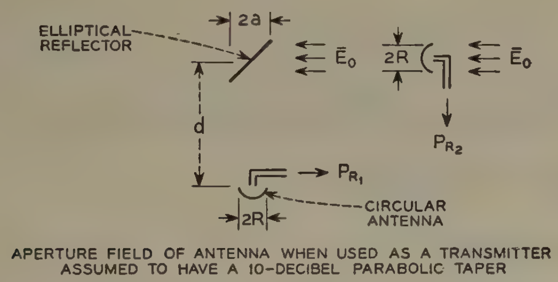

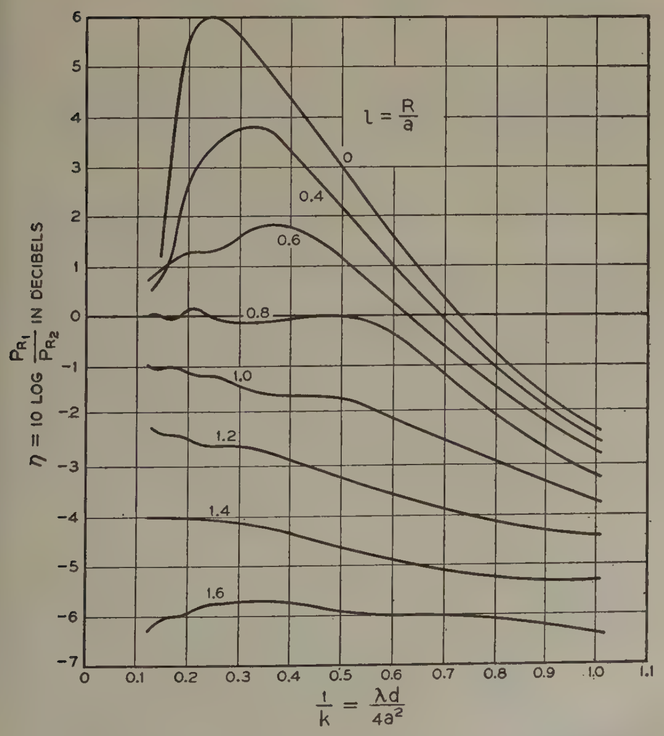

Fig. 4—Ratio of the power received by the antenna under the reflector to that which it would receive if subject to the same field incident on the reflector for various values of a, d, R, λ.

and $\lambda d/4a^2<0.6$ the system is essentially uniform in response over a 5:1 frequency band at a given height, or, conversely, over a 5:1 variation in height at a given frequency.

Appendix

I. Reflected Field

The reflector may be replaced by a circular aperture of radius a, as shown in Fig. 2. The incident field is assumed to be E_0 and the diffracted field E_1. By Huygens' principle [provided $(R+a/d)\leqq 0.176$, $(a/\lambda)>1$],

$$E_1 = \frac{iE_0}{\lambda}\int_{\Sigma}\frac{e^{-i\beta l}}{l}\,ds, \qquad \left(\beta = \frac{2\pi}{\lambda}\right) \tag{1}$$

or

$$E_1 \doteq \frac{iE_0}{\lambda d}e^{-i\beta(d+r^2/2d)}\int_0^a e^{-i\beta\rho^2/2d}\rho\,d\rho \cdot \int_0^{2\pi} e^{i(\beta/d)r\rho\cos(\theta-\phi)}d\phi; \tag{2}$$

using the approximate formula for l [valid to 1 per cent for $(R+a/d)\leqq 0.176$]

$$l \doteq d + \frac{\rho^2+r^2-2r\rho\cos(\theta-\phi)}{2d}. \tag{3}$$

The integral on ϕ in (2) may be evaluated directly, giving

$$E_1 = imE_0e^{-i\beta d - i(m\xi^2/2)}\int_0^1 J_0(m\xi t)e^{-i(m/2)t^2}t\,dt \equiv E_0e^{-i\beta d}g(\xi), \tag{4}$$

where

$$t = \rho/a, \quad \xi = r/a, \quad m = \frac{\beta a^2}{d}. \tag{5}$$

Note that E_1 is independent of θ.

Equation (4) defines the function $g(\xi)$. By taking $(d/d\xi)g(\xi)$ and comparing this to the integral by parts of $g(\xi)$ one gets a differential equation for $g(\xi)$,

$$g'(\xi)e^{i(m/2)\xi^2} - mJ_1(m\xi)e^{-i(m/2)} = 0, \tag{6}$$

with initial condition

$$g(0) = 1 - e^{-i(m/2)}. \tag{7}$$

$g(0)$ gives the field variation along the z-axis, and $g(\xi)$ gives the field variation in the x-y plane for a given value of d.

Equation (6) was solved by the Bell Laboratories General Purpose Analogue Computer for values of $m=k\pi/2$, $k=1, 2, 3 \cdots 8$, giving both real and imaginary parts of $g(\xi)=u(\xi)+iv(\xi)$.

II. Power Relations

Suppose the aperture field of the antenna when used

for transmitting is

$$E_{TRANS} = E_T h(\xi), \ h(\xi) \text{ real and } |h(\xi)| \leq 1. \tag{8}$$

The ratio of the power which would be received by the antenna (area $=s$) when subjected to an incident field E_1 to that transmitted is given by[1]

$$\frac{P_{R_1}}{P_T} = \frac{\left| \int_s E_0 e^{-i\beta d} g(\xi) E_T h(\xi) ds \right|^2}{\left[\int_s E_T^2 h^2(\xi) ds \right]^2}, \tag{9}$$

where

$$E_1 = E_0 e^{-i\beta d} g(\xi). \tag{10}$$

The ratio of the power which would be received by the antenna when subjected to an incident field E_0 to that transmitted is

$$\frac{P_{R_2}}{P_T} = \frac{\left| \int_s E_0 E_T h(\xi) ds \right|^2}{\left[\int_s E_T^2 h^2(\xi) ds \right]^2}. \tag{11}$$

$$\frac{P_{R1}/P_T}{P_{R2}/P_T} = \frac{\left| \int_0^l g(\xi) h(\xi) \xi d\xi \right|^2}{\left[\int_0^l h(\xi) \xi d\xi \right]^2} = \frac{P_{R_1}}{P_{R_2}}, \tag{12}$$

where $l = R/a$.

The integral

$$\int_0^l g(\xi) h(\xi) \xi d\xi \tag{13}$$

was evaluated by the Analogue Computer for values of $l = 0.4, 0.5, 0.6 \cdots 1.6$. The transmitted aperture field was taken as

$$h(\xi) = 1 - .684 \frac{\xi^2}{l^2} \text{ (10 db parabolic taper).}$$

The function $\eta(k, l) = 10 \log (P_{R_1}/P_{R_2})$ is plotted in Fig. 4.

[1] Unpublished memorandum by S. P. Morgan.

Statistical Fluctuations of Radio Field Strength Far Beyond the Horizon*

S. O. RICE†, SENIOR MEMBER, IRE

Summary—**When a sinusoidal radio wave of extremely high frequency is sent out by a transmitter, the wave received far beyond the horizon is often observed to fluctuate. Here some of the statistical properties of this fluctuation are derived on the Booker-Gordon assumption; namely, that the received wave is the sum of many little waves produced when the transmitter beam strikes "scatterers" distributed in the troposphere. Expressions are obtained for the periods of the fluctuations in time, in space, and in frequency. These expressions extend closely related results obtained by Booker, Ratcliffe and others.**

I. Introduction

SINCE AIR CURRENTS are generally turbulent, the atmosphere has small irregularities in its density and hence in its electrical properties. When these irregularities are struck by a radio wave they scatter energy. According to the Booker-Gordon[1] theory of radio scattering, the field at points far beyond the horizon is due solely to this scattered energy

Suppose that a radio transmitter sends out a steady sine wave of extremely high frequency. When the signal is received at points far beyond the horizon it is no longer steady. The time fluctuations of the field strength are explained by ascribing a random motion to the irregularities.

The strength of the received signal may also fluctuate with relatively small changes in the position of the receiver and with changes in the transmitter frequency. In this paper we study the fluctuations of the received wave with (*a*) the time, (*b*) the position of the receiver, and (*c*) the frequency. The time fluctuation results are substantially the same as the ones given by Booker and Gordon[1] for the troposphere, and by Ratcliffe,[2] and Booker, Ratcliffe and Shinn[3] in connection with moving centers of scattering in the ionosphere. Since they fit in naturally with our method of dealing with the remaining types of fluctuation, they are included for the sake of completeness. The results obtained for the fluctuation with position are also somewhat related to those given by Ratcliffe and Shinn.

We shall make use of the simplified Booker-Gordon model shown in Fig. 1. The transmitter at T sends out a sine wave which becomes, in effect, a plane wave by the time it reaches the cloud of irregularities at O. The irregularities scatter the energy of the incident wave so that part of it reaches the receiver at P. The surface of the earth is not shown in Fig. 1, but P is supposed to be over the horizon from T.

* Decimal classification: R113.242. Original manuscript received by the Institute, May 2, 1952.

† Bell Telephone Laboratories, 463 West St., New York 14, N. Y.

[1] H. G. Booker and W. E. Gordon, "A theory of radio scattering in the troposphere," Proc. I.R.E., vol. 38, pp. 401–412; April, 1950.

In the original form of the Booker-Gordon theory, only those scatterers which lie in both the transmitter and receiver beams are of importance. The intersection of these two beams cuts out a volume which we simulate by the cloud of scatterers centered at O. In our simplified model this cloud has spherical symmetry, at least statistically. The density of the cloud is assumed to decrease as we move away from its center in order to imitate the weakening of the transmitter and receiver beams as we move away from their centers.

We assume the scatterers to be clustered about O according to a three-dimensional normal law. Each of the three rectangular co-ordinates is assumed to be independent of the other two, and to have a standard deviation of l. Since the rms distance of a scatterer from O turns out to be $l\sqrt{3}$, we can think of the effective diameter of the cloud as being $2l\sqrt{3}$. This is indicated by the dotted circle in Fig. 1. It seems that l will be of the order of thousands of meters.

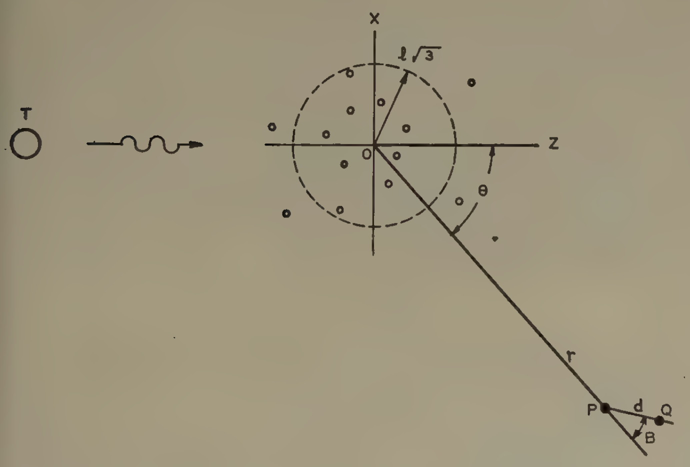

Fig. 1—This diagram shows the positions of the transmitter T, receiver P, and cloud of scatterers clustered about O. The rms distance of the scatterers from O is $l\sqrt{3}$ and their rsm speed is $u\sqrt{3}$

The individual scatterers are taken to be small compared to a wavelength.

The scatterers do not stand still. We assume that they move in much the same way as do the molecules of a gas. If we examine the components of their velocities along any line, such as OX, OY, or OZ we find a normal distribution having an average value of zero and a standard deviation of u. There is no correlation between the various components. Thus the rms speed of the scatterers is $u\sqrt{3}$. We might expect u to be of the order of several meters per second.

If a steady drift, such as would be caused by a steady wind, were added to the random motion it appears that the time rate of fluctuation would increase somewhat and there would be a shift in the average frequency of the received signal due to the Doppler effect.

One might wonder whether the *simplified* Booker-Gordon model just described leads to trustworthy results on fluetuation. For example, it predicts that the incident energy will be scattered in all directions (because of the small size assumed for the scatterers); but this is not in agreement with recent experimental results which show that beam width is preserved. On the other hand, the model does possess the virtue that formulas may be derived from it. We shall proceed with the hope that even though the model is not perfect, the results contain enough truth to give a rough idea of the fluctuations, and of the factors which influence them.

The field at the receiver may be expressed as the sum of waves coming from the individual scatterers. The situation is similar to that found in the theory of random noise where the resultant voltage can be regarded as the sum of many small voltages. The results given here are obtained by using the same sort of analysis as is used in random noise theory.

Let the radio wave sent out by the transmitter at T strike the spherical cloud of moving scatterers at O as shown in Fig. 1. Assume that the only energy arriving at the receiver at P comes from the scatterers. The following results give formulas for the fluctuations with time, with the position of the receiver, and with the frequency, respectively. In other words, Result (a) deals with the rate of fading, Result (b) with "space diversity," and Result (c) with "selective fading."

Result (*a*)

Let the transmitter at T send out a steady sine wave of frequency f_0. The signal at the receiver fluctuates in amplitude and in frequency. It behaves exactly like thermal noise which has been passed through a narrow band filter with a normal law characteristic centered on f_0.

Distortion of this sort has been encountered in other fields, one of which is picture transmission, and has been called "multiplicative noise" or "noise modulation."

The power spectrum of the received signal is proportional to $\exp\left[-(f-f_0)^2/2\sigma_a^2\right]$, where

$$\sigma_a = 2f_0u[\sin(\theta/2)]/c. \tag{1}$$

The width of the spectrum is roughly $2\sigma_a$, and the rms deviation of the frequency of the received signal from f_0 is σ_a. In (1) f_0 is the transmitter frequency, u the rms value of a velocity component of a scatterer, θ the angle between the transmitter and receiver beams, and c is the velocity of light.

The correlation coefficient between the envelope of the signal received at time t and the envelope at a later time $t+\tau$ is given approximately by

$$\rho_a(\tau) \approx \exp\left[-(2\pi\sigma_a\tau)^2\right]. \tag{2}$$

Here τ is the difference in the two times.

Ratcliffe[2] gave these results in 1949 for the case where $\theta = 180$ degrees. They were extended to general values of θ in 1950 by Booker, Ratcliffe and Shinn.[3] It should also

[2] J. A. Ratcliffe, "Diffraction from the ionosphere and the fading of radio waves," *Nature*, vol. 162, pp. 9–11; January, 1948.

[3] H. G. Booker, J. A. Ratcliffe, and D. H. Shinn, "Diffraction from a random screen with applications to ionosphere problems," *Phil. Trans.*, vol. 242, pp. 579–609; 1950.

be mentioned that Siegert[4] investigated a somewhat similar problem in 1943 in connection with radar.

An idea of the order of magnitude of σ_a may be obtained by taking $u=3$ meters/sec., $f_0=4{,}000$ mc and $\theta=2$ degrees. This value of θ corresponds to a distance of about 140 miles between the transmitter and receiver. Using these figures, the value of σ_a comes out to be about 1.4 cps.

The above results on time fluctuation may be put in a slightly different form. If the envelope of the received signal were plotted as a function of the time it would have maxima spaced at irregular intervals. The expected number of maxima per second is

$$2.52\sigma_a = 5.04 f_0 u\,[\sin(\theta/2)]/c. \tag{3}$$

When we use the same values of f_0, u, and θ as before, (3) predicts that the envelope will have about 3.5 maxima per second, on the average.

Since θ is nearly proportional to the distance between the transmitter and receiver, (3) says that the rate of fading (far beyond the horizon) varies directly with the distance and with the frequency used by the transmitter.

The 2.52 appearing in (3) comes from the theory of random noise when it is used to study the effect of a normal-law filter. Of course, the last 2 in 2.52 is not of much significance in our problem.

We now deal with the fluctuation as a function of the position of the receiver.

Result (b)

Let the situation be the same as that assumed in Result (a) with the transmitter sending out a steady sine wave of frequency f_0 and wavelength λ_0. Suppose that the field be frozen at some instant. When we explore this field near the receiver at P we find that it consists of concentric ripples centered at O (Fig. 1) and of wavelength λ_0. The ripples will have an envelope which varies slowly and randomly.

Result (b) states that as we move away from P along the line PQ (shown in Fig. 1) and examine the envelope as we go, we find

$$2.52\sigma_b = 2.52 l\,|\sin B|/r\lambda_0 \tag{4}$$

maxima per meter. As mentioned earlier, l is a length such that $2l\sqrt{3}$ is the effective diameter of the cloud of scatterers. In turn, this diameter may be taken to be the beam width at the point where the transmitter and receiver beams intersect. B is the angle between the lines PQ and OP, r is the distance between the center of the cloud of scatterers and the receiver, and λ_0 is the wavelength. When we assume a beam width of 3 degrees and take the example given earlier, we get $l=1$ mile, $r=70$ miles, and $\lambda_0=7.5$ cm. Our formula predicts about one maximum every two meters, on the average, as we travel at right angles to the direction of propagation (so that $B=90$ degrees).

[4] A. J. F. Siegert, chapt. 6, "Threshold Signals" by J. L. Lawson and G. E. Uhlenbeck, vol. 24 of M.I.T. Radiation Lab. Series, McGraw-Hill Book Co., Inc., 1950.

For a given angular beam width, l and r increase directly with the distance between the transmitter and receiver. Thus (4) tends to be independent of this distance.

The correlation coefficient $\rho_b(d)$ between the envelope at P and the envelope at Q is given approximately by

$$\rho_b(d) \approx \exp\left[-(2\pi\sigma_b d)^2\right], \tag{5}$$

where d is the distance between P and Q, and σ_b is defined by

$$\sigma_b = l\,|\sin B|/\lambda_0 r. \tag{6}$$

Since the expression for $\rho_b(d)$ is an exponential function in which the exponent is squared, it decreases very rapidly when d becomes large. This rapid decrease of the correlation coefficient should not be taken too seriously. It comes from the assumption that the density of the scattering cloud varies according to a normal law. This assumption was made to simulate the weakening of a radio beam as we go away from its center. Other assumptions could be made which would lead to a slower decrease of the correlation coefficient. Hence, we should regard our expression for $\rho_b(d)$ as giving no more than an idea of the order of magnitude, and this only when d is not too large. Incidentally, (6) indicates that the correlation coefficient should be almost independent of the distance between the transmitter and receiver.

The formulas of Result (b) are based on the assumption that l is so large that we have

$$l/r \gg u/c, \qquad l \gg d, \tag{7}$$

where u is the scatterer velocity used in Result (a), and c is the velocity of light.

We now take up the fluctuation of the received signal with frequency.

Result (c)

Let the transmitter frequency f_0 be changed so rapidly that the time fluctuations of Result (a) need not be considered. The envelope of the wave received at P will change because of this change in frequency. When the envelope is plotted as a function of frequency a randomly fluctuating curve is obtained. The same curve could be obtained by having an array of transmitters at T with each one using a different frequency.

The average distance between the maxima of this curve is approximately

$$\frac{1}{2.52\sigma_c} = \frac{c}{5.40 l \sin(\theta/2)}\ \text{cps.} \tag{8}$$

Note that the answer is given in cycles per second. For the values $l=1$ mile and $\theta=2$ degrees used before, this formula predicts about 2 mc for the average distance between the maxima.

If we take l and θ to vary directly with the distance between the transmitter and the receiver, (8) says that the separation between the maxima varies inversely with the square of the distance. Thus, if the transmitter and receiver were 280 miles apart instead of the 140 of

our example, the separation between the maxima would only be $\frac{1}{2}$ mc instead of 2 mc.

The correlation coefficient $\rho_c(f_2-f_1)$ between the envelopes of two signals, one at frequency f_1 and the other at f_2, is given approximately by

$$\rho_c(f_2 - f_1) = \exp\left[-(2\pi\sigma_c)^2(f_2 - f_1)^2\right], \tag{9}$$

where

$$\sigma_c = 2l[\sin(\theta/2)]/c. \tag{10}$$

Just as in Result (b) we cannot expect (9) to give us more than a rough idea of the behavior of the correlation coefficient.

These were our three main results. In our formulas u has been associated with the velocity of the moving scatterers. If it should turn out that our model is altogether wrong, there is still a chance that the formulas of Result (a) will hold provided u is interpreted as some sort of velocity which gives a measure of the time rate of change of the medium. The same may be true for l and Results (b) and (c). $2l\sqrt{3}$ represents the effective sidewise spread of the wave (or rays) in getting from the transmitter to the receiver, and is vaguely similar to the first Fresnel zone.[5]

The nature of our model causes the parameter l to appear in both Results (b) and (c). This indicates that there may be a relation between the "space diversity" and the "selective fading" correlation coefficients $\rho_b(d)$ and $\rho_c(f_2-f_1)$. Equations (5) and (9) give

$$\begin{aligned}\rho_b(d) &= \exp\left[-(2\pi\sigma_b d)^2\right]\\ &= \exp\left[-(2\pi\sigma_c)^2(\sigma_b d/\sigma_c)^2\right] \qquad (11)\\ &= \rho_c[\sigma_b d/\sigma_c],\end{aligned}$$

where the ratio σ_b/σ_c may be computed from (6) and (10). If it should turn out that the "normal law" expressions are incorrect, there is still the possibility that $\rho_b(d)$ may be obtained from $\rho_c(f_2-f_1)$ by putting

$$\sigma_b d/\sigma_c = \frac{f_0|\sin B|d}{2r\sin(\theta/2)} \tag{12}$$

in place of f_2-f_1.

The results of reference 3 suggest that if the scattering were due to a number of moving clouds instead of the one stationary cloud of our model, the pattern of Result (b) would move at a rate determined by the speed of the clouds and produce time fluctuations. If the work leading to Result (a) is repeated for the case where a steady drift is superposed on the random motion (to do this, replace u_n by u_0+u_n, etc., where u_0, v_0, w_0 are the components of the drift velocity, and repeat the work of Section IV. It is now necessary to consider the terms linear in x_n, y_n, z_n in $1/p_n$) we find that the σ_a appearing in (2) and (3) is given by

$$\sigma_a = (f_0/c)\left[(2u\sin(\theta/2))^2 + (V_s l/r)^2\right]^{1/2}, \tag{13}$$

instead of by (1). Here V_s is the component of the steady-drift velocity perpendicular to OP. Thus besides producing a Doppler shift in the average received frequency, the steady drift tends to increase the time rate of fading.

There does not appear to be a great deal of published data on the types of fluctuation considered here. However, the formulas stated above seem to give results of the correct order of magnitude in the very few cases tested.

[5] I am indebted to Mr. F. W. Schott for data (on space-diversity reception) which indicate that under certain conditions $2l\sqrt{3}$ corresponds to an angular spread of only one or two degrees even though the transmitter and receiver beams may be much wider. These data have been explained by assuming highly directive, i.e., large, scatterers. In this investigation, which was performed at the Naval Electronics Laboratory at San Diego, a wavelength of 1.26 inches was used. The receiver and transmitter were 46 miles apart on level desert ground, and were well over the horizon from each other.

II. Examination of Results from a Physical Point of View

Before taking up the mathematical work leading to the results stated in the Introduction, it is worth while to examine them from a physical point of view. Here we try to make them seem reasonable through arguments of the kind often used in optics and X-ray theory.

Result (a) depends upon the Doppler principle. Consider a scatterer to move towards A along the line AB shown in Fig. 2 with the speed u. It moves towards the transmitter at a speed of $u \sin(\theta/2)$. Since it is moving *into* the wavefronts coming from the transmitter more

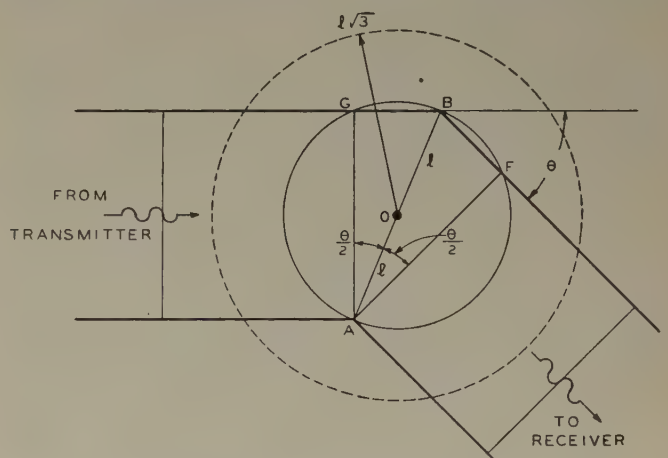

Fig. 2—Diagram used to establish rough versions of Results (a) and (c) of the Introduction.

waves are crossing over it than if it were standing still. These waves cause it to vibrate at a frequency of $f_0+(u/\lambda_0)\sin(\theta/2)$. It is also moving towards the receiver at a speed of $u\sin(\theta/2)$. The Doppler effect produces another increase in frequency so that the received frequency is $f_0+(2u/\lambda_0)\sin(\theta/2)$. When the scatterer moves towards B the received frequency decreases to $f_0-(2u/\lambda_0)\sin(\theta/2)$.

We expect motion in the direction AB to produce the greatest change in the received frequency, because in motion at right angles to AB the change in vibration frequency is just cancelled by the Doppler effect. We can separate the scatterers into two groups according to whether their component of velocity along AB points

from B to A or from A to B. If each group were approximated by a large scatterer moving along AB with speed $\pm u$ the received wave would have a beat note of $(4u/\lambda_0)\sin(\theta/2)$ cps. This is also the number of maxima its envelope would have in one second. Comparison with (3) of Result (a) shows that there is agreement except for a coefficient of 5.04 instead of 4.

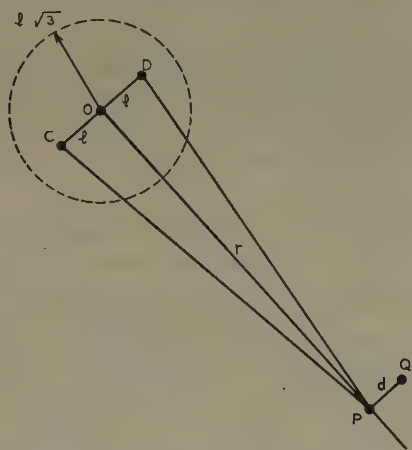

Fig. 3—Diagram used to establish rough version of Result (b) of the Introduction.

In order to obtain a rough form of Result (b) imagine the scatterers to be divided into two groups with each group sending a wave to the receiver. One group has its center at C and the other at D, where the line COD is perpendicular to OP as shown in Fig. 3. Since the effective radius of the cloud of scatterers is about $l\sqrt{3}$, we rather arbitrarily take C and D to be separated by a distance of $2l$. Assume that the wave from each group comes from its center. Also assume, for the sake of argument, that the two waves received at P from C and D are in phase. As an exploratory point moves at right angles to OP ($B=90$ degrees) towards Q, the two waves alternately cancel and reinforce each other. Let Q be the first point beyond P where the two waves reinforce each other and let $PQ=d$. These are particular instances of the Q and d used in the Introduction. Then, since $CP=DP$, $CQ=DQ+\lambda_0$. From Fig. 3 we see that if $l \ll d$,

$$CP = DP = [r^2 + l^2]^{1/2} = r + l^2/2r + \cdots$$
$$CQ = [r^2 + (l+d)^2]^{1/2} = r + (l+d)^2/2r + \cdots$$
$$DQ = r + (l-d)^2/2r + \cdots$$
$$\lambda_0 = CQ - DQ = 2ld/r + \cdots .$$

It follows that the distance between the maxima at P and Q is about

$$d = r\lambda_0/(2l).$$

This gives $2l/(r\lambda_0)$ maxima per meter compared to the value $2.52l/(r\lambda_0)$ given by (4) for $B=90$ degrees.

To study Result (c) we return to Fig. 2. The scatterers are again divided into two groups with their centers at A and B instead of at C and D. The distance AB is taken to be $2l$ and the wave from each group is assumed to come from its center. Incidentally, the line AF in Fig. 2 is parallel to the line CD in Fig. 3. Suppose that at the transmitter frequency f_1 the waves sent out by A and B are in phase at the receiver. Then the path difference GBF is an integral number of wavelengths, say $n\lambda_1$

$$2(2l)\sin(\theta/2) = n\lambda_1 = nc/f_1.$$

Let the frequency increase from f_1. After going through a region of interference, the two waves from A and B will again be in phase and produce a maximum. Let this frequency be f_2 and the corresponding wavelength be λ_2. Then

$$4l\sin(\theta/2) = (n+1)\lambda_2 = (n+1)c/f_2.$$

Equating the values of n obtained by solving these two equations gives

$$(f_2 - f_1) = c/[4l\sin(\theta/2)].$$

This is the distance between successive maxima of the curve showing the envelope amplitude as a function of frequency. It is to be compared with (8) of Result (c) which has 5.04 in the denominator instead of 4.

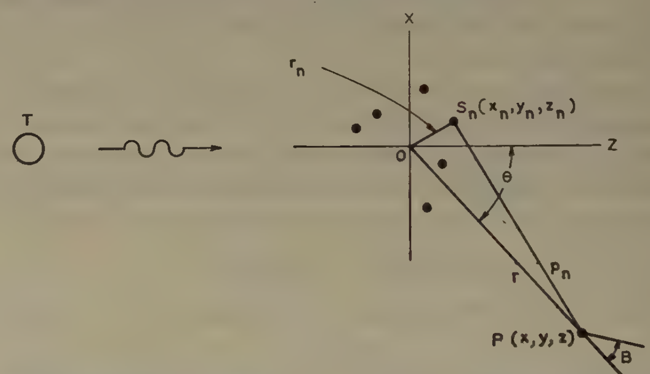

Fig. 4—Geometry of transmitter T, receiver P and nth scatterer S_n at time $t=0$. The scatterers move with random velocities.

III. Expressions for the Received Signal

By a rather long but straightforward consideration of the retarded potentials[6] the following result may be obtained: Let the transmitter T in Fig. 4 send out a radio wave which may be regarded as a plane polarized wave by the time it reaches O. Let its electric vector point in the OX direction. Let the dielectric constant ϵ of a scatterer be greatest at the center of the scatterer, and decrease smoothly towards the value ϵ_0 of free space as we move away from the center. Denote the value of the integral of $\epsilon - \epsilon_0$ taken over the space occupied by the scatterer by the product $U\epsilon_2$. We write a product instead of a single symbol in order that we may interpret U as the effective volume and ϵ_2 as the effective dielectric constant of the scatterer. U and ϵ_2 will never appear separately in our work. Let the dimensions of the scatterer be small compared to a wavelength, and let ϵ/ϵ_0 be close to unity. Let the co-ordinates (x_n, y_n, z_n) of the nth scatterer S_n at time $t=0$ be such that r_n/r (see Fig. 4) is small compared to unity. Let the velocity com-

[6] A discussion of retarded potentials is given in a number of text books on electromagnetic theory. See, for example, J. A. Stratton, "Electromagnetic Theory," McGraw-Hill Book Co., Inc., 1941.

ponents (u_n, v_n, w_n) of S_n be small in comparison with the speed of light c.

Let $E_x = F(t)$ be the electric field produced at O (and indeed all along the line OX) at time t by the transmitter T. The electric field produced at point $P(x, y, z)$ by S_n is the same as that produced by an electric dipole at S_n polarized in the OX direction. Thus the electric intensity at P is perpendicular to S_nP and is of amplitude

$$E = \frac{\epsilon_2 U}{\epsilon_0 4\pi p_n} \frac{\sin \gamma_n}{c^2} F''\left[\left(t - \frac{p_n}{c}\right)\left(1 + \frac{W_n \cos \psi_n - w_n}{c}\right) - \frac{z_n}{c}\right], \quad (14)$$

where the double prime on F'' denotes its second derivative and

$$\begin{aligned} \gamma_n &= \text{angle between the } OX \text{ and } S_nP \text{ directions,}\\ p_n &= \text{distance } S_nP \text{ at time } t=0,\\ W_n &= \text{speed of } S_n = [u_n^2+v_n^2+w_n^2]^{1/2},\\ \psi_n &= \text{angle between direction of motion of } S_n \text{ and } S_nP \text{ direction, and} \quad (15)\\ p_nW_n \cos\psi_n &= u_n(x-x_n)+v_n(y-y_n)+w_n(z-z_n). \end{aligned}$$

The most important part of the expression (14) for the electric intensity, as far as our needs are concerned, is the argument of the function F''. This argument may be termed the "retarded time at P." Since the derivation of (14) is omitted, it seems appropriate to give a physical discussion which leads to the retarded time in question.

Fig. 5 shows the line of motion of the nth scatterer S_n. The position of S_n on this line at time t is given by the co-ordinates x_n+u_nt, y_n+v_nt, z_n+w_nt. p_n is the distance between S_n and the receiver at P at time $t=0$.

Consider now the state of affairs at time t. The electric intensity E along the line OX is given by $F(t)$. The value of E at the scatterer is the value E had at OX at an earlier time, the delay being $(z_n+w_nt)/c$ where c is the velocity of light. Thus the value of E at S_n is

$$F\left(t - \frac{z+w_nt}{c}\right).$$

This is the value of E being scattered at time t. It will not affect the electric intensity at P until some later time which is $t+$(distance between S_n and P at time t)/c.

However, we are interested in the field at P at time t. This field must have been scattered from S_n at some time before t. Let this time be called $t-\tau$. At time $t-\tau$ the co-ordinates of S_n were

$$x_n + u_n(t-\tau), \quad y_n + v_n(t-\tau), \quad z_n + w_n(t-\tau),$$

and the value of E was

$$F\left[t - \tau - \frac{z_n + w_n(t-\tau)}{c}\right].$$

The distance the scattered disturbance travels between the initial time $t-\tau$ and the final time t is $c\tau$. This distance is the separation between S_n and P at time $t-\tau$. Thus

$$\begin{aligned} c^2\tau^2 &= [x-x_n-u_n(t-\tau)]^2 + \text{similar terms in } y \text{ and } z\\ &= (x-x_n)^2 - 2(x-x_n)u_n(t-\tau) + u_n^2(t-\tau)^2 + \text{similar terms in } y \text{ and } z\\ &= p_n^2 - 2[(x-x_n)u_n+(y-y_n)v_n+(z-z_n)w_n](t-\tau)\\ &\quad + [u_n^2+v_n^2+w_n^2](t-\tau)^2\\ c\tau &= p_n - [(x-x_n)u_n+(y-y_n)v_n+(z-z_n)w_n](t-\tau)/p_n\\ &\quad + \cdots. \end{aligned}$$

When we use the last line of (15) to simplify this expression we find that τ is given approximately by

$$c\tau = p_n - (t-\tau)W_n \cos\psi_n + \cdots.$$

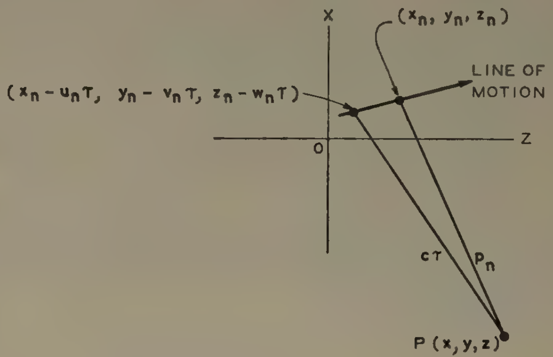

Fig. 5—Diagram for calculating the retarded time at P.

From this it follows that

$$t - \tau = t - \frac{p_n}{c} + \frac{(t-\tau)}{c} W_n \cos\psi_n + \cdots.$$

If we assume that the scattering occurs instantaneously, the field at P at time t is determined by the field at the scatterer at time $t-\tau$. This is

$$\begin{aligned} &F\left[t-\tau-\frac{z_n+w_n(t-\tau)}{c}\right]\\ &= F\left[(t-\tau)\left(1-\frac{w_n}{c}\right)-\frac{z_n}{c}\right]\\ &\approx F\left[-\frac{z_n}{c}+\left(t-\frac{p_n}{c}\right)\left(1-\frac{w_n}{c}\right)\Big/\left(1-\frac{W_n}{c}\cos\psi_n\right)\right]\\ &\approx F\left[-\frac{z_n}{c}+\left(t-\frac{p_n}{c}\right)\left(1-\frac{w_n}{c}\right)\left(1+\frac{W_n}{c}\cos\psi_n\right)\right]\\ &\approx F\left[\left(t-\frac{p_n}{c}\right)\left(1+\frac{W_n\cos\psi_n - w_n}{c}\right)-\frac{z_n}{c}\right]. \quad (16) \end{aligned}$$

This is the electric intensity at the scatterer S_n at time $t-\tau$. It is the value of E which determines the field at P at time t. Actually, the re-radiation process of the scatterer brings in the second derivative of F instead of F itself. However, the time dependence is that shown by either (16) or (14).

When the transmitter sends out a sinusoidal wave we let $F(t) = \cos\omega_0 t$ and ignore the slight differences in the directions (at P) of the E vectors from the individual scatterers. Since $F''(t) = -\omega_0^2 \cos\omega_0 t$, the electric intensity at P produced by N scatterers clustered about the origin O shown in Fig. 4 is then

$$E = A\sum_{n=1}^{N} \cos \omega_0\left[\left(t - \frac{p_n}{c}\right) \cdot \left(1+\frac{W_n \cos \psi_n - w_n}{c}\right) - \frac{z_n}{c}\right], \quad (17)$$

where

$$A = -\frac{\epsilon_2 U\omega_0^2 \sin \gamma}{\epsilon_0 4\pi r c^2}, \quad \gamma = \text{angle } XOP. \quad (18)$$

This follows directly from (14). The notation is explained there.

IV. Fluctuation of Envelope with Time

For this purpose we write (17) as

$$E = A\sum_{n=1}^{N} \cos\left[\omega_0 t\left(1 + \frac{W_n \cos \psi_n - w_n}{c}\right) + \phi_n\right], \quad (19)$$

where the time independent terms have been gathered into the phase angle ϕ_n. It is apparent that E consists of the sum of N sinusoidal components, the nth of which has the frequency.

$$f_n = f_0\left(1 + \frac{W_n \cos \psi_n - w_n}{c}\right) \quad (20)$$

$$f_0 = \omega_0/2\pi.$$

From the definitions (15) of W_n and ψ_n it follows that

$$\begin{aligned} f_n - f_0 &= f_0[u_n(x - x_n) + v_n(y - y_n) \\ &\quad + w_n(z - z_n) - p_n w_n]/p_n c \\ &\approx f_0[u_n x + v_n y + w_n(z - r)]/rc, \end{aligned} \quad (21)$$

where we have neglected x_n, y_n, z_n in comparison with x, y, z, and have replaced p_n by its approximate value, r=distance $OP = [x^2+y^2+z^2]^{1/2}$.

Since (21) expresses $f_n - f_0$ as the sum of the three normally distributed random variables it follows that $f_n - f_0$ is itself a normal random variable with zero mean and rms value

$$\begin{aligned} \sigma_a &= f_0 u[x^2 + y^2 + (z - r)^2]^{1/2}/rc \\ &= f_0 u(2 - 2z/r)^{1/2}/c \\ &= f_0 u 2\left(\sin \frac{\theta}{2}\right)\Big/ c, \end{aligned} \quad (22)$$

where u is the rms value of u_n, v_n, w_n and the other notation is that shown in Fig. 4.

Because the nth component of E has the random phase angle ϕ_n, and because the number of components having frequencies between f and $f+df$ is

$$\frac{Ndf}{\sigma_a\sqrt{2\pi}} \exp\left[-(f-f_0)^2/2\sigma_a^2\right],$$

it follows that E behaves like a random noise with the power spectrum[7]

$$w(f) = \frac{NA^2}{2\sigma_a\sqrt{2\pi}} \exp\left[-(f - f_0)^2/2\sigma_a^2\right]. \quad (23)$$

The average power in each component is $A^2/2$.

Two other results given in reference 3 will be of interest in the following work. The first states that the autocorrelation coefficient of the envelope $R(t)$, defined as

$$\rho_a(\tau) = \frac{\text{ave. } (R(t) - \overline{R})(R(t + \tau) - \overline{R})}{\text{ave. } (R(t - \overline{R})^2}, \quad (24)$$

is given approximately by

$$\rho_a(\tau) \approx \left|\int_{-f_0}^{\infty} w(f_0 + u) \exp(2\pi i u\tau)du\right|^2 \cdot \Big/ \left|\int_{-f_0}^{\infty} w(f_0 + u)du\right|^2. \quad (25)$$

The averages in (24) are taken over time and $\overline{R}$ denotes the time average of $R(t)$. The lower limit of integration is $-f_0$ instead of the $-\infty$ of reference 3 because here we take the power spectrum $w(f)$ to extend only from $f=0$ to $f=\infty$. This result goes back to some work of Uhlenbeck's.

The second result we take from reference 3 is obtained when (23) for $w(f)$ is inserted in (25), and f_0 assumed to be so large that the lower limits $-f_0$ may be replaced by $-\infty$ without appreciably changing the values of the integrals. Thus the auto-correlation coefficient of $R(t)$ is approximately

$$\rho_a(\tau) \approx \exp\left[-(2\pi\tau\sigma_a)^2\right]. \quad (26)$$

In addition, it is interesting to note the theory of random noise[8] tells us the envelope has, on the average,

$$2.52\sigma_a = \frac{5.04 f_0 u \sin(\theta/2)}{c} \quad (27)$$

maxima per second.

V. Fluctuation of Envelope with Position

A description of this case is given under Result (b) of the Introduction. In the analysis we take the time of freezing to be $t=0$. The exploration of the region around P is accomplished by moving a distance α away from P in the direction defined by the direction cosines a_1, a_2, a_3. We denote the original position of P by the co-ordinates (x_0, y_0, z_0) and the position of the exploratory point Q by (x, y, z):

$$\begin{aligned} x &= x_0 + a_1\alpha \\ y &= y_0 + a_2\alpha \qquad a_1^2 + a_2^2 + a_3^2 = 1. \\ z &= z_0 + a_3\alpha \end{aligned} \quad (28)$$

Setting $t=0$ in (17) gives us the function we have to examine:

$$E = A\sum_{n=1}^{N} \cos \frac{\omega_0}{c}\left[p_n\left(1+\frac{W_n \cos \psi_n - w_n}{c}\right) + z_n\right]. \quad (29)$$

[7] A special case ($\theta=\pi$) of this result was given by Ratcliffe[2] in 1948. The general case was given by Booker, Ratcliffe and Shinn[3] in 1950.

[8] S. O. Rice, "Mathematical analysis of random noise," *Bell Sys. Tech. Jour.*, vol. 24, p. 87; 1945.

By expanding p_n in ascending powers of α, x_n, y_n, z_n and using the assumptions $l/r \gg u/c$, $l \gg \alpha$, we can (after considerable algebra) reduce (29) to the form

$$E = A \sum_{n=1}^{N} \cos \left[\frac{\omega_0}{c} \alpha \cos B + \phi_n + \frac{\omega_0}{c} \frac{\alpha}{r_0} \left(\left(\frac{x_0 \cos B}{r_0} - a_1 \right) x_n + \cdots \right) \right], \quad (30)$$

where ϕ_n is the random phase angle containing terms independent of α and the distance OP is now r_0. The angle B is shown in Fig. 1. In this reduction we make use of

$$p_n^2 = (x_0 + a_1\alpha - x_n)^2 + \cdots .$$

$$r_0 \cos B = a_1 x_0 + a_2 y_0 + a_3 z_0.$$

When we write the expression for p_n^2 as $r_0^2 + 2r_0 G + H^2$, where G and H are of the same order as l, we have the helpful result

$$p_n = r_0 + G + (H^2 - G^2)/2r_0 + \cdots .$$

Expression (30) is quite similar to the expression for the fluctuation of E with respect to time. Here α plays the same role that t played in Section IV. The rapidly varying term $\omega_0\alpha(\cos B)/c$ gives rise to the "ripples" of wavelength $\lambda = c/f_0$ in the frozen wave, since when we go radially from (x_0, y_0, z_0), $\cos B = 1$, and when we go transversely, $\cos B = 0$. The remaining coefficient of α gives rise to the envelope variations. The analogy is given in Table I (where $2\pi\sigma_b$ is computed by making use of the fact that l is the rms value of x_n, y_n, z_n).

TABLE I

Equation (19) t in seconds	Equation (30) α in meters
$\omega_0 t(W_n \cos \psi_n - w_n)/c \approx \omega_0 t[u_n x + v_n y + w_n(z - r)]/rc$	$\omega_0\alpha \left[\left(\frac{x_0 \cos B}{r_0} - a_1 \right) x_n + \cdots \right] /cr_0$
Above coefficient of t is a normal variate with rms value (in radians/sec.) $2\pi\sigma_a = 2\omega_0 u[\sin(\theta/2)]/c$	Above coefficient of α is a normal variate with rms value (in radians/meter) $2\pi\sigma_b = \omega_0 l \lvert\sin B\rvert/cr_0$
Correlation coefficient between values of envelope observed at times spaced τ seconds apart $\rho_a(\tau) = \exp[-(2\pi\sigma_a\tau)^2]$	Correlation coefficient between values of envelope observed at points spaced d meters apart along line PQ $\rho_b(d) = \exp[-(2\pi\sigma_b d)^2]$
Average number of maxima of envelope per second is $2.52\sigma_a = 5.04 f_0 u[\sin(\theta/2)]/c$	Average number of maxima of envelope per meter is $2.52\sigma_b = 2.52 l \lvert\sin B\rvert/(\lambda r_0)$

The second column of the table gives the results stated under Result (b) of the Introduction.

VI. Fluctuation of Envelope with Frequency

In order to obtain Result (c) of the Introduction, we replace ω_0 by $\omega_0 + 2\pi\alpha$ in (17) (where α is now the change in frequency measured in cps) and examine E at time $t = 0$. The expression to be investigated is then

$$E = A \sum_{n=1}^{N} \cos \left(\frac{\omega_0 + 2\pi\alpha}{c} \right) \cdot \left[p_n \left(1 + \frac{W_n \cos \psi_n - w_n}{c} \right) + z_n \right]. \quad (31)$$

When we use r_n to denote the distance of the nth scatterer from the origin we obtain

$$\begin{aligned} p_n^2 &= (x - x_n)^2 + (y - y_n)^2 + (z - z_n)^2 \\ &= x^2 - 2xx_n + x_n^2 + \cdots \\ &= r^2 - 2(xx_n + yy_n + zz_n) + r_n^2 \\ r^2 &= x^2 + y^2 + z^2 \\ p_n &= r\left[1 - \frac{xx_n + yy_n + zz_n}{r^2} + 0(r_n^2/r^2) \right]. \end{aligned}$$

By making use of the assumption $l/r \gg u/c$ introduced earlier it is seen that the term $(W_n \cos \psi_n - w_n)/c$, which is $O(u/c)$, can be neglected in comparison with the second term in the expression for p_n, which is $O(l/r)$. Writing the terms which contain ω_0 as a random phase angle ϕ_n, we see that (31) may be reduced to

$$\begin{aligned} E &= A \sum_{n=1}^{N} \cos \left[\frac{2\pi\alpha r}{c} \left(1 - \frac{xx_n + yy_n + zz_n}{r^2} \right) + 2\pi\alpha z_n/c + \phi_n \right] \\ &= A \sum_{n=1}^{N} \cos \left[\frac{2\pi\alpha r}{c} - \frac{2\pi\alpha}{cr} (xx_n + yy_n + zz_n - rz_n) + \phi_n \right]. \end{aligned} \quad (32)$$

This again is of the same form as (19) and may be analyzed by adding a third column to Table I to read

Equation (3) α in cps

$$-2\pi^\alpha[xx_n + yy_n + (z - r)a_n]/rc.$$

Above coefficient of α is a normal variate with rms value (in radians/(cps))

$$2\pi\sigma_c = 4\pi l[\sin(\theta/2)]/c.$$

Correlation coefficient between values of envelope observed at frequencies f_1 and f_2 (measured in cps)

$$\rho_c(f_2 - f_1) = \exp[-(2\pi\sigma_c)^2(f_2 - f_1)^2].$$

Average number of maxima of envelope per (cps) is

$$2.52\sigma_c = 5.04 l[\sin(\theta/2)]/c.$$

The average distance between the maxima is the reciprocal of the last expression.

$$\frac{1}{2.52\sigma_c} = \frac{c}{5.04 l \sin(\theta/2)} \text{ cps.} \quad (33)$$

These results have been stated under Result (c) of the Introduction.

Acknowledgment

It gives me pleasure to acknowledge the many useful comments I have received from my colleagues during the preparation of this paper. I am especially indebted to Pierre Mertz for his interest in the work given here.

Remodulation in Electron Multiplier Cascades*

HEINZ E. KALLMANN†, SENIOR MEMBER, IRE

Summary—**A method is described to increase the originally low depth of modulation in electron multiplier cascades. The modulation is derived as voltage on an intermediate dynode and applied to a control grid following a later dynode. Results of tests are given.**

ELECTRON MULTIPLIER CASCADES offer in a single envelope very high gains extending from dc to very high frequencies. In many applications, however, only a comparatively slight signal modulation of the "standing" direct current is of interest, for instance, light signals in the presence of ambient light received by a photo-multiplier, or modulation by a control grid in the initial triode stage of a cascade. Wherever the depth of the desired modulation is slight, the usefulness of electron multipliers is severely limited by the presence of large standing currents. If multiplication were continued until the signals had reached the desired amplitude then the standing currents would have grown to enormous values, beyond the capacity of a reasonable power supply, and would require large electrodes for heat dissipation. Thus it is necessary to break off the multiplication at a tolerable level of standing current and to feed the still feeble signals via an ac coupling to another amplifier. Such arrangements require, besides the added amplifier tube or tubes, supply circuits for plate and heater current not needed for the multiplier.

The method here described permits an increase, within the multiplier cascade, of the depth of modulation for a selected range of frequencies, to values approaching 100 per cent. The scheme is inherently simple but for full effectiveness requires a control grid not found in present electron multiplier tubes.

Not all types of multipliers are equally suited for the introduction of a control grid between dynodes. In one type, electrons are guided in a zigzag path between solid dynodes; this path depends on the relations between successive accelerating voltages. In another type, the dynodes are pervious to electrons, each composed of slats forming a louver.[1] Many such louver dynodes may be arranged in parallel planes behind each other. In such a cascade, the field on one side of a louver is substantially unaffected by the field on the other side.

As may be seen in Fig. 1, the required changes in the conventional multiplier circuitry are (1) the introduction in one dynode lead—dynode D_9—of a load Z_D of high impedance at least for the desired range of modulation frequencies, and (2) provision of the ac coupling, e.g. via the condenser C and grid resistor R_G, to a control grid G after the next—D_{10}—, or a later, dynode.

It will be noted that the current i_9 through Z_D consists of the difference between the electron stream i_{8-9} reaching the dynode D_9 from the preceding dynode, and the stream of secondary electrons i_{9-10} leaving the dynode D_9 for the next dynode. For the usual secondary-emission ratio of four, the latter current is about four times larger and the current i_9 is thus about $\frac{3}{4}i_{9-10}$, and

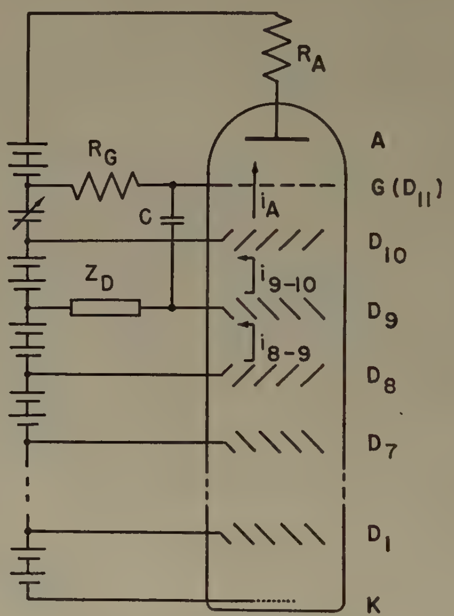

Fig. 1—Remodulating circuit.

of a polarity such that the dynode D_9 is the more positive relative to its supply potential the larger the currents i_{8-9} and i_{9-10}.

Let the gain of the multiplier cascade preceding D_9 be sufficient to yield approximately one volt peak modulating voltage $E_m = \frac{3}{4}Z_D i_{9-10}$ on dynode D_9. This voltage is amply sufficient to modulate an electron stream by means of a control grid such as grid G. Since the current from dynode D_{10} through grid G already carries the slight original modulation it emerges from the grid G modulated twice, and in the same sense, by the same signal. If the original modulation coefficient is α and the subsequent modulation of the standing current and its modulation, by means of the control grid G, is made M times larger, $M\alpha$, then the resulting total modulation will be $(1+\alpha)M\alpha = M(\alpha+\alpha^2)$. The nonlinear (square law) distortion due to remodulation thus has an upper limit α; since α is presumed to be small, under 10 per cent, such distortion will usually not merit correction.

* Decimal classification: R339. Original manuscript received by the Institute May 21, 1952; revised manuscript received, September 17, 1952.
† Consulting Engineer, New York, N. Y.
[1] J. S. Allen, "Recent applications of electron multiplier tubes," Proc. I.R.E., vol. 38, pp. 346–358; April, 1950. See Fig. 9, p. 352 of E.M.I. type VX 5031.

The control grid acts by repelling a large part of the electron stream leaving the preceding electrode. Thus, if the control grid were introduced immediately following the dynode D_9, it would substantially reduce or even cancel the excess of current leaving D_9 over that arriving there, and so obliterate the signal voltage developed on Z_D. Another dynode, D_{10}, or a space-charge grid, should therefore separate the control grid from the dynode on which the control voltage is developed. The signal-coupling circuit may be a simple condenser-resistor combination, or a transformer, and it might control more than one control grid. If the control grid is placed prior to the dynode whence it is controlled feedback oscillation, or at least distortion, is to be expected.

The method was tested, by using a louver-type dynode as substitute for the control grid, on a regular E.M.I. photo-multiplier of the type 5659. This tube has a transparent photocathode followed by eleven louver-type dynodes and an anode and is designed for an over-all multiplication of 10^7 with 160 volts on each stage. The test gave useful results since a louver-type dynode, when used without accelerating voltage, will act not unlike a control grid, with negligible current entering or leaving it.

In the first series of tests the last dynode D_{11} was so used, with a grid resistance of 4.7 megohms. The load impedance Z_D in the lead of dynode D_9 was a resistor of one megohm. Of two separate power supplies, one, adjustable for first-gain control, supplied about 140 volts to each stage from cathode to D_9, with the supply point of the latter at ground potential. The other supply provided regulated 130 volts between ground and D_{10}, adjustable voltage between D_{10} and D_{11}, and about 160 volts between D_{11} and the anode load of usually 0.2 megohms. The signal source consisted of two neon bulbs, one fed with adjustable dc to produce constant background illumination, and the other to provide the signal in the form of brief flashes at a rate of a few hundred per second, usually adjusted for about 10 per cent peak modulation. The coupling capacity C consisted of two ceramic condensers in series, with their junction connected to ground by a switch. With the switch closed, both electrodes D_9 and D_{11} were free of signal voltage, and rapid comparison was possible without any change in dc conditions. The direct current through Z_D was of the order of 10 μ amps that through the anode load about 6 μ amps.

The increase in signal modulation in the anode circuit, observed by oscilloscope, was about fivefold, with zero volt bias between D_{10} and D_{11}. Greater gain was noticed with D_{11} a few volts positive, but this arrangement tends to instability since during the signal peaks the secondary-emission current from D_{11} through the large resistor R_G drives that electrode further positive until it reaches and maintains a potential of about +80 volts relative to D_{10} and then acts as a regular multiplier dynode. It can thus be seen that the improvement due to remodulation is modest only if a dynode is used as a substitute for a control grid. By varying the signals and the first-gain control, or by applying a sinusoidal signal voltage from an audio oscillator to the dynode D_{11}, it was found that all observations could be described by a single characteristic, relating depth of anode current modulation to signal voltage on D_9 and D_{11}. The plot in Fig. 2 shows that the remodulation characteristic starts out linearly at a rate of 33 per cent modulation per volt, but grows nonlinear above 50 per cent even though pulse modulation well above 100 per cent could be had without difficulty.

With an anode current of 6 μ amps, the signal amplitude on the anode was correspondingly small. Therefore, in the second series of tests, the whole unchanged remodulation circuit was moved by one electrode towards the cathode, with Z_D now in the lead to D_8, 130 volts between D_8 and D_9, zero volt bias on D_{10}, and with 140 volts each between D_{10} and D_{11} and between D_{11} and

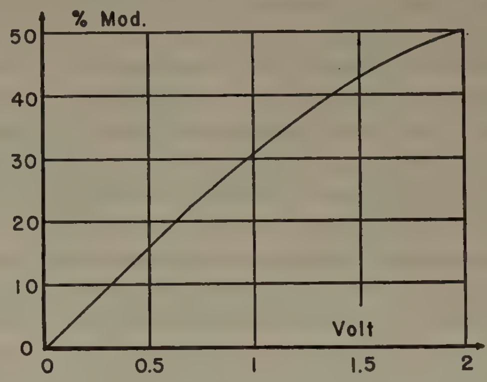

Fig. 2—Remodulation characteristic.

the anode load. By adjusting the first gain control the required signal voltage was again provided on Z_D; and by inserting the dynode D_{11} between the control grid D_{10} and the anode the remodulated current was once more multiplied before reaching the anode. No substantial change in the behavior of the remodulating circuit was noted. The increase in modulation was about fivefold, but the anode current was now about 40 μamps. The plot of Fig. 2 was found to apply to these tests also but with the slightly better efficiency of initially 50 per cent per volt.

A suitably designed control grid should do rather better than these tests. The ultimate limit of improvement is set by the bandwidth of the required signal, capacity and heat dissipation of the dynodes, and the initial depth of signal modulation. If for instance the capacity of the controlling dynode does not permit a load impedance Z_D of more than 50,000 ohms over the required frequency range and if heat dissipation limits the dc current from the controlling dynode to 0.5 ma, then for 0.5 volt peak signal on Z_D the initial modulation would have to be 2 per cent peak.

Measurement of Tropospheric Index-of-Refraction Fluctuations and Profiles*

C. M. CRAIN†, MEMBER, IRE, A. P. DEAM†, MEMBER, IRE, AND J. R. GERHARDT†

Summary—This paper presents measurements of index-of-refraction fluctuations and profiles made with a direct reading microwave refractometer over the Atlantic Ocean and coastal areas near Lakehurst, N. J., in April 1951 and over the vicinity of Wright-Patterson Field, Dayton, Ohio, in June 1951.

I. Introduction

IN RECENT YEARS various theories[1,2,3] have been advanced which suggested that the existence beyond the horizon of high-frequency radio-field strengths which are greater than can be accounted for on the basis of refraction theory may be due to scatter by atmospheric index-of-refraction discontinuities. As no measured data were available on the nature of these discontinuities, it was necessary, in advancing the theories, to make use of secondary factors. Megaw deduced the order of magnitude and the average size of these inhomogeneities in atmospheric refractive index from stellar scintillation data. Booker and Gordon made use of temperature-fluctuation data obtained a few feet above the surface of the earth. Megaw arrived at an integral scale of turbulence up to about a kilometer which he stated was some 1,000 times as large as was used by Booker and Gordon (100 meters versus 10 cm).

Previously reported measurements[4,5,6] of index-of-refraction rapid fluctuations have been limited to heights above the ground of less than 300 feet. While the results of these measurements have considerable value in the study of atmospheric turbulence, their use in radio-propagation studies is limited. This paper presents the result of the first directly recorded index-of-refraction fluctuation and profile measurements at altitudes up to 10,000 feet mean sea level.

II. Measurements over the Atlantic Ocean and Coastal Areas

In April 1951, through the co-operation of the Naval Air Station, Lakehurst, N. J., measurements were made on four different days of the index-of-refraction fluctuations up to 5,000 feet over the Atlantic Ocean and the Lakehurst coastal area, The measurements were made with a direct reading microwave refractometer, which is essentially the same as previously used[7] for fluctuation studies near the ground. Arrangements were made to change, in steps, the gain of the metering circuit so that full scales of 8, 16, 32, or 60 N-units[8] could be used. Temperature fluctuations were also recorded using a Western Electric bead-type thermistor, No. D-176980, as the sensitive element.

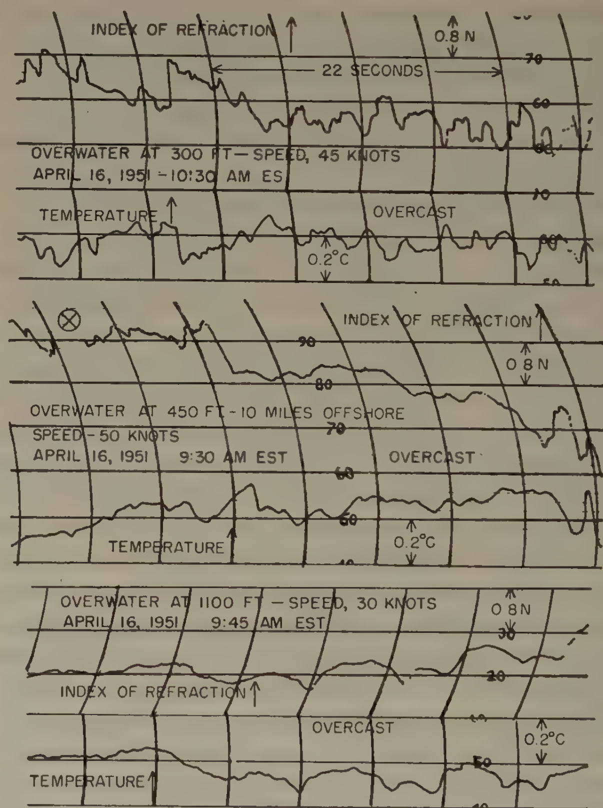

Fig. 1—Simultaneous index-of-refraction and temperature fluctuations over water at altitudes of 300, 450, and 1,100 feet, April 16, 1951.

The equipment was mounted in a front compartment of a Navy Type M airship some 60 to 70 feet in front of the ship's propellors. The perforated measuring-cavity resonator and thermistor were mounted two feet out from the skin of the airship.

Fig. 1 shows typical simultaneous index-of-refraction and temperature fluctuation on April 16, 1951, at altitudes of 300, 450, and 1,100 feet some 10 miles off shore.

* Decimal classification: R113.230.9. Original manuscript received by the Institute, November 29, 1951; revised manuscript received July 15, 1952. Research supported by the Office of Naval Research under Contract N5ori-136, P. O. I.

† The University of Texas, Austin, Texas.

[1] H. G. Booker and W. E. Gordon, "A theory of radio scattering in the troposphere," Proc. I.R.E., vol. 38, pp. 401–412; April, 1950.

[2] E. C. S. Megaw, "Scattering of electromagnetic waves by atmospheric turbulence," *Nature*, vol. 166, p. 1100; December, 1950.

[3] Krasil'nikov, *Bull. Acad. Sci.* (*URSS*), vol. 13, pp. 33–57; 1949.

[4] C. M. Crain and J. R. Gerhardt, "Some preliminary studies of the rapid variations in the index-of-refraction of atmospheric air at microwave frequencies," *Bull. Amer. Met. Soc.*, vol. 31, pp. 330–335; September, 1950.

[5] C. M. Crain and J. R. Gerhardt, "Measurements of the parameters involved in the theory of radio scattering in the troposphere," Proc. I.R.E., vol. 40, pp. 50–54; January, 1952.

[6] G. Birnbaum, "Fluctuations in the refractive indes of the atmosphere at microwave frequencies," *Phys. Rev.*, vol. 82, pp. 110–111; January, 1951.

[7] C. M. Crain, "Apparatus for recording fluctuation in the refractive index of the atmosphere at 3.2 centimeters wave-length," *Rev. Sci. Instr.*, vol. 21, pp. 456–457; May, 1950.

[8] $N=(n-1)10^6$, where n is the index-of-refraction.

Fig. 1 is representative of the data obtained on three of the four observation periods wherein the over-water air temperature structure showed a weak inversion from the water surface up to about 1,000 feet.

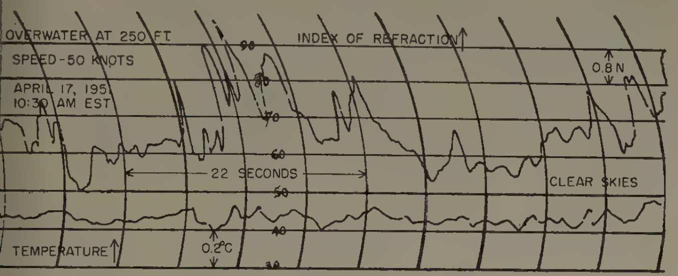

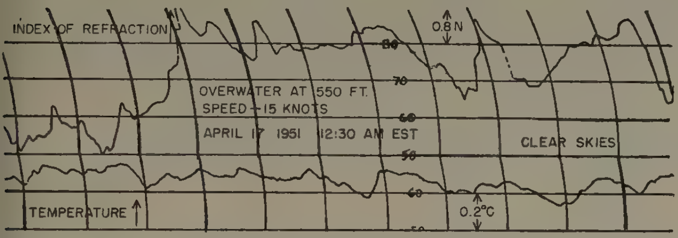

Fig. 2(a)—Simultaneous index-of-refraction and temperature fluctuations over water at altitudes of 250 and 550 feet, April 17, 1951.

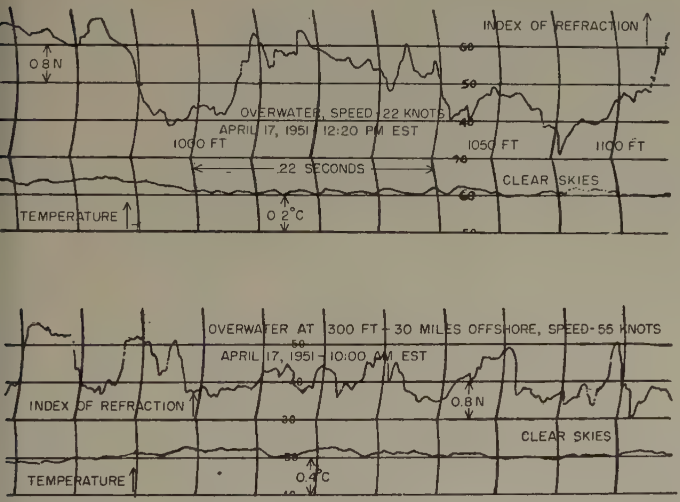

Fig. 2(b)—Simultaneous index-of-refraction and temperature fluctuations over water at altitudes of 1,000 and 1,300 feet, April 17, 1951.

Figs. 2(a), (b), and (c) show typical data obtained on April 17 at various heights from 250 to 4,500 feet some 35 miles off shore. In both cases magnitude of fluctuations decreased while the scale increased with altitude.

Fig. 2 was taken during a period wherein cold air was flowing out over a warmer water surface, giving rise to a relatively uniform adiabatic temperature lapse rate up to all observation levels. Note here that the temperature index correlation, though small, is positive at levels near the surface while the corresponding correlation for Fig. 1 is negative. This and the observed decrease in correlation with height agrees with previously reported studies near the ground.[9]

The rms fluctuation intensity for the over-water data of April 16 was never greater than about 0.8 N-unit at the lowest altitude for which measurements were made (300 feet) and decreased near 0.1 N-unit or less at altitudes of the order of 1,100 feet. The average size of the refractive-index inhomogeneities, as determined by averaging the distance represented by the major amplitude fluctuations on the recorded trace, was of the order of 60 feet at an altitude of 300 feet and 100 feet at an altitude of 1,100 feet. On April 17 the over-water rms fluctuation intensity decreased from about 0.7 N-units to 0.2 N-units in the height interval 250 to 4,500 feet.

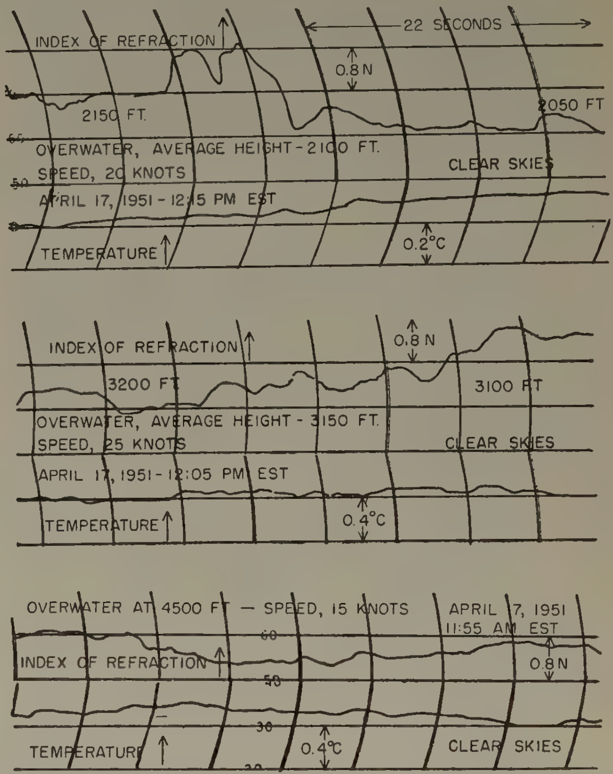

Fig. 2(c)—Simultaneous index-of-refraction and temperature fluctuations over water at altitudes of 2,150, 3,200, and 4,500 feet, April 17, 1951.

As a general rule, the fluctuations were of greater intensity near the coast line and over land than over water several miles off shore. Fig. 3, a typical over-land recording of April 17, may be compared with Fig. 2(a) and (b) for obtaining the general, though not always consistent, pattern observed during the tests.

Except for the measurements over land of April 24, the fluctuations shown in Figs. 1, 2, and 3 were the largest observed during the Lakehurst tests. On April 24, however, while flying over irregular patches of land and water near the coastline, at an altitude of 1,050 feet, peak-to-peak fluctuations as large as 15 N-units (rms value near 3 N-units) were observed. The average size of these inhomogeneities was of the order of 300 to 500 feet. From simultaneously obtained temperature fluctuations it was possible to determine that these index-of-refraction fluctuations were primarily due to

[9] Crain and Gerhardt, *op. cit.*, p. 2.

fluctuations in air moisture content, the latter exhibiting variations up to 4 to 5 millibars for the April 24 over-land data.

It should be emphasized that the Lakehurst tests were made during a period over which there were no great contrasts between air and water temperatures, and that on three of the observation periods a weak temperature inversion existed over water up to heights of

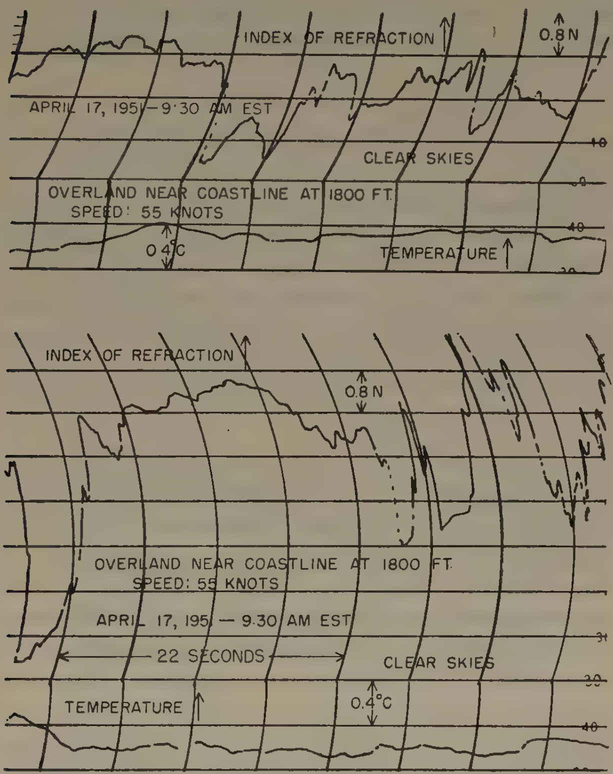

Fig. 3—Simultaneous index-of-refraction and temperature fluctuations over land at an altitude of 1,800 feet, April 17, 1951.

the order of 1,000 feet. Thus, with average springtime values of air temperature and moisture, it would appear that the atmospheric conditions during the tests were such that the measured fluctuation should be, relatively speaking, small. Measurements made under conditions of higher sea and air temperature would normally be expected to indicate fluctuations of greater magnitude due to the greater possible moisture content of the air and increased thermal turbulence.

It is obvious, in view of the fluctuation measurements reported above and those which follow, that in the application of the various scattering equations, both the intensity of the fluctuations and their statistical size should be treated as functions of the co-ordinates, in particular, height, and not as constants.

III. Measurements over Southern Ohio up to 11,000 Feet, Mean Sea Level

During four days of June 1951, through the cooperation of the Aircraft Radiation Laboratory, Wright-Patterson Air Force Base, Dayton, Ohio, measurements were made of refractive-index profiles and fluctuations up to as high as 11,000 feet (approximately 10,000 feet above the local terrain) over the region of Wright-Patterson Air Force Base. The refractometer was carried aloft in a type C-46 aircraft. Details of the equipment installation and operation and also a discussion of errors and limitations of the equipment are given elsewhere.[10] It should be mentioned here, however, that a recording meter having a time constant of approximately 0.5 second was used; thus, with indicated air speeds of the order 100 to 150 mph, fluctuations occurring over distances of less than 100 feet were inaccurately recorded. In this connection, previous measurements at Lakehurst made at speeds as low as 15 mph indicated that fluctuations having periods of less than 100 feet are of minor intensity.

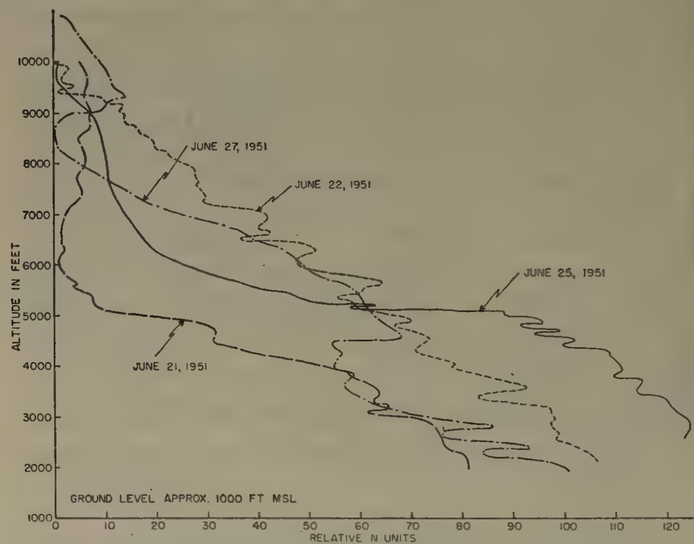

Fig. 4—Typical measured index-of-refraction profiles over land, June 21 to 27, 1951.

Fig. 4 shows typical index-of-refraction profile curves obtained on each of the four days during which measurements were made. These plotted profiles are greatly smoothed, as may be seen by examining the original recorded data shown in Figs. 5 and 6. Figs. 5 and 6 also show the magnitude of the fluctuation encountered during the flights. The symbol ⊕, shown on the various curves, indicates that the resonant frequency of the measuring cavity was mechanically modified so as to keep the recording pen on scale.

The curves in Fig. 4 are in close over-all agreement with those obtained simultaneously by means of an Aircraft Radiation Laboratory psychograph; however, due to the much smaller refractometer time constant, the refractometer data shows much more of the fine structure of the profile.

Except for a small correction caused by changes in the cavity dimensions during the flight (approximately 10 N-units for the curves shown over a 10,000 foot

[10] C. M. Crain and A. P. Deam, "An airborne microwave refractometer," *Rev. Sci. Instr.*, vol. 23, pp. 149–151; April, 1952.

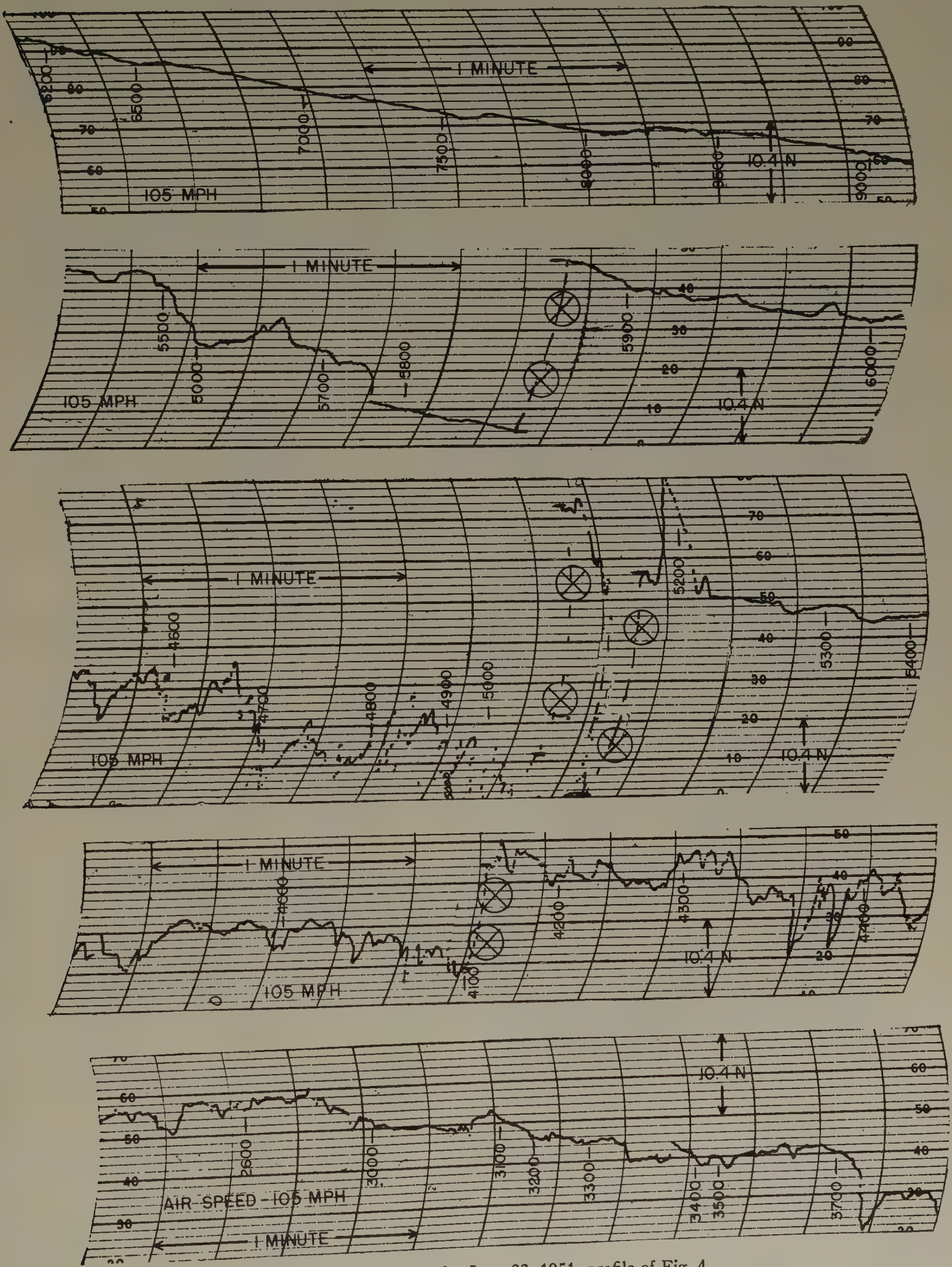

Fig. 5—Original data for June 22, 1951, profile of Fig. 4.

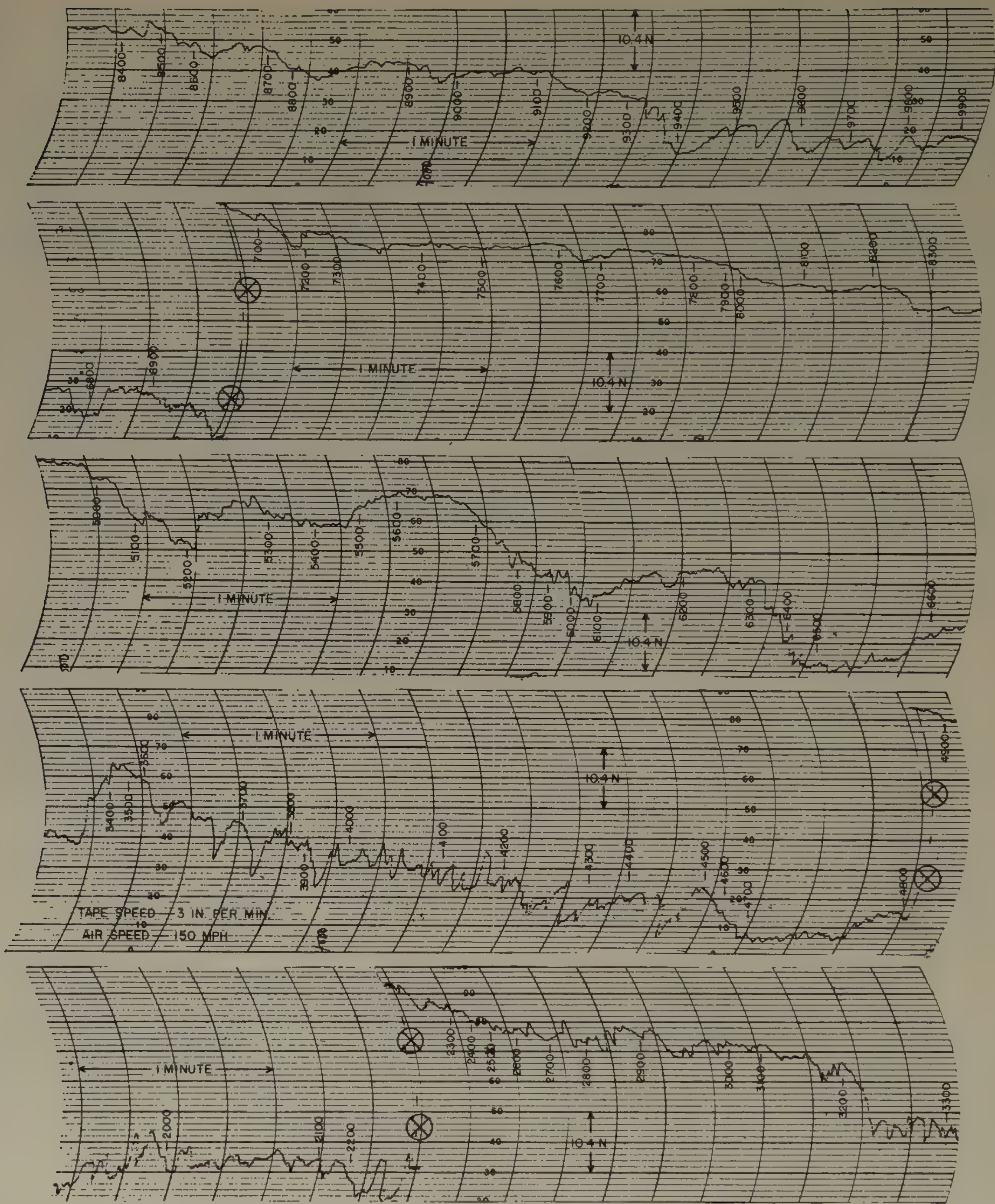

Fig. 6—Original data for June 25, 1951, profile of Fig. 4.

height interval), the profile curves were plotted directly from the recorded data.

In order to obtain a better measurement of the index fluctuations, more sensitive scales were occasionally used. Fig. 7 shows typical fluctuation data as obtained on June 27 at different heights. Fig. 8 shows an entirely different type of index-of-refraction variation which was recorded on June 25 with the airplane maintaining a constant elevation of 5,000 feet. At this elevation, the plane was flying through the tops of scattered "fair-weather cumulus" clouds. Bursts of white mist were observed through the plane's window simultaneously with the "pegging" of the recording pen as shown. The fact that the recording pen returned to its previous average reading very rapidly after leaving the edge of the cloud would seem to indicate that the increase in the recorded refractive index was real and not due to water condensation in the cavity, in which case, the pen would be quite slow in returning to its previous average position.[11]

Fig. 8 also indicates the effect of indicated air speed

[11] Since submission of this paper, additional measurements have indicated that the sharp increase in index of refraction at certain cloud boundaries may be as great as 40 N-units.

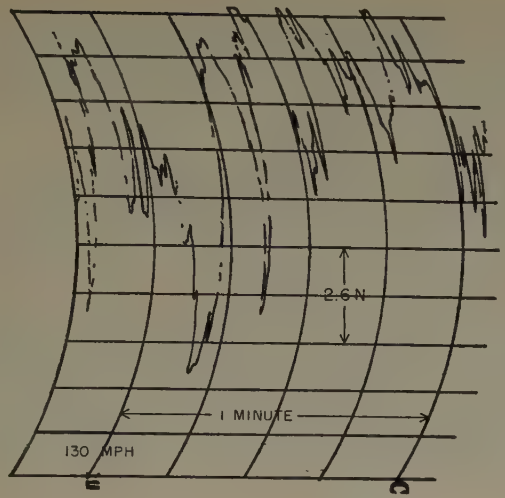

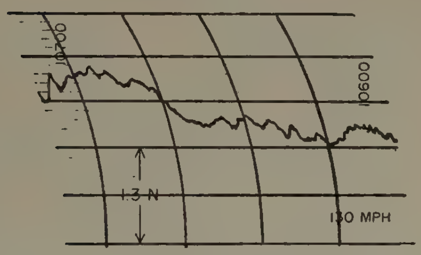

Fig. 7—Typical index-of-refraction fluctuation data at 2,000 and 10,000 feet, June 27, 1951.

on the recorded index-of-refraction. Many speed runs of this nature were made in order to determine air-speed effect. Although no particular effort was made to correct these observations for possible horizontal inhomogeneities in the refractive index over the test path,

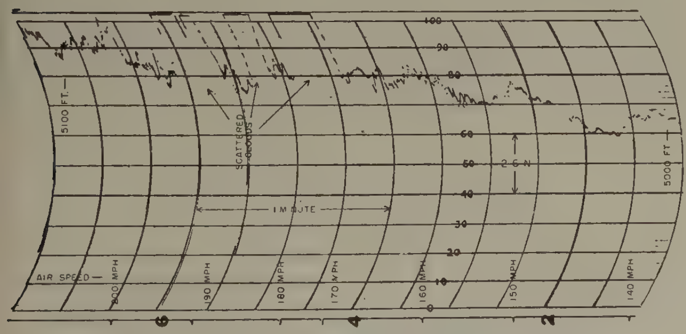

Fig. 8—Fluctuations in refractive index obtained while flying through scattered clouds, June 15, 1951.

a critical examination of the results of several tests indicated that the effect of increasing the indicated air speed from 100 to 200 mph caused an increase in the recorded indicated index-of-refraction of about 5 to 7 N-units. Thus, for profile measurements made with indicated air speeds with a 10-mph limit of variation, it would appear that the dynamic correction to the indicated index-of-refraction profile is negligible (less than 1 N-unit).

For an adequate explanation of the measured profile shapes a meteorological analysis for the various days is necessary, but it is impractical to include such an analysis here. This information and further results of the airborne measurements are given in detail elsewhere.[12,13] It might be pointed out, however, that on June 21 and June 25 the flights were in polar air and scattered clouds existed in the vicinity of the air mass boundaries (the top of the clouds appeared to be very close to the base of the layer). On June 22 and 27 the flights were made in tropical air. On June 22 clouds existed intermittently at nearly all levels up to 8,000 feet; however, all clearly visible clouds were avoided during the flight for which the profile is shown. On June 27 scattered clouds were found at levels of approximately 4,000, 11,000, and 12,000 feet.

It might well be noted here that there were two major types of index-of-refraction fluctuations observed in these tests. One is that resulting from turbulence-produced time and space variations in an essentially homogeneous atmosphere. Here the intensity of the fluctuations is relatively uniform; rms values of the order of 1.0 N-unit or less near the surface fall to a small fraction of this value at 10,000 feet, although peak changes may be as large as 5.0 N-units; scale of turbulence increases with height. The other type of index-of-refraction fluctuations pattern occurs as a result of the existence of either horizontal gradients of N within the air mass or of significant changes in the vertical gradients of N within the air mass, or at boundaries separating air masses. The former situation is well illustrated by the flight at a constant altitude through clouds (Fig. 8) where major horizontal gradients of index-of-refraction exist between free air and cloud. The latter case would occur when flying horizontally at some layer over which the index-of-refraction was changing rapidly with height. Here, small changes in plane altitude and the normal turbulent mixing of the atmosphere could result in extremely large index-of-refraction variations.

Repeated flights from near ground level of 10,000 feet often revealed that quite rapid changes in the measured patterns were occurring with time. For example, the inversion shown at 8,700 feet on the profile in Fig. 4 for June 27 rose some 1,000 feet, maintaining approximately the same shape, in some 35 minutes.

Without exception, when the plane's motion indicated rough air, relatively large amplitude, rapid index-of-refraction variations were encountered; however, the reverse was not necessarily true.

[12] C. M. Crain, A. P. Deam, and J. R. Gerhardt, "A Preliminary Study of the Variations in Refractice Index Over a 5,000 foot Height Interval Above the Earth's Surface," Electrical Engineering Research Laboratory Report No. 53, University of Texas, Austin, Texas; 1951.

[13] C. M. Crain and A. P. Deam, "Measurement of Tropospheric Index-of-Refraction Profiles with an Airplane Carried Direct Reading Refractometer," Electrical Engineering Research Laboratory Report No. 54, University of Texas, Austin, Texas; August 31, 1951.

IV. Conclusions

Rapid variations of index-of-refraction of the order of several N-units were measured up to elevations of the order of 11,000 feet. On most occasions it was found that the intensity of the inhomogeneities decreases with magnitude and their average size increases with altitude. For example, the typical average size of the major fluctuations measured a few feet above ground ranged from 6 to 15 feet,[5] while the size of those measured at heights greater than 1,000 feet above ground level were in the order of a few hundred feet.

In the case of sharp changes in the vertical index gradient (for example, see the curve for June 25, Fig. 4, and the original data, Fig. 6) more intense fluctuations were observed in the vicinity of the change in gradient than at lower or higher altitudes.

Measurements to date indicate that tropospheric index-of-refraction fluctuations vary greatly.

(a) from day to day at a fixed location,
(b) at a given time with location,
(c) at a given location with time in the order of minutes.

All high-altitude measurements have been made during the daylight hours. Probably on the average the night-time fluctuations will be smaller (and perhaps follow a different pattern from that indicated for the daytime fluctuations) because of decreased thermal activity in the atmosphere.

Network Alignment Technique*

JOHN G. LINVILL†, ASSOCIATE, IRE

Summary—**A method is presented whereby the response of production networks can be adjusted to a standard response by making single adjustments in the elements one at a time. The only requirement, apart from the linearity of the networks, is that their elements be within reasonable range of the correct values at the outset. In the example described, this range included deviations from 10 to 20 per cent. The technique reduces simply to the adjustment of the elements, one at a time, until an indicating instrument reads zero.**

Introduction

Inaccuracies in the element values of production networks result in deviations of their responses from that of a perfectly aligned network. The adjustment of trimming elements to bring the response into close correspondence with that of a standard network is complicated in that ordinarily the whole of the response is affected by changes in each element to be adjusted. The problem of alignment is hence the determination of the proper combination of changes in the elements to effect the correction of the response at all points of interest. A method is presented in the following for alignment of elements one at a time to their correct values in the presence of inaccuracies of other elements. Experimentally, the alignment method amounts to the following procedure. The difference in response to a periodic excitation (square wave, pulses, or swept-frequency sinusoid) of the production network from that of a standard network is fed onto one coil of a wattmeter (or any device that indicates the average product). On the other coil is applied the difference in response of a standard network and a test network of the same configuration as the standard network but with elements which are appropriately misaligned. The wattmeter reading is proportional to the deviation of an element value in the production network from its standard value. That element is then simply varied until the wattmeter reads zero. It is then in adjustment whether other elements are slightly out of adjustment or not. The same procedure is carried through for all of the variable elements in the network in turn, each time using a test network which is appropriately misaligned for the element being adjusted. Fig. 1 is a block diagram illustrating this operation. The only requirement on the method, apart from the linearity of the networks, is that the network be within reasonable range of alignment at the outset. In the experimental case to be described, element deviations of 10 to 20 per cent were within reasonable range; however, for the larger deviations it is sometimes necessary to do the alignment in two steps to obtain close tolerances.

Fig. 1—Block diagram illustrating circuit to align element A in production network irrespective of other element deviations.

Laboratory Verification—Broader Applicability of the Method

A block diagram illustrating the laboratory set-up used to verify the method is shown in Fig. 2. The excitation generator is a General Radio 769A square wave generator fed by an audio oscillator operating at 40 cps.

* Decimal classification: R143×R200. Original manuscript received by the Institute, March 18, 1952; revised manuscript received, July 7, 1952. The work reported here was done at the Research Laboratory of Electronics, M.I.T., and was partly supported by the Signal Corps, the Air Matériel Command and ONR.
† Massachusetts Institute of Technology, Cambridge, Mass.

The difference amplifiers are Hewlett-Packard 450A amplifiers, one feeding the potential coil of a sensitive wattmeter, the other feeding the current coil in series

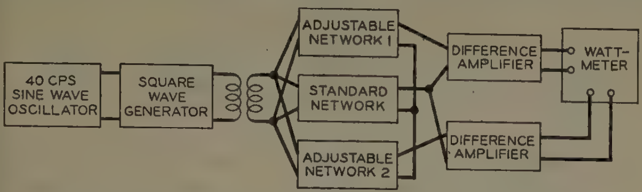

Fig. 2—Block diagram of complete laboratory set-up.

with 1,500 ohms. The three networks shown are of the same configuration (Fig. 3), two are adjustable, the third being fixed. The upper adjustable network plays the role of the production network, the lower plays the role of each of the appropriately misaligned networks in turn. In the circuits the inductors were not variable. It is significant that the method works whether all elements are variable or not. Of course, if some fixed elements are incorrect, the network response can not be made perfect, but this method achieves the best compromise possible in the sense that the integral of deviation squared is minimized.

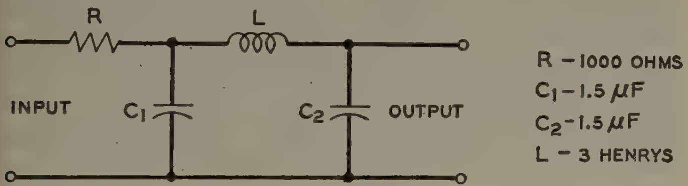

Fig. 3—Configuration and nominal element values of networks used in a laboratory test.

The general method employed here to align networks is applicable in a large number of different situations. The experimental verification described was made simple to facilitate its rapid completion. In some instances the wattmeter used as an averaging-multiplier might be profitably replaced by an electronic device more suitable in higher frequency ranges. Here the whole of the response curve was used. It is possible to select only a number of matching points, at least as great as the number of elements to be adjusted but preferably several times as large, making all computations in terms of the response at these points. In this approach, the problem becomes a digital one and a type of digital computation is required. Finally, it is worth noting that once the set-up has been made, the alignment of networks does not require the judgment of an observer. A completely automatic machine could be made for the problem of aligning a network if the magnitude of operations were sufficient to sustain cost of a completely automatic machine.

Mathematical Formulation of the Problem and Its Solution

The primary physical facts on which the alignment method is based are the following. Changes in response of a linear network to any given excitation are linearly proportional to changes in the element values, for small changes. For small deviations, the rate of change of response due to adjustment of any one element is very nearly independent of small changes in other elements.

The characteristics just stated make it possible for one to write

$$\Delta f \cong \Delta E_1 f_{a1} + \Delta E_2 f_{a2} + \cdots + \Delta E_n f_{an}, \tag{1}$$

where

Δf is the change in the response of the network to a standard excitation;

ΔE_i is the change in element "i";

f_{ai} is the unit adjustment function associated with element "i," it is the change in response resulting from a unit increase in element "i."

That the characterization indicated is valid and that the approximation indicated in (1) is good follows from the fact that the response of any linear network to any given excitation is a continuous function of the element values. Equation (1) is then simply the approximation for finite increments corresponding to the exact following relationship for differential increments.

$$df = \frac{\partial f}{\partial E_1} dE_1 + \frac{\partial f}{\partial E_2} dE_2 + \cdots + \frac{\partial f}{\partial E_n} dE_n. \tag{2}$$

In the alignment problem the response difference in which one is primarily interested is the change required to make the response of an imperfect network come into alignment with the ideal response. For any such network one can define this desired change as Δf_d. The problem of alignment then becomes simply the solution for ΔE's in an equation of the form of (1) where Δf becomes Δf_d.

$$\Delta f_d = \Delta E_1 f_{a1} + \Delta E_2 f_{a2} + \cdots + \Delta E_n f_{an}. \tag{3}$$

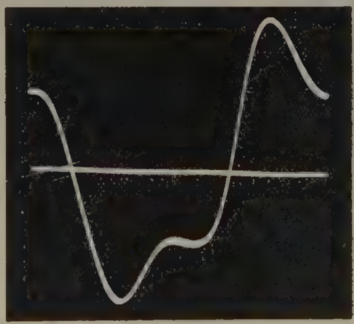

(ALL OSCILLOGRAMS START WITH DECREASING EDGE OF SQUARE WAVE AT INPUT)

Fig. 4—Response of standard network to input wave.

The functions just mentioned are easily associated with the experimental set-up shown in Fig. 2. Where the upper network represents the production network, the response of the upper difference amplifier represents $-\Delta f_d$ magnified. If a single element in the lower adjustable is one unit too large, the output of the lower difference amplifier is f_{ai} magnified. Photographs were taken of the responses of the difference amplifiers for set deviations of the elements one at a time in the experimental network. The response of the standard network represented in Fig. 3 to a 40-cps square wave is the oscilloscope pattern shown in Fig. 4. Multiples of the

unit adjustment functions for this network are shown as oscilloscope patterns in Fig. 5. From the photographs it is clear that the property of linearity of changes in response with changes in element value holds very well for the network of Fig. 3.

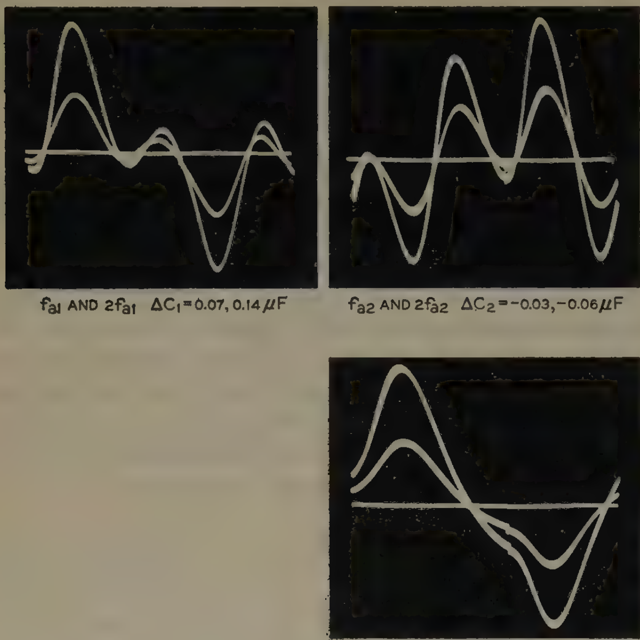

Fig. 5—Multiples of unit adjustment functions showing linearity of response changes.

The solution for the ΔE's of (3) can be viewed as the selection of co-efficients of the sum represented in (3) to best approximate Δf_d. The approximation of Δf_d is facilitated by operations with linear combinations of the unit adjustment functions which form an ortho-normal set rather than with the unit adjustment functions themselves. Fortunately, the problem of finding the ortho-normal set is susceptible to easy treatment experimentally, and the ortho-normal set is generated easily with the networks of Fig. 2. One designates this new set of functions as

$$\begin{aligned} f_{n1} &= a_{11}f_{a1} \\ f_{n2} &= b_{21}f_{n1} + a_{22}f_{a2} = a_{21}f_{a1} + a_{22}f_{a2} \\ &\cdots\cdots\cdots\cdots\cdots\cdots \\ f_{nn} &= b_{n1}f_{n1} + b_{n2}f_{n2} + \cdots + a_{nn}f_{an} \\ &= a_{n1}f_{a1} + a_{n2}f_{a2} + \cdots + a_{nn}f_{an}. \end{aligned} \tag{4}$$

The co-efficients, a's or b's, are selected to fulfill the conditions of ortho-normality over the range of time (time response case) or range of frequency (frequency response case) of interest. The conditions of normality and orthogonality are given in (5).

$$\begin{aligned} \int_0^T f_{ni}\cdot f_{nj}dx &= 1, \quad \text{if} \quad i = j \\ &= 0, \quad \text{if} \quad i \neq \;. \end{aligned} \tag{5}$$

In (5), x is the time or frequency depending upon which variable is of interest. In (4) one could consider only the a's, the b's are introduced there only to facilitate the mechanics of solution for the a's. By taking the scalar product of the first of (4) with itself, one sees that

$$a_{11} = \frac{1}{\sqrt{\int_0^T f_{a1}\cdot f_{a1}dx}}\,. \tag{6}$$

Experimentally, this amounts to saying that if one simultaneously increases element 1 of the two adjustable networks in Fig. 2, other elements being left at their correct values, when the wattmeter reads 1, the amount of increase of the adjustable elements is a_{11}. By taking the scalar product of the first and second equations of (4) one can verify that

$$-\frac{b_{21}}{a_{22}} = \int_0^T f_{n1}\cdot f_{a2}dx. \tag{7}$$

Experimentally, this ratio is easy to measure also. With network 1 so adjusted that the differencing circuit connected to it provides f_{n1}, and with network 2 set so that only element 2 is one unit too large, the wattmeter reads $-b_{21}/a_{22}$. It is clear that the b's in (4) are significant in that they are useful to determine the relative size of deviations of the various elements in the generation of a normal-orthogonal function. For example, from (4) one can deduce that in the generation of f_{n2} the ratio of deviation of element 1 to that of element 2 is $b_{21}a_{11}/a_{22}$. One now can determine a_{22} by identically and simultaneously varying in the two adjustable networks in Fig. 2 the first and second elements in this established proper proportion until the wattmeter reads unity. The deviation at that time of element 2 in the two networks is a_{22}. In exactly a similar way the solution of the succeeding equations in (4) is derived in two kinds of steps. The first kind is the determination of the correct proportion of deviations of the elements and this will be indicated by wattmeter readings. The second kind of step is the adjustment of the magnitude of these deviations, keeping the right proportion, to make a wattmeter reading come to unity.

A family of orthogonal functions which are linear combinations of the unit adjustment functions shown in Fig. 5 are shown in Fig. 6. These functions are generated by setting the adjustable network in the particular way indicated with each photograph and recording the response of the differencing amplifier. The element deviations corresponding to the orthogonal functions were found as indicated above. The first orthogonal function is a function of the unit adjustment function of C_1 only, the second is a combination of the unit adjustment functions of C_1 and C_2, the third orthogonal function is a combination of the unit adjustment functions of all of the adjustable elements.

The approximation of Δf_d as a linear combination of the ortho-normal functions has a simple explicit solution.

$$\Delta f_d = c_1f_{n1} + c_2f_{n2} + \cdots + c_nf_{nn}. \tag{8}$$

This solution is easily obtained by taking the scalar product of (8) with $f_{n1}, f_{n2}, \cdots f_{nn}$ in succession. These operations give:

$$
\begin{aligned}
c_1 &= \int_0^T \Delta f_d \cdot f_{n1} dx \\
c_1 &= \int_0^T \Delta f_d \cdot f_{n2} dx \\
&\cdots\cdots\cdots \\
c_n &= \int_0^T \Delta f_d \cdot f_{nn} dx.
\end{aligned} \tag{9}
$$

One can easily express the ΔE's which solve (3) in terms of the c's given above.

$$
\begin{aligned}
\Delta E_1 &= a_{11}c_1 + a_{21}c_2 + a_{31}c_3 + \cdots + a_{n1}c_n \\
\Delta E_2 &= \qquad\quad a_{21}c_2 + a_{32}c_3 + \cdots + a_{n2}c_n \\
&\cdots\cdots\cdots\cdots\cdots\cdots \\
\Delta E_n &= \qquad\qquad\qquad\qquad\qquad a_{nn}c_n.
\end{aligned} \tag{10}
$$

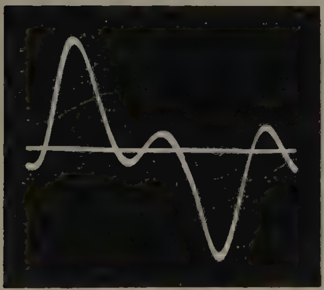

f_{n1} $\Delta C_1 = 0.16\mu F$

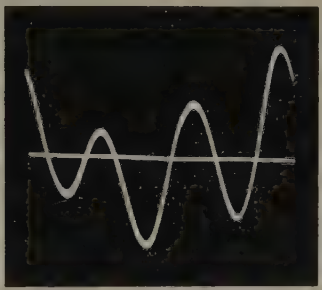

f_{n2} $\Delta C_1 = -0.17\mu F$, $\Delta C_2 = 0.09\mu F$

f_{n3} $\Delta C_1 = -0.215\mu F$, $\Delta C_2 = 0.02\mu F$, $\Delta R = 78$ OHMS

Fig. 6—Normal orthogonal functions which are linear combinations of f_{a1}, f_{a2} and f_{a3}.

Mathematically, (10) completes the solution of the alignment problem. These expressions of the solution can be written in a slightly different form which makes evident the manner in which one can obtain, in terms of a single wattmeter reading, the deviation of any element in spite of small deviations of other elements.

$$
\begin{aligned}
\Delta E_1 &= \int_0^T (a_{11}f_{n1} + a_{21}f_{n2} + \cdots + a_{n1}f_{nn}) \cdot \Delta f_d dx \\
\Delta E_2 &= \qquad \int_0^T (a_{22}f_{n2} + \cdots + a_{n2}f_{nn}) \cdot \Delta f_d dx \\
&\cdots\cdots\cdots\cdots\cdots\cdots \\
\Delta E_n &= \qquad\qquad\qquad \int_0^T a_{nn}f_{nn} \cdot \Delta f_d dx.
\end{aligned} \tag{11}
$$

Suppose one misaligns the third network of Fig. 1 so that the output of the lower differencing circuit is f_{nn}. By the last of (11) it is clear that the wattmeter reading is proportional to the misalignment of the nth element in the production network. If one adjusts the nth element of the production network until the wattmeter reads zero, then that element is in alignment. In a similar way one can determine the misalignment of any other element in the production network. If one adjusts the third network so that the output of the lower differencing amplifier is $a_{11}f_{n1} + a_{21}f_{n2} + \cdots + a_{n1}f_{nn}$, for instance, the wattmeter reading is proportional to the misalignment of element 1 in the production network. The matter of adjusting the network in the third box so that the connected differencing circuit has the output $a_{11}f_{n1} + \cdots + a_{n1}f_{nn}$ simply requires that each element is deviated from the correct value by a_{11} times the deviation required to generate f_{n1}, plus a_{21} times the deviation required to generate f_{n2}, and so on.

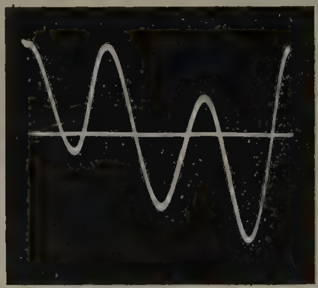

TO ANALYZE R
$\Delta C_1 = -0.215$, $\Delta C_2 = 0.02$, $\Delta R = 78$

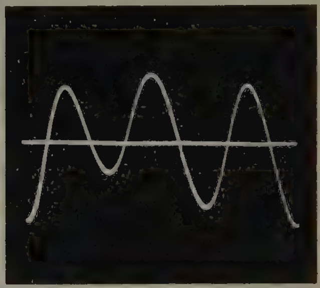

TO ANALYZE C_1
$\Delta C_1 = 0.222$, $\Delta C_2 = -0.04$, $\Delta R = -35$

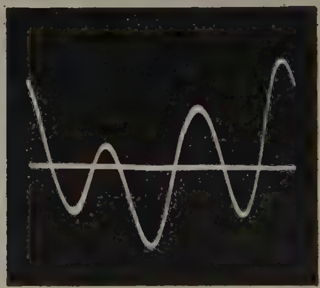

TO ANALYZE C_2
$\Delta C_1 = -0.20$, $\Delta C_2 = 0.09$, $\Delta R = 20$

Fig. 7—Responses of difference amplifiers with test network set to analyze particular elements of production network.

Pertinent functions for alignment of experimental network of Fig. 3 are shown in Fig. 7. These are oscillograms of response of differencing amplifier when one adjustable network is appropriately misaligned for diagnosis of a particular element's deviation in the other adjustable network. Element values for photographs of Fig. 7 were calculated on the basis of (11), and final adjustment of the values near the calculated values was made experimentally. With the test network settings indicated in Fig. 7, it was found that misadjustments of the top network in Fig. 2 could be readily determined by wattmeter indication. The top network could ordinarily be aligned in a single series of corrections if its elements were no more than 10 to 20 per cent in error, two series of corrections being required only for large deviations.

Correspondence

Some Notes on Theory of Radio Scattering in a Randomly Inhomogeneous Atmosphere

Booker and Gordon[1] have defined an autocorrelation function of capacitivity as a space correlation:

$$\rho_1 = \frac{1}{v\overline{(\Delta\epsilon)^2}}\int_v (\Delta\epsilon)(\Delta\epsilon')^* dv, \qquad (1)$$

where $\Delta\epsilon$ is the deviation from the mean value of capacitivity at point P and $\Delta\epsilon'$ is the corresponding value at the point P', both $\Delta\epsilon$ and $\Delta\epsilon'$ being the values at the same instant of time t'. The * indicates a complex conjugate. They consider the scattered power on an instantaneous basis. Since the turbulent motion in the atmosphere causes the capacitivity to vary with time, ρ_1 would vary with time and be very difficult to evaluate experimentally, involving as it does a large volume integral over a very short period of time (during which $\Delta\epsilon$ and $\Delta\epsilon'$ are relatively constant).

Recently Staras[2] has proposed the use of a time correlation function

$$\rho_2 = \lim_{T\to\infty}\frac{1}{2T}\int_{-T}^{T}\left(\frac{\Delta\epsilon}{\epsilon_0}\right)\left(\frac{\Delta\epsilon'}{\epsilon_0}\right)^* dt, \qquad (2)$$

where ϵ_0 is the average capacitivity. This correlation is easily measurable, as Staras points out, but requires the assumption that ρ_2 is the same for all pairs of points P and P' so long as the distance between them is the same. He derives an expression for the received average scattering power rather than the instantaneous power of Booker and Gordon. From practical considerations it would seem that this average power is more useful than the instantaneous power which fluctuates greatly with time.

Adopting the premise that the time average power received from scattering is the more useful concept, a third definition of correlation is proposed, namely, correlation function in the time-space domain Thus, we can define

$$\rho_3 = \lim_{T\to\infty}\frac{1}{2Tv\overline{(\Delta\epsilon)^2}} \cdot \int_{-T}^{T}\int_v (\Delta\epsilon)(\Delta\epsilon')^* dv dt. \qquad (3)$$

This value of correlation may be considered as the time average of the Booker-Gordon definition or the space average of the Staras concept, i.e.,

$$\rho_3 = \lim_{T\to\infty}\frac{1}{2T}\int_{-T}^{T}\rho_1 dt = \frac{\epsilon_0^2}{\overline{(\Delta\epsilon)^2}v}\int_v \rho_2 dt. \qquad (3a)$$

ρ_3 therefore is more general than the correlation defined by (1) or (2) since it does not require an assumption of uniformity in time or space. It is also measureable since it involves only the space average of the Staras correlation.

Applying the time average to the scattered power equations (2i) and (2s) of Booker and Gordon, we obtain almost identically the same formulas.

$$\bar{p} = \lim_{T\to\infty}\frac{1}{2T}\int_{-T}^{T}\tfrac{1}{2}EH^* dt$$
$$= \tfrac{1}{2}Y^*E_0^2\{(k^2\sin X)/4\pi R\}^2 I, \qquad (4)$$

where

$$I = 4\pi j\frac{\overline{\left(\frac{\Delta\epsilon}{\epsilon}\right)^2}v}{2k\sin\frac{1}{2}\theta}\int_0^\infty \rho_3 \cdot \exp\{-j2kr\sin\tfrac{1}{2}\theta\} r dr. \qquad (5)$$

Assuming an isotrophic medium, let us consider the variation of ρ_3 as a function of the distance r between points P and P'. If we were to plot in a scatter diagram all the $\Delta\epsilon'$ versus the $\Delta\epsilon$ for a given separation r, then as a first approximation the regression line would be

$$\Delta\epsilon' = \rho_{3r}\Delta\epsilon. \qquad (6)$$

Define ρ_{3l} as the correlation between two points spaced a unit distance l apart. Then for points spaced $r/l=1$ unit apart,

$$\Delta\epsilon' = \rho_{3l}\Delta\epsilon. \qquad (7)$$

The relationship for another point P'' spaced 2 units from P and 1 unit from P' would be

$$\Delta\epsilon'' = \rho_{3l}\Delta\epsilon', \qquad (8)$$

or substituting (8) into (7),

$$\Delta\epsilon'' = \rho_{3l}^2\Delta\epsilon. \qquad (9)$$

This process may be continued to give the general formula for a spacing of r/l units between P and P',

$$\Delta\epsilon' = \rho_{3l}^{r/l}\Delta\epsilon. \qquad (10)$$

Substituting (10) into (5), there results

$$I = 4\pi j\frac{v\overline{\left(\frac{\Delta\epsilon}{\epsilon}\right)^2}}{2k\sin\frac{1}{2}\theta}\int_0^\infty \rho_{3l}^{r/l} \cdot \exp\{-j2kr\sin\tfrac{1}{2}\theta\} r dr$$
$$= 4\pi j\frac{v\overline{\left(\frac{\Delta\epsilon}{\epsilon}\right)^2}}{2k\sin\frac{1}{2}\theta}\left[\frac{1}{l}\ln\rho_{3l} - j2k\sin\tfrac{1}{2}\theta\right]^{-2}. \qquad (11)$$

The real part of I is then

$$ReI = -\frac{8\pi v\overline{\left(\frac{\Delta\epsilon}{\epsilon}\right)^2}l^3\ln\rho_{3l}}{\{\ln^2\rho_{3l} + (2kl\sin\frac{1}{2}\theta)^2\}^2}. \qquad (12)$$

In the above, ReI is a positive quantity since ρ_{3l} is less than unity. If the unit spacing l were chosen so that ρ_{3l} equal $1/e$ then (12) reduces to (2t) in the Booker-Gordon paper.

Harry Fine
Technical Research Division
Federal Communications Comm.
Washington, D. C.

[1] H. G. Booker and W. E. Gordon, "A theory of radio scattering in the troposphere," Proc. I.R.E., p. 403; April, 1950.

[2] H. Staras, "Scattering of Electromagnetic Energy in a Randomly Inhomogeneous Atmosphere," National Bureau of Standards Report No. 1662, Washington, D. C.

On the Possibilities of a Neutrino Communication System

Hammond[1] has called attention to the fact that the neutrino fulfills most of the conditions required for a telepathic transmitting phenomenon when the assumption of the reality of telepathic communication is made as by Bibbero,[2] Hollman,[3] and Stockman.[4] It is interesting to note that a source of neutrinos is available in human organisms, in that potassium is radioactive,[5] and the major portion of the ractioactivity is caused by the beta process from the isotope of weight 40, *viz*,

$$^{40}_{19}K \rightarrow ^{40}_{20}Ca + e.$$

As documented by Hammond, the beta decay is attended by the emission of a neutrino.

The invariably found incidence of the $^{40}_{19}K$ is 0.011 per cent and the accepted half life of the radioactive isotope is 2.4×10^8 years.[5] The older literature lists the potassium content of the brain as approximately 4 grams.[6] Thus it is computed that the emission of neutrinos would approach a value of 4.4×10^2 neutrinos per second from the brain.

It is also of interest to note that it is widely recognized that potassium deficiencies in the human are attended by mental confusion, impairment of memory, as well as by deterioration of muscular activity, and other symptoms.

The information cited above apparently usefully extends the proposal of Hammond, and also probably contains no contrary evidence concerning the assumption of telepathic communication elsewhere proposed.

G. N. Tyson, Jr.
ElectroCircuits, Inc.
Pasadena, California

[1] A. L. Hammond, "A note on telepathic communication," Proc. I.R.E., vol. 40, p. 605; May, 1952.

[2] R. J. Bibbero, "Telepathic communication," Proc. I.R.E., vol. 39, pp. 290–291; March, 1951.

[3] H. H. Hollman, "Telepathic communication," Proc. I.R.E., vol. 29, p. 841; July, 1951.

[4] H. Stockman, "More on telepathic communication," Proc. I.R.E., vol. 39, p. 1571; December, 1951.

[5] N. V. Sidgwick, "The Chemical Elements and Their Compounds," vol. 1, Oxford University Press, London, Eng., pp. 62–63; 1950.

[6] A. T. Shohl, "Mineral Metabolism," Reinhold Publishing Corp., New York, N. Y., p. 19; 1939.

Correspondence

A Note on Pulse Codes*

The diagram (Fig. 1) indicates one possible method whereby recognizable English characters may be communicated as telegraphic pulses which are recorded at the receiver in a directly readable form. Numerals have not been included, but these may be designed along the same lines.

Three independent channels are shown, each of which uses pulses of fixed amplitude but variable duration. It is assumed that means are available at the transmitter for printing the characters on a tape, and for photo-electric scanning of the pulse crests, independently for each channel. The resulting pulses are recorded oscillographically in their respective channels to reconstruct the message on a tape at the receiver.

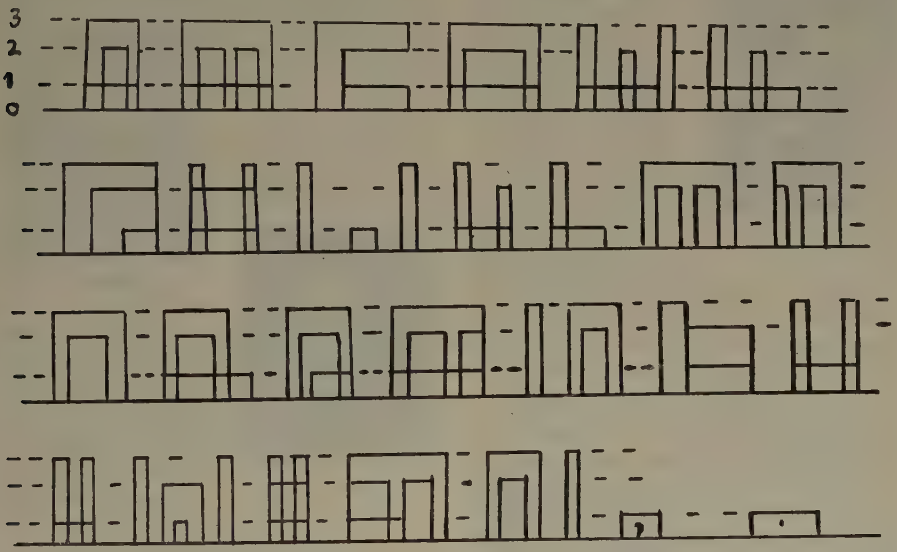

Fig. 1

The characters $B, D, E, F, P, R, S, T, Y$, and Z are oriented at right angles to the normal to facilitate their conversion into pulse form, and it will be assumed that automatic means are provided to reorient them correctly at the receiver by means of associated control signals. The three channels may be impressed on a single carrier by using any known band-sharing technique.

Students of information theory may find interest in comparing a code of this type (or an improved version) with Morse, Baudot, or other binary code. A casual comparison will show that the code illustrated uses 2.93 pulses per character (average) against 3.36 pulses per character for Morse. The corresponding binary digits per character are 4 and 9 respectively.

It appears that a code such as that outlined promises advantages, in certain applications, of higher speed of operation and narrower over-all bandwidth. Also design and cost considerations are favorable.

Charles M. Sweet
24 Newberry Rd.
Lucknow, India

* Received by the Institute, July 28, 1952.

New Linear Passive Nonreciprocal Microwave Circuit Component*

Studies of propagation of guided microwaves through an anisotropic electron gas have been in progress at Federal Telecommunication Laboratories since the summer of 1950. In the course of these studies, particular attention was paid to the case where the anisotropy was produced by a uniform constant magnetic field permeating the electron-gaseous medium in a direction parallel to the waveguide axis.

The study of propagation of electromagnetic waves through a dielectric medium made anisotropic in this way goes back quite far in the history of electromagnetism. Faraday, by sending plane-polarized light waves through a transparent medium of reasonably high refractive index with a magnetic field across it in the direction of propagation, discovered the effect bearing his name, which consists of rotation of the polarization plane of the light waves. Furthermore, he noted that the sense of rotation is the same for the reflected wave as for the incident wave. Thus, for example, a fixed observer noting a clockwise rotation of the incident wave would note an equal additional clockwise rotation of the reflected wave on its return through the medium. If the Faraday experiment is translated into radio and microwave frequencies, a behavior may be observed that produces nonreciprocity when the signal traverses the magneto-anisotropic medium between input and output terminals. Indeed, the failure of the various reciprocity theorems when electrons in a magnetic field are involved is a fact long familiar to students of electromagnetic phenomena in the ionosphere.

We have performed Faraday-type experiments with waves launched in the linearly polarized TE_{11} mode in a circular waveguide at frequencies in the range of 4,600 to 5,500 mc, the dielectric being the electrons present in the plasma of a gas discharge. The composite element, consisting of a section of waveguide with an electron-gas generating tube inside it and with a magnetic field generator surrounding the whole, may be referred to as a "magneto-optic" component. For magnetic fields not too near that field corresponding to electron gyroresonance with the signal frequency, not only were the expected Faraday rotations obtained, but they were of quite large magnitude. The results of our experiments were summarized in two brief publications.[1,2] It is evident, in view of the preceding discussion, that the magneto-optic component that produces these rotations constitutes a linear passive[3] nonreciprocal microwave circuit element which is furthermore an electronic element. This was pointed out by us in our presentations of these results at the Eleventh Annual Conference on Physical Electronics at the Massachusetts Institute of Technology in March, 1951 and at the Electron Devices Conference of the Institute at the University of New Hampshire in June, 1951. In addition, we pointed out a particularly cogent application of such a component exploiting its nonreciprocal nature, namely, as a lossless buffer between a signal source and its load, completely independent of reflections at the load (this being accomplished by a 45-degree rotation of the plane of polarization of the signal in the component).

Recently our attention has been called to two articles by Tellegen[4,5] bearing on the general problem of constructing linear passive nonreciprocal network elements. To relate his work to ours, we may note that the Maxwell equations, as modified by the presence of electrons in a constant magnetic field, are contained implicitly in his equa-

* Received by the Institute, March 27, 1952. The work discussed in this letter was sponsored by the Signal Corps Engineering Laboratories, Fort Monmouth, N. J.

Since this letter was written and the necessary clearance obtained for publication, an article by Hogan appeared in the January, 1952 issue of the *Bell System Technical Journal*, which describes a realization of Tellegen's gyrator by means of the Faraday effect in a ferromagnetic medium. The Faraday rotations are produced in such a medium by interaction of the radio-frequency magnetic field with the medium. In mathematical terms, the permeability is a second-order tensor and the dielectric constant is a scalar. In the dielectric Faraday effect studied by us, the rotations are produced by interaction of the radio-frequency electric field with a free-electron gas; that is, the dielectric constant is a second-order tensor and the permeability is a scalar. A very considerable practical advantage in the dielectric Faraday effect, as obtained in our experiments, is that the electron gas medium may itself be modulated or pulsed. In the ferromagnetic Faraday effect, only the magnetic field can practically be modulated.

[1] L. Goldstein, M. A. Lampert, and J. F. Heney, "Magneto-optics of an electron gas with guided microwaves," *Phys. Rev.*, vol. 82, pp. 956–957; June 15, 1951.

[2] L. Goldstein, M. A. Lampert, and J. F. Heney, "Magneto-optics of an electron gas for guided microwaves: propagation in rectangular waveguides," *Phys. Rev.*, vol. 83, p. 1255; September 15, 1951.

[3] Although power is required for production of a free-electron gas, the device is passive insofar as interaction of the free electrons, which lack any significant drift velocity, and the propagating microwave signal is concerned.

[4] B. D. H. Tellegen, "The gyrator, a new electric network element," *Philips Res. Rep.*, vol. 3, pp. 81–101; April, 1948.

[5] B. D. H. Tellegen, "The synthesis of passive resistanceless fourpoles that may violate the reciprocity relation," *Philips Res. Rep.*, vol. 3, pp. 321–337; October, 1948.

tions (33) of the gyrator article. The modification of the Maxwell equations are precisely the replacement of the scalar dielectric constant by a second-order tensor dielectric "constant," the "new" parts of which depend on the magnetic flux density. Tellegen, however, did not pursue the case of anisotropy in a dielectric because voltage step-up is unobtainable in such a medium.[6]

[6] He discusses this on page 99 of reference 4.

Though, indeed, our magneto-optic component is simply a one-to-one voltage transformer, it still is an eminently realizable linear passive nonreciprocal microwave circuit component. It is furthermore a completely electronic element in that the electron-gaseous medium can itself be modulated or pulsed on and off. Furthermore, one can visualize the nonreciprocal character of the device directly from its rotation properties without recourse to mathematical discussion.

Ladislas Goldstein
University of Illinois
Urbana, Ill.

Murray A. Lampert
Federal Telecommunication
Laboratories, Inc.
Nutley 10, N. J.

Contributors to Proceedings of the I.R.E.

William G. Anderson (A'52) was born in Morris, Ill., on January 30, 1924. He received the B.S. degree in electrical engineering from the University of Texas in 1946. Upon graduation he was commissioned in the U. S. Naval Reserve.

W. G. Anderson

From 1946 to 1948, Mr. Anderson was employed by the Westinghouse Electric Corporation in the Special Products Division, where he was concerned with servomechanism development. Concurrently, he attended the Graduate School of the University of Pittsburgh.

Since 1948, Mr. Anderson has been engaged in the development of feedback control systems and analog computers at the Collins Radio Company. The primary application of these devices is in the field of aircraft control and guidance.

Mr. Anderson is a member of Tau Beta Pi and an associate member of the A.I.E.E.

❖

Louis L. Bailin was born in Chicago, Ill. on May 28, 1922. He received the B.A. degree in physics from U. C. L. A. in 1943. After a year as a teaching assistant in physics in the specialized service training programs at this University, he joined the technical staff of the Naval Ordnance Laboratory in Washington, D. C. He returned to U. C. L. A. in 1945 for graduate study in physics, and received the M.A. degree in 1946 and the Ph.D. degree in 1949.

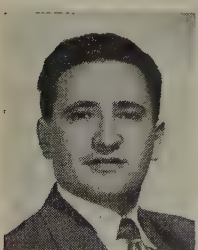

L. L. Bailin

In 1948 Dr. Bailin was employed as a mathematician by the Institute for Numerical Analysis of the National Bureau of Standards. Since November, 1949 he has been a member of the technical staff of the Hughes Aircraft Company engaged in microwave propagation and antenna studies.

Dr. Bailin is a member of A.P.S., Sigma Xi, R.E.S.A., and Pi Mu Epsilon.

P. A. T. Bevan was born on January 8, 1909 near Newport, Monmouthshire, England. He was graduated from the University of Wales and Cardiff Technical College in 1930, and spent the following three years as a graduate apprentice (Design and Research) at the Rugby works of the British Thomson-Houston Co. Ltd.

P. A. T. Bevan

He joined the Engineering Division of the British Broadcasting Corporation in 1934 as a member of the small group of specialist radio and power engineers who then formed the Station Design Department which subsequently became the Planning and Installation Department. Initially, as a power engineer, he became known for his work in connection with the development of high voltage steel tank rectifiers for high power transmitters, and since 1936, as a radio and television engineer, he has been closely associated with most of the major engineering projects and technical developments in the BBC's sound and television broadcast services, especially in the high-power transmitting station field. He was one of the pioneer team responsible for developing the technical facilities for starting the high definition public television service from the London Television Station at Alexandra Palace, and for its subsequent expansion.

During World War II, while the Television Service was closed down, Mr. Bevan supervised the project planning and engineering of medium- and short-wave transmitting stations, and, in particular, the group of very high power sound broadcasting stations, including the 800-kw Ottringham station, constructed by the BBC for its war-time European Service. Since 1947 he has been mainly concerned with developments in vhf broadcasting, the construction of the experimental vhf FM-AM transmitting station at Wrotham, Kent, and more recently with planning the new group of high-power television broadcast stations required by the BBC's expansion of the British Television Service to give national coverage.

Mr. Bevan is now a senior member of the Engineering Division of the BBC and occupies the consultant position of senior planning engineer. He has authored several papers, received the Duddell Premium of the IEE in 1951, and presented the survey paper on "Television Broadcasting Stations" at the 1952 Convention on "The British Contribution to Television." He is a member of the IEE, serving on a number of IEE and British Standards committees, and the editorial advisory board of the *Wireless Eng.*

❖

Kenneth K. Clarke (S'46–A'49) was born in Miami, Fla., on June 7, 1924. He attended Cornell University from 1941 to 1943. From 1943 to 1946 he was in the U. S. Army Air Forces as a Communications Officer with the AACS. He received his M.S. in electrical engineering from Stanford University in 1948.

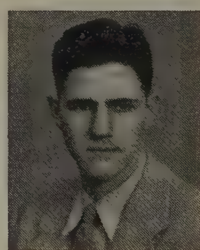

K. K. Clarke

From 1949 to 1950 Mr. Clarke was a Senior Research Fellow at the Microwave Research Institute, Brooklyn, N. Y., and did postgraduate study in the School of Electrical Engineering at the Polytechnic Institute of Brooklyn. He taught at the Madras Institute of Technology, Madras, India, in 1951 and 1952. He is currently lecturer in telecommunication at the University of Ceylon.

Mr. Clarke is a member of Tau Beta Pi.

❖

Cullen M. Crain (S'42–M'49) was born in Goodnight, Texas, in 1920. He received the B.S. degree in electrical engineering from the University of Texas in 1942. After a year with the Philco Radio and Television Corporation in Philadelphia, Pa, he returned to the University of Texas as an instructor in electrical engineering.

C. M. Crain

From 1944 to 1946 Mr. Crain was on active duty in the U. S. Naval Reserve, attached to the Bureau of Ordnance, where he worked in the mine

Contributors to Proceedings of the I.R.E.

program, and to the office of Research and Inventions, where he worked on the development of radar bombing trainers.

Since 1946 Mr. Crain has been associated with the University of Texas, where he received the M.S. degree in electrical engineering in 1947. He is at present an assistant professor in the electrical engineering department, and a radio engineer with the electrical engineering research laboratory.

Mr. Crain is a member of Tau Beta Pi, Eta Kappa Nu, and Sigma Xi.

❖

A. P. Deam was born in Dallas, Tex. on December 10, 1917. He received the B.S.E.E. degree from the Agricultural and Mechanical College of Texas in 1940 and M.S.E.E. degree from the University of Texas in 1949.

A. P. Deam

During 1941 and 1942 he was employed by the Dallas Power and Light Company as an assistant engineer.

He has been employed by the University of Texas since, both in a teaching and research capacity. Presently, he is a radio engineer at the Electrical Engineering Research Laboratory of the University of Texas. Work at this laboratory has been primarily related to radio wave propagation.

❖

M. J. Ehrlich (SM'51) was born in Baltimore, Md. in May, 1920. He received the B.E. degree in electrical engineering from the Johns Hopkins University in 1941, the M.S. degree in electrical engineering in 1947, and the Ph.D. degree in 1951 from the University of California at Berkeley.

M. J. Ehrlich

From 1942 to 1946 Dr. Ehrlich served as a mine warfare officer in the U. S. Navy. He joined the Radiation Laboratory, University of California, Berkeley in 1946 as a member of the linear accelerator group. In 1948 he joined the Antenna Laboratory, University of California, as a research engineer, and engaged in diffraction and scattering studies. Since 1950 Dr. Ehrlich has been associated with the Microwave Research Department of Hughes Aircraft Company.

Dr. Ehrlich is a member of the A.P.S. and Sigma Xi.

❖

Edgar H. Fritze (S'48–A'50) was born in St. Paul, Minn. on January 15, 1924. He received the B.E.E. degree from the University of Minnesota in 1944 and the M.S. degree in electrical engineering from the University of Wisconsin in 1948.

E. H. Fritze

Mr. Fritze served in the U. S. Navy from 1944 to 1946, during which time he received technical radar training at the Massachusetts Institute of Technology and later was assigned duty in airborne electronics. After release from the service, he was employed by the Boeing Aircraft Company as an instrumentation development engineer. Since 1948 he has been employed by the Collins Radio Company, and has been engaged in the development of servomechanisms and analog computers primarily for radar and aircraft control applications.

Mr. Fritze is a member of Tau Beta Pi and Eta Kappa Nu.

❖

J. R. Gerhardt was born in Omaha, Neb., on April 29, 1918. He received the B.S. degree in engineering in 1940 from the Illinois Institute of Technology. Entering the Air Force in 1941, he was graduated from the New York University meteorology course for weather officers in 1943. Following a period of special training in radio and radar propagation, he was engaged on special Air Force projects involving the forecasting and analysis of the meteorological parameters affecting radar propagation with the Radiation Laboratory, MIT, the AAF Board at Orlando, Fla., and the OCSiGO on radio relay projects in California and Florida.

J. R. Gerhardt

Since 1946 Mr. Gerhardt has been associated with the electrical engineering research laboratory of the University of Texas, formerly as chief meteorologist and currently as assistant director. This laboratory is engaged in research in radio wave propagation and micrometeorology.

Mr. Gerhardt is a member of Phi Lambda Upsilon, Sigma Xi, the American Meteorological Society, the American Geophysical Union, and the New York Academy of Sciences.

For a photograph and biography of Marcel J. E. Golay, see page 1252 of the October, 1952 issue of the Proceedings of the I.R.E.

❖

Robert Graham, Jr. (S'48–A'50) was born in East Orange, N. J. on September 6, 1924. Upon graduation from high school in 1942 he entered the Navy and served three years. After being discharged he entered the Newark (N.J.) College of Engineering, and was awarded the B.S. degree in electrical engineering in 1950. He has done graduate study at the Newark College of Engineering and at Rutgers University.

R. Graham, Jr.

Since 1950 Mr. Graham has been employed by Coles Signal Laboratory ofthe Signal Corps Engineering Laboratories where he is engaged in development and procurement of radio relay sets for military use. Mr. Graham has been a licensed radio amateur for several years.

❖

William L. Hughes (S'48–A'50) was born in Rapid City, S. D., on December 2, 1926. He received the B.S. degree in electrical engineering from South Dakota State School of Mines and Technology in 1949, and the M.S. and Ph.D. degrees in electrical engineering from Iowa State College in 1950 and 1952, respectively.

W. L. Hughes

Mr. Hughes worked as a transmitter engineer for the Black Hills Broadcast Co. of Rapid City while a student and was active in the engineering development of Iowa State's television station WOI-TV. During World War II he worked for two years in aviation electronics for the U. S. Navy. At present he is assistant professor of electrical engineering at Iowa State College.

Mr. Hughes is an associate of Eta Kappa Nu, Sigma Xi, and Pi Mu Epsilon.

❖

For a photograph and biography of William C. Jakes, Jr., see page 1253 of the October, 1952 issue of the Proceedings of the I.R.E.

Contributors to Proceedings of the I.R.E.

Heinz E. Kallmann (A'38–M'41–SM'43) was born on March 10, 1904, in Berlin, Germany. He received the Ph.D. degree in physics from the University in Goettingen in 1929. From 1929 to 1934, Dr. Kallmann was a research engineer in the Laboratories of the C. Lorenz A. G. in Berlin, concerned with the development of rf test equipment, and of ultra-short-wave receivers for communications and for wide-band television. He was also in charge of television development.


H. E. Kallmann

From 1934 to 1939, Dr. Kallmann was a television engineer with Electric and Musical Industries, Ltd., Hayes, England, doing research and advanced circuit development. Since 1939, he has been a consulting engineer in New York, N. Y., except for the period from 1943 to 1945, when he joined the Radiation Laboratory of the Massachusetts Institute of Technology, where he had charge of the circuit section of the test equipment group, and was a member of the fundamental microwave research group.

Dr. Kallmann is a member of the American Physical Society and has served on various RMA committees on uhf and color television systems.

❖

For a photograph and biography of John G. Linvill see page 727 of the June, 1952 issue of the Proceedings of the I.R.E.

❖

J. R. Mentzer was born in Arch Spring, Pa. on June 16, 1916. He received the B.S. and M.S. degrees in electrical engineering from Pennsylvania State College in 1942 and 1948, respectively, and the Ph.D. degree in physics from the Ohio State University in 1952.


J. R. Mentzer

From 1942 to 1946 Dr. Mentzer was associated with the Radio Division of the Westinghouse Electric Corporation in Baltimore, Md. where he worked on the design of receivers for search radar. In 1946 he accepted an appointment in the Ordnance Research Laboratory at the Pennsylvania State College. There he held the position of head of the Theory Section until 1948, when he joined the staff of the Antenna Laboratory at the Ohio State University. In 1952 he became a member of the research staff at the Massachusetts Institute of Technology.

Dr. Mentzer is a member of A.P.S. and Sigma Xi.

❖

For a photograph and biography of Alan A. Meyerhoff see page 1127 of the September 1952 issue of the Proceedings of the I.R.E.

❖

For a biography and photograph of W. W. Mumford see page 1128 of the September, 1952 issue of the Proceedings of the I.R.E.

❖

Glenn W. Preston (A'51) was born in Welch, W. Va. on March 30, 1922. He received the B.S. and M.S. degrees in physics from Trinity College in June, 1947 and Yale University in 1949, respectively.

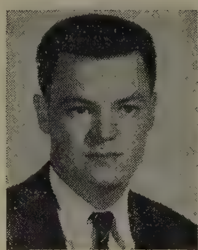
G. W. Preston

During World War II, Mr. Preston served as blimp pilot and radar officer with the U. S. Navy. During 1950 and the early part of 1951, he was group leader of an applied mathematics group at the Goodyear Aircraft Corporation.

Since February, 1951, Mr. Preston has been associated with the Philco Corporation in the capacity of consultant engineer in the Research Division, supervising a mathematical consulting group, responsible for planning and directing theoretical investigations concerned with various military and domestic research programs involving radar, radio, television, and allied fields.

Mr. Preston is a member of A.P.S., the Society for Industrial and Applied Mathematics, and the Econometric Society.

❖

S. O. Rice was born on November 29, 1907, in Shedds, Ore. He was graduated from Oregon State College with a B.S. degree in 1929. The following year he attended California Institute of Technology and then joined the technical staff of Bell Telephone Laboratories.


S. O. Rice

From 1930 to 1934 Mr. Rice was concerned with non-linear circuit theory, with special emphasis on modulation studies. He spent the academic years 1934 and 1935 at California Institute of Technology, assisting in a mathematical project, then returned to Bell Laboratories. A member of the systems studies department, he is now concerned with telephone transmission theory, including noise theory and applications of electromagnetic theory.

❖

Joseph C. Tellier (S'35–A'37–SM'45) was born in Des Moines, Iowa on June 24, 1914. He received the B.S. degree in electrical engineering from the Moore School of Electrical Engineering, University of Pennsylvania, in 1935. In 1936 he joined Philco Corporation, and since 1937 has been associated with the Research Division of that company. He has been interested primarily in the circuit development aspects of AM, FM, and television receivers, and has been connected with and been in charge of various classified research and development projects.


J. C. Tellier

At present Mr. Tellier is a Section Engineer in the Philco Research Division, supervising a group engaged mainly in the development of color television circuitry.

Mr. Tellier is a member of Eta Kappa Nu and Tau Beta Pi.

❖

Yeo Pay Yu (A'48) was born on August 27, 1919, in Canton City, China. He received the M.S. in E.E. degree in 1940 from Lehigh University and the Ph.D. degree in 1942 from the Brooklyn Polytechnic Institute.

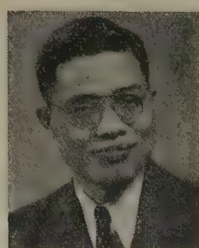
Yeo Pay Yu

From 1942 to 1946 Dr. Yu was a project engineer engaged indevelopment of special electronic instruments and FM and AM receivers in industry. From 1947 to 1949 he was associate professor of electronics in the School of Engineering, North Dakota State College. From 1949 to 1952 he was associated with Allen B. DuMont Laboratories as a senior engineer engaged in research and development of high-speed oscilloscopes. Since August Dr. Yu has been with the Advance Electronics Company as president and chief engineer, doing research and development work on electronic instruments.

Dr. Yu has published more than fifteen papers on the results of his research and development in electron-tube circuits and instruments.

Institute News and Radio Notes

Calendar of COMING EVENTS

IRE-AIEE-ASME Southwest Conference on Feedback Circuits, Southern Methodist University, Dallas, Tex., March 12–13

IEE Symposium on Insulating Materials, London, Eng., March 16–18

1953 IRE National Convention, Waldorf-Astoria Hotel and Grand Central Palace, New York, N. Y., March 23–26

IRE New England Radio Engineering Meeting, Storrs, Conn., April 11

9th Joint Conference of RTMA of United States and Canada, Ambassador Hotel, Los Angeles, Calif., April 16–17

IRE Seventh Annual Spring Technical Conference, Cincinnati, Ohio, April 18

IRE-Polytechnic Institute of Brooklyn, Symposium on Non-Linear Circuit Analysis Engineering Societies Building, N. Y., April 23 and 24

SMPTE Convention, Statler Hotel, Los Angeles, Calif., April 26–30

IRE-URSI Spring Meeting, National Bureau of Standards, Washington, D. C., April 27–30

NARTB Convention, Biltmore Hotel, Los Angeles, Calif., April 28–May 1

Electronic Components Symposium, Shakespeare Club, Pasadena, Calif., April 29–May 1

1953 National Conference on Airborne Electronics, Dayton, Ohio, May 11–14

National Electronics Conference, Hotel Sherman, Chicago, Ill., September 28–30

1953 IRE-RTMA Radio Fall Meeting, Toronto, Ont., October 26–28

Electric Components Symposium Set for April

The American Institute of Electrical Engineers, Institute of Radio Engineers, Radio-Television Manufacturers' Association, and West Coast Electronic Manufacturers Association will be sponsors of the 1953 Electronic Components Symposium to be held April 29–May 1, at the Shakespeare Club, Pasadena, Calif.

The Symposium is one of a series on electronic component parts held annually to bring together those interested in the development, design, performance, and future of electronic component parts.

Technical papers are now being considered for the program of this meeting. For further information write to: D. A. M. Zarem, Electronic Components Symposium Headquarters, Stanford Research Institute, Suite 1011, 621 South Hope St., Los Angeles 17, Calif.

Record Attendance at Computer Conference

A record attendance of 1144 engineers registered at the Second Annual Computer Conference and Exhibition, Park Sheraton Hotel, New York, N. Y., December 10–12, 1953. The meeting was jointly sponsored by the IRE Professional Group on Electronic Computers, the American Institute of Electrical Engineers, and the Association for Computing Machinery.

Twenty-seven technical papers and exhibits by 15 manufacturers and scientific organizations stressed the conference's theme of "Input and Output Equipment Used in Computing Systems" for business accounting, automatic factory operation, and scientific investigations.

Copies of the Proceedings of the Second Annual Computer Conference may be obtained by sending checks for $4.00, payable to the American Institute of Electrical Engineers, to R. S. Gardner, AIEE, 33 W. 39 St., New York, N. Y.

A list of the papers presented at the conference may be found in the November, 1952 issues of the PROCEEDINGS OF THE I.R.E., page 1613.

Guggenheim Fellowships Offered to Engineers

Applications are now open for The Daniel and Florence Guggenheim Jet Propulsion Fellowships, which are awarded annually for graduate study at Princeton University and the California Institute of Technology.

From nine to twelve fellowship grants, totaling $18,000, are available at each institution. The individual grant will provide for tuition and stipend from $1,000 to $2,000.

Complete information and application blanks may be had by writing to: The Daniel and Florence Guggenheim Foundation, 120 Broadway, New York 5, N. Y.

Instrumentation Conference Scheduled for March

The electrical engineering department of Michigan State College, in co-operation with the National Science Foundation, the National Bureau of Standards, Instrument Society of America, and the American Society for Engineering Education, will hold an invitational National Collegiate-Industry-Government Conference on Instrumentation, March 19–20, 1953, Michigan State College, East Lansing, Mich.

The objectives of the conference will be: to relate the role and needs of instrumentation in production and research to college interests and responsibilities, to review current instrumentation activities in the college, to suggest specific activities the colleges might undertake in this field, and to suggest specific ways by which industry might assist the colleges in these activities.

The program will present authorities of the instrumentation industry and will include, among others, Paul Klopsteg, National Science Foundation; A. V. Astin, National Bureau of Standards; Porter Hart, Instrument Society of America; and E. A. Walker, Pennsylvania State College.

Additional information concerning the conference may be requested from: Professor R. J. Jeffries, Department of Electrical Engineering, Michigan State College, East Lansing, Mich.

Technical Committee Notes

Under the Chairmanship of D. C. Ports the **Antennas and Waveguides** Committee met on November 12, 1952. The Committee finished reviewing written comments submitted on the Definitions of Wave Guide Terms. The definition of Q was discussed at some length by the Committee. Mr. Ports offered to have duplicated the written Q summaries which were prepared by A. G. Fox and Seymour Cohn. The comments will be distributed as guides to Committee members in order that the Q definitions can be resolved by all. The Chairman suggested that the list of Proposed Wave Guide Component Definitions be discussed at future meetings.

The **Facsimile** Committee met on November 7, 1952, under the Chairmanship of R. J. Wise. J. H. Hackenberg outlined briefly the work of last season and the status of the various subjects under consideration. Samples were exhibited of a test chart used by Bell Laboratories. The chart is similar to those used by other organizations and it was suggested that further discussion of test charts be deferred until a later date in order that various changes of definitions which have been proposed might be considered. The first of these to be considered was that for Definition (1F12). There was a general agreement that 1F12 of the 1942 Standards on Facsimile (as written) was of little practical value; however, there was no agreement as to how it should be changed. Although a number of suggestions were made, none of the proposals seemed on an acceptable basis to rewrite the definition; decision on the matter was deferred until another meeting. A new definition (direct recording), originally proposed by I. H. Frankel at the January 4, 1952 meeting, was revised and approved. A proposed revision of "Electrochemical Recording" was rejected and it was voted to retain the definition unchanged. Both "Electrolytic Recording" and "Electrothermal Recording" were revised. It was agreed to retain the definition of "Electromechanical Recording."

The **Circuits** Committee met on November 14, 1952. In the absence of C. H. Page, W. R. Bennett took the Chair. A letter received by R. L. Dietzold from Professor Otto J. M. Smith, University of California, expressing a desire to participate in the work of the Circuits Committee was presented. Mr. Dietzold will offer Professor Smith the chairmanship of a subcommittee on the Pacific Coast to help in framing definitions for a selected group from the backlog of terms now in the domain of Subcommittee 4.2 and Subcommittee **4.9**. The Committee

(*Continued on following page*)

(*Technical Committee Notes continued*)

does not foresee any immediate action here on these definitions. Formation of a new Subcommittee 4.1 on Transistor Circuitry was approved and J. G. Linvill was appointed Chairman. Membership will be selected by Dr. Linvill. J. G. Kreer has pointed out that the Subcommittee 4.4 definitions on bilateral and unilateral networks which are now on the Grand Tour do not agree with the corresponding definitions on transducers published as standards. The Committee agreed to modify their classification of terms to conform with the transducer groups. A list of feedback definitions prepared by the Subcommittee 4.7, on May 16, 1952, was received by mail from Chairman W. A. Lynch who was not able to attend the present meeting. After some discussion the definition of feedback loop was approved. With regard to series, shunt, and bridge feedback, it is felt that if a satisfactory quantitative definition of feedback itself could be agreed upon, the above terms which have already been defined would be acceptable. It was suggested that illustrative drawings must accompany these definitions.

On December 4, 1952, the **Symbols** Committee met under the Chairmanship of A. G. Clavier. In the absence of C. D. Mitchell, Chairman of Subcommittee 21.2 on Symbols for Semiconductor Devices, a report was read by the Secretary. A. C. Reynolds, Jr. reported on the work done by the Subcommittee on Symbols for Functional Operation of Control, Computing, and Switchboard Equipment. In the absence of A. F. Pomeroy, R. E. Thiemer reported on the status of ASA Standardization of Graphical Symbols and Reference Designations. A final draft has been completed by the ASA Subcommittee and submitted through channels for approval as an American Standard. Two meetings of an Editorial Task Group have been held to decide on the format. After adoption of the format to be used, the standard, which has been adopted by the IRE Standards Committee, will be submitted for the PROCEEDINGS. A foreword will be written for the IRE Standard, giving credit to all concerned and stating that although the IRE has adopted the whole document, it did not participate in formulation of the power symbols included. H. P. Westman will prepare a foreward draft which he will distribute to the membership for comment. In the absence of F. M. Bailey, F. J. Louden reported that Dr. Bailey's new Subcommittee on Symbols for Feedback Control Systems is in the process of being formed. Mr. Louden requested clarification of the scope of the Subcommittee's work and asked if both letter symbols and graphical symbols are to be covered. It was agreed that both of these items as well as abbreviations peculiar to Feedback Control Systems should be surveyed by the Subcommittee. Accordingly, the name of the Subcommittee was revised to read "Subcommittee on Abbreviations, Letter Symbols, and Graphical Symbols for Feedback Control Systems." Chairman Clavier advised Mr. Louden that the Subcommittee should keep in close touch with all other groups working on feedback control and servomechanism in order to avoid any conflicts.

Professional Group News

Airborne Electronics

The Board of Directors has been appointed for the National Conference on Airborne Electronics, to be held in Dayton, Ohio, May 12–14, 1953 and sponsored by the Professional Group on Airborne Electronics. They are as follows: President, S. M. Schram, Jr.; Vice-President, Joseph General; Secretary, E. M. Turner; Treasurer, James DeLuna; Budget, R. J. Doran; Dayton Section Representative, J. L. Dennis; Professional Group Representative, Maurice Jacobs; Committee Chairmen, G. F. Guernsey, N. L. Laschever, P. R. Murray, D. J. Dietrich, Yale Jacobs, Paul Clark, A. P. Parker, Mrs. T. Duckwitz.

The Airborne Electronics Group appointed its Administrative Committee members, who took office January 1, 1953. They are: N. Winter, Sperry Gyroscope Company; J. A. Marsh, North American Aviation Company; E. A. Post, United Air Lines; J. F. Morrison, Bell Telephone Laboratories; W. H. Rothammer, Wright Air Development Center.

Audio

The Cincinnati Chapter of the Audio Group has been holding meetings at the Engineering Society Headquarters Building, Cincinnati, Ohio.

During one of the meetings W. H. Breunig spoke on "The Historic Development of the Louspeaker" in which he discussed the development of the moving coil loudspeaker from a patent viewpoint. At a second meeting Robert Holden presented a lecture entitled "Quiet Please" with a demonstration film showing the uses of acoustic treatment, elementary theory of its operation, and reasons for its use. Another meeting featured H. A. Hartley from London, England, who presented a paper on "British Audio." Mr. Hartley discussed his views and thoughts on what constitutes good sound reproduction and demonstrated audio equipment manufactured in his country.

The Chicago Chapter of the Audio Professional Group held its December meeting at the Western Society of Engineers Building, Chicago, Ill. O. C. Bixler, Magnecord, Inc., presented a paper on "A Binaural Recording System." Mr. Bixler reviewed the theoretical factors involved in binaural recording and reproduction, along with a description of some equipment developed to provide a high quality system consistent with reasonable cost. Some novel problems and effects in the development program as well as in recording techniques were described as encountered in radio, court reporting, and test instrumentation.

Broadcast and Television Receivers

A joint meeting was held recently by the Chicago Chapters of the Broadcast and Television Receivers and the Broadcast Transmission Systems Groups, at the Western Societies of Engineers Building, Chicago, Ill. W. E. Berkey presided at the meeting, and L. L. Lewis of Station WOI, Ames, Iowa, presented a paper on "Diesel Power for TV Transmitter Operation."

Broadcast Transmission Systems

A meeting of the Boston Chapter of the Broadcast Transmission Systems Group was held at Radio Station WEEI, Boston, Mass. P. K. Baldwin, Chairman of the Chapter, presided over an attendance of ninety-three. Seventeen broadcast stations were represented.

During the meeting, a paper was presented on "High-Power Klystron and Helical Antenna for UHF Telecasting," by H. B. Fancher, General Electric Company, Syracuse, N. Y.

Circuit Theory

The Chicago Chapter of the Circuit Theory Group held a meeting recently at the Western Society of Engineers, L. E. Pepperberg, Chairman. Joseph Markin of Raytheon Television and Radio Corporation presented a paper on "UHF Measurements and the Smith Chart."

Electronic Computers

The Los Angeles Chapter of the Electronic Computers Group held a meeting recently at the Institute for Numerical Analysis, UCLA. W. F. Gunning was chairman.

During the meeting, R. R. Bennett of the Hughes Aircraft Company spoke on "An Introduction to Analogue Computers," in which he described the basic elements of analogue computers and gave an operational description of their performance in a typical system. T. A. Rogers of the University of California spoke on "The Solution of Partial Differential Equations on an Analogue Computer." Professor Rogers discussed techniques for generating the solutions for a wide variety of partial differential equations utilizing amplifier type computer elements.

Nuclear Science

At a meeting of the Chicago Chapter of the Nuclear Science Group held recently, E. R. Rathbun, Nuclear Instrument and Chemical Corporation, spoke on "Detection of Radiation with Scintillation Counters." The material presented involved the physical processes in the interaction of gamma rays with matter.

Vehicular Communications

The Los Angeles Chapter on Vehicular Communications held a December meeting at the Institute of Air Sciences Building, Los Angeles, Calif., M. E. Kennedy, Chairman.

C. N. Gregory presented a paper entitled "The Use of Microwave Equipment in Modern Communications Systems," and demonstrated his discussion with color film taken during and after construction of the mountain-top microwave relay stations.

A joint session of the Chicago Chapters of the Vehicular Communications and Broadcast and Television Receivers Groups was held recently. R. B. Holt, Transistor Products, Inc., presented a paper "Current Status of Transistor Manufacture and Applicability of Available Types."

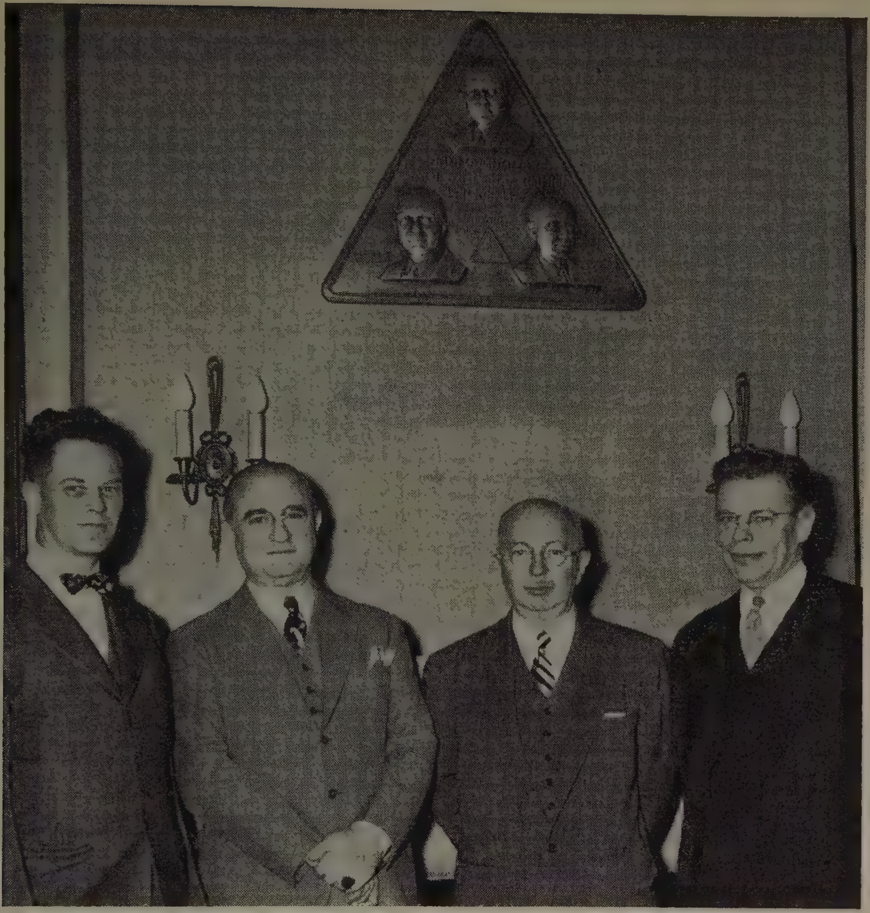

Left to right) D. B. Sinclair, 1952 President; A. N. Goldsmith, Editor; J. V. L. Hogan; J. W. McRae, 1953 President, standing before the recently unveiled plaque commemorating the three founders of the Institute. At top of the plaque is a likeness of R. H. Marriott; lower left, A. N. Goldsmith; lower right, J. V. L. Hogan.

JTAC Outlines Plans for Studying Radiation Problem

In response to a request by the Federal Communications Commission for engineering information on interference caused by spurious radiation, the Joint Technical Advisory Committee has drawn up a threefold plan for dealing with the Commission's request. The plan was outlined in a letter dated December 23, 1952, from JTAC Chairman Ralph Brown to Paul A. Walker, Chairman of the FCC.

Part 1 of the plan calls for the formation of a subcommittee of JTAC to compile existing information on the principles and methods of dealing with spurious radiation problems, and to organize this material into an engineering reference handbook.

Under *part 2* of the plan, the JTAC is requesting the IRE to set up a temporary committee which can work closely with JTAC to formulate and systematize the available information on measurement methods pertinent to the spurious radiation question. The committee will also clearly outline those areas where such information is lacking so that means can be considered for filling these gaps.

In accordance with *part 3* of the plan, the JTAC has taken the initial step of asking the Radio-Television Manufacturers Association for their viewpoint on the problem of spurious radiation from transmitters and receivers in television broadcasting, and requesting information on any plans which they have, or may propose, to cope with it.

1953 IRE Convention News

A well-rounded and comprehensive program of over 200 technical papers and 400 exhibits has been scheduled for the 1953 IRE National Convention, to be held on March 23–26, at the Waldorf-Astoria Hotel and Grand Central Palace in New York City.

❖

Technical Sessions

The technical program will be highlighted by an all-day seminar and nine symposia organized by Professional Groups of the IRE.

On Wednesday, March 25, 1953, the Professional Group on Audio will initiate a new experiment in sessions at the IRE National Convention. An entire day (two full sessions) is being devoted to a seminar on "Acoustics for the Radio Engineer." The seminar will be conducted by a panel of six speakers and will be of a tutorial nature. Discussion both among the members of the panel and between the audience and the panel will be encouraged. Both sessions will be held at the Gold Room of the Grand Central Palace and will be open to members and non-members of the Professional Group on Audio. Wide interest is expected among non-audio people both because of the material to be presented and the excellent panel of speakers. The morning session will be devoted to a talk and discussion on Fundamental Theory, by L. L. Beranek, M.I.T., Microphones, by H. F. Olson, Radio Corporation of America, and Loudspeakers, by H. S. Knowles, Industrial Research Products. The afternoon session will feature Phonograph Reproducers, by B. B. Bauer, Shure Brothers, Inc., Tape Recording, by M. Camras, Armour Research Foundation, and Studio Acoustics, by H. J. Sabine, The Celotex Corporation.

Not only will the papers present the material in a clear fashion adjusted to the desires of the radio engineer, but the ensuing discussion will bring to light and answer many of the questions in every radio engineer's mind.

Nine symposia, specially prepared by Professional Groups, will cover the subjects of television broadcasting and uhf, wideband amplifiers, large scale digital computers, engineering management, transistor measurements, manufacture of microwave equipment, nucleonics, and mobile communications. The program will be rounded out by 32 sessions encompassing every phase of activity in the radio engineering field.

❖

Exhibits

The Radio Engineering Show, comprising over 400 exhibits of the latest communications and electronic equipment and their applications, will occupy all four floors of Grand Central Palace. For the convenience of members and visitors, many of the exhibits will be grouped according to subject. The exhibits will be complemented by several demonstration rooms and two lecture halls.

❖

Convention Record

In order that the papers presented at the convention may be of greater benefit to the radio engineering profession, plans have been made to publish all convention papers in a new publication, to be called the Convention Record of the I.R.E. The Convention Record will be issued in ten parts, with each part devoted to papers in one general field, to be available approximately two months after the convention. Orders for the Convention Record will be taken during the convention.

Of particular interest to members of IRE Professional Groups is the fact that plans are under consideration whereby every paid Group member will automatically receive, free of charge, the particular Convention Record Part pertaining to the technical field of his Group.

❖

Further Details

Final details regarding the technical program, exhibits, and the Convention Record will appear in the March issue of the Proceedings.

IRE People

Hubert J. Schlafly, Jr. (A'41–A'42–SM'47) has been elected vice president in charge of engineering of the TelePrompTer Corporation.

H. J. Schlafly

Mr. Schlafly was born in St. Louis, Mo., August 14, 1919, and received the B.S. degree in electrical engineering from the University of Notre Dame in 1941. He then joined the advanced development laboratory of the General Electric Company, and in 1944, he was assigned by General Electric to the Radiation Laboratory at the Massachusetts Institute of Technology, in charge of the engineering of a gunfire control system.

After World War II, Mr. Schlafly returned to General Electric's marine engineering section, and in 1947, he joined 20th Century Fox as director of television research. Recently, he spent several months at the Federal Institute of Technology in Zurich, Switzerland, working with the inventors of the Eidophore principle and was subsequently responsible for the technical aspects of the first demonstration of the system in the United States last summer.

Mr. Schlafly has served as a member of the board of directors of the TelePrompTer Corporation. He is a fellow of the Society of Motion Picture and Television Engineers.

❖

Francis M. Wiener (SM'52) has been appointed section head in the engineering department of Spencer-Kennedy Laboratories, Cambridge, Mass.

F. M. Wiener

Dr. Wiener, a native of Czechoslovakia, received his B.S. degree from the Institute of Technology, Prague, Czechoslovakia, in 1934. He worked at the Radio Techna Corporation in Prague until 1938, when he came to the United States and started his graduate studies at Harvard University. He received the M.S. and Ph.D. degrees at Harvard in 1939, and 1941.

After working for a time in the research department of the Stromberg-Carlson Company, Dr. Wiener returned to the electro-acoustic laboratory at Harvard and remained there until 1946. He then joined the Bell Telephone Laboratories to work on acoustic theory and, later, on fundamental communication aspects of speech, as well as classified problems for the Office of Naval Research.

Dr. Wiener has been an adjunct professor of electrical engineering at the Polytechnic Institute of Brooklyn where he now teaches a course in acoustic wave theory. He is a member of Sigma Xi, and a fellow of the Acoustical Society of America.

Edwin A. Speakman (A'43–M'44–SM'48) has been appointed general manager of the Fairchild Guided Missiles Division, Wyandanch, N. Y. Previously, Mr. Speakman has been vice chairman of the Research and Development Board, Department of Defense.

E. A. Speakman

Receiving the B.S. degree in physics at Haverford College, Haverford, Pa., Mr. Speakman remained there for three years as an instructor in physics. As part of his graduate study, he developed a photo-electric timing system on which he holds a patent.

From 1934–1937, Mr. Speakman was associated with the research laboratories of the Philco Corporation, where he invented the telescopic rod antenna which is used on most radio-equipped automobiles today.

Mr. Speakman was appointed to the Naval Research Laboratory in Washington, D. C., in 1939, to serve as assistant superintendent of the Radio Division and head of the Countermeasures Branch of the Laboratory. During this time he initiated developments for naval radar equipment for which he received the Navy's Meritorious Civilian Service Award in 1946.

In 1949, Mr. Speakman joined the Research and Development Board as executive director of the committee on electronics. He is a member of the American Physical Society and a former member of the United States Civil Service Board of Examiners for Scientific and Technical personnel.

❖

Alfred W. Russell (A'44–SM'51) has been appointed head of the instrument divisions' electrical design section of the Dumont Laboratories, Inc. He was formerly a senior engineer.

Mr. Russell, a native of England, received the B.S. degree in physics from the University of London Kings College, in 1934. He spent two years doing research under Sir Edward Appleton before joining the research staff of Mullard Radio in England.

In 1948, Mr. Russell came to the United States and joined the receiver division of the General Electric Company in Syracuse, N. Y. He became associated with the Dumont Laboratories, Inc., in 1951.

❖

Wilmer T. Spicer (M'49) has been named administrative assistant to the director of engineering research, radio division, of Bendix Aviation Corporation, Towson, Md.

Mr. Spicer was born in Cambridge Md., and received the B.E.E. degree from Johns Hopkins University in 1938. In 1940 he joined the technical publications department at Bendix and was instrumental in the development of that section.

Donald L. Herr (SM'46) has been elected president and director of American Electronic Manufacturing, Inc., Los Angeles, Calif.

D. L. Herr

Dr. Herr, a native of Pennsylvania was the winner of numerous student prizes and awards at the Moore School of Electrical Engineering. He took his graduate work as a National Tau Beta Pi fellow and MIT scholar at the Massachusetts Institute of Technology. He received the Ph.D. degree from the Polytechnic Institute of Brooklyn in 1951, where he was an adjunct professor in electrical engineering.

Dr. Herr has been associated with the Bell Telephone Laboratories, the RCA Manufacturing Company, the General Electric Company, the Control Instrument Company, and the Reeves Instrument Company. During World War II, he served in the U. S. Navy as officer in charge of the electrical minesweeping section, Bureau of Ships, and with the Office of Naval Research, for which he received two commendations for his outstanding work.

The recipient of numerous awards for his work in the technical field, Dr. Herr also has written many articles and one textbook and holds more than a score of patents in the fields of computers, precision components, servomechanisms, networks, and military naval technology. He is a fellow of the New York Academy of Sciences, honorary member of the American Society of Naval Engineers, member of the American Institute of Electrical Engineers, American Society of Mechanical Engineers, American Association for the Advancement of Science, and many others.

❖

F. Clark Cahill (S'38–A'40–SM'45) has been appointed chief engineer of the engineering and production division of Airborne Instruments Laboratory, Inc., Mineola, N. Y. He has been a member of the Laboratory since 1945.

F. C. Cahill

Mr. Cahill was born on April 27, 1914, in Dixon Ill. He received the B.A. and E.E. degrees from Stanford University in 1936 and 1938, respectively.

In 1938 Mr. Cahill joined Heintz and Kaufman, Ltd. as an engineer. During World War II, he was associated with the Radio Research Laboratory at Harvard University as head of a war research work division. At this same time he was associate director of the affiliated American-British Laboratory in Great Britain.

Mr. Cahill is a member of Phi Beta Kappa and Tau Beta Pi.

Vladimir K. Zworykin (M'30–F'38) has been awarded the 1952 Edison Medal of the American Institute of Electrical Engineers. The medal was presented "for outstanding contribution to the concept and design of electronic components and systems."

V. K. Zworykin

Dr. Zworykin was born in Mourom, Russia, in 1889. He received the E.E. degree from the Petrograd Institute of Technology in 1912, the Ph.D. from the University of Pittsburgh in 1926, and the D.Sc. from Brooklyn Polytechnic Institute in 1938.

In 1920, Dr. Zworykin came to the United States and joined the research staff of Westinghouse Electric and Manufacturing Company. In 1930 he became associated with the Radio Corporation of America as director of the electronic research laboratory, and in 1947, he was elected vice-president and technical consultant of the RCA Laboratories Division.

During World War II, he served on the Scientific Advisory Board to the Commanding General of the United States Army Air Forces, the Ordnance Advisory Committee on Guided Missiles, and three subcommittees of the National Defense Research Committee, also directing important research work.

Dr. Zworykin received the IRE Morris Liebmann Memorial Prize in 1934, as well as numerous other awards for basic contributions to television, electron microscopy, and other phases of radio and electronics. He is a fellow of the American Institute of Electrical Engineers, the American Physical Society, and the American Association for the Advancement of Science, and a member of the Electron Microscope Society of America and Sigma Xi.

❖

William W. Dean (A'43–SM'46) has been appointed director of engineering of the Langevin Manufacturing Corporation, New York, N. Y.

W. W. Dean

Mr. Dean was born in Chicago, Ill., in 1913, and received the B.S. degree in electrical engineering in 1941. From 1933–1941, he was associated with the technical staff of radio station WWJ in Detroit, Mich., and then transferred to the General Electric Company, Syracuse, N. Y.

During World War II, Mr. Dean was in the radio transmitter engineering department at General Electric, where he worked on high-power transmitters and military radio equipment. In 1945 he became an audio facilities project engineer.

Mr. Dean is a member of the IRE Audio Techniques Committee.

Henri Polak (M'50) has been appointed scientific attaché at the Netherlands Embassy, Washington, D. C.

Dr. Polak, a native of Netherlands East India, was born on June 14, 1918. He received the Ph.D. degree in engineering physics from the Delft Institute of Technology, in 1943.

From 1940–1946, Dr. Polak was a research physicist for the technical physics laboratory at Delft Institute of Technology, and then became the scientific investigator of the French zone of Germany for the Netherlands Ministry of Foreign Affairs. In 1947, he was a technical and scientific adviser with the Netherlands Embassy in Washington, D. C., and in 1948, he became the Netherlands representative and technical liaison for government research, to the United States.

Dr. Polak is a member of the American Physical Society, Royal Institute of Engineers (Netherlands), Netherlands Institute of Physics, and Netherlands Radio Society.

❖

R. K. Frazier (A'41) has been named technical assistant to the director of engineering and research, of the radio division of Bendix Aviation Corporation, Towson, Md. Prior to his assignment, he was chief engineer of the communication and navigation engineering department.

Mr. Frazier is a native of Newton, Kans., and a graduate of Montana State College. He has been with the Bendix organization since 1940.

❖

Commander Newell A. Atwood (A'46–SM'49) has been assigned senior program officer for Radio and Sound at the Naval Research Laboratory. He has been on active navy duty since 1941.

N. A. Atwood

Commander Atwood was born in Urbana, Ohio, in 1907, and received the B.A. degree from the University of Michigan in 1932, and the LL.B. degree from the George Washington University. He joined the United States Naval Communications Reserve in 1933.

From 1926–1927, Commander Atwood was connected with the research laboratories of the National Carbon Company, Cleveland, Ohio, and from 1929–1936, he was on the faculty of the University of Michigan. He then practiced patent law in Washington, D. C., until 1941. During World War II, he served with the Naval Research Laboratory, the Bureau of Ships, the Office of Naval Research, and the Norfolk Naval Shipyard. After the war he served as an electronics engineering officer.

Since 1950, Commander Atwood has been on duty in London, England and other European countries in connection with the Mutual Security foreign aid program.

Ralph A. Hackbusch (A'26–M'30–F'37), president and managing director of Stromberg-Carlson Company Limited, has been re-elected president of the Canadian Radio Technical Planning Board.

R. A. Hackbusch

Mr. Hackbusch, a native of Hamilton, Ontario, has been active in the Canadian radio industry for many years. In addition to his associations with Stromberg Carlson, he was the vice-president and director of the Radio Division of the Canadian Government Research Enterprises Ltd. He also has served as vice-president and president of the Radio Manufacturers' Association of Canada.

Mr. Hackbusch was the IRE Vice President in 1944, and has served on such IRE Committees as, Admissions, Awards, Public Relations, and Standards. He has been the Secretary and Chairman of the IRE Toronto Section.

❖

E. G. Lomas (A'46–M'48–SM'51) has been appointed to form an engineering sales division within the PSC Applied Research Limited, an associated company of the Photographic Survey Corporation Limited, Toronto, Ont., Canada.

E. G. Lomas

Mr. Lomas, a native of Canada, was born December 6, 1917. He received the B.S. degree in mathematics and physics at Sir George Williams College in 1946.

For eight years Mr. Lomas was associated with the radio aviation division of the Department of Transport, Montreal, and in 1947 he became a communications sales engineer of Femco. In 1948, he transferred to the Royal Canadian Air Force, where he was initially engaged as a section head in charge of microwave and vhf communications. In addition, he was responsible for RCAF representation on the Electronic Standards Subcommittee of the Joint Telecommunications Committee.

Prior to his recent appointment, Mr. Lomas was chief of telecommunications specifications and publications branch Air Materiel Command Headquarters, RCAF.

❖

L. E. Florant (S'52) has been named head of the engineering services section at the Dumont Laboratories, Inc. He was formerly an intermediate engineer.

Mr. Florant, a native of New York, was born on May 2, 1925. He received the B.S. degree at Howard University in 1947, and the B.S. E.E. degree from the University of Michigan in 1950. He recently has been attending the City College of New York.

Books

Statistical Theory with Engineering Applications by A. Hald (4504)

Published by John Wiley and Sons, Inc., 440 Fourth Ave., New York 16, N. Y. 760 pages+20-page index+xii pages. 150 figures. 235 tables. 9¼×6¼. $9.00.

A. Hald is professor of statistics, University of Copenhagen, Denmark.

In this text, intended primarily for non-statisticians, the author establishes the definitions and axioms of the calculus of probabilities in such a manner as to make the calculus of probabilities and the calculus of frequencies isomorphic. He then develops the calculus in an elementary manner, slanting it toward the needs of the statistician.

The plan of the author's treatise, as outlined in chapter 25, is a program of statistical analysis, suggested by R. A. Fisher, consisting of five basic steps which follow:

1. The first is the planning of the investigation and, in particular, the sampling method and the number of observations. The necessity for insuring that observations are the results of a random operation is considered and techniques for randomizing are developed. The number of observations required to obtain a given accuracy of the estimate of the population mean is shown to depend on the population variance whether the population includes a finite or an infinite number of elements. Methods are developed for dividing the population into a number of homogeneous subpopulations, sampling from the subpopulations and eliminating variations between the subpopulations by handling data in accordance with the principles of the analysis of variance. Basic principles pertaining to the design of experiments are discussed in connection with the analysis of variance. Methods are developed for determining the number of observations nec essary to obtain a reliable decision from the power function of the test to be applied.

2. The next step, specification, is the formulation of a mathematical-statistical model which gives a satisfactory description of the data. This is not really a statistical task but belongs to the professional subject from which the observations have been derived. Since, as is often the case in practice, the professional knowledge is too meager to permit the formulation of a theoretical model, it becomes necessary to establish a phenomenological description of the observed phenomenon. The theory of statistics includes a collection of standard models, for example, the various systems of distribution functions and regression and correlation analysis which are well suited to application to such a phenomenological description. Since the choice of a model is largely arbitrary, the guiding principles here are in satisfactory agreement between the observed data and the model and simplicity in the description—either a mathematically simple description or simple tests of significance. Dangers resulting from basing the specification solely on an analysis of the data are discussed, and it is shown that an effective test of the model cannot be carried out by using the same data both for construction and testing the model.

3. The estimating the parameters step follows the specification of the mathematical form of the distribution of the population. A classification of estimates is attempted on the basis of properties derived from their sampling distributions. Examples of such classes of estimates are: consistent, efficient, sufficient, and unbiased estimates. Further methods of deriving estimates include the method of maximum liklihood and the method of least squares. Most of the estimates used in this book are sufficient, or, if sufficient tests do not exist, efficient. In the greater part of the problems treated, it is assumed that the observations are randomly drawn from a normally distributed population, and the estimates of the parameters have been derived using the method of least squares which in this case leads to sufficient estimates.

4. In the investigation of the agreement between the model and the observations, methods are described for employing probability paper to formulate a distribution function. After computing estimates of the parameters, the expected distribution may be compared with the observed distribution by means of the Chi-squared test. Other tests are also described, for example, the V-squared test for the linearity of the regression curve.

5. The last step, tests of significance, includes some of the principle tests that have been developed, and references are given to others. It is assumed that no observations from a normally distributed population with known variance and unknown mean are given and the so-called significance test is developed to determine the soundness of the hypothesis that the mean has a given specified value. The procedure used for investigating this problem is a prototype for all significance tests.

The author has illustrated by a great number of examples practically every concept employed and every theorem developed. This has resulted in a lengthy but at the same time a very readable text. Most of the illustrations are taken from the properties of materials.

It is the feeling of the reviewer that the author has succeeded in presenting his material in such a way as to make it readily accessible as a tool to the nonprofessional statistician.

LLOYD T. DEVORE
General Electric Company
Syracuse, N. Y.

The Magnetron by R. Latham, A. H. King, and L. Rushforth (4505)

Published (1952) by Chapman & Hall Ltd., 37 Essex St., W.C. 2, London, Eng. 138 pages+4-page index+ix pages. 82 figures. 5½×8¾. Price, 18s.

R. Latham is a staff member of the Imperial College of Science and Technology, South Kensington; A. H. King is a staff member of Clifton College, Bristol; and L. Rushforth is a staff member of the British Thomson-Houston Company, Ltd., research laboratory, Rugby, Eng.

The authors of this book were actively engaged, during World War II, in the British development of the multiresonator magnetron, from its early concept through the production stages. This book, written with a historical viewpoint, describes the vast problems and the adverse conditions in the developing of empirical designs, new construction techniques, and, finally, the factory production of magnetrons for aid in the defense of England as well as attacking the enemy. This story of the development of the "heart" of microwave radar is one of the great scientific epics of the war.

The book was written for engineers unfamiliar with microwave techniques but also is of interest to those actively engaged in such work. Only simple treatment is presented; however, the large number of references of unclassified war-time literature allows others to pursue the subject further.

The first three chapters describe the need for microwave radar, the comparison of magnetrons with other microwave oscillators, and the early development of multiresonator magnetrons. Chapters four and five discuss the anode block and RF systems and the problems involved in extracting energy from the tube.

A simple electronic theory is presented in chapters six, seven, and eight where the threshold voltage, energy conversion, and mode stability are covered. Chapters nine and ten discuss construction problems and the construction techniques employed by the British. The following two chapters cover magnetron testing techniques and the application of the magnetron to radar use.

This light treatment of magnetrons is recommended for those who wish to become acquainted with this family of tubes. For those who desire a more intimate knowledge of magnetrons, volume six of the MIT Radiation Laboratory Series entitled "Microwave Magnetrons," edited by G. B. Collins, might be suggested.

J. R. BLACK
W. G. DOW
University of Michigan
Ann Arbor, Mich.

Instrument Engineering by C. S. Draper, W. McKay, and S. Lees (4506)

Published (1952) by McGraw-Hill Book Company, Inc., 330 West 42 St., New York 36, N. Y. 260 pages+8-page index+2-page bibliography+xvi pages. 94 figures.

C. S. Draper is department head and W. McKay and S. Lees are professors of the Aeronautical Engineering Department, Massachusetts Institute of Technology, Cambridge, Mass.

This is the first volume of a three-volume set; the other volumes are scheduled to appear shortly. The text is subtitled, "methods for describing the situations of instrument engineering."

The major portion of this book is devoted to organizing a generalized system of notation and procedures for handling the operating systems involved in instruments. A discussion of the principles of dimensional analysis is included along with some reviewing of the methods of statistical analysis. The representation of functions by power series, exponential series, and Fourier series are treated briefly. Pulse functions and sinusoidal response characteristics are also discussed.

While the examples are mainly based on aeronautical instruments, the general notation and procedures apply to other forms of instrumentation; the whole approach is closely linked to servomechanisms.

The generalized notation developed in this book is systematic, versatile, and extensive and is characterized by "self-defining symbols" and a multiplicity of subscripts. Here is shown the result of much effort to produce a comprehensive system for use with instruments of any degree of complexity. However, because of the multiplicity of subscripts, it is difficult to use the book as a reference without a thorough initial study of the text. A short summary of the notation principles and list of the most used symbols could be added to simplify its use.

Since generalized terms are used, parts of the book are hard to follow. For example, a 12-word term like "input function product-reference input function product reference frequency function ration function" is not usually comprehended at a glance.

A number of minor errors in the text are noticeable. Some of the "proofs" could be replaced by plausibility arguments with a resulting improvement in the text. For instance, while the authors state that their mathematical discussions are not intended to be rigorous, the manipulations of figure 12-11, on impulse functions, are unjustified so that in the opinion of this reviewer they are seriously misleading to the student. More discussion of the limitations of the methods described would help to compensate for the lack of rigor.

The decibel is suggested for logarithmic co-ordinates; however, no mention is made of the restrictions that apply to its use. It appears that it would be preferable to avoid the decibel and to use the logit instead in this book. The example in the chapter on statistical methods concerning vacuum-tube characteristics appears unrealistic. Some discussion of the problem of maintaining control to ensure "similarity" would be helpful. A warning against extensive rejections of large deviations might also be desirable.

It will be interesting to see how the comprehensive approach of this volume is used in the applications of the set's third volume, which should constitute the real proof of the usefulness of the background developed in this first volume.

ARNOLD P. G. PETERSON
General Radio Co.
Cambridge, Mass.

Harmonics Sidebands and Transients in Communications Engineering as Studied by the Fourier and Laplace Analyses by C. Louis Cuccia (4507)

Published (1952) by the McGraw-Hill Book Company, Inc., 330 West 42 St., New York 36, N. Y. 446 pages+14-page index+6-page appendix+ix pages. 263 figures. 9×6. $9.00.

C. Louis Cuccia is a research engineer at RCA Laboratories Division, Princeton, N. J.

This book was written to "treat the highly important field of mathematics of harmonic and transient analysis applied to the communications field, while at the same time providing a treatment of communication engineering in its own right." Also, according to the preface, it "has been written to provide not a collection of solutions but rather an organized and integrated textbook . . . ." The author achieves his aims to a large degree, although he sometimes falls short of his objectives.

The first four chapters are a brave, but inadequate, attempt to cover the essential mathematical techniques required throughout the text. These chapters are titled, Elementary Functions of a Complex Variable; The Fourier Series; The Fourier Transform; The Laplace Transform. The remaining eighteen chapters cover a very diversified group of topics, which includes, among others, linear network analysis; distortion and harmonics in amplifiers; rectifier circuits; filter networks; amplifier response; integrating, differentiating, and scanning systems for television; reactance tubes; modulating systems; amplitude modulated waves; single tone fm; indirect frequency modulation and wave interference; multi-tone frequency modulated waves and pulse width modulation; spectral analysis of finite wave trains; wave transmission through linear networks; traveling waves in communication systems; reception in electrical communications.

The book possesses some very fine features and a wealth of material which is not readily available in book form. It serves well to provide many examples of practical problems which are directly and completely solved by mathematical techniques which more and more are becoming the normal working tools of the analytic engineer. It provides a high degree of perspective of many of the important considerations in communication engineering. A comparison of this book with works of several decades ago clearly shows some of the progress made in the field of communication engineering.

There are a number of details in the book with which one might take some issue. A few are noted here. (a) A complete equivalence seems to be drawn between the cisoidal or exponential time function, the trigonometric function, and complex number theory, with a very inadequate explanation of the basis for and limitations of such representations. (b) It is perhaps unfortunate that the author did not see fit to adopt the IRE and AIEE recommended "phasor" instead of "rotating vector." (c) On page 5, there appears a rather strange statement that, "if the rotating vector represents a current, then the real part represents that current which can be read with meters. . . . The imaginary part is not physically realizable and may be considered to be that part of the current which completes its mathematical representation." (d) The author is consistently negligent in specifying the reference positive for potential, and often neglects to specify the reference direction of current, when network diagrams are drawn. (e) One often sees such statements as, "the emf source is a rotating vector-voltage generator." (f) In many places lower case letters e and i are used to denote instantaneous time expressions for potential and current. In other cases, but without explanation, they are used to denote the complex number (or phasor) representations for a single frequency, such as, equation (41), page 100. (g) To refer to the current source equivalent representations of a vacuum tube as an application of Norton's theorem (page 135) is extending the Norton theorem to applications that are not justified from general network considerations. (h) The "per cent ripple" appears on page 165, in connection with rectifier circuits, but the more important "ripple factor" is not introduced. (i) Some mention should have been made of the fact that the integral in equation (56), page 365, has the value $\pi/2$, so that $f(t)$ as given agrees with equation (51), but that its form was retained for considerations in the next section.

There is some doubt about the adaptability of this book for regular classroom purposes, since much of this subject matter appears scattered in courses of the usual undergraduate and graduate curriculum, such as: electronics, radio engineering, network analysis, transient analysis, communications systems. It is a book which should find considerable appeal to the practicing engineer and to others who desire a broad view of communications engineering problems, with the new techniques of solution.

SAMUEL SEELY
Syracuse University
Syracuse, N. Y.

Electrical Measurements Manual by C. H. Dunn and H. J. Barker (4508)

Published (1952) by Prentice-Hall, Inc., Publishers, 70 Fifth Ave., New York 11, N. Y. 112 pages +viii pages. 61 figures. 5⅜×8⅜. $4.35.

C. H. Dunn and H. J. Barker are assistant professors of electrical engineering, Rensselaer Polytechnic Institute, Troy, N. Y.

This manual, designed for an elementary laboratory course in electrical measurements, is prepared with a special reference to college students, although it may be adaptable to courses in other institutions giving laboratory work in electricity.

An introductory chapter on laboratory techniques thoroughly treats laboratory methods in general, the recording of data, the presentation of results, and the writing of reports.

The book contains 35 experiments covering conventional methods for measuring voltage, current and power, resistance, inductance, and capacitance. Both deflection and zero methods are included. A few electronics experiments appear in the list, but experiments on dc and ac power machinery are not presented. The selection of material is comprehensive and sufficiently flexible to allow combinations of experiments in demonstrating circuit theorems.

Each of the experiments includes diagrams of connections, a list of necessary apparatus, measurements to be recorded, and calculations to be included in the report. Searching questions for the students to answer are appended to each experiment.

In some cases a brief introductory discussion precedes the order of procedure, but it is assumed that the essential theory of each experiment is to be gained elsewhere in the course, presumably from lecture notes or another textbook. For the most part, choice of actual apparatus and working value details for working conditions are not specified but are left to the discretion of the instructor to whom the student is referred.

The authors are to be congratulated on their choice of a well-balanced and useful list of fundamental experiments.

FREDERICK W. GROVER
Union College
Schenectady, N. Y.

Books

Applications of the Electronic Valve in Radio Receivers and Amplifiers, Volume II by B. G. Dammers, J. Haantjes, J. Otte, and H. Van Suchtelen (4509)

Published (1951) by the Philips Technical Library (N. V. Philips Gloeilampenfabrieken) Eindhoven, Holland. 425 pages+3-page index+xviii pages. 343 figures. 6×9.

The authors are members of the scientific staff of the Philips Company, Eindhoven, Holland.

This is Book V of a series of seven new books on electronic valves being published by the Philips Company. Book V is the second of three related volumes which together cover the field of applications of the electronic valve in radio receivers and amplifiers. Volume I considers the reception of a radio signal through detection. Volume II considers AF amplification, the output stage, and the power supply. Volume III covers feedback, stability, interference, and related problems.

The present book will be very useful to those who design and develop audio equipment. The coverage of the subject is thorough and detailed, including much practical information such as the influence of the power supply regulation on the performance of the amplifier, deviations from normal operating conditions, and the design of transformers. Many of the subjects treated often are not found in similar books. Proponents of high fidelity may feel that some consideration should have been given to the many unusual audio circuits such as cathode follower power output, single ended push-pull output, and so on; however, their omission is understandable since they are not found in commercial radio receivers.

All books of this series are being translated from Dutch into English, French, and German. It is a commendable undertaking.

L. J. Giacoletto
RCA Laboratories Division
Princeton, N. J.

UHF Practices and Principles by Allan Lytel (4510)

Published (1952) by John F. Rider Publishers, Inc., 480 Canal St., New York 13, N. Y. 366 pages+6-page appendix+7-page bibliography+10-page index+ix pages. 285 figures. 5½×8½. $6.60.

Allan Lytel is a lecturer in electronics, Temple University Technical Institute, Philadelphia, Pa.

Those IRE members who were originally power engineers, and who through today's evolutionary tendencies in the field of communications have perforce become familiar with the principles of ultra-high-frequency practices, may find this book useful as a basic introduction. The author states that it is designed for the student or technician, and this statement, based on the contents of the book, is reasonably adequate.

Eleven chapters direct the reader from a simple introduction of uhf, through the regular units of communication equipment and developmental tubes, to a final chapter on test equipment and techniques. A brief listing of test equipment is contained in this last chapter, and the information here contained might be useful to broadcast engineers who are mainly familiar with AM operations and who wish to expand their thinking to uhf for new television operations.

Considering the limitations of space, the book, in general, seems to be a résumé and repetition of material of the many articles which have appeared in the past ten years on uhf communications. For this reason it does present in an easily understood and readable form many uhf fundamentals and removes the need of searching for this type of information in various periodicals. A comprehensive bibliography is included and should be valuable. Also, there is an almost complete absence of mathematics which tends to enhance the book's appeal and readability for student technicians.

The author's preface is dated August, 1952, and we realize that there are long delays between completion of manuscripts and the appearance of finished books. However, it is unfortunate that the author's only main reference to uhf television and the FCC is built around the July 11, 1949 release and refers to proposals as tentative and lacking in definite information concerning the starting point (470 to 500 mc) of the uhf television band. Also, a number of very erratically cropped pages, in the reviewer's copy, was unexpected for a book of this caliber.

John H. Battison
National Radio Institute
Washington, D. C.

Advanced Antenna Theory by Sergei A. Schelkunoff (4511)

Published (1952) by John Wiley & Sons, Inc. 440 Fourth Ave., New York 16, N. Y. 190 pages+15-page appendix+10-page index+xii pages. 56 figures. 5¾×9. $6.50.

Sergei A. Schelkunoff is a member of the technical staff of Bell Telephone Laboratories, Inc., Murray Hill, N. J.

The preface to this book states that Dr. Schelkunoff presents a compact but general exposition of Hallen's methods of obtaining asymptotic solutions for linear antennas, Stratton and Chu's theory of spheroidal antennas of arbitrary size, and Dr. Schelkunoff's theory of biconical antennas and thin antennas of arbitrary size. However, the reviewer feels that Hallen's method of obtaining the solutions for cylindrical antennas should have been explained at greater length. The discussion of this method is in chapter 5, pages 140–150 inclusive. Dr. Schelkunoff explains this by stating in the preface that he has condensed some developments which can be found in fuller form elsewhere. Since the text is only 190 pages, it appears that the material could have been handled more fully.

Otherwise, the material of the book does stay within the author's aims in presenting mathematical methods for solving antenna problems. The text is divided into six sections: spherical waves, mode theory of antennas, spheroidal antennas, integral equations, cylindrical antennas, and natural oscillations. Although the mathematics is difficult to follow, it must be remembered that this is not an easy subject. Nevertheless, the reviewer would like to have seen the mathematics presented in more detail. For example, on page 101, the author states that equation (316), which is an equation taken from Tai, may be obtained from equations (56), (57), (62), and (63). After stating the manipulations in three sentences, the author gives an intermediate complex result and in another sentence states the final manipulations necessary for the desired equation.

The book contains a great deal of information and should be welcomed by advanced antenna students. Used in conjunction with the author's previous book on electromagnetic waves, it should prove very helpful. This would be a useful book in a class where Dr. Schelkunoff's theory of biconical antennas is presented and where the mathematics is discussed in detail.

Nathan Marchand
Marchand Electronic Laboratories
Greenwich, Conn.

Analysis of Alternating-Current Circuits by W. R. LePage (4512)

Published (1952) by McGraw-Hill Book Company, Inc., 330 West 42 St., New York 36, N. Y. 391 pages+42-page appendix+2-page reference+8-page index+xiii pages.

W. R. LePage is professor of electrical engineering, Syracuse University, Syracuse, N. Y.

This new introductory text is designed for a sophomore or junior college course. The general treatment and content seem to be at a lower level than would be expected, since there is more arithmetic than algebra.

In the contents of the book, simple resonant circuits are withheld until page 125; the general discussion of variation of impedance with frequency is postponed until chapter 14, and coupled-tuned circuits are not discussed. The Wye-Delta and Delta-Wye transformations are stated, although their derivation is not indicated except in a footnote appearing in Appendix B. In favor of the material, however, is a chapter devoted to 3-phase systems.

The insistence on the use of "sinor" and "phasor" for special vectors, and the use of "potential difference" for the emf induced by a changing magnetic field is not agreeable to this reviewer. In addition to these matters of style, there are various misleading statements. For example, the chapter entitled "Variable-Response Networks" implies in its introduction that variations of circuit elements are considered, as well as variations of frequency, and adds, "It is only necessary to carry through a solution with the variable paramenter in literal form." This chapter (14) discusses only the selectivity effects of tuned circuits and filters, and "the term response is used broadly to include impedance and admittance." Again, on page 32, of the text, it is concluded that a coil 10 cm long may be expected to obey the $L\ di/dt$ law to 30 mc.

The preface mentions the rigid adherence to definitions, yet an iron-cored inductor "can no longer be considered as a passive element," because it is a source of harmonics. The impedance of a series combination of black boxes is called the "equivalent impedance" of the combination, and this is claimed to be an extension of the concept of impedance.

For the most part, the book is disappointing in its content and treatment.

Chester H. Page
National Bureau of Standards
Washington, D. C.

Abstracts and References

Compiled by the Radio Research Organization of the Department of Scientific and Industrial Research, London, England, and Published by Arrangement with that Department and the *Wireless Engineer*, London, England

NOTE: The Institute of Radio Engineers does not have available copies of the publications mentioned in these pages, nor does it have reprints of the articles abstracted. Correspondence regarding these articles and requests for their procurement should be addressed to the individual publications, not to the I.R.E.

The number in heavy type at the upper left of each Abstract is its Universal Decimal Classification number and is not to be confused with the Decimal Classification used by the United States National Bureau of Standards. The number in heavy type at the top right is the serial number of the Abstract. DC numbers marked with a dagger †) must be regarded as provisional.

The Index to the Abstracts and References published in the PROC. I.R.E. from February, 1952, through January, 1953, is in course of preparation and will, it is hoped, be available in February, price 3s.9d. (including postage). As supplies are limited our Publishers ask us to stress the need for early application for copies. Included with the Index is a selected list of journals scanned for abstracting, with publishers addresses.

ACOUSTICS AND AUDIO FREQUENCIES

016:534 **1**
References to Contemporary Papers on Acoustics—R. T. Beyer. (*Jour. Acous. Soc. Amer.*, vol. 24, pp. 548–555; September, 1952.) Continuation of 3298 of 1952.

534:061.6 **2**
The Physikalisch-Technische Bundesanstalt, Brunswick—M. Grützmacher. (*Ricerca sci.*, vol. 22, pp. 1333–1347; July, 1952.) A description with special reference to the acoustics laboratories.

534:727.5(68.01) **3**
The Electro-acoustics Laboratory at the School for the Deaf, Worcester, C. P.—J. P. A. Lochner and A. Semmelink. (*Trans. S. Afr. IEE*, vol. 43, part 7, pp. 212–221; July, 1952.) General description of the laboratory and its functions, with a more detailed description of the construction of the anechoic chamber.

534.231.3:621.3.011.21].001.362 **4**
Incomplete Analogy between Electrical and Acoustical Characteristic Impedances, and Consequences relating to Echoes in Continuously Stratified Media—G. Eckart and P. Liénard. (*Acustica*, vol. 2, pp. 157–161; 1952. In French.) The acoustical characteristic impedance of a medium is defined by analogy with the corresponding electrical quantity. In the case of em waves, there is no internal reflection in a continuously stratified medium if the characteristic impedance remains constant. This, however, is not true for sound waves, which should in all circumstances be reflected by a stratified atmosphere.

534.232:538.652 **5**
Magnetostriction Transducer Measurements—H. J. Round. (*Radio Tech. Dig., Ed. franç.*, vol. 6, pp. 123–133; 1952.) Adaptation in French of paper noted in 1494 of 1952, with 14 additional references.

534.24 **6**
Acoustic Radiation Pressure of Plane Compressional Waves at Oblique Incidence—F. E. Bornis. (*Jour. Acous. Soc. Amer.*, vol. 24, pp. 468–469; September, 1952.) Simple analysis is given for a system comprising a sound beam of finite cross section propagated in a nonviscous medium and incident on a plane reflector. For the special case of a reflector in the form of a wedge of angle 90°, the pressure due to a beam incident symmetrically on the edge of the wedge is independent of the coefficient of reflection.

534.321.9 **7**
Ultrasonic Velocity, Dispersion, and Absorption in Dry, CO_2-Free Air—C. Ener, A. F. Gabrysh and J. C. Hubbard. (*Jour. Acous. Soc. Amer.*, vol. 24, pp. 474–477; September, 1952.) Measurements were made at 32° C and pressures p from 0.02 to 1 atm, using frequencies f of 2 and 3 mc. The variation of dispersion and absorption with f/p is discussed. Changes in velocity, absorption and internal specific heat are interpreted as the result of the slowing of energy exchange between translational and rotational states.

534.6:534.321.9 **8**
New Method for the Visualization and Measurement of Ultrasonic Fields—G. S. Bennett. (*Jour. Acous. Soc. Amer.*, vol. 24, pp. 470–474; September, 1952.) Details are given of a method depending on the ability of ultrasonic vibrations to accelerate chemical reactions, particularly the starch-iodine reaction. $BaTiO_3$ disks were used as ultrasonic sources, operating in a dilute solution of iodine, and glass plates coated with starch paste were used as detectors. Photographs are shown of near-field patterns obtained.

534.76 **9**
Masking of Tones by White Noise as a Function of the Interaural Phases of Both Components: Part 1—500 Cycles—L. A. Jeffress, H. C. Blodgett and B. H. Deatherage. (*Jour. Acous. Soc. Amer.*, vol. 24, pp. 523–527; September, 1952.)

534.78 **10**
On the Effect of Frequency and Amplitude Distortion on the Intelligibility of Speech in Noise—I. Pollack. (*Jour. Acous. Soc. Amer.*, vol. 24, pp. 538–540; September, 1952.) A comparison of the effects of noise and of frequency limiting on the intelligibility of speech (*a*) subjected to no amplitude distortion, and (*b*) subjected to infinite peak clipping.

534.78 **11**
Solid Sound—L. G. Kersta. (*Bell Lab. Rec.*, vol. 30, pp. 354–357; September, 1952.) A method is described for preparing three-dimensional models showing the variation with time of the energy spectrum representing speech sounds. Models of the spoken words "five" and "nine" are illustrated.

534.845.1 **12**
Room-Acoustics Investigations with Directive Transmitters and Receivers—E. Meyer and H. G. Diestel. (*Acustica*, vol. 2, pp. 161–166; 1952.. In German.) The material whose absorption was to be measured completely covered one wall of a four-sided room. Measurements on three different materials were made in the range 500–1,000 cps, using directive transmitters. Results for normal incidence are independent of the wall surface on which the material is fixed and agree with values obtained by means of Kundt's tube, and also qualitatively with results obtained at grazing incidence of the sound beam.

534.845.1 **13**
Long-Tube Method for Field Determination of Sound-Absorption Coefficients—E. Jones, S. Edelman and A. London. (*Jour. Res. Nat. Bur. Stand.*, vol. 49, pp. 17–20; July, 1952.) Portable equipment has been developed by means of which the method previously described by London (1846 of 1950) can be used for the nondestructive testing of acoustic materials already installed; measurements are made at 512 cps. The method enables the appearance of the materials to be correlated with their sound absorption coefficient; variations due to differences in plasterer workmanship are discussed.

534.846.4 **14**
Acoustic Correction in the Church of St. Anthony of Padua in Vienna $\overline{X}$.—(*Radio Tech.* (Vienna), vol. 28, pp. 317–318; July, 1952.) The church has a reverberation time of 7 seconds. The arrangement of 5 loudspeaker arrays to obviate echo is described.

534.87(204.1):621.396.822 **15**
Thermal-Noise Limit in the Detection of Underwater Acoustic Signals—Mellen. (See 106.)

621.395.616 **16**
Electrical Input Resistance of the Capacitor Microphone—H. Grosskopf. (*Arch. elekt. Übertragung*, vol. 6, p. 351; August, 1952.) Comment on 18 of 1952 (Kirschner).

621.395.623.7 **17**
The Assessment of the Transient Distortion of Loudspeakers from the Frequency Response—E. Seemann. (*Tech. Mitt. schweiz. Telegr.-TelephVerw.*, vol. 30, pp. 121–127; April 1, 1952. In German.) The transient distortion (crackles etc.) produced by different loud-

speakers can be compared by an objective method making use of the "mean-value" frequency response curve proposed by Hentsch (2898 of 1951). The basic subjective measurements and the apparatus devised for obtaining the mean-value response curve are described. Examples show good agreement between the objective and subjective assessments.

621.395.623.7 18
Metal-Cone Loudspeaker—F. H. Brittain. (*Wireless World*, vol. 58, pp. 440–443; November, 1952.) An account is given of development work on a high-quality metal-cone loudspeaker. A dip in the response curve at a frequency between 2 and 3 kc was traced to interference between vibrations from different parts of the cone and was eliminated by inserting a rigid "bung" in the cone cavity. A peak in the response curve at about 8 kc was eliminated by slotting the cone circumferentially and bending the parts adjacent to the slots.

621.395.623.73+681.85].001.42 19
Objective Testing of Pickups and Loudspeakers—K. R. McLachlan and R. Yorke. (*Jour. Brit. IRE*, vol. 12, pp. 485–496; September, 1952.) Analytical and experimental techniques used to assess the performance of pickups and moving-coil loudspeakers are described. Analysis by electrodynamic analogies enables a general mathematical solution to be obtained of the problem of determining performance characteristics. Apparatus used to determine steady-state and transient response is described and examples of typical tests are given, together with details of the methods used for indicating and recording the mechanical vibrations of (*a*) the various components of pickups and (*b*) loudspeaker cones. The analysis for pickups affords an explanation of all the phenomena observed experimentally. A similar general agreement has not yet been reached for loudspeakers, the work on which is still in its initial stages.

621.395.625.3 20
The Mechanical Properties of Various Magnetic Recording Tapes and their Influence on the Quality of the Recording—P. H. Werner. (*Tech. Mitt. schweiz. Telegr.-Teleph-Verw.*, vol. 30, pp. 173–180; May 1, 1952. In French and German.) Extraneous modulation may occur at frequencies up to 50 cps due to slow variations of tape speed and at frequencies between about 1 and 3 kc due to longitudinal oscillations of the tape. Extension/tension curves are plotted for 14 commercial tapes. A formula is given relating the elastic modulus and the frequency of the longitudinal oscillations, and these frequencies are tabulated for metre lengths of the 14 tapes. The production of noise by friction between tape and rollers is discussed, and an experimental arrangement is described for investigating this effect. An indication is given of steps to be taken in the design and construction of the recording machine to reduce this noise.

621.395.625.3 21
Magnetic Recording in Film Production—N. Leevers. (*Jour. Brit. IRE*, vol. 12, pp. 421–427; August, 1952.) Description of equipment using twin-channel magnetic tape, one channel carrying pulse signals at picture frequency, or a multiple thereof, for synchronizing with the corresponding picture film.

621.395.625.3(083.74) 22
Standardization of Magnetic-Recording Technique—H. Schiesser and O. Schmidbauer. (*Frequenz*, vol. 6, pp. 222–229; August, 1952.) Proposals made at the 1950 Berne conference and at the 1951 C.C.I.R. meeting at Geneva are discussed, and methods of measurement of magnetic characteristics of recording and reproducing heads, and magnetic tapes, etc., are considered.

621.395.97+621.397.24 23
Relaying the Sound and Television Signals at the South Bank Site—H. J. Barton-Chapple. (*Jour. Telev. Soc.*, vol. 6, pp. 381–384; April/June, 1952.) A general description of arrangements during the Festival of Britain; reliability was the main factor determining the choice of amplifying equipment and associated control gear. Vision signals were distributed on 61.75 mc and television sound at 58.25 mc except for the Telekinema, where the sound was distributed at AF.

621.396.645.371.029.3:621.395.667 24
Negative-Feedback Tone Control—Baxandall. (See 64.)

ANTENNAS AND TRANSMISSION LINES

621.392+621.315.212].018.44 25
Mathematical Theory of Laminated Transmission Lines: Part 1—S. P. Morgan, Jr. (*Bell Sys. Tech. Jour.*, vol. 31, pp. 883–949; September, 1952.) The theory presented by Clogston (2908 of 1951) is extended and analysis is given for both parallel-plane and coaxial cables using laminated conductors, the present paper dealing mainly with the class of structure in which the conductors are separated by a space filled with a continuous dielectric. Lines of this type are termed Clogston-1 as opposed to the Clogston-2 type in which the whole space is filled with laminated material. The problems studied include: determination of the propagation constants and the fields of the various transmission modes; the choice of optimum dimensions for the lines; calculation of the frequency dependence of attenuation due to the finite thickness of the laminae; losses caused by dielectric mismatch in Clogston-1 lines and by nonuniformity of the laminae in Clogston-2 lines; and the effects of dielectric and magnetic dissipation. See also 2988 of 1952 (Black *et al.*).

621.392.21 26
Analysis of Multiconductor Systems with Transverse Electromagnetic Waves at High Frequencies—H. J. von Baeyer and R. Knechtli. (*Z. angew. Math. Phys.*, vol. 3, pp. 271–286; July 15, 1952.) The transmission-line equations for current and voltage on each conductor are derived in a generalized form involving matrix symbols. Boundary conditions are considered and the generalized equations are applied in theory of the transmission-line directional coupler and in simplified theory of the folded dipole antenna.

621.392.26 27
The Relative Power-Carrying Capacity of High-Frequency Waveguides—H. M. Barlow. (*Proc. IEE*, part III, vol. 99, p. 323; September, 1952.) Discussion on 1196 of 1952.

621.392.26:[621.315.61+621.315.5 28
Dielectric and Metal Waveguides—H. Kaden. (*Arch. elekt. Übertragung*, vol. 6, pp. 319–332; August, 1952.) An idealized planar type of waveguide is considered, for which a system of transcendental equations is derived; these apply to dielectric waveguides if the dielectric constant of the material is assumed preponderantly real with a small imaginary component which accounts for the losses. For metal waveguides the dielectric constant is assumed to be purely imaginary and of magnitude very large compared with that of free space. The results of the analysis indicate that for the transmission of centimetre waves the dielectric hollow waveguide is better than either the metal waveguide or the Goubau surface-wave line. Quantitative results are presented in two tables, the first giving comparative figures for the properties of dielectric hollow and solid waveguides, metal waveguides, and surface-wave transmission lines, of the same outside dimensions, for free-space wavelengths from 100 to 1 cm, the second comparing the properties of dielectric hollow and solid waveguides, and surface-wave transmission lines, with the same amount of insulating material, for the same range of wavelengths. Theory of the transmission of TM and TE waves in the general type of waveguide is given, the formulas for the type here considered being derived as special cases.

621.392.26:621.392.43 29
Broad-Band Matching with a Directional Coupler—W. C. Jakes, Jr. (PROC. I.R.E., vol. 40, pp. 1216–1218; October, 1952.) Theoretical and experimental investigation of a method of using a directional coupler to cancel standing waves. The method gives a wide-band match which is independent of the relative locations of the directional coupler and the discontinuity causing the original mismatch. Good agreement was obtained between experimental results and theoretical curves.

621.392.43 30
Bandwidth of Quarter-Wave Sections—E. G. Fubini and F. H. Rockett, Jr. (*Electronics*, vol. 25, pp. 138–139; October, 1952.) Charts are given from which can be read the bandwidth over which a prescribed degree of matching is obtainable, using either single- or double-$\lambda/4$ matching sections; the matched bandwidth is considerably greater in the latter case.

621.396.67 31
On the Theory of Antenna Beam Shaping—A. S. Dunbar. (*Jour. Appl. Phys.*, vol. 23, pp. 847–853; August, 1952.) A theoretical investigation is made up of the diffraction pattern produced by radiation from a given aperture, (*a*) for controlled variation of the amplitude distribution over the aperture with given uniform phase, and (*b*) for controlled variation of phase over the aperture with given uniform amplitude. The method used by Chu (*M.I.T. Research Laboratory of Electronics, Technical Report 40;* 1947) for calculating cylindrical reflectors is adapted to derive a general formulation for an amplitude distribution on a curved surface. The theory is applied to the design of progressive-phase antennas. Experimental results obtained with channel-guide and slot-array antennas support the theory.

621.396.67 32
Mutual Radiation Resistance of Aerials and Arrays—H. L. Knudsen. (*Wireless Eng.*, vol. 29, pp. 301–305; November, 1952.) A simple expression for the mutual resistance of two antenna arrays with known characteristics is derived on the basis of the Poynting-vector method. The application of the expression is demonstrated by the examples of (*a*) two parallel linear antennas, and (*b*) two concentric ring arrays.

621.396.67:621.316.54 33
Aerial Exchange—(*Wireless World*, vol. 58, p. 444; November, 1952.) Description of equipment installed at one of the Admiralty's high-power transmitting stations for connecting any one of 10 transmitters to any one of 20 antenna systems. The switching system is partly motorized and comprises a semicylindrical structure of radius 14 feet and height about 16 feet, with traveling carriages, 11 moving horizontally and 20 others vertically.

621.396.67:621.392:621.397.61 34
Suspended Television Feeder—(*Wireless World*, vol. 58, pp. 473–474; November, 1952.) Description of antenna feeder arrangements at the B.B.C. stations at Kirk O'Shotts and Wenvoe. See also 244 below.

621.396.67:621.396.823 35
Loop Aerial Reception—G. Bramslev. (*Wireless World*, vol. 58, pp. 469–472; November, 1952.) An indication is given of the advantages of using a loop antenna for long-wave reception with an ordinary broadcast receiver, from the point of view of reducing interference from electrical apparatus. The loop is less responsive than the ordinary capacitive antenna to the locally produced electric fields mainly responsible for the interference. Design

details are given for the loop and the coupling circuit to the receiver.

621.396.67:621.396.826 36
Electromagnetic Back-Scattering from Cylindrical Wires—C. T. Tai. (*Jour. Appl. Phys.*, vol. 23, pp. 909–916; August, 1952.) The problem dealt with previously by Van Vleck *et al.* (3035 of 1947) is here investigated using the variational method of Schwinger (*Phys. Rev.*, vol. 72, p. 742; 1947.) Different trial functions are used to determine the numerical values of the back-scattering cross section for broadside incidence. The boundary conditions for the currents at the ends of the wires are examined. See 2716 of 1952 (Dike and King).

621.396.67:621.397.5+621.396.97.029.6 37
Combined Transmitting Aerials for Television and U.S.W. Broadcasting—W. Berndt. (*Telefunken Ztg*, vol. 25, pp. 158–168; August, 1952.) The horizontal and vertical radiation diagrams of various simple unit arrangements of dipoles or slot antennas are discussed, and several antenna systems consisting of vertical assemblies of such units, with which television and sound signals can be transmitted simultaneously, are described, with illustrations of N.W.D.R. antenna systems at Witzleben, Berlin, and at Bielstein, Teutoburger Wald.

621.396.67.013.34 38
Impulse Electromagnetic Fields—R. Kitai. (*Trans. S. Afr. IEE*, vol. 43, part 7, pp. 200–211; July, 1952.) Expressions are developed for the fields of the Hertzian dipole and the magnetic dipole in terms of dipole moments. The expressions hold when the derivatives of the dipole moments are continuous for all values of time. By assuming that the moment M obeys the law $M \propto \tanh(kt)$, an insight into the nature of impulsive fields is obtained by considering the condition $k \rightarrow \infty$, when the function becomes a step function. General expressions for impulse fields are derived and the properties of such fields are illustrated by a worked-out example. Static, induction and radiation fields are found to have different shapes.

621.396.676 39
The Magnetic Dipole Antenna Immersed in a Conducting Medium—J. R. Wait. (Proc. I.R.E., vol. 40, pp. 1244–1245; October, 1952.) Explicit expressions for the fields are derived for a magnetic dipole at the center of a spherical insulating cavity in a conducting medium such as sea water. An expression for the total power radiated is given for the case when all displacement currents in the conducting medium are negligible.

621.396.677 40
Simultaneous Radiation of Odd and Even Patterns by a Linear Array—C. B. Watts, Jr. (Proc. I.R.E., vol. 40, pp. 1236–1239; October, 1952.) A method is described for obtaining odd and even patterns from a broadside array, both patterns being free of minor lobes. An experimental array consisted of 18 uniformly spaced vertical slots in the narrower face of a horizontal rectangular waveguide about 105 feet long and of cross section 41×78 inches. The slots were end-loaded to bring them near $\lambda/2$ resonance for the operating frequency of 109.1 mc. A hybrid junction was used to feed the signals for the odd and even patterns. Performance is limited to a comparatively narrow band of frequencies. Application is in connection with runway localizers for instrument landing.

621.396.677.012.12† 41
Analysis of Microwave-antenna Side-Lobes—N. I. Korman, E. B. Herman and J. R. Ford. (*RCA Rev.*, vol. 13, pp. 323–334; September, 1952.) A simple method, based on Wheeler's theory of "paired echoes" (3642 of 1939), is described which allows manufacturing tolerances to be expressed in terms of the side-lobe level for the majority of large microwave reflectors. The method is also useful for prediction of the radiation pattern of a reflector whose mechanical deviations from the perfect shape are known.

621.396.679 42
Design of Optimum Buried-Conductor R.F. Ground System—F. R. Abbott. (Proc. I.R.E., vol. 40, p. 1160; October, 1952.) Correction to paper noted in 2729 of 1952.

CIRCUITS AND CIRCUIT ELEMENTS

621.3.012.2 43
Universal Circle Diagram for Certain Radio Systems—J. Coulon. (*Compt. Rend. Acad. Sci.* (Paris), vol. 235, pp. 608–609; September 22, 1952.) When the Q of a system (e.g. a Lecher line) is nearly constant over the pass band, circle diagrams similar to those previously obtained for quartz crystals (3160 of 1952) can be established.

621.314.7 44
Transistors: Part 3—J. Malsch and H. Beneking. (*Arch. elekt. Übertragung*, vol. 6, pp. 333–346; August, 1952.) Discussion of (*a*) transistor equivalent circuits, (*b*) analogies between transistors and electronic tubes, (*c*) practical transistor circuits, (*d*) noise, (*e*) operational frequency limits. Part 2: 1643 of 1952 (Malsch).

621.314.7:621.396.615 45
Transistor Oscillators—E. A. Oser, R. O. Endres and R. P. Moore, Jr. (*RCA Rev.*, vol. 13, pp. 369–385; September, 1952.) Detailed discussion of various transistor circuits, including different types of sine-wave generator, relaxation oscillators, and a combination of the two giving self-quenching oscillations or stabilized frequency division.

621.316.726.029.64 46
Frequency Stabilization in the Microwave Range—B. Koch. (*Arch. tech. Messen*, nos. 198 and 200, pp. 155–158 and 203–204; July and September, 1952.) Descriptive review of different methods, including those using frequency-discriminator circuits and spectral-line systems.

621.316.86 47
Production Control of Printed Resistors—W. H. Hannahs and J. W. Eng. (*Electronics*, vol. 25, pp. 106–109; October, 1952.) Factors affecting the reproducibility of resistors produced by the silk-screen process are discussed; those requiring especially careful control are carbon concentration, squeegee speed, temperature of application, curing schedule and application of protective coating.

621.318.57 48
Electronic Switching Elements for Communications Engineering—K. Steinbuch. (*Fernmeldetech. Z.*, vol. 5, pp. 349–356; August, 1952.) A review of the characteristics of available glow-discharge tubes, thermistors, thyratrons, transistors, and multi-electrode counter tubes, with discussion of their possible applications in telephony circuits.

621.318.57:621.387.032.212 49
New Trigger Circuits for use with Cold Cathode Counting Tubes—J. L. W. Churchill. (*Jour. Brit. IRE*, vol. 12, pp. 497–504; September, 1952.) A description is given of several trigger circuits devised for use particularly with dekatron tubes [2066 of 1950 (Bacon and Pollard)]. The circuits can be used in the construction of a scaling unit which can subtract as well as add. The counting losses of such a unit when used on random pulses are considered.

621.318.572:621.387.4 50
High-Speed Counter uses Ternary Notation—R. Weissman. (*Electronics*, vol. 25, pp. 118–121; October, 1952.) The basis of the counter is a flip-flop circuit modified to have three stable states by insertion of a diode coupling circuit between the cathodes. A nine-stage circuit is described, operating reliably up to counts of 175,000 per second. The indicating system may use either one or two lights per stage.

621.319.4 51
R.F. Characteristics of Capacitors—T. E. Clarke. (*Wireless World*, vol. 58, pp. 457–458; November, 1952.) Comment on 2740 of 1952 (Davidson).

621.319.47 52
Development of Vacuum Capacitors—S. J. Borgars. (*Proc. IEE* (London), part III, vol. 99, pp. 307–315; September, 1952.) Vacuum capacitors are particularly suitable for hf hv operation in airborne radio equipment. An account is given of the development of two types, one having a capacitance of 50 pf within ±5 per cent at a peak working voltage of 6 kv, the corresponding figures for the other being 100 pf and 8.5 kv. Electrical and mechanical test methods are outlined.

621.392.4:517.54 53
Resonance Characteristics by Conformal Mapping—P. M. Honnell and R. E. Horn. (Proc. I.R.E., vol. 40, pp. 1211–1215; October, 1952.) The expression $f(\lambda) = a\lambda + b + c/\lambda$, where $\lambda = \sigma + j\omega$, is termed the "resonance function." It represents the impedance of the series-connected LRS circuit ($S = 1/C$) or the admittance of the parallel-connected $CG\tau$ circuit ($\tau = 1/L$). Conformal mapping of the λ-plane on to the $f(\lambda)$-plane gives a figure which illustrates the meaning of the resonance function for complex frequencies. Typical examples illustrate the application of the figure to the parallel $CG\tau$ circuit and to one of its intrinsic generalizations. The mapping of the reciprocal functions $1/f(\lambda)$ and $1/\{1+f(\lambda)\}$ is also considered.

621.392.5:621.396.645 54
Networks with Maximally Flat Delay—W. E. Thomson. (*Wireless Eng.*, vol. 29, p. 309; November, 1952.) Corrections to paper noted in 3375 of 1952.

621.392.5.018.7 55
Waveform Computations by the Time-Series Method—N. W. Lewis. (*Proc. IEE* (London), part III, vol. 99, pp. 294–306; September, 1952.) The time-series method greatly reduces the work of computation in the solution of waveform or transient-response problems of cascade-connected linear quadripoles. Practical procedures for dealing with time series are described and illustrated by numerical calculations relating to waveform tests on a 100-mile coaxial-cable television link with a nominal upper cut-off frequency of 3 mc.

621.392.52 56
The Numerical Calculation of Filter Circuits with Generalized Parameters, using Modern Theory with Special Attention to Cauer's Work—V. Fetzer. (*Arch. elekt. Übertragung*, vol. 6, pp. 350–351; August, 1952.) Corrections to paper abstracted in 1545 of 1952.

621.392.52 57
The Transmission Range of Two-Circuit Band-Pass Filters, particularly for Large Band-widths—H. Meinke. (*Fernmeldetech. Z.*, vol. 5, pp. 362–371; August, 1952.) Graphical methods of calculation are developed which give results with accuracy adequate for practical purposes. The methods are applicable to unsymmetrical and wide-band filters, and also to narrow-band symmetrical filters.

621.392.52 58
Filters—Synthesis of Narrow-Band Direct-Coupled [waveguide] Filters—H. J. Riblet. (Proc. I.R.E., vol. 40, pp. 1219–1223; October, 1952.) A general synthesis procedure is described that is based on an approximate first-order equivalence between direct-coupled and $\lambda/4$-

coupled filters. The transmission characteristics computed for a 6-cavity filter with an over-all Q of 37.6 are in excellent agreement with measurements.

621.392.52 59
A Frequency-Eliminating Transconductance Bridge—W. C. Michels and R. C. Barbera. (*Rev. Sci. Instr.*, vol. 23, pp. 293–295; June, 1952.) Description of a bridge circuit which completely eliminates a single frequency component and also partially suppresses a band of frequencies whose width can be varied within wide limits by suitable choice of circuit parameters. Applications to ripple elimination and to band-elimination amplifiers are discussed.

621.392.52:621.396.621:621.396.822 60
Optimum Filters for the Detection of Signals in Noise—Zadeh and Ragazzini. (See 205.)

621.392.52:621.396.621:621.396.822 61
The Detection of a Sine Wave in the Presence of Noise by the Use of a Nonlinear Filter—Slattery. (See 206.)

621.392.6 62
A General Network Theorem, with Applications—B. D. H. Tellegen. (*Philips Res. Rep.*, vol. 7, pp. 259–269; August, 1952.) It is proved that, in a network configuration with branch currents i satisfying the node equations and branch voltages v satisfying the mesh equations, Σiv, summed over all branches, is zero. Using this result it is possible to prove the energy theorem and the reciprocity relation of networks, and to show that if arbitrarily varying voltages are applied to a $2n$-pole network at rest, the difference between the electric and the magnetic energy at any instant depends only on the admittance matrix of the $2n$-pole network and not on the particular network used to realize this matrix.

621.394/.396].6:003.63 63
The Utility Factor in Circuit Diagrams—C. E. Williams. (PROC. IRE (Australia), vol. 13, pp. 345–349; September, 1952.) The importance is stressed of laying out circuit diagrams so that the working of the circuit can be easily and clearly grasped. The common type of drawing-office diagram may look neat, but usually requires to be radically rearranged to indicate circuit functions. It is suggested that circuit diagrams should be drawn on the same general plan as block diagrams, a standard lay-out being used for common sub-circuits, and only lines carrying signals being included.

621.395.667:621.396.645.371.029.3 64
Negative-Feedback Tone Control—P. J. Baxandall. (*Wireless World*, vol. 58, pp. 402–405 and 444; October and November, 1952.) The circuit described provides independent control of bass and treble response without switching. The RC arrangement on each side of a bass-control potentiometer p_1 is made symmetrical so that it may be combined in the feedback line with a treble-control circuit, the potentiometer of which has an earthed center-tap. At medium and high frequencies p_1 is effectively shorted. With both potentiometers at a middle setting, response is level.

621.396.611.1 65
Parallel-Tuned Circuit Periodically Switched to a Direct-Current Source—L. J. Giacoletto. (*RCA Rev.*, vol. 13, pp. 386–416; September, 1952.) Circuit phenomena with the switch (*a*) closed, (*b*) open, are analyzed in turn, linear solutions being obtained. The complete solution is then obtained by matching the boundary conditions for the two cases. This solution includes sinusoidal, sawtooth, and complex waveforms, dependent on circuit parameters and switching period. Elimination of dissipative circuit elements simplifies the general solution, with resulting clarification of the operation of the circuit. Tests with a mechanically switched circuit verified the theory, the entire gamut of waveforms being obtained by variation of circuit parameters and switching period.

621.396.611.3:621.392.26 66
On the Scattering Matrix of Symmetrical Waveguide Junctions—A. E. Pannenborg. (*Philips Res. Rep.*, vol. 7, pp. 131–157; 169–188 and 270–302; April, June and August, 1952.) Fundamental properties of the scattering matrix are derived. Tomonaga's theory for lossless resonant structures is extended to include the effect of losses. The structural symmetry of microwave circuits is discussed, junctions consisting of two parallel sections of rectangular waveguide with one side common being particularly considered. The theory of directional couplers with such symmetry is developed. An attenuator and standard matching transformer, each having a directional coupler as a basic unit, are described. Other forms of resonant coupling are discussed.

621.396.611.4 67
Natural Electromagnetic Oscillations in a Rectangular Cavity with Walls of Finite Conductivity—R. Müller and E. Ruch. (*Z. angew. Phys.*, vol. 4, pp. 254–258; July, 1952.) In the limiting case of infinite wall conductivity, the *TE* and *TM* self-oscillations have the same frequency. This does not hold for finite wall conductivity, in which case linear combinations of the *TE* and *TM* oscillations, with the same frequency, exist. These combinations, termed "matched" oscillations, represent to a first approximation the natural oscillations of the actual resonator. The determination of the characteristics of these matched oscillations is based on the solution of a simple geometrical problem, from which the damping and mistuning are calculated.

621.396.615 68
Oscillator Systems including Elements having Inertia—N. Minorsky. (*Compt. Rend. Acad. Sci.* (Paris), vol. 235, pp. 604–605; September, 1952.) Analysis is given for oscillator circuits, both with and without tubes, including elements whose resistance varies with temperature.

621.396.645 69
Amplification and Bandwidth of Video Amplifiers—F. J. Tischer. (*Arch. elekt. Übertragung*, vol. 6, pp. 309–315; August, 1952.) The characteristics of the ideal amplifier with constant amplification and constant phase transit time throughout the pass band are briefly reviewed, and the principal types of amplifier are analyzed, with particular reference to amplification and bandwidth. The theoretical maximum values of these parameters are determined for the various types and compared with the values obtained in practice and with one another. Arrangements using distributed amplification and having very wide pass bands are considered briefly.

621.396.645:621.315.61 70
A Mathematical Analysis of a Dielectric Amplifier—L. A. Pipes. (*Jour. Appl. Phys.*, vol. 23, pp. 818–824; August, 1952.) The fundamental principles of operation of dielectric amplifiers are outlined and a basic circuit with resistive load is analyzed in detail. It is assumed that the hysteresis curve of the dielectric is represented by a hyperbolic-sine function. Expressions are calculated for the steady-state input and output currents, and the time constant of the amplifier is estimated from consideration of the transient response.

621.396.645.35:621.317.3 71
High-Gain D.C. Amplifiers—Kandish and Brown. (See 172.)

621.396.645.35:621.318.435.3 72
The Design of a Practical D.C. Amplifier based on the Second-Harmonic Type of Magnetic Modulator—S. W. Noble and P. J. Baxandall. (*Proc. IEE* (London), part II, vol. 99, pp. 327–344; August, 1952. Discussion, pp. 344–348.) Description of the development of an amplifier based on the work of Williams and Noble (152 of 1951), including details of (*a*) a 1.5-kc oscillator with second-harmonic distortion <0.0005 per cent, (*b*) a low-pass filter to prevent power from the oscillator reaching the dc source, (*c*) a phase-sensitive rectifier, (*d*) switching and over-all dc negative-feedback arrangements.

621.396.645.37:621.387.424 73
A Circuit for the Limitation of Discharge in G-M Counters—W. C. Porter and W. E. Ramsey. (*Jour. Frank. Inst.*, vol. 254, pp. 153–163; August, 1952.) A two-tube feedback amplifier is used to limit the discharge to a small part of the total length of the wire, full sensitivity being restored in about 1 μs.

GENERAL PHYSICS

537.224 74
Electrets—J. Euler. (*Z. Ver. dtsch. Ing.*, vol. 94, pp. 481–483; June 1, 1952.) General discussion of the properties of electrets. Applications in electrometers and in apparatus for detecting the presence of radioactive radiation are noted.

537.291+538.691 75
The Motion of Changed Particles in the Magnetic Field of a Linear Current, and the Electric Field of a Cylindrical Capacitor—V. M. Kel'man and I. V. Rodnikova. (*Zh. Eksp. Teor. Fiz.*, vol. 21, pp. 1364–1369; December, 1951.) The particle trajectories for such a system are determined. Under certain conditions the system may be used for focusing beams of charged particles.

537.291+538.691]:537.122 76
An Integrable Case of Electron Motion in Electric and Magnetic Field—H. Poritsky and R. P. Jerrard. (*Jour. Appl. Phys.*, vol. 23, pp. 928–930; August, 1952.) The case is considered of a two-dimensional electric field, with the potential given by $V=A+B\ (x^2-y^2)/2$, applied together with a uniform magnetic field in the z direction. The path of an electron is an ellipse whose center moves in a hyperbola; the electron may drift into regions of higher or lower potential.

537.291+538.691]:537.122 77
Calculation of Plane Electron Trajectories in Particular Electric and Magnetic Fields by means of Complex Vector Loci—H. Kleinwächter. (*Arch. elekt. Übertragung*, vol. 6, pp. 315–318; August, 1952.) Further examples of the method previously described (4449 of 1939) include (*a*) trajectories in a time-variable homogeneous magnetic field, (*b*) circular paths in a suitable em field, as for the betatron.

537.311.33 78
A Note on the Theory of Semiconductors—P. T. Landsberg. (*Proc. Phys. Soc.* (London), vol. 65, pp. 604–608; August 1, 1952.) Two different theories are obtained, depending on whether the free energy due to the spin of electrons in impurity centers is or is not taken into account. The second of these alternatives is essentially that adopted by Wilson (*Proc. Roy. Soc. A*, vol. 133, p. 458 and vol. 134, p. 277; 1931) and has been used almost universally, though the first, which is that adopted by Mott and Gurney (*Electronic Processes in Ionic Crystals*, 2nd ed., p. 157; 1948) can be applied to degenerate semiconductors and is preferable.

537.311.4:621.396.822 79
A Theory of Contact Noise—R. L. Petritz. (*Phys. Rev.*, vol. 87, pp. 535–536; August 1, 1952.) The outlines of a theory of contact noise are presented, based on the idea that it is due to temperature fluctuations in the neighborhood of the contact. Detailed theory is being prepared for publication.

537.311.62+538.52 80
The Apparent High-Frequency Resistance of a Conducting Layer of Finite Width parallel to an Infinite Plane Conductor. Opposing Field and Induced Currents—A. Colombani and M. Gourceaux. (*Compt. Rend. Acad. Sci.* (Paris), vol. 235, pp. 605–608; September 22, 1952.) Formulas are derived for the case where the conducting strip comprises a winding with a number of separate turns.

537.311.62+538.52 81
Currents Induced in a Plane Conductor of Great Width by a Plane Strip of Small Width carrying a High-Frequency Current. Approximate Formulae giving the Variations of Resistance and Self-Inductance of the Inductor—M. Gourceaux and A. Colombani. (*Compt. Rend. Acad. Sci.* (Paris), vol. 235, pp. 650–652; September 29, 1952.) Continuation of analysis noted in 80 above.

537.323:546.28 82
Thermoelectric Measurements on *p*-Type Silicon—J. Savornin and F. Savornin. (*Compt. Rend. Acad. Sci.* (Paris), vol. 235, pp. 465–467; August 18, 1952.) The thermoelectric power, positive with respect to Cu, is about 700 μv/1° C for material of purity 99.85 per cent, falling to about 550 μv/1° C for 99.4 per cent purity and rising again to 590 μv/1° C for 98 per cent purity.

537.523/.527].029.6 83
High-Frequency Electrical Breakdown of Gases—W. P. Allis and S. C. Brown. (*Phys. Rev.*, vol. 87, pp. 419–424; August 1, 1952.) Theory is presented which is applicable to any gas over a wide range of pressure. Experimental results for H are in agreement with the theory.

537.523.4:538.639 84
Sparking Potentials in a Transverse Magnetic Field—J. M. Somerville. (*Proc. Phys. Soc.* (London), vol. 65, pp. 620–629; August 1, 1952.) By taking account of the distribution of electron free paths, and of electron recapture by the cathode, a theory is developed which is in better agreement with observation than that of Valle (*Nuovo Cim.*, vol. 7, p. 174; 1950).

537.525.72:538.63:621.396.822 85
A Resonance Phenomenon in Electrodeless H.F. Gas Discharges with Superposed Magnetic Field—A. Lindberg, H. Neuert and H. Weidner. (*Naturwiss.*, vol. 39, pp. 374–375; August, 1952.) Experiments in atmospheres of H_2 and Ar are described which show that the resonance effect previously noted [614 of 1951 (Koch and Neuert)] is associated with a sharp drop between two peaks in the intensity of the emitted light; it occurs always at the same value of the field strength.

537.77 86
Dimensions and Units—M. Berger. (*Compt. Rend. Acad. Sci.* (Paris), vol. 235, pp. 872–874; October 20, 1952.) By considering the expression for power in terms of the dimensions M, L and T on the one hand and in terms of current and voltage on the other hand, it follows that quantity of electricity may be regarded as having the dimensions L^3. Using this result, all the other electrical magnitudes can be expressed in terms of M, L and T with integral indices. The separate question of the best system of units is discussed briefly; the M.K.S. system fits well with the above dimensional system.

538.2 87
Some Post-War Developments in Magnetism—L. F. Bates. (*Proc. Phys. Soc.* (London), vol. 65, pp. 577–594; August 1, 1952.) Presidential address to the Physical Society, May 1952. The extension of knowledge of the ferromagnetic domain through the work of Néel and others and the systematic use of the Bitter powder-figure techniques is surveyed, and the main resonance phenomena and experiments on the diffraction of neutrons by antiferromagnetic crystals are described.

538.566:535.42 88
Diffraction of Electromagnetic Waves by a Half-Plane—B. N. Harden. (*Proc. IEE* (London), part III, vol. 99, pp. 229–235; September, 1952.) The observed intensity and phase values of the field near the edge of a thin high-conductivity sheet are compared with Sommerfeld's rigorous solution for an infinitely thin perfectly conducting half-plane, good agreement being obtained. Results for sheets of different thicknesses and conductivities show the importance of these factors in determining the field near the diffracting edge.

538.566:537.562 89
Experimental Demonstration in the Laboratory of the Existence of Magneto-hydrodynamic Waves in Ionized Helium—W. H. Bostick and M. A. Levine. (*Phys. Rev.*, vol. 87, p. 671; August 15, 1952.)

538.566.2 90
Reciprocity of the Transmissive Properties of Any Multiple Layer for Electromagnetic Waves—C. v. Fragstein. (*Optik* (Stuttgart), vol. 9, pp. 337–359; 1952.) A full analytical proof is given that the transmission of a perpendicularly incident plane em wave through a multiple layer consisting of any number of plane-parallel absorbing or nonabsorbing components is the same in both directions if the first and last media have the same absorption index, i.e. if $\chi_1=\chi_n$. If χ_1 and χ_n are different, the ratio of the transmission factors in the two directions is $(1+\chi_1^2)/(1+\chi_n^2)$. Treatment is simplified by applying quadripole theory, but this does not give a closed expression for the over-all transmission factor. The validity of the Kirchhoff inversion principle is illustrated.

538.569.4.029.65:546.21 91
Line-Breadths of the Microwave Spectrum of Oxygen—R. S. Anderson, W. V. Smith and W. Gordy. (*Phys. Rev.*, vol. 87, pp. 561–568; August 15, 1952.) The microwave absorption band for O_2 consists mainly of 25 lines around the wavelength 5 mm, with spacings of only a few hundred mc. The intensity of the band depends on the variation of line widths with pressure; this variation is expressed in terms of the "line-breadth parameter," defined as the half-width, measured at half intensity, of an absorption line at a pressure of 1 atm. Determinations of this parameter made with a Zeeman modulation spectrograph are reported and discussed, and an interpretation of the self-broadening collision process is developed. Measurements are also reported for broadening due to collisions with foreign molecules.

GEOPHYSICAL AND EXTRATERRESTRIAL PHENOMENA

523.72+523.85]:621.396.822 92
Radio-Astronomy—M. Ryle and J. A. Ratcliffe. (*Endeavour*, vol. 11, pp. 117–125; July, 1952.) A general review of the subject, with a description of methods of measurement and discussion of the theory of galactic and solar RF radiation.

523.72:621.396.822.029.65 93
Solar Outbursts at 8.5-mm Wavelength—J. P. Hagen and N. Hepburn. (*Nature* (London), vol. 170, pp. 244–245; August 9, 1952.) Report of results obtained at the Naval Research Laboratory, Washington, D. C., with an antenna having an aperture of 24 inch and beam width of 1.1°, and correlation with observations at 3-cm wavelength and with the occurrence of solar flares. Typical records are reproduced. The 8.5-mm bursts are in general of smaller amplitude and of much shorter duration than the bursts observed on greater wavelengths.

523.78:523.72 94
Radio Observations of the Solar Eclipses of September 1, 1951, and February 25, 1952—J. F. Denisse, E. J. Blum and J. L. Steinberg. (*Nature* (London), vol. 170, pp. 191–192; August, 1952.) Preliminary report of results which were confirmed during the February eclipse by observations at Marcoussis, near Paris, and at Dakar, French West Africa. See also 1282 of 1952 (Bosson *et al.*).

523.841.11:621.396.822 95
Radio-Frequency Radiation from Tycho Brahe's Supernova (A.D. 1572)—R. H. Brown and C. Hazard. (*Nature* (London), vol. 170, pp. 364–365; August 30, 1952.) Observations at a frequency of 158.5 mc revealed a radio source whose coordinates agree closely with those of the supernova of 1572. Data for the supernovae of A.D. 1054 and 1572 are compared.

523.85:621.396.822 96
Line Emission from Interstellar Material in the Radio-Frequency Range—R. Lüst. (*Naturwiss.*, vol. 39, pp. 372–374; August, 1952.) Historical review of published results, including particular reference to the hydrogen emission line at 1.42 kmc.

523.854:621.396.822:523.165 97
On the Possible Relation of Galactic Radio Noise to Cosmic Rays—G. W. Hutchinson. (*Phil. Mag.*, vol. 43, pp. 847–852; August, 1952.) The possibility is considered that cosmic rays are accelerated in regions of the galaxy with intermediate particle density ($\sim 10^3$/cm^3). A conservative estimate of the magnetic fields in such regions would lead to a radio-noise flux of the observed order of magnitude; the observed spectrum could easily be produced.

523.99:523.8:621.396.822:523.755 98
Occultation of a Radio Star by the Solar Corona—K. E. Machin and F. G. Smith. (*Nature* (London), vol. 170, pp. 319–320; August 23, 1952.) Interferometers of high resolving power were used to reduce the amplitude of the record from the undisturbed sun during observations of the radio star in Taurus as it passed near the sun's southern limb. A decrease of amplitude occurred on both 38 mc and 81.5 mc when the angular separation of star and sun was as great as ten times the angular radius of the visible disk, the amplitude decrease being greatest when the angular separation approached its minimum value. The results will be discussed in a later paper. See also 1281 of 1952.

537.226.2:]546.212+551.311.234.5 99
On the Dielectric Constant of the Water in Wet Clay—L. S. Palmer. (*Proc. Phys. Soc.* (London), vol. 65, pp. 674–678; September 1, 1952.) An explanation is put forward of the variation with moisture content of the permittivity of soil samples previously observed by Cownie and Palmer (2793 of 1952). It is suggested that relatively dry clay consists of closely packed water-coated particles in an air matrix, while relatively wet clay consists of particles uniformly distributed in a water matrix, the effective permittivity of the water increasing from the value for "bound" water (about 3) to that for "free" water (about 80) as the percentage of water is increased.

550.385:535.13 100
Maxwell's Equations for Three-Layered Media and their Application to the Theory of the Movement of a Magnetic Storm—M. Matschinski. (*Rev. Sci.* (Paris), vol. 90, pp. 91–103; March/April, 1952.) Solutions of the characteristic equations for ideal and for real three-layered media are given. Application is made to discussion of the characteristics of the marginal layers and calculation of the velocity of propagation of the elements of a magnetic storm. Other possible applications of the theory given are noted.

551.510.535 101
Ionospheric Disturbance of 23rd–28th February 1952—H. Siedentopf and A. Behr. (*Naturwiss.*, vol. 39, pp. 377–378; August, 1952.) A short account of observed variations of night-sky brightness, F_2-layer limiting frequency, radiocommunication with North America, and radiosonde measurements of air temperature. A solar origin for the disturbance cannot be assigned with certainty.

551.510.535 102
A Self-Consistent Calculation of the Dissociation of Oxygen in the Upper Atmosphere—H. E. Moses and Ta-You Wu. (*Phys. Rev.*, vol. 87, pp. 628–632; August 15, 1952.) A model is considered similar to that previously proposed (129 of 1952) but with the requirement of radiative energy balance abandoned and with a particular temperature distribution assumed. Calculations indicate a much narrower dissociation region, occurring at a lower altitude.

551.510.535:621.396.11 103
The B.B.C. Ionospheric-Storm-Warning System—T. W. Bennington and L. J. Prechner. (*BBC. Quart.*, vol. 7, pp. 107–119; Summer, 1952.) The various data on which the B.B.C. warning system is based are noted and a statistical review is presented of the correlation between actual and forecast ionospheric conditions in the period 1947–1950. The accuracy of the forecasts during this period was of the order of 60–70 per cent.

551.594.11:523.78 104
Observations of the Electric Field of the Atmosphere at Khartoum during the Total Solar Eclipse of 25th February 1952—A. Dauvillier. (*Compt. Rend. Acad. Sci.* (Paris), vol. 235, pp. 852–854; October 20, 1952.) No effect due to the eclipse was observed in measurements of the electric field near the ground. This result supports that obtained by Chauveau in 1912 but disagrees with more recent observations, e.g. those made by Sucksdorff in Finland (2561 of 1946).

551.594.6:621.396.65 105
Correlation between the Mean Level of Atmospherics and the Degree of Intelligibility in a Kilometre-Wave Radio Link—F. Carbenay. (*Compt. Rend. Acad. Sci.* (Paris), vol. 235, pp. 423–425; August 11, September 29, 1952.) Measurements made on 26th–27th June 1952, at the Laboratoire National de Radioélectricité, using a wavelength of 11 km, are reported. The signaling speed was 40 words/minute and the signal strength at the receiver 340 μv/m. A vertical antenna was used, and atmospherics were received simultaneously with the signal. The numbers of wrong or indecipherable figures and letters received are indicated on a graph of mean field strength of atmospherics plotted against hour of day. Good correlation is observed.

LOCATION AND AIDS TO NAVIGATION

534.87(204.1):621.396.822 106
Thermal-Noise Limit in the Detection of Underwater Acoustic Signals—R. H. Mellen. (*Jour. Acous. Soc. Amer.*, vol. 24, pp. 478–480; September, 1952.) Experimentally found spectra of sea noise, for different sea states, are compared with the thermal-noise spectrum for an ideal medium as derived from classical statistical mechanics; the difference between the two is a function of frequency and sea state. The intensity of the smallest plane-wave signal detectable against the noise background by a linear reversible hydrophone is determined in terms of the directivity ratio, the bandwidth and the operating noise factor.

621.396.9 107
Radio Echoes and Lightning—V. G. Miles. (*Nature* (London), vol. 170, pp. 365–366; August 30, 1952.) Report of effects observed on the ppi screen of radar equipment, with a vertically directed beam, during passage of a thunderstorm overhead, when echoes were obtained coincident with lightning flashes.

621.396.9:523.531 108
Radio-Echo Observations of the Major Night-Time Meteor Streams—G. S. Hawkins and M. Almond. (*Mon. Not. R. Astr. Soc.*, vol. 112, no. 2, pp. 219–233; 1952.) An account of determinations made during 1946–1951 of the radiant coordinates and meteor velocities of the Perseids, Geminids and Quadrantids. Data are included for five other streams.

621.396.9:629.13 109
Search Radar for Civil Aircraft—P. L. Stride. (*Jour. Brit. IRE*, vol. 12, pp. 445–460; August, 1952.) Consideration of the basic design problems of equipment intended primarily for (*a*) detection of storm clouds, (*b*) avoidance of high ground, (*c*) navigation by "map painting," indicates that a pulse power of 10 kw at 3-cm wavelength, with a beam width of 6°, is adequate. Roll and pitch stabilization of the scanning axis is essential. A general description is given of suitable equipment, with details of the scanner and its stabilized mounting, the servo amplifier, the transmitter-receiver, the indicator, and the control unit. Results of performance tests are illustrated by typical displays.

MATERIALS AND SUBSIDIARY TECHNIQUES

533.5:678.14-415 110
Use of Membranes in Vacuum Technique—Prugne and P. Garin. (*Le Vide*, vol. 7, pp. 1197–1199; May, 1952.) The fitting of thin rubber membranes, either flat or corrugated, in pressure taps and tubes is described.

535.37:621.397.621.2 111
A Single-Component White Luminescent Screen for Television Tubes—F. A. Kröger, A. Bril and J. A. M. Dikhoff. (*Philips Res. Rep.*, vol. 7, pp. 241–250; August, 1952.) The development of a new phosphor, (Zn, Cd)S-Ag-Au-Al, is described. This exhibits white luminescence when excited by ultraviolet, X or cathode rays. Efficiency and current saturation are about the same as for the commonly used sulphide mixtures.

537.226:546.431.82 112
The Effect of the Polarizing Field on the Value of the Dielectric Constant and Dielectric Losses of $BaTiO_3$—E. V. Sinyakov, E. A. Stafiychuk and L. S. Sinegubova. (*Zh. eksp. teor. Fiz.*, vol. 21, pp. 1396–1402; December, 1951.) A report on an experimental investigation, the main conclusions of which are as follows: (a) a constant electric field decreases the dielectric constant and loss angle particularly within the ferroelectric range of temperatures near the Curie point, and (b) the distorting action of the field displaces the Curie point towards higher temperatures.

537.226:621.396.677 113
Isotropic Artificial Dielectric—C. Süsskind. (PROC. I.R.E., vol. 40, p. 1251; October, 1952.) Comment on 2523 of 1952 (Corkum).

537.311.33 114
The Physical Mechanism of [conduction] Phenomena in Complexes of Electronic Semiconductors—J. Martinet. (*Compt. Rend. Acad. Sci.* (Paris), vol. 235, pp. 874–876; October 20, 1952.) Observed I/V characteristics are presented for various semiconductors formed by compacting and sintering iron-oxide powders; these characteristics are linear when plotted on a double-logarithmic scale. The investigation covers only low values of applied voltage. The results justify the hypothesis that the current travels in the same way through an agglomerate as through a potential barrier.

537.311.33 115
On the Variations of Lattice Parameters of some Semiconducting Oxides—L. D. Brownlee and E. W. J. Mitchell. (*Proc. Phys. Soc.* (London), vol. 65, pp. 710–716; September, 1952.) The investigations made by Verwey *et al.* (905 of 1951) on Ni(Li)O systems have been extended to $Fe_2(Ti)O_3$ systems and to reduced Mg_2TiO_4.

537.311.33:546.289 116
Impurity Effects in the Thermal Conversion of Germanium—W. P. Slichter and E. D. Kolb. (*Phys. Rev.*, vol. 87, pp. 527–528; August 1, 1952.) Experiments on the growth of single crystals of Ge of very high purity have revealed no thermal acceptors as a consequence of the process of growth. Heat treatment of crystals after immersion in very dilute $CuSO_4$ solution resulted in extensive conversion. The results in general support the conclusion that conversion is associated with the rapid diffusion of Cu into the Ge.

537.311.33:546.289 117
Contact Properties of *p*-Type Germanium—J. W. Granville, H. K. Henisch and P. M. Tipple. (*Proc. Phys. Soc.* (London), vol. 65, pp. 651–652; August 1, 1952.) Typical characteristics are shown (*a*) for an unformed *W* point contact on etched and on polished samples of *p*-type Ge, (*b*) for contacts between two samples of *p*-type Ge. Curves for the *n*-type material from which the *p*-type material was prepared by heat shock are included for comparison.

537.311.33:546.289 118
Area Contacts on Germanium—J. W. Granville and H. K. Henisch. (*Proc. Phys. Soc.* (London), vol. 65, pp. 650–651; August 1. 1952.) The I/V relations of large-area contacts, prepared by evaporation in vacuo of Au on to *n*-type Ge, are qualitatively similar to those for point contacts. No significant differences are found with contacts of Au, Ag or Cu and no improvement of the rectifying properties could be achieved by processes of the type used for "forming" point contacts. Observation results are shown graphically, together with results for formed and unformed *W* point contacts.

537.311.33:546.289 119
Copper as an Acceptor Element in Germanium—C. S. Fuller and J. D. Struthers. (*Phys. Rev.*, vol. 87, pp. 526–527; August 1, 1952.) Report of results indicating that Cu is a surface impurity responsible for the "thermal conversion" of Ge [see also 2235 of 1952 (Fuller *et al.*)]. Experiments on Si at 1,100°C show that Cu diffuses into it at a rate comparable with that for Ge, and that an increase of hole conductivity occurs.

537.311.33:546.817.221 120
The Conductivity and Hall Coefficient of Sintered Lead Sulphide—E. H. Putley. (*Proc. Phys. Soc.* (London), vol. 65, pp. 736–737; September 1, 1952.) Values measured over a range of temperatures are shown in graphs and compared with values obtained previously on single crystals. The variation of the Hall coefficient is substantially the same for sintered specimens as for single crystals of comparable purity. The variation of conductivity is similar for the two types down to the temperature of minimum conductivity; below this temperature intergranular boundaries affect the conductivity of the sintered specimens.

537.311.33:621.314.7 121
On the Distribution of Transistor Action—T. H. Tønnesen. (*Proc. Phys. Soc.* (London), vol. 65, pp. 737–739; September 1, 1952.) Results are reported of experiments on a large number of semiconductors prepared in the form of filaments; about 40 of the materials are considered likely to show transistor action.

537.311.33:621.396.822 122
Electrical Noise in Semiconductors—H. C. Montgomery. (*Bell Sys. Tech. Jour.*, vol. 31, pp. 950–975; September, 1952.) A survey is made of the noise characteristics of Ge diodes

and triodes, in the light of existing theories. Experiments with single-crystal Ge filaments carrying current are described; the results indicate that the noise is produced by variations in the concentration of the minority carrier (i.e. holes in *n*-type material, electrons in *p*-type). Noise voltages in adjacent portions of a filament were quantitatively correlated with the life time and transit time of the minority carriers, and the effect of a magnetic field on the noise was found to agree with the calculated changes of the life time of the minority carriers.

538.221 123

Magnetic Viscosity under Discontinuously and Continuously Variable Field Conditions—R. Street, J. C. Woolley and R. B. Smith. (*Proc. Phys. Soc.* (London), vol. 65, pp. 679–696; September 1, 1952.)

538.221 124

Vibralloy—a New Ferromagnetic Alloy—M. E. Fine. (*Bell Lab. Rec.*, vol. 30, pp. 345–348; September, 1952.) An alloy of Fe with 43 per cent Ni and 9 per cent Mo, developed from elinvar, has elastic and magnetic properties combining to make it highly suitable for vibrating reeds.

538.221 125

The Magnetoresistance of Ferromagnetic Al-Si-Fe Alloys—R. Parker. (*Proc. Phys. Soc.* (London), vol. 65, pp. 616–620; August 1, 1952.) By extending the treatment previously given (3018 of 1951), an equation is derived for the saturation magnetoresistance of some mixed ferromagnetic alloys as a function of composition and temperature. Results calculated from this equation are in good agreement with measured values for various Al-Si-Fe alloys.

538.221:621.314.2.042.143 126

The Change of Shape of the Hysteresis Loop of Transformer Sheet exhibiting Magnetic Creep—R. Feldtkeller. (*Z. angew. Phys.*, vol. 4, pp. 281–284; August, 1952.) Observations are reported on sheets of carbon-containing Si-Fe alloy subjected to a weak sinusoidally varying magnetic field. Immediately after switching on the field the hysteresis loop exhibits a marked constriction at the center; the constriction disappears after some hours at room temperature and more quickly at higher temperatures. The presence of the constriction corresponds with the existence of short-lived overtones in opposite phase to the stable overtones corresponding to the points of the hysteresis loop. The constriction results from the peculiar statistical nature of the Barkhausen jumps in demagnetized material.

538.221:669.862.5.721 127

Ferromagnetism of Certain Gadolinium-Magnesium Alloys—F. Gaume-Mahn. (*Compt. Rend. Acad. Sci.* (Paris), vol. 235, pp. 352–354; August 4, 1952.)

538.221:681.142 128

Behavior of Rectangular-Hysteresis-Loop Magnetic Materials under Current-Pulse Conditions—E. A. Sands. (Proc. I.R.E., vol. 40, pp. 1246–1250; October, 1952.) An account of an investigation of the effect of variation of magnetic and physical parameters on the time needed to change a magnetic toroid from a condition of residual flux to that of saturation.

538.632:546.431-31 129

The Hall Effect in Single Crystals of Barium Oxide—E. M. Pell. (*Phys. Rev.*, vol. 87, pp. 457–462; August 1, 1952.) Measurement results obtained by an ac method for the temperature range 400–800°K are presented. Conduction was predominantly *n*-type.

538.652 130

Investigations of the Variation of the Partial Processes in Magnetostriction—E. Bailitis, C. Hagen and H. H. Rust. (*Z. angew. Phys.*, vol. 4, pp. 284–291; August, 1952.) Observations confirm that when a ferromagnetic material is magnetized, both reversible and irreversible changes of length occur, the over-all longitudinal magnetostriction representing a resultant effect. Three separate component variations are isolated, designated respectively as the main, remanence and inertia components; on superposition these give the over-all characteristic found by Nagaoka. Materials investigated include invar, indilatans extra, superinvar, Si-Cr-Fe, Ni, Ni-Mn and silver steel. The three magnetostriction components differ widely between these materials. Making some simplifying assumptions, a distribution function for the arrangement of the Weiss moments is derived which provides a satisfactory explanation of the experimental results. Discontinuous variation of length is observed, when the magnetizing force is decreased, for values less than the coercive force.

538.652:538.221 131

Magnetostriction of Cobalt Ferrites as a Function of Composition—R. Vautier. (*Compt. Rend. Acad. Sci.* (Paris), vol. 235, pp. 356–358; August 4, 1952.) Nonoriented Co ferrites have high negative magnetostriction, while oriented samples exhibit a slight positive effect in the direction of orientation and larger negative effects perpendicular to the orientation direction. Measurement results are shown graphically for CoO contents of 35–48 per cent.

538.221:538.652 132

Temperature Variation of the Magnetostriction of a Cobalt Ferrite—R. Vautier. (*Compt. Rend. Acad. Sci.* (Paris), vol. 235, pp. 417–419; August 11, 1952.)

539.231:546.48-31 133

Electrical Conductivity and Structure of Sputtered CdO Layers—G. Helwig. (*Z. Phys.*, vol. 132, pp. 621–642; August 19, 1952.) The specific conductivity depends not only on the sputtering time, but also on the electrical power used in the process and on the oxygen content of the N-O or Ar-O mixtures. Test methods and results are described.

539.24:537.311.31:546.92 134

Electrical Conduction of Thin Films of Platinum covered with a Dielectric Layer by Evaporation in a Vacuum—C. Feldman and B. Vodar. (*Compt. Rend. Acad. Sci.* (Paris), vol. 235, pp. 414–417; August 11, 1952.) The effect on the resistance of the Pt film of covering it with a layer of SiO_2 is to increase the variation with temperature and to decrease the variation with applied electric field. See also 3126 of 1952 (Feldman).

546.482.21 135

Single Synthetic Cadmium Sulfide Crystals—S. J. Czyzak, D. J. Craig, C. E. McCain and D. C. Reynolds. (*Jour. Appl. Phys.*, vol. 23, pp. 932–933; August, 1952.) A procedure is described which results in the growth of single crystals in the form of hexagonal prisms, starting with chemically pure CdS powder.

621.315.61:537.222.5 136

Characteristics and Measurement of Brush-Discharge Ionization in Dielectrics—D. Renaudin. (*Bull. Soc. franç. Élect.*, vol. 2, pp. 431–435; August, 1952.) Local ionization at comparatively low voltages due to impurities in the dielectric is discussed and qualitative methods of measurement are noted. A quantitative measurement of mean ionization density is made by a comparative method, using the recurrent rapid discharge of a capacitor with controlled ionization. Results of such measurements on hv transformers, some of which were oil-filled, are shown.

621.315.612:546.882/.883]-3 137

Niobate and Tantalate Dielectrics—E. Wainer and C. Wentworth. (*Jour. Amer. Ceram. Soc.*, vol. 35, pp. 207–214; August 1, 1952.) The ceramic and electrical properties of the niobates and tantalates of the elements of the first and second groups are described in detail, with numerous tables and diagrams. The materials include members of the perovskite crystal system which are ferroelectric and have Curie points in the range 350–475°C. The materials $NaNbO_3$ and $NaTaO_3$ are of particular interest. The results obtained indicate that $Cd_2Nb_2O_7$ is the ceramic and dielectric analogue of $SrTiO_3$, and that the binary compound $NaNbO_3$. $Cd_2Nb_2O_7$ is the analogue of $BaTiO_3$, except that its high dielectric constant and piezoelectric properties are maintained over a much wider range of temperature. Study of these compounds has indicated means for extending the temperature range of usefulness of perovskite-type ceramics for capacitor and electromechanical applications.

621.315.616.96 138

Some Physical Constants of Araldite—P. André. (*Le Vide*, vol. 7, pp. 1200–1202; May, 1952.) Dielectric characteristics are shown as functions of temperature and frequency.

621.317.011.5:[546.212+612.1 139

A Comparison of the Dielectric Behaviour of Pure Water and Human Blood at Microwave Frequencies—H. F. Cook. (*Brit. Jour. Appl. Phys.*, vol. 3, pp. 249–255; August, 1952.) Methods of measuring the complex dielectric constant at frequencies from 1.7 kmc to 24 kmc are described. The results for water at temperatures in the range 0–60°C are analyzed in relation to the Debye and the Cole-Cole dispersion equations, and the possibility that the dispersion is characterized by a narrow spectrum of relaxation times is discussed. Results for whole blood are given for the temperature range 15–35°C; the observed dispersion is attributed entirely to water relaxation. 41 references.

621.396.611.21 140

Some Characteristics of Quartz Crystals—J. Coulon. (*Rev. gén. Élect.*, vol. 61, pp. 373–380; August, 1952.) Operational characteristics related to two particular points on the resonance curve of a quartz crystal are discussed, and a method for determining the constants of quartz crystals, making use of a circle diagram, is described. See also 2549 and 2550 of 1952.

666.1.037:621.3.032.7 141

Techniques of Sealing by Optical Polishing—J. Bleuze and P. Dussaussoy. (*Le Vide*, vol. 7, pp. 1182–1190; May, 1952.) In the basic technique fusion occurs between polished glass surfaces at a steady temperature of about 500°C. A steady low pressure is maintained during the complete process. Either flat or curved surfaces are used. Enamel or colloidal Ag may be applied before sealing. The technique also applies to metals and ceramics. The application in tube manufacture is described, with details of the processes of surfacing the glass and mounting the electrodes. The characteristics of some types of tube have been much improved by adoption of this method of sealing.

666.1.037.5 142

A High-Conductivity Glass-to-Metal Seal—J. C. Turnbull. (*RCA Rev.*, vol. 13, pp. 291–299; September, 1952.) A method is described for plating kovar with high-conductivity metals (Cu and Cr) before sealing to glass. This procedure reduces the hf heating of the seals.

666.22:546.244-31 143

Tellurite Glasses—J. E. Stanworth. (*Jour. Soc. Glass Tech.*, vol. 36, pp. 217–241; August, 1952.) A detailed account of the work noted in 2834 of 1952.

MATHEMATICS

517.941.91 144

An Integral Variant associated with the Wave Equation—F. H. van den Dungen. (*Compt. Rend. Acad. Sci.* (Paris), vol. 235, pp. 532–533; September 8, 1952.)

517.948 145
Solution of Systems of Linear Equations by Minimized Iterations—C. Lanczos. (*Jour. Res. Nat. Bur. Stand.*, vol. 49, pp. 33–53; July, 1952.) The general principles previously developed (1418 of 1951) are applied to the solution of large systems of linear algebraic equations.

681.142 146
A Universal Unit for the Electrical Differential Analyzer—R. Tomovich. (*Jour. Frank. Inst.*, vol. 254, pp. 143–151; August, 1952.)

681.142 147
Automatic Programme Planning for Programme-Controlled Computers—H. Rutishauser. (*Z. angew. Math. Phys.*, vol. 3, pp. 312–313; July 15, 1952.) Methods for using the computer itself to determine the program for a given problem have been worked out; details are described in a booklet to be published soon.

681.142 148
Digital to Analog Converter—M. Miller, B. L. Waddell and J. Patmore. (*Electronics*, vol. 25, pp. 127–129; October, 1952.) Data in digital form, e.g. on punched cards, are converted into direct voltages; the basic elements of the equipment comprise timer, two temporary storage units, two dc converters and a control panel.

681.142:517.392 149
Development of a Product Integrator—P. Germain. (*HF* (Brussels), vol. 2, pp. 69–75; 1952.) The two functions whose product is to be integrated are represented by curves drawn on the two halves of a cylindrical drum. Photoelectric equipment gives the ordinate of each curve for any particular value of the variable x, and electrical pulse methods are used to obtain the product of the ordinates and to integrate the successive products for n equidistant values of x.

681.142:[621.392.26+621.396.611.4 150
The Solution of Waveguide and Cavity-Resonator Problems with the Resistance-Network Analogue—G. Liebmann. (*Proc. IEE* (London), part III, vol. 99, pp. 316–319; September, 1952.) Digest only. See 2839 of 1952.

681.142:621.396.6:511.124 151
A High-Accuracy Time-Division Multiplier—E. A. Goldberg. (*RCA Rev.*, vol. 13, pp. 265–274; September, 1952.) Equipment for use in analogue-type computers is described which produces a train of rectangular pulses whose amplitude is proportional to one variable, and whose duration is proportional to another variable. The average or dc component of the pulse train is then proportional to the product of the two variables. Accuracy to within 0.01 per cent of full scale is achieved by use of (*a*) a feedback system for establishing accurate timing, (*b*) steep-fronted switching pulses, (*c*) an electronic switch of predictable performance independent of tube characteristics, (*d*) precision resistors and reference voltages.

MEASUREMENTS AND TEST GEAR

531.765:621.396.615.17 152
Sawtooth-Current Generator with Long Sweep Time for Recording of Time Intervals—H. Lueg and E. Oberhausen. (*Arch. tech. Messen*, no. 198, pp. 145–146; July, 1952.) Description, with detailed circuit diagram, of equipment based on the Miller integrator [347 of 1949 (Briggs)], with a linear time scale up to 20 seconds and with a frequency constancy, under normal operating conditions, to within ±1 per cent. For a sweep of 100 seconds, time errors up to 3 per cent may occur. With the addition of a univibrator and recorder, time intervals are registered directly as ordinates.

621.3.018.41(083.74):621.317.361:529.77 153
The Estimation of Absolute Frequency in 1950–51—H. M. Smith. (*Proc. IEE* (London), part II, vol. 99, pp. 407–409; August, 1952. *Ibid.*, part III, vol. 99, pp. 320–321; September, 1952.) Summary only. Measurements at Greenwich of the mean annual fluctuation of the period of the earth's rotation show a diminution of 40 per cent in amplitude compared with the mean of published values for the period 1934–1949. A table is given which shows the mid-monthly deviations from the nominal frequency of the frequency standards at Abinger (2), Greenwich (1), Dollis Hill (G.P.O.) (4), and Teddington (N.P.L.) (1) for 1950 and 1951. A criterion of the quality of these standards is furnished by the mean absolute value of the tabulated deviations over a period. For five of the standards the criterion is about 1 part in 10^9 and for the other three about 2 parts in 10^9 per month per month.

621.317:061.3 154
Electrical Engineering Measurement Technique—(*Electronica*, vol. 5, pp. 121–127; August 2, 1952.) Report of papers and discussions at a conference held at Delft in May 1952.

621.317.029.6:621.396.621.54 155
Principles and Applications of Converters for High-Frequency Measurements—D. A. Alsberg. (Proc. I.R.E., vol. 40, pp. 1195–1203; October, 1952.) The use of heterodyne methods enables measurements to be made over wide ranges of frequency, with the reference standards operating at a fixed frequency. The accuracy of such measurements depends on the performance characteristics of the transducers or converters used. Design principles are outlined for maximum linearity and dynamic range of converters and for minimum zero corrections. These principles are applied in equipment for point-by-point and sweep measurements of delay, phase, impedance, and transmission characteristics.

621.317.328.029.63 156
600-Mc/s Field-Strength Meter—A. C. Gordon-Smith. (*Wireless Eng.*, vol. 29, pp. 306–308; November, 1952.) Receiving equipment is described suitable for the accurate comparison of field strengths over the frequency range 500–700 mc. For measuring modulated signals, the equipment comprises a crystal frequency changer, a 30-mc IF amplifier incorporating a piston attenuator, and a 1-kc selective amplifier followed by rectifier and dc meter. For measuring unmodulated signals the AF amplifier is omitted. Calibration was performed both by the field-radiation method and by the direct-injection method; good agreement was obtained between the two methods.

621.317.332:621.396.615.141.2 157
Conductance Measurements on Operating Magnetron Oscillators—M. Nowogrodzki. (Proc. I.R.E., vol. 40, pp. 1239–1243; October, 1952.) The conductance terms in formulas for the equivalent circuit of a magnetron oscillator can be obtained from measurements of the Q-factor of the magnetron in the oscillating and nonoscillating conditions. The "operating" Q-factors are determined from measurements of the variations of output power and oscillation frequency caused by a specified load mismatch. Experimental data are quoted.

621.317.34:621.315.212 158
Measurement of the Characteristics of a Cable for Radio-Frequency Transmission—H. Vigneron. (*HF* (Brussels), vol. 2, no. 3, pp. 77–80; 1952.) Theoretical formulas are derived which are less general, but which are both easier to obtain and to manipulate than those given by Hontoy (3169 of 1952). Hontoy's notation is used. A simpler method of measurement is also described, based on an acceptable approximation in which a spiral on a Smith's diagram is replaced by a circle. The method also furnishes a supplementary constant of the cable.

621.317.341.029.62 159
Measurement of Transmission-Line Attenuation—(*Tech. News Bull. Nat. Bur. Stand.*, vol. 36, pp. 133–135; September, 1952.) The method applies to balanced unscreened transmission lines. A sliding polystyrene fitting holds a small pickup loop at a constant distance from the resonant line, both ends of which are shorted. A rectifier and filter attached to the fitting are connected to a galvanometer measuring the standing waves along the line. Attenuation is approximately equal to $\coth^{-1}\alpha$, where α is the swr. Matching difficulties are avoided; accuracy to within 1 per cent is attainable.

621.317.35 160
Methods of obtaining Amplitude-Frequency Spectra—A. E. Hastings. (*Rev. Sci. Instr.*, vol. 23, pp. 344–346; July, 1952.) The frequency components of an arbitrary function of short duration are obtained from the discrete spectrum which results when the function is repeated at a fixed rate. The analysis is presented, and alternative practical arrangements are described involving optical or cr scanning or recording on magnetic tape.

621.317.35:519.272.119 161
Device for Computing Correlation Functions—A. E. Hastings and J. E. Meade. (*Rev. Sci. Instr.*, vol. 23, pp. 347–349; July, 1952.) An analogue device is described in which the original time function is recorded on magnetic tape and is reproduced by two pickups with the desired time separation. An electrodynamic wattmeter is used to multiply the outputs together.

621.317.351 162
Cathode-Ray-Tube Beam Intensifier—R. W. Rochelle. (*Electronics*, vol. 25, pp. 151–153; October, 1952.) To obtain the very high operating speed required for examining small portions of pulse edges, the intensifier circuit uses a hard tube for gating, together with two thyratrons for shutting off the beam. Timing is controlled by use of appropriate lengths of delay cable.

621.317.353.2/.3 163
Double-Tone and Intermodulation Methods of Distortion Measurement: Differences between the Results obtained, and their Causes—H. Müller. (*Telefunken Ztg.*, vol. 25, pp. 142–148; August, 1952.) Conversion of the results obtained by one method into those given by the other is only found possible if the equipment under test has the same frequency response characteristic both for the primary tones used in the double-tone method and for the distortion products. Discussion of transit distortion and load distortion is based on consideration of the characteristics of the circuit equivalent of a distorting network, consisting of a quadripole producing nonlinear distortion connected between two other quadripoles producing only linear distortion. Analysis and measurement results show that neither of the two methods furnishes correct values in all cases. The intermodulation method is recommended for use in the lower third of the AF range and the double-tone method for the upper part of the range.

621.317.4:621.397.621 164
Field Plotting in Deflection Yoke Design—Sieminski. (See 256.)

621.317.444 165
Magnetic-Field Measurements with the Iron-Cored Magnetometer by the Harmonic Method—R. Kühne. (*Arch. tech. Messen*, no. 199, pp. 175–178; August, 1952.) Discussion of basic principles of the method and review of practical equipment. 28 references.

621.317.7:061.4 166
Electrical Measurement Technology—W. Hunsinger. (*Z. Ver. dtsch. Ing.*, vol. 94, pp. 619–626; July 1, 1952.) Review of the measurement equipment shown at the 1952 Technical Fair, Hanover, with short descriptions of selected exhibits and 147 references to relevant

621.317.725+621.317.79.018.78 167
Voltage and Distortion Meters without Valves, as Examples of Rectifier-Type Instruments—K. Hagenhaus. (*Frequenz*, vol. 6, pp. 217–222; August, 1952.) Description of (*a*) a rectifier-capacitor-bridge type of voltmeter with ranges covering 1–500 v and with scale errors not exceeding 2 per cent from 30 cps to 300 mc, (*b*) a distortion meter with a range of 0.5–30 per cent, suitable for measurement of hum and harmonic distortion of equipment for transmission of speech or music, using fixed frequencies of 160, 180, 3,000 and 5,000 cps.

621.317.733:621.311.6 168
Precision Voltage Source—W. J. Cunningham. (*Wireless Eng.*, vol. 29, p. 309; November, 1952.) Comment on 3505 of 1952 (Attree).

621.317.733.029.54/.55 169
Impedance Bridges for the Megacycle Range—H. T. Wilhelm. (*Bell Sys. Tech. Jour.*, vol. 31, pp. 999–1012; September, 1952.) Three bridges designed for precision measurements on networks and components for wide-band coaxial-line transmission systems are described in detail: (*a*) general-purpose 20-mc unit operating both as admittance and series-impedance bridge and covering a reactance range from a few ohms to nearly one megohm; (*b*) 5-mc Maxwell inductance bridge for the range 0.001 μH–10 μH; (*c*) 10-mc admittance bridge especially for determining the temperature coefficients and frequency characteristics of small capacitors up to 200 pF, with an accuracy to within 0.01 pF. Standards having a range of several decades are provided.

621.317.734 170
Two Electronic Resistance or Conductance Meters—L. B. Turner. (*Proc. IEE* (London), part III, vol. 99, p. 322; September, 1952.) Digest only. See 2853 of 1952.

621.317.761+621.396.621.54 171
Direct-Reading Frequency-Measurement Equipment for the Range 30 c/s–30 Mc/s—L. R. M. Vos de Wael. (*Onde élect.*, vol. 32, pp. 351–356; August/September, 1952.) See 2855 of 1952.

621.396.645.35:621.317.3 172
High-Gain D.C. Amplifiers—K. Kandish and D. E. Brown. (*Proc. IEE* (London), part II, vol. 99, pp. 314–326; August, 1952. Discussion, pp. 344–348.) Critical review of various methods of measuring small currents and voltages, with discussion of the use of negative feedback, dc/ac conversion by means of a contact modulator, magnetic modulators, and correction of zero drift in direct-coupled amplifiers.

621.396.645.35:621.318.435.3 173
The Design of a Practical D.C. Amplifier based on the Second-Harmonic Type of Magnetic Modulator—Nobe and Baxandall. (See 72.)

OTHER APPLICATIONS OF RADIO AND ELECTRONICS

531.552:621.396.9 174
Radar Measurement of the Velocity of Projectiles—B. Koch. (*Onde élect.*, vol. 32, pp. 357–371; August/September, 1952.) Detailed account of a method of using the Doppler-Fizeau effect to derive a continuous indication of the velocity of a projectile. Wavelengths in the dm or cm range are used, the transmitting and receiving equipment being preferably located close to the projectile path. In the case of cannon, the equipment is installed either directly behind or in front of the gun. Typical records are reproduced and numerous measurements quoted which show the accuracy to be at least equal to that given by classical methods.

537.533.72:538.691 175
Two-Directional Focusing with Short Uniform Magnetic Fields—C. Reuterswärd. (*Ark. Fys.*, vol. 4, pp. 159–171; August 14, 1952.) Analysis with application to ion lenses.

621.314.3†:621.316.728 176
Power Control with Magnetic Amplifiers—E. L. Harder. (*Electronics*, vol. 25, pp. 115–117; October, 1952.) The use of magnetic amplifiers to control high-power industrial equipment and other devices is described.

621.317.3.029.5:677 177
High-Frequency Measurement Methods in the Textile Industry—H. Locher. (*Bull. schweiz. elektrotech. Ver.*, vol. 43, pp. 653–658; August 9, 1952.)

621.365.54†:061.4 178
Equipment for Inductive Heating—W. Stuhlmann. (*Z. Ver. dtsch. Ing.*, vol. 94, pp. 653–654; July 1, 1952.) Review of exhibits at the 1952 Technical Fair, Hanover.

621.365.54†:621.935 179
High-Frequency Tempering of the Points of the Teeth of a Band-Saw—F. P. Pietermaat and R. Antoine. (*HF* (Brussels), vol. 2, no. 3, pp. 53–54; 1952.) Illustrated description of the arrangements for inductive heating of the teeth, using a 1-mc generator, and subsequent quenching in an oil shower.

621.383:621.96 180
An Electronic Tracing Head for Oxygen Cutting—H. E. Newton. (*Metrop. Vick. Gaz.*, vol. 24, pp. 227–231; September, 1952.) Description of pantograph-type apparatus including travel motor, steering motor and optical system with photoelectric control causing the tracing head to follow the outline of a drawing in Indian ink on white paper.

621.384.611 181
The Oak Ridge 86-Inch Cyclotron—R. S. Livingston. (*Nature* (London), vol. 170, pp. 221–223; August 9, 1952.) Description, with operating details, of an accelerator giving an internal proton beam of intensity $>$1 ma at 24 mev.

621.384.612 182
The Electron Synchrotron—S. E. Barden. (*Metrop. Vick. Gaz.*, vol. 24, pp. 207–217; August, 1952.) An outline of synchrotron theory, with some details of the 375-mev synchrotron built for Glasgow University.

621.384.612.1† 183
Cyclotron—Please note that 621.384.611 will be used in future for cyclotrons in place of 621.384.612.1† used hitherto.

621.384.62 184
An Electrostatic Generator for 1 MV—N. Forsberg and P. Isberg. (*Ark. Fys.*, vol. 3, pp. 519–524; August 5, 1952.) Description of a nonpressurized van de Graaff generator constructed for nuclear research at the Royal Institute of Technology, Stockholm. The linear accelerator used with the generator is also described.

621.385.833 185
Measurement of the First and Second Derivatives of the Axial Field of a Powerful Magnetic Lens—P. Gautier. (*Compt. Rend. Acad. Sci.* (Paris), vol. 235, pp. 361–364; August 4, 1952.)

621.385.833 186
New Type of Electrostatic Immersion Objective with High Resolving Power—A. Septier. (*Compt. Rend. Acad. Sci.* (Paris), vol. 235, pp. 652–654; September 29, 1952.) A system comprising essentially a plane cathode followed by a unipotential lens was investigated in order to obtain a very strong extractor field. A resolution of the order of 100 mμ was obtained.

621.385.833 187
Resolving Power of the Electrostatic Immersion Objective—A. Septier. (*Compt. Rend. Acad. Sci.* (Paris), vol. 235, pp. 609–611; September 22, 1952.) For a particular metallurgical electron microscope the value found in practice for the resolving power is better than the theoretical value.

621.385.833 188
The Focal Properties and Spherical-Aberration Constants of Aperture Electron Lenses—M. M. MacNaughton. (*Proc. Phys. Soc.* (London), vol. 65, pp. 590–596; August 1, 1952.)

621.385.833 189
Investigation of Magnetic Lenses having the Axial Field $H(0, z) = \gamma/z^n$—U. F. Gianola. (*Proc. Phys. Soc.* (London), vol. 65, pp. 597–603; August 1, 1952.)

621.385.833:061.3 190
German Society for Electron Microscopy. Fourth Annual Conference—T. Mulvey. (*Nature* (London), vol. 170, pp. 271–273; August 16, 1952.) Summaries are given of some of the 80 papers read, selected to indicate the general scope of the conference held at Tübingen, June 1952.

621.387.464:621.396.822 191
Discrimination against Noise in Scintillation Counters—R. J. T. Herbert. (*Nucleonics*, vol. 10, pp. 37–39; August, 1952.)

621.396:623.5 192
Acoustic Firing Error Indicator—M. C. Eliason and W. G. Hornbostel. (*Electronics*, vol. 25, pp. 98–101; October, 1952.) Equipment enabling useful information to be obtained from misses as well as hits comprises two radio transmitters mounted on the airborne target and radio receivers located near the gun. The transmitters are associated with special flat-response capacitor microphones which pick up the shock waves from passing bullets; the receivers indicate magnitude and sense of the error.

621.791.3:621.316.7.076.7 193
Electronic Control of Soldering Machines—J. Dusailly. (*Tech. Mod.* (Paris), vol. 44, pp. 141–143; May, 1952.) Description of equipment using thyratrons for timing and heating-current control of soldering operations.

621.791.7:621.317.313 194
Measurement of the Effective Values of Welding Currents—R. Peretz. (*HF* (Brussels) vol. 2, pp. 55–67; 1952.) Two methods of measurement are described, one using a series manganin resistor and the other a magnetic amplifier, with electronic equipment for measuring the short welding time. Single-phase currents up to 20 ka, with thyratron control, were measured. Results obtained by the two methods were in good agreement.

PROPAGATION OF WAVES

538.566 195
The Nonexistence of Sommerfeld's Surface Wave—P. Poincelot. (*Compt. Rend. Acad. Sci.* (Paris), vol. 235, pp. 350–352; August 4, 1952.) A source of error in Sommerfeld's analysis is noted, from which it is concluded that the surface wave does not exist. See also 2892 of 1949 (Kahan and Eckart).

538.566:551.510.535 196
The Mean Velocity of the Energy in a Nonuniform Ionized Absorbing Medium with Slowly Varying Parameters [stratified medium]—H. Arzeliès. (*Compt. Rend. Acad. Sci.* (Paris), vol. 235, pp. 421–423; August 11, 1952.) Theory is developed without assuming the propagated wave to be transverse and the electric and magnetic vectors both linearly polarized. Two parameters are introduced, characterizing respectively the phase velocity and the wave attenuation; these depend not only on the location of the point considered, but also on the angle between the phase velocity and the planes of stratification. There are two simple sets of polarization conditions possible: the electric vector is linearly polarized and the magnetic vector elliptically polarized, or vice versa. The first case arises if the wave penetrat-

ing the medium has its electric vector parallel to the strata. Simple formulas are derived for the mean energy velocity, the Poynting vector, and the energy density.

621.396.11:519.2 197
Fundamentals of Probability Theory—G. Bangen and H. W. Fastert. (*Tech. Hausmitt. NordwDtsch. Rdfunks*, Special No: Bases for planning of usw networks, pp. 35–44; 1952.) An outline of the principal features of the calculus of probability, with particular reference to its application to the phenomena of the propagation of em waves. Section A deals with the one-dimensional random variable, with explanation of the characteristics of normal distribution and extension to random variables dependent on two parameters. Section B considers the case of two-dimensional random variables and explains the concept of correlation and also some special formulas.

621.396.11:537.562 198
The Propagation of Electromagnetic Signals in an Ionized Gas—N. G. Denisov. (*Zh. Eksp. Teor. Fiz.*, vol. 21, pp. 1354–1363; December, 1951.) An exact solution of the problem in terms of Lommel's functions of two variables is obtained. Using an integral representation of these functions, an asymptotic form of the solution in terms of Fresnel integrals is derived which describes the field of the main part of the signal which has passed over sufficiently large distances. For this case, relatively simple formulas are obtained for determining the envelope of the oscillations of the field; this makes the solution more convenient for practical application.

621.396.11:551.510.535 199
Calculation of Sky-Wave Field Strength—K. Rawer. (*Wireless Eng.*, vol. 29, pp. 287–301; November, 1952.) The first account in English of the method used by the French Service de Prévision Ionosphérique Militaire, in which the different paths actually followed in ionospheric propagation are considered separately and their effects combined. Absorption and blanketing by the lower ionosphere layers, and the geometrical optics of the reflection layer are taken into account. Comparison is made with the C.R.P.L. method. See also 2812 of 1951.

621.396.11:551.510.535 200
The B.B.C. Ionospheric-Storm-Warning System—Bennington and Prechner. (See 103.)

621.396.11.029.55 201
Scatter Sounding: A New Technique in Ionospheric Research—O. G. Villard, Jr., and A. M. Peterson. (*Science*, vol. 116, pp. 221–224; August 29, 1952.) See also 2579 of 1952.

621.396.11.029.55 202
Marked Deterioration of Radio-Propagation Conditions recently observed on Intercontinental Circuits using Decametre Waves—J. Maire. (*Ann. Radioélect.*, vol. 7, pp. 221–224; July, 1952.) After a relatively calm period of several years, a long succession of ionospheric storms commenced towards the middle of August 1950, which seriously affected communications on the Paris-New York circuit. Whereas in 1948 only two frequencies (10 and 18 mc) or at most three (7, 10 and 18 mc) sufficed for uninterrupted communication, five frequencies (5, 7, 10, 15 and 18 mc) were found necessary during the winters 1950–51 and 1951–52. The relation of the effect to sunspot activity and geomagnetic variations is discussed. Both annual and 27-day-period variations have been noted. Since the minimum phase of solar activity is being approached, a diminution of the trouble is probable in the coming years.

621.396.11.029.64:621.396.812.3 203
Some Aspects of Microwave Fading on an Optical Path over Sea—A. G. Bogle. (*Proc. IEE* (London), part III, vol. 99, pp. 236–240; September, 1952.) Observations of the fading of 3.26-cm and 9.2-cm signals transmitted across Cook Strait, New Zealand, were made for about 15 months during 1949 and 1951. Most of the equipment used was identical with that used in the Cardigan Bay tests described by Megaw (518 of 1947). Two principal types of fading were distinguished: (*a*) "roller" fading in which broad maxima were separated by narrow deep minima at intervals ranging from a few minutes to about an hour; (*b*) slow shallow fading, usually associated with "scintillation" and sometimes persisting for as long as six hours. From the evidence available it is concluded that the deep fading is caused by the random coincidence of two conditions, (*a*) phase opposition of the direct and indirect signals, which is dependent on the variation of the effective gradient of the modified refractive index over the path, (*b*) equality of the two signal strengths, which depends on the distribution of discontinuities of refractive index along the path, attributed to turbulence.

RECEPTION

621.396.621:621.396.619.11/.13 204
Circuit Technique of the New Valves for A.M./F.M.—D. Hopf and H. Bock. (*Funk-Technik* (Berlin), vol. 7, pp. 433–434, 441; August, 1952.) Design details for an efficient AM/FM receiver using two Type-ECH81 tubes and one each of Types EF85, EABC80, and EL41.

621.396.621:621.396.822:621.392.52 205
Optimum Filters for the Detection of Signals in Noise—L. A. Zadeh and J. R. Ragazzini. (PROC. I.R.E., vol. 40, pp. 1223–1231; October, 1952.) An optimum predetection filter is defined as one which maximizes the difference between the signal and noise components of the output in terms of a suitable difference function. In a special case, this definition leads to the criterion used by North (3419 of 1944) and yields filters which maximize the signal/noise ratio at a specified instant of time. North's theory of such filters is extended to the case of nonwhite noise and finite-observation-time filters. Explicit expressions for the pulse responses of such filters are developed and two practical examples are considered.

621.396.621:621.396.822:621.392.52 206
The Detection of a Sine Wave in the Presence of Noise by the use of a Nonlinear Filter—T. G. Slattery. (PROC. I.R.E., vol. 40, pp. 1232–1236; October, 1952.) Basic theory of the design of nonlinear filters for the detection of signals in noise is reviewed, and an account is given of the construction of such a filter for the detection of a sine wave of unknown frequency in the presence of random noise.

621.396.621.53.029.51/.55 207
The All-Wave Receiver, Type E 103 AW/4—H. Behling. (*Telefunken Ztg.*, vol. 25, pp. 185–193; August, 1952.) Description of a double-heterodyne receiver covering from 100 kc to 30 mc in seven ranges with adequate overlap. As regards quality of reproduction, sensitivity and selectivity, the receiver is intermediate between a good broadcasting receiver and a high-quality commercial receiver. Performance data for the sw band are compared with results for a special sw receiver of the "Köln" type.

621.396.622:621.396.619.11 208
Linear Detection of Amplitude-Modulated Signals—H. Hellerman and C. R. Cahn. (PROC. I.R.E., vol. 40, p. 1251; October, 1952.) Analysis leading to an expression for the output of a type of linear detector suitable for AM signals, in a form which clearly indicates the theoretical limitations of the detection process.

621.396.823:621.396.67 209
Loop Aerial Reception—Bramslev. (See 35.)

STATIONS AND COMMUNICATION SYSTEMS

621.396:656.22(43) 210
Radio Communication Technique used on German Railways—M. Finck and F. Pepping. (*Telefunken Ztg.*, vol. 25, pp. 176–184; August, 1952.) An account of developments starting with the period 1920–1924, when long-wave telegraphy systems were used for communication between district head-offices and also for communication with relief trains. Modern usw equipment is described.

621.396.1.029.6:061.3 211
European V.H.F. Broadcasting—(*Wireless World*, vol. 58, pp. 433–434; October, 1952.) Summary of plans considered at the Stockholm conference, June 1952, for the allocation of frequency bands for television and sound. See also 3560 of 1952.

621.396.41 212
A Time-Division Multiplex Terminal—O. E. Dow. (*RCA Rev.*, vol. 13, pp. 275–290; September, 1952.) Detailed description of the equipment for a 22-channel pam system with channel transmission bands from 100 cps to 3.4 kc. Each channel is sampled 8333 times per second by means of an electronic distributor. The resulting AM pulses of both plus and minus polarities are used for FM of the RF carrier. A method of noise reduction and a crosstalk-balancing circuit are described and performance details of the system are given.

621.396.61.029.62:621.396.8:519.2 213
Simplified Method of Determining Service Probability and its Application to the Planning of U.S.W. Networks—R. Gressmann and K. H. Kaltbeitzer. (*Tech. Hausmitt. NordwDtsch. Rdfunks*, pp. 3–17; 1952. Special No: Bases for planning of usw networks.) The F.C.C. statistical treatment of field strength is outlined and its suitability for application to the conditions existing in Germany is critically discussed. The logarithmic-normal statistical field-strength distribution is explained. Practical examples illustrate the application of the statistical method for estimating the service area of a transmitter (*a*) with no interference, (*b*) with a single interfering signal, (*c*) with several interfering signals. Only simple mathematics is used. A map shows the estimated service areas of various television transmitters in Western Germany.

621.396.61.029.62:621.396.8:519.2 214
Method for Determining the Service Probability in the Field of a Transmitter affected by Any Number of Interfering Transmitters—J. Grosskopf. (*Tech. Hausmitt. NordwDtsch. Rdfunks*, pp. 18–34; 1952. Special No: Bases for planning of usw networks.) A detailed explanation is given of the statistical method of service-area estimation described in the Report of the Ad Hoc Committee, F.C.C., Washington, D. C. The effects of interfering fields are taken into account, and since the F.C.C. Report omits the greater part of the mathematical basis for the numerous formulas given, sufficient mathematics is included here to make the formulas intelligible.

621.396.65:551.594.6 215
Correlation between the Mean Level of Atmospherics and the Degree of Intelligibility in a Kilometre Wave Radio Link—Carbenay. (See 105.)

621.396.65:621.396.5 216
Radio Relay Stations of the TD-2—W. L. Tierney. (*Bell Lab. Rec.*, vol. 30, pp. 326–332; August, 1952.) Illustrations and brief descriptions of typical stations along the 2992-mile circuit.

621.396.65.029.6 217
Microwave Radio Links—A. T. Starr and T. H. Walker. (*Proc. IEE* (London), part III, vol. 99, pp. 241–255; September, 1952. Discussion, pp. 289–293.) Propagation phenomena are discussed in relation to the design of multichannel radio links, and a detailed treatment is given of a FM link, thermal and intermodulation noise being calculated in terms of the system parameters and the frequency devia-

tion determined for minimum total noise. Preemphasis is discussed and the bandwidth necessary to meet specified requirements is determined. Statistical problems are not considered, and all used channels are assumed to have signals of equal amplitude. The mathematical analysis is given in appendices.

621.396.65.029.62:621.3.018.78 218
Multipath Distortions on a F.M. U.S.W. Beam Link and their Effect on its Operation—H. J. Fründt. (*Telefunken Ztg.*, vol. 25, pp. 149–157; August, 1952.) Investigations of a radio link between Berlin and the Harz mountains, operating in the 60-mc band with a frequency swing of ±150 kc, showed multipath-transmission effects with a transit-time difference of about 1.7 μs and an amplitude ratio of about 0.15, with corresponding fluctuations of cross-talk between the telephony channels. In spite of this the noise level was 6 N below and the crosstalk 5.7 N below the signal level. Multipath effects were not observed on a similar link between Berlin and the Harz mountains (2614 of 1952). This operates in the same frequency band and has a frequency swing of ±500 kc, but the two paths are several kilometers apart and have different ground profiles.

621.396.65.029.64:621.396.61/.62 219
Microwave Techniques for Communication Links—G. King, L. Lewin, J. Lipinski and J. B. Setchfield. (*Proc. IEE* (London), part III, vol. 99, pp. 275–288; September, 1952. Discussion, pp. 289–293.) An account of theoretical and practical work in connection with the development of microwave components for the frequency band 3.6–4.2 kmc, including hybrid-T junctions, waveguide horns for feeding parabolic reflectors, low-reflection crystal mounting, antenna matching devices, etc. Measurement techniques required to ensure satisfactory performance are outlined and a detailed description is given of a precision microwave signal generator and a piston attenuator suitable for measurements on microwave circuits and components.

621.396.65.029.64:621.396.61/.62 220
Circuit Technique in Frequency-Modulated Microwave Links—H. Grayson, T. S. McLeod, R. A. G. Dunkley and G. Dawson. (*Proc. IEE* (London), part III, vol. 99, pp. 256–274; September, 1952. Discussion, pp. 289–293.) Discussion of circuit problems in wide-band microwave radio links is illustrated by reference to the development of links operating at frequencies around 4 kmc for 180-channel telephony or for television. Modulating and demodulating circuits with very nearly linear characteristics, and IF amplifiers with uniform time-delay, are described, together with the techniques required to assess their performances. The optimum type of wide-band low-noise IF amplifier consists of earthed-grid triodes in cascade. High-level IF microwave mixers, and afc systems, are described and the special problems of television video-frequency circuits are discussed.

621.396.71+621.397.7](71) 221
The Radio Canada Building in Montreal—A. Frigon. (*BBC. Quart.*, vol. 7, pp. 100–106; Summer, 1952.) General description of the arrangements of the broadcasting and television sections in the adapted 12-story building in Dorchester St. West, Montreal.

621.396.712(434.1) 222
Transmitter Installation on the Hoher Meissner, North Hesse, Germany—P. Eich. (*Telefunken Ztg.*, vol. 25, pp. 194–197; August, 1952.) Outline description of the station equipment, which at present includes a medium-wave 20-kw transmitter, and a 10-kw usw transmitter feeding an 8-stack double-slot antenna. Programs are transmitted over an usw link from the Feldberg.

621.396.712.2/.3 223
Auxiliary Circuits in a Studio—W. Roos. (*Tech. Mitt. schweiz. Telegr.-TelephVerw.*, vol. 30, pp. 140–144; April 1, 1952. In German.) Description of control system and circuits installed at the Zürich studios enabling actors playing in separate studios to hear studio effects and speeches made in the other studios as necessary. Circuits for communication between sound engineer and actors are also described.

621.396.73 224
New Equipment for Outside Broadcasts—S. D. Berry. (*BBC. Quart.*, vol. 7, pp. 120–128; Summer, 1952.) Description of amplifier and associated equipment, comprising 4-channel mixer, Type-OBA/9 amplifier and program meter (two per set), distribution and general control unit, loudspeaker amplifier and isolating amplifier, and power unit, together with loudspeaker, spares and accessories. Special features of the various units are noted.

621.396.931 225
Investigations on Train Radiotelephony—H. Kobierski. (*Telefunken Ztg.*, vol. 25, pp. 169–175; August, 1952.) An account of experiments carried out in a specially equipped coach on the electrified line from Nuremberg to Ratisbon. Frequencies in the 80-mc and 160-mc bands were used; their relative advantages and disadvantages are discussed. The results favor the use of a diversity transmission system in which the frequency separation between the two transmitters is about 30 kc (twice the FM deviation). The receivers are automatically tuned to the transmitter giving the stronger signal.

621.396.933:061.4 226
Air Radio Developments—(*Wireless World*, vol. 58, pp. 397–400; October, 1952.) Review of airborne and ground equipment on view at the exhibition organized by the Society of British Aircraft Constructors, Farnborough, September 1952.

SUBSIDIARY APPARATUS

621-526 227
The Stability of a Multiple Linear Servo System—F. H. Raymond. (*Compt. Rend. Acad. Sci.* (Paris), vol. 235, pp. 508–510; September 1, 1952.)

621.311.69:534.113 228
Recent Developments in Vibrators and Vibrator Power Packs—J. H. Mitchell. (*Jour. Brit. IRE*, vol. 12, pp. 431–444; August, 1952.) Discussion of the Grade-1 type of vibrator which is expected to give at least the 1,000-hour life required for Services equipment. Reasons are given for specializing mainly on synchronous split-reed separately driven types. An outline is given of extensive investigations of contact phenomena, vibrator design, and the circuits fed by the vibrator. A range of vibrators is described with outputs from a few milliwatts to over 200 w. Very high conversion efficiencies have been obtained.

621.314.63:546.824-3 229
Titanium-Dioxide Rectifiers—R. G. Breckenridge and W. R. Hosler. (*Jour. Res. Nat. Bur. Stand.*, vol. 49, pp. 65–72; August, 1952.) A detailed account of work carried out up to the present on the TiO_2-film rectifiers previously noted (3567 of 1952). A feature of great practical importance is the improvement in performance with increase of temperature. For a particular steam-treated sample the forward current increased, while the backward current decreased slightly, as the temperature was increased up to 140°C. Heating to 200°C, however, causes irreversible damage. Differences of characteristics observed with different counter-electrode metals are discussed, a marked change of properties being noted when Zn was used. Further investigations are in progress.

621.316.722:621.316.86 230
Voltage Regulators using Nonlinear Elements—N'Guyen Thien-Chi and J. Suchet. (*Ann. Radioélect.*, vol. 7, pp. 189–198; July, 1952.) A simple method of determining the parameters of circuits providing reference voltages working into a constant load is described, and is illustrated by calculations for arrangements using either a single element or a pair of the nonlinear resistors manufactured by the Compagnie général de T.S.F. (3364 of 1952). Power limitations restrict the field of application of this type of voltage regulator.

621.316.722:621.384.5 231
How to Design V.R. Tube Circuits—R. C. Miles. (*Electronics*, vol. 25, pp. 135–137; October, 1952.) Families of supply-voltage/supply-series-resistance curves for various voltage-regulator tubes are used as the basis for designing stabilized direct-voltage supply circuits.

TELEVISION AND PHOTOTELEGRAPHY

621.397:061.4 232
The (Television) Society's Annual Exhibition—(*Jour. Telev. Soc.*, vol. 6, pp. 326–329 and 390–393; January/March and April/June, 1952.) Brief descriptions are given of television and associated equipment exhibited at Century House, London, December 1951.

621.397.24:621.395.97 233
Relaying the Sound and Television Signals at the South Bank Site—Barton-Chapple. (See 23.)

621.397.3 234
The Energy Spectrum of the Television Image—F. Winckel. (*Arch. elekt. Übertragung*, vol. 6, pp. 385–387; September, 1952.) The investigations of Mertz and Gray (1934 Abstracts) are discussed. The gaps in the energy spectrum of the television image are evaluated by analyzing picture content, taking the particular case of a vertical bar rotated through 360°. The width of the video-frequency sideband is shown to be proportional to the tangent of the angle of rotation. The gaps in the spectrum tend to become filled as the number of scanning lines decreases; interlacing turns this to advantage.

621.397.331.2 235
A Note on the Design of Constant-Resistance Cathode-Ray Deflection Circuits—R. C. Webb. (*RCA Rev.*, vol. 13, pp. 335–343; September, 1952.) Description of a horizontal-deflection circuit which is particularly useful with small television pickup tubes like the vidicon, and allows several hundred feet of transmission line to be interposed between the amplifier tube and the deflection coil, which forms part of a network that appears as a pure resistance matching the line impedance. The efficiency of the system is low, but the resulting transient disturbances in video circuits are small.

621.397.335:535.623 236
Frame Synchronization for Color Television—D. Richman. (*Electronics*, vol. 25, pp. 146–150; October, 1952.) Analysis indicates that the present F.C.C. monochrome synchronizing waveform is able to provide reliable triggered frame synchronization with the N.T.S.C. color system [175 of 1952 (Hirsch *et al.*)]. A suitable circuit is described.

621.397.5 237
Present Stage of Development of Television—V. K. Zworykin. (*Ricerca sci.*, vol. 22, pp. 1893–1927; October, 1952.) A survey covering choice of television standards, tube developments, color systems and applications in industry. 30 references.

621.397.5:535.623 238
Gamma Correction in Constant-Luminance Color-Television Systems—S. Applebaum. (PROC. I.R.E., vol. 40, pp. 1185–1195; October, 1952.) Analysis of the effects of precorrection of the red, green and blue image coordinates to provide unity over-all gamma.

621.397.5:535.623 239
Colour Television—A. Karolus. (*Z. angew. Phys.*, vol. 4, pp. 300–320; August, 1952.) A survey paper reporting developments to date, especially in the U.S.A. 63 references.

621.397.5:535.623 240
A Summary of Recent Advances in 'Dot-Sequential' Color TV Systems—B. D. Loughlin. (*Proc. NEC* (Chicago), vol. 7, p. 361; 1951.) Summary only. See 826 of 1952.

621.397.5:535.88 241
An Experimental System for Slightly Delayed Projection of Television Pictures—P. Mandel. (PROC. I.R.E., vol. 40, pp. 1177–1184; October, 1952.) Description of a system comprising a flying-spot scanner for pictures on 35-mm film, a microwave relay transmitting the picture signals to the receiving station, where the picture is reproduced on the screen of a cr tube, photographed on synchronously driven 16-mm film, which is developed, fixed and dried in 60 seconds and then run through a standard cinema projector for display on a large screen. Tests carried out in Paris indicate that the loss in fine detail is about 10 per cent. The slight delay of 60 seconds should not be objectionable.

621.397.5:621.396.65 242
British Television Relay Network—(*Elec. Commun.*, vol. 29, pp. 171–178; September, 1952.) A short description of the design and characteristics of the various links in this network, with special emphasis on the features of the RF relay chains.

621.397.5(41):061.3 243
The Convention on "The British Contribution to Television"—(*Onde élect.*, vol. 32, pp. 372–388; August/September, 1952.) Summaries of the papers presented at the convention, with an introduction by General Leschi. See also 2629 of 1952.

621.397.61 244
B.B.C. Television Transmitting Stations—(*Engineer* (London), vol. 194, pp. 227–229; August 15, 1952.) Some details are given of the high-power equipment brought into use at the Kirk o' Shotts stations in August 1952. The vision transmitter uses low-level modulation, the output power of 50 kw being obtained with a pair of water-cooled triodes, Type BW. 165, in the final stage. The sound transmitter is of conventional design using class-B modulation, with a carrier output of 18 kw at 100 per cent modulation. The transmission line feeding the common antenna at the top of the 750-foot mast consists of a 5-inch Cu tube with an axial inner conductor of locked-coil wire rope with outer wires of high-conductivity Cu, the rope having a 2-ton load at the lower end. This construction reduces echo effects. Power supplies are noted and a map shows estimated field-strength contours. See also 2640 of 1952.

Details are also given of the equipment of the new station at Wenvoe, near Cardiff, which commenced transmissions in August 1952, using medium-power transmitters, the vision transmitter has a peak-white output of 5 kw, modulation being effected at the 500 w level; the sound transmitter, has an output of 2 kw and uses a class-B modulator. As at Holme Moss and Kirk o' Shotts, a combining unit is used with a single transmission line feeding the common antenna at the top of the 750-foot mast. Programs will ultimately be transmitted from London via a new coaxial cable, but until this is ready the transmissions will be routed over an experiment vhf link between London and Cardiff.

621.397.61(43) 245
The First [German] 10-kW Television Transmitter—(*Funk-Technik*, (Berlin), vol. 7, pp. 396–397; August 1, 1952.) Technical details of the directional transmitter shortly to be brought into operation in Nikolassee, Berlin, to serve Berlin and Western Germany. The frequency range is 174–216 mc, with a video-frequency bandwidth of 5 mc.

621.397.61(494) 246
The Suitability of the Dôle as a Site for a Television Transmitter—H. Laett. (*Tech. Mitt. schweiz. Telegr.-Teleph Verw.*, vol. 30, pp. 167–172; May 1, 1952. In German.) For a station to serve an area including Lausanne and Geneva, the "Combe gelée" plateau at about 1,500 m altitude, on the Swiss side of the Dôle, was considered likely to be a suitable site. Tests were made over the period July–October 1951, using a B.B.C. television transmitter (carrier power 500 w, frequency 62.25 mc) with a wide-band directional antenna giving horizontal polarization, and pulse equipment for making reflection measurements. Field-strength distribution at height 3 m is shown on a map; the value at height 10 m is on the average 7 db below that at 3 m. It is estimated from the measurements that using a 5-kw transmitter and two antennas directed respectively towards Lausanne and Geneva, more than half a million people could be served; within the service zone the coverage would be 84 per cent.

621.397.61.029.6:621.317.7 247
Ultra-High-Frequency Television Monitor—F. D. Lewis. (*Proc. NEC* (Chicago), vol. 7, pp. 440–448; 1951.) Description of equipment for carrier-frequency monitoring of the video transmitter, and both carrier-frequency and modulation monitoring of the FM sound transmitter. A single precision reference crystal is used for independent monitoring of both carrier frequencies. A new harmonic generator using Ge diodes has been developed for the uhf stage of the crystal-controlled multiplier chain. Heterodyne methods are applied to derive signals suitable for operating cycle-counter types of frequency-deviation meters.

621.397.611/.621).2 248
Scanning-Current Linearization by Negative Feedback—A. W. Keen. (PROC. I.R.E., vol. 40, p. 1215; October, 1952.) Summary only. See 1752 of 1952.

621.397.611.2 249
Performance of the Vidicon, a Small Developmental Television Camera Tube—B. H. Vine, R. B. Janes and F. S. Veith. (*Proc. NEC* (Chicago), vol. 7, pp. 449–453; 1951.) See 2914 of 1952.

621.397.62 250
Television A.G.C. Circuit—G. F. Johnson. (*Wireless World*, vol. 58, pp. 424–426; October, 1952.) Description of a simple system of stabilizing mean brightness by maintaining a constant difference of average voltage between the grid of the first IF amplifier and the grid of the synchronizing-signal separator.

621.397.62 251
Problems of Television Projection-Type Receivers—E. Schwartz. (*Elektrotech. Z., Ed. B*, vol. 4, pp. 249–253; September 21, 1952.) Effects associated with the cr tube, including halation, reflection from the tube walls, effect of screen thickness on luminous intensity, secondary and x-ray emission, and thermal loading of screen, are discussed and the optics of projection systems and the characteristics of picture screens are considered briefly.

621.397.62 252
An Economical Sync Clipper of Unusual Noise Immunity—M. Marks. (*Proc. NEC* (Chicago), vol. 7, pp. 352–360; 1951.) Impulse noise strong enough to disturb the operation of most types of synchronizing circuit is rendered innocuous by the synchronizing-signal clipper described. A single conventional receiver tube is operated so that noise pulses, distinguished from desired signals by their higher peak amplitude, produce no output. Synchronization pulses, on the contrary, are clipped at top and bottom as usual and fed to the horizontal and vertical sweep systems. Practical circuits are described.

621.397.62:535.623 253
Synchronous Demodulator for Color TV—R. B. McGregor. (*Electronics*, vol. 25, pp. 214, 230; October, 1952.) In the N.T.S.C. system the color information is carried at a subcarrier frequency, the hue and saturation information being embodied respectively in the modulation of two subcarrier components with a mutual phase separation of 90°. The two signals are separated by applying to the suppressor grid of the detector tube an oscillating voltage of the same frequency as that of the subcarrier applied to the control grid, and in phase with one of the components.

621.397.62:621.396.622.72 254
A Constant-Input-Impedance Second Detector for Television Receivers—W. K. Squires and R. A. Goundry. (*Proc. NEC* (Chicago), vol. 7, pp. 362–368; 1951.) See 2059 of 1952.

621.397.621 255
Faulty Interlacing—W. T. Cocking. (*Wireless World*, vol. 58, p. 457; November, 1952.) Comment on 2918 of 1952 (Patchett), stressing that the first requirement for correct interlacing is that the frame synchronizing pulses applied to the sawtooth-wave generator shall be identical in successive frames for such time as they are capable of influencing the generator.

621.397.621:621.317.4 256
Field Plotting in Deflection-Yoke Design—E. Sieminski. (*Electronics*, vol. 25, pp. 122–126; October, 1952.) Simple apparatus including a probe coil is described for measuring the field of magnetic deflection yokes for television tubes; the test procedure makes it easy to relate a difference of tube performance to a particular design variation.

621.397.621.2 257
Using C.R. Tubes with Internal Pole Pieces—C. V. Fogelberg, E. W. Morse, S. L. Reiches and D. P. Ingle. (*Electronics*, vol. 25, pp. 102–105; October, 1952.) By including part of the magnetic focusing system inside the cr tube, the focusing-energy requirements can be reduced and the focusing field better controlled. Various examples of internal pole pieces are illustrated and methods of mounting them in television tubes are described.

621.397.645+621.397.61 258
Ekco Amplifier/Converter. New TV Retransmitting Equipment—(*Electrician*, vol. 149, pp. 537–538; August 22, 1952.) Short description of equipment comprising high-gain receivers for the sound and vision channels, together with frequency-changer units, low-level amplifiers, sound and vision transmitters, and a mains-operated power unit. Such equipment provides good reception over some 150 square miles in fringe or shadow areas. Provision is made for retransmission on either the British, American or European line standards.

621.397.7+621.396.71](71) 259
The Radio Canada Building in Montreal—Frigon. (See 221.)

621.397.813 260
Modulation Distortion in Television Reception, and the Possibility of its Compensation—F. Kirschstein and H. Bödeker. (*Fernmeldetech. Z.*, vol. 5, pp. 357–361; August, 1952.) The deformation of television signals transmitted by a ssb system is analyzed, use being made of data furnished by Kell and Fredendall (2063 of 1949) on transient phenomena in vestigial-sideband transmission. The analysis was checked by tests carried out on the Feldberg experimental transmitter. A simple practical compensation arrangement is described which uses an RC circuit, with a time constant of 0.25 μs, as a frequency-dependent feedback unit in the cathode circuit of the video-amplifier output tube. This restores the rectangular form of the distorted wave from the demodulator.

TRANSMISSION

621.396.61:621.396.97 261
Automatic Broadcasting: Remote Control and Automatic Monitoring of Third Programme Transmitter—R. W. Leslie and C. Gunn-Russell. (*Wireless World*, vol. 58, pp. 449–451; November, 1952.) See 2924 of 1952.

621.396.619.231.018.783† 262
The Problem of Distortion in Anode-Voltage-Modulated Transmitters—W. T. Runge. (*Telefunken Ztg.*, vol. 25, pp. 135–142; August, 1952.) In the final HF stage, conversion distortions are small because the external resistance is sufficiently high compared with the tube internal resistance determined by the mutual conductance and penetration factor. Load distortion, however, cannot be neglected. A decrease of these distortions can be obtained by reducing the internal resistance of the control stage. Distortions in the modulation transformer are discussed by considering its equivalent circuit, and the nonlinear distortion factors are calculated. In the final stage of the modulator, nonlinear distortion also occurs, a 5 per cent deviation of the amplitude of the fundamental wave producing a distortion of about 1 per cent, a value which also results if the phases of the two half-waves differ by about 0.7°. Certain requirements can be deduced for the preliminary modulation stages; a modulator satisfying these requirements is described. Application of the knowledge gained in these investigations to the design of the 20-kw medium-wave transmitter installed on the Hoher Meissner resulted in the distortion being very small. Measurement results are quoted.

TUBES AND THERMIONICS

537.533:621.396.619 263
Analysis of Modulated Electron Beams—W. W. Cannon and L. E. Bloom. (*Proc. NEC* (Chicago), vol. 7, pp. 59–63; 1951.) Description of experimental equipment for analyzing the velocity and density distribution of an electron beam modulated by a 3-kmc signal.

621.314.7+621.396.622.63 264
Industrial Applications of Semiconductors: Part 5—Crystal Valves—A. Lindell and G. M. Wells. (*Research* (London), vol. 5, pp. 317–323; July, 1952.) The construction and operating characteristics of point-contact and junction-type Ge and Si diodes and triodes are reviewed.

621.314.7:53.01 265
The Physics of Transistors—E. Billig. (*Brit. Jour. Appl. Phys.*, vol. 3, pp. 241–248; August, 1952.) Some of the fundamental concepts of the solid state which are required for an understanding of transistor action are discussed, electron energy levels, contact potential and potential barriers, rectification, extrinsic and intrinsic semiconductors, and transistor action being considered.

621.383.27:621.387.464 266
Two New Photomultipliers for Scintillation Counting—M. H. Greenblatt, M. W. Green, P. W. Davison and G. A. Morton. (*Nucleonics*, vol. 10, pp. 44–47; August, 1952.) Detailed description of a high-efficiency tube, Type H-5037, with a large-area photocathode. and of a high-gain tube, Type 4646, with a large output current. Typical applications are discussed briefly.

621.384.5:621.316.722 267
The Characteristics of some Miniature High-Stability Glow-Discharge Voltage Regulator Tubes—G. Grimsdell:F. A. Benson. (*Jour. Sci. Instr.*, vol. 29, p. 301; September, 1952.) Comment on 1772 of 1952 and author's reply.

621.385:537.525.92 268
Space-Charge-Wave Propagation in a Cylindrical Electron Beam of Finite Lateral Extension—P. Parzen. (*Elec. Commun.*, vol. 29, pp. 238–242; September, 1952.) Reprint. See 2371 of 1952.

621.385:621.392.21 269
Transmission-Line Tubes—V. J. Fowler. (*Proc. NEC* (Chicago), vol. 7, pp. 318–330; 1951.) Proposals are advanced for the development of a new type of wide-band amplifier tube whose construction is based on that of amplifiers with distributed amplification, which are here termed 'chain amplifiers.'

621.385.004(083.75) 270
General Considerations in Regard to Specifications for Reliable Tubes—C. R. Knight and K. C. Harding. (Proc. I.R.E., vol. 40, pp. 1207–1210; October, 1952.) Proposals are made for a specification accurately describing the characteristics of the finished product and including details of inspection and acceptance tests. The lot-acceptance system, in conjunction with an adequate sampling procedure, is considered preferable to 100 per cent screening.

621.385.004.15 271
Concerning the Reliability of Electron Tubes—M. A. Acheson and E. M. McElwee. (Proc. I.R.E., vol. 40, pp. 1204–1206; October, 1952. *Sylvania Technologist*, vol. 4, pp. 38–40; April, 1951.) Analysis of various causes of tube failure, serving to indicate the direction of research and development programs for production of reliable tubes.

621.385.004.15 272
Technique of Trustworthy Valves—E. G. Rowe. (Proc. I.R.E., vol. 40, pp. 1166–1177; October, 1952.) Condensed reprint. See 1776 of 1952.

621.385.029.6 273
Low-Noise Traveling-Wave Tube—A. G. Pfeifer, P. Parzen and J. H. Bryant. (*Proc. NEC* (Chicago), vol. 7, pp. 314–317; 1951; *Elec. Commun.*, vol. 29, pp. 234–237; September, 1952.) Outline description of a tube operating in the range 4.2–5.2 kmc, with a gain of 15 db, an output power of 0.5 mw, and a noise figure of 10 db. A new version under construction will have a gain of about 30 db, with a comparable noise figure.

621.385.029.6 274
Some Recent Developments in Traveling-Wave Tubes for Communication Purposes—J. H. Bryant, T. J. Marchese and H. W. Cole. (*Proc. NEC* (Chicago), vol. 7, pp. 299–303; 1951; *Elec. Commun.*, vol. 29, pp. 229–233; September, 1952.) Basic features of traveling-wave tubes are reviewed and typical performance characteristics and applications are considered. A new type of tube is described which is of rugged construction and is specially designed for ease of handling. The operating frequency range is 5.9–7.1 kmc, gain 25 db, power output 10 w and operating voltage 1.2 kv, this voltage permitting a reduction of over-all length. An experimental permanent-magnet system for this type of tube is shown.

621.385.029.6 275
Experimental Low-Noise Amplifying Valve—G. Convert. (*Ann. Radioélect.*, vol. 7, pp. 225–234; July, 1952.) Theory serving as a basis for the development of a low-noise traveling-wave tube is presented, and an experimental tube is described with an optimum noise factor of 10 db and a gain of 14 db. The gain is a linear function of the cube root of the beam current. Variation of the noise factor as a function of the voltage of the second anode and as a function of the beam current is shown in curves. Pertinent theory has previously been published (2397 of 1952).

621.385.029.62/.64 276
Generalities on Travelling-Wave-Valve Feedback Self-Oscillators. Theory of the Reflex Travelling-Wave Valve—M. Denis. (*Ann. Radioélect.*, vol. 7, pp. 169–188; July, 1952.) The properties of traveling-wave-tube oscillators with internal or external em feedback are reviewed, and the advantages of using high-dispersion transmission lines to obtain satisfactory operation of such oscillators are discussed. Theory indicates that optimum performance should be obtained with a line having minimum abnormal dispersion, i.e., one in which the group velocity is negative and equal to the velocity of light. Such lines are best used in oscillators of the type termed "carcinotron" [3616 of 1952 (Guénard *et al.*)]. A tentative theory is developed for the reflex type of traveling-wave tube, using a method of exposition similar to that of Bernier (2974 of 1947) for the normal type. Reflex tubes have a wide range of electronic tuning and are easily controlled by adjustment of anode and repeller voltages. Results obtained with an experimental reflex tube confirm the theoretical predictions except as regards power output, which was much lower than expected.

621.385.029.63/.64 277
Low-Noise Traveling-Wave Amplifier—R. W. Peter. (*RCA Rev.*, vol. 13, pp. 344–368; September, 1952.) Design considerations for the electron gun and the circuit of wide-band low-noise traveling-wave amplifiers are discussed, and detailed theory is given of the "three-region" low-noise gun, which is the essential factor in the design of such amplifiers. The construction of a demountable traveling-wave tube is described and measurements on experimental tubes are presented which show the dependence of the noise factor on various tube parameters. The type of traveling-wave amplifier developed can compete with the best crystal-mixer amplifiers as regards noise factor. The best performance obtained with a 500-v wide-band amplifier operating at frequencies near 3 kmc was a noise factor of 8.5 db with a 15-db gain.

621.385.029.63 278
Amplification by Space-Charge Waves in an Electron Beam acted on by Crossed Electric and Magnetic Fields—R. Warnecke, H. Huber, P. Guénard and O. Doehler. (*Compt. Rend. Acad. Sci.* (Paris), vol. 235, pp. 470–472; August 18, 1952.) It has previously been shown [333 of 1950 (Warnecke *et al.*)] that amplification can result from the interaction of two beams, with different velocities, in crossed fields. Amplification is also found possible with a single beam in which a high space-charge density introduces differences of velocity. Theory for small-amplitude signals [1022 of 1951 (Warnecke *et al.*)] shows that the gain is proportional to the relative change of velocity, which is calculable in terms of known parameters. Experimental arrangements are described with which a power output of 20 w, a gain of 15 db and an efficiency of 5 per cent have been obtained at a frequency of 1.2 kmc.

621.385.029.64 279
The Excitation of Electromagnetic Fields by Current Waves—H. Kleinwächter. (*Arch. elekt. Übertragung*, vol. 6, pp. 376–378; September, 1952.) Theory is developed from Maxwell's equations to show that em fields corresponding to a plane or H_{01} wave can be excited by traveling current waves. The appropriate transverse current wave with phase velocity greater than the velocity of light is produced by a multielement waveguide arrangement as described in 2075 of 1952. Space-charge effects are not considered, hence the formulas apply only for weak fields and low-density beams.

621.385.029.64 280
Experimental Verification of Small-Signal Theory for the Traveling-Wave Valve with Helix—H. Schnitger and D. Weber. (*Arch. elekt. Übertragung*, vol. 6, pp. 369–376; September, 1952.) Measurements were made to determine the extent to which wave velocity, helix characteristic impedance and tube gain are affected by enclosing the helix in a glass tube, which is a common practice. From the values of wave velocity found experimentally, the dependence of the gain on current and voltage variations was calculated and compared with measured values; good agreement was ob-

tained. In the experimental wide-band tubes used, no extra attenuation was necessary to prevent self-oscillation. The measurements covered the wavelength range 10.5–30 cm.

621.385.032.213:621.396.822 281

Space-Charge Reduction of Low-Frequency Fluctuations in Thermionic Emitters—T. B. Tomlinson. (*Jour. Appl. Phys.*, vol. 23, pp. 894–899; August, 1952.) A report of experiments to investigate the difference between the space-charge reduction factor for flicker noise and for shot noise. An indirect method is described, using a triode (*a*) connected as a retarding-field diode, and (*b*) with normal connections. By making one pair of measurements at low frequency and another pair at high frequency it is shown that the reducing effect of space charge is greater for flicker than for shot noise.

621.385.032.213.1 282

The Transient Behaviour of Thermionic Filaments with Temperature-Limited Emission—F. H. Hibberd. (*Jour. Sci. Instr.*, vol. 29, pp. 280–283; September, 1952.) The time lag of a filament in responding to variations of heating current is investigated; methods are described for calculating and for measuring its magnitude. The value of the thermal time constant depends on whether the power is supplied at constant voltage or at constant current, being somewhat greater in the former case. For W filaments its value may lie between about 0.03 and 0.3 second.

621.385.032.213.1:536.2 283

Temperature Distribution at the End of a Hot Wire—J. A. Prins, J. Schenk and J. M. Dumoré. (*Appl. Sci. Res.*, vol. A3, no. 4, pp. 272–278; 1952.) Analysis is presented leading to a more general solution than that obtained by Clark and Neuber (1024 of 1951). See also 375 of March (Fischer).

621.385.032.216 284

Spectral Dependence of Thermionic Emission with Activation from (Ba-Sr)O Cathodes over the Visible Region—T. Hibi and K. Ishikawa. (*Phys. Rev.*, vol. 87, pp. 673–674; August 15, 1952.) A 750-w lamp was used with filters as a monochromatic light source to illuminate the cathode incorporated in a test diode. Results are shown in curves and discussed in relation to trapping levels.

621.385.032.216 285

The Decay and Recovery of the Pulsed Emission of Oxide-Coated Cathodes—R. M. Matheson and L. S. Nergaard. (*Jour. Appl. Phys.*, vol. 23, pp. 869–875; August, 1952.) Full paper. Summary abstracted in 2080 of 1950.

621.385.032.216 286

Industrial Applications of Semiconductors: Part 6—Oxide Cathodes—S. Wagener. (*Research* (London), vol. 5, pp. 355–362; August, 1952.) The properties of the semiconducting oxide coating are reviewed and performance levels achieved in modern tubes are quoted. The structure and formation of the interface semiconductor are discussed and its effect on tube performance and life is considered.

621.385.032.44 287

On Extending the Operating Voltage Range of Electron-Tube Heaters—J. Kurshan. (*RCA Rev.*, vol. 13, pp. 300–322; September, 1952.) A survey of possible means of increasing the present voltage tolerance limits of ±10 per cent to ±20 per cent indicates that, even with a heater material having an extremely high temperature coefficient of resistance, ±16 per cent is a fundamental physical limit.

621.385.12:621.318.572 288

Electronic Switching—E. A. R. Peddle. (*Wireless World*, vol. 58, pp. 421–423 and 465–468; October and November, 1952.) Part 1: Principles of the use of Cold-Cathode Gas-Discharge Tubes. Part2: Applications of the Cold-Cathode Gas-Discharge Triode.

621.385.15 289

Theoretical and Experimental Investigation of Dynamic Secondary-Electron Multipliers—H. Beneking. (*Z. angew. Phys.*, vol. 4, pp. 258–267; July, 1952.) Design formulas for electron multipliers are derived and are confirmed by experiments which, among other things, indicate a value of 2–3 ev for the emission energy of the secondary electrons. Data for practical applications are presented graphically and the production and characteristics of multiplier tubes with Mg-MgO secondary-emissive anodes are described.

621.385.2 290

High-Frequency Diode Admittance with Retarding Direct-Current Field—K. S. Knol. and G. Diemer. (*Philips Res. Rep.*, vol. 7, pp. 251–258; August, 1952.) Formulas are developed for the susceptance of a planar diode with a negative anode voltage. The terms due to reflected electrons (total-emission susceptance) and electrons reaching the anode (exponential susceptance) are evaluated separately. Results obtained agree qualitatively with experimental findings.

621.385.2:537.525.92 291

The Space-Charge Smoothing Factor: Part 2—C. S. Bull. (*Proc. IEE* (London), part III, vol. 99, pp. 319–320; September, 1952.) Digest only. Analysis showing a decided difference between fluctuation phenomena in diodes and in resistors. The mean-square deviation $\overline{\epsilon^2}$ of the conductance of a resistor is shown to be zero, so that even for signals as small and as rapidly changing as thermal fluctuations, its conductance is the same as that obtained by ordinary measurements. For diodes, experimental results indicate a value of $\overline{\epsilon^2}/N$ of about 0.5, where N is the number of fluctuating elements regarded as constituting the diode. In an ordinary case N is of the order of 10^4. Part 1: 2058 of 1951.

621.385.2.032.21:537.212+537.525.4 292

Relation between the Phenomenon of Sparking and the Electric Field at the Surface of a Cathode—H. Bonifas. (*Bull. Soc. franc. élect.*, vol. 2, pp. 553–554; October, 1952.) Determination of the es field at the surface of the cathode, using equations previously developed (2084 of 1952), enables an explanation to be given of the mechanism of sparking and of the detachment of cathode active material in rectifying diodes. Discussion indicates that in order to avoid these effects, the cathode surface should be as smooth as possible, with uniform emissivity and low transverse resistivity.

621.385.3/.4 293

High-Transconductance Tubes for Broad-Band Telephone System Uses—G. T. Ford and E. J. Walsh. (*Proc. NEC* (Chicago), vol. 7, pp. 304–313; 1951.) See 1165 of 1952.

621.385.5 294

Screen Dissipation of Pentodes—S. C. Dunn. (*Wireless Eng.*, vol. 29, pp. 309–310; November, 1952.) It is suggested that the usual information and characteristics supplied by tube manufacturers should be supplemented by a statement of optimum screen voltage. The influence of this parameter on the available working area in the I_a-V_a plane is discussed.

621.387 295

Investigation of Gas-Filled Valves for Industrial Applications—C. Biguenet and M. Vassilian. (*Le Vide*, vol. 7, pp. 1191–1196; May, 1952.) Thyratron action is analyzed and the suitability of X_e as a gas filling is illustrated.

621.387.42:621.318.57 296

Gas-Filled Counter and Switching Valves—H. Harmuth. (*Elektrotech. u. Maschinenb.*, vol. 69, pp. 310–313; July 1, 1952.) Description of a neon-filled counter tube essentially similar to that of Lamb and Brustman (266 of 1950), and of suitable decade-counter and switching circuits using such tubes.

621.396.615.141.2 297

The Possibility of Generating Millimetre Waves with Pulsed Multislot Magnetrons of the Rising-Sun Type—W. Praxmarer. (*Nachr-Tech.*, vol. 2, pp. 277–282; September, 1952.) Analysis is presented which leads to the production of diagrams determining oscillation range, operation conditions, and also mechanical dimensions. A second oscillation range is found below 5-mm wavelength, and with suitable mechanical design it appears possible to reach a wavelength of 0.8 mm.

621.396.615.142.2:621.317.332 298

Conductance Measurements on Operating Magnetron Oscillators—Nowogrodzki. (See 157.)

MISCELLANEOUS

621.3:061.4 299

Radio Technology and Electroacoustics—W. Althans. (*Z. Ver. dtsch. Ing.*, vol. 94, pp. 632–636; July 1, 1952.) Review of equipment shown at the 1952 Technical Fair, Hanover, including radio and television receivers, high-power hf transmitting tubes, portable R/T sets, navigation aids, magnetic recorders, uhf measurement equipment, etc.

621.39:061.4 300

Radio Exhibition Review—(*Wireless World*, vol. 58, pp. 384–397; October, 1952.) Detailed discussion of trends in the design of television and broadcast receivers, cr tubes and valves as exemplified in exhibits at the 19th National Radio Exhibition in September 1952. Other equipment reviewed includes a new design of metal-cone loudspeaker and a stencil-cutting system for reproducing pictorial matter. See also 3539 of 1952.

621.396/.397:061.4 301

The British National Radio Exhibition—L. Carduner. (*Audio Eng.*, vol. 36, pp. 12, 81; October, 1952.) An American's impressions of the show.